UNIVERSITY OF CALIFORNIA, SAN DIEGO

The Export of Carbon Mediated by Mesopelagic Fishes in the Northeast Pacific Ocean

A dissertation submitted in partial satisfaction of the requirements for the degree Doctor of Philosophy

in

Oceanography

by

Peter Charles Davison

Committee in charge:

David M. Checkley, Jr., Chair
Jeffrey B. Graham
Philip A. Hastings
J. Anthony Koslow
Mark D. Ohman
Robert Pinkel
Frank L. Powell

2011

ProQuest LLC.
789 East Eisenhower Parkway
P.O. Box 1346
Ann Arbor, MI 48106 - 1346

The dissertation of Peter Charles Davison is approved, and it is acceptable in quality and form for publication on microfilm and electronically:

_____

_____

_____

_____

_____

_____

_____

Chair

University of California, San Diego

2011

DEDICATION

In recognition that her marriage vow did not include clauses for "graduate school," "student stipend," or "husband at sea," and that much was tolerated by her, this dissertation is dedicated to my wife, Lisa.

TABLE OF CONTENTS

LIST OF FIGURES

LIST OF TABLES

ACKNOWLEDGEMENTS

I intended to keep the acknowledgement section brief, but it soon became clear that a great many people have contributed to my education and research here at SIO.

First, I have benefited much from my advisor Dave Checkley, who not only provided the opportunity and funding for me to study at SIO, but taught me how to think and, just as importantly, write as a scientist (it remains a work in progress). Dave continually surprises me with his depth-of-knowledge and experience in the fields of oceanography, biology, mathematics, and ecology. It seems like every time I explore an arcane topic, Dave has already studied it. Dave continually challenged me and set a high standard, to my profit.

My committee was a carefully-chosen team of scientists who all had expertise bearing on my research topic. Although I ended up with a committee of seven members, who could be counted on to give me several different opinions regarding a given issue or manuscript section, I found most of those opinions insightful and often not mutually exclusive as I searched for "the eighth way". Each of my committee members was very helpful and found time for me in their schedule to review manuscripts, attend committee meetings, and to discuss problems.

Jim Bishop, Dave Checkley, and Dave Demer all guided me on funding proposals. My research would not have been possible without a fellowship from NASA, who believed (and funded) me when I proposed to study fish from space. The relationship did indeed turn out to be significant (Figure 4.4).

Dave Demer and his lab provided acoustic advice regarding the set-up and calibration of Tony Koslow's new EK60 sonar that I used for Chapter 3. Dave Demer,

Jules Jaffe, Alex de Robertis, and Rob Pinkel also provided help and advice on an ADCP manuscript that unfortunately didn't work out.

I'd like to thank my co-authors Rebecca Asch, Ana Lara-Lopez, Tony Koslow, and Dave Checkley for their hard work, for their ideas, and for greatly improving my manuscripts.

Oceanography is difficult without ship-time, and I was fortunate to participate in the CCE-LTER program with Mark Ohman and Mike Landry. Trawling is time-intensive, and Mike tolerated schedule overruns by the trawl with more grace than others might have. Mark was generous with wire time, and probably more so than he intended to be before his own instrument malfunctioned in 2008. The core of my final chapter came from the 2008 NOAA ORCAWALE cruise. This excellent opportunity was provided by George Watters and Jay Barlow through the agency of Tony Koslow, and Annette Henry was extremely helpful with logistics. I am grateful for the two successful proposals and cruises, as well as an SIO-277 class cruise, funded through the UC Ship Funds program that provided data for two chapters of this dissertation. The Kaisei Foundation/Ocean Voyages Institute provided funding to extend the SEAPLEX for an additional, much-needed, week at sea.

Trawling is labor-intensive as well as time-intensive. I would like to acknowledge all the faculty, students, volunteers, postdocs, restechs, and crew members who helped launch, retrieve, repair, and process the many trawls that I made. A partial list includes Tony Koslow, Jim Leichter, Sam McClatchie, Jian Liu, Ana Lara-Lopez, Rebecca Asch, Jesse Powell, Andrew King, Brian Hopkinson, Brian Seegers, Ryan Rykaczewski, Chelsea Rochman, Andrew Titmus, Josh Jones, Jared Cox, Ioana Ionescu,

Lilian Carswell, Lara Dickens, Darcy Taniguchi, Marco Hatch, Emy Daniels, Meg Rippy, Moira Decima, Mike Stukel, Rosalie Raymond, Brian Overcash, Dave Jensen, Sara, Haili Wang, Jim Dorrance, Matt Durham, Gus Aprans, Megan Donohue, Karin Malmstrom, Mario Aguilera, Doug Woodring, and Timbo Stillinger. Andrey Suntsov, assisted by Jason Blackburn and Shannon Lyday, led the trawling effort for two legs of the ORCAWALE cruise while I was on the LTER cruise.

I borrowed gear and chemicals from Dave Checkley, Tony Koslow, Jay Hildebrand, Dave Griffith, George Watters, the Pelagic Invertebrate Collection, and the Marine Vertebrate Collection. Shonna Dovel and Megan Roadman taught me how to set up a wet lab preservation station and provided much help along the way. Cindy Klepadlo and HJ Walker from the Marine Vertebrate Collection provided training, identification keys, storage shelves, and lab space in return for over 40,000 dead fishes. I hope they were enough. Some fishes were donated from zooplankton nets by Miriam Goldstein, Moira Decima, Jesse Powell, Mark Ohman, and Ryan Rykaczewski.

My fellow BO students made classes and research fun here at SIO, especially the 2004 cohort of Pincelli Hull, Kate Hanson, Jenny Prairie, Mike Stukel, and Moira Decima. I look forward to following their future careers. I could not have asked for better office-mates than Ryan Rykaczewski and Jesse Powell, both of whom helped me repair formaldehyde carboys at sea. We will now live forever, or at least never decompose. I had many interesting discussions with Rebecca Asch, Ana Lara-Lopez, and Miriam Goldstein, although usually not about the same sort of things.

There are many stellar lecturers here at SIO, who literally taught me everything that I know about the ocean. In particular Lisa Levin, Ken Smith, Mark Ohman, Dave

Checkley, Nick Holland, Myrl Hendershott, Peter Franks, Jules Jaffe, and Phil Hastings taught memorable classes. And finally, who can forget the day when Jeff Graham blew my mind in a lecture by informing me that my pet catfish (*Corydoras* sp.) possessed an air-breathing surface in its posterior intestine? I still don't know how I failed to observe that in high school.

While I was a student at SIO I married and had two children. My degree would not be possible without their support and sacrifice, especially that of my wife Lisa. I was at sea for the last four months of her first pregnancy, and she was still here when I returned. This was not permitted for the second pregnancy, but I remain indebted to her for life. I would also like to acknowledge my parents, Richard and Barbara Davison, who did not even try to talk me out of leaving a good job to become an oceanographer.

Chapter 2, in full, is a reprint of the material as it appears in ICES Journal of Marine Science 68 (10), 2064-2074, Davison, P., 2011. The dissertation author was the primary investigator and author of this paper.

Chapter 3, in full, has been submitted for publication of the material as it may appear in the Journal of the Acoustical Society of America, Davison, P., Lara-Lopez, A., and Koslow, J.A., 2011. The dissertation author was the primary investigator and author of this paper.

Chapter 4, in full, is currently being prepared for submission for publication of the material. Davison, P.C., Checkley, D.M., Koslow, J.A., and Barlow, J. The dissertation author was the primary investigator and author of this paper.

VITA

1987	Bachelor of Science, Electrical Engineering, University of Illinois, Champaign-Urbana
1988-1989	National Semiconductor Corporation
1990	Master of Science, Computer Engineering, University of Wisconsin, Madison
1990-2004	Intel Semiconductor Corporation
2004-2011	Graduate student researcher, University of California, San Diego, Scripps Institution of Oceanography
2007	Teaching assistant, "The Oceans," University of California, San Diego
2011	Doctor of Philosophy, Oceanography, University of California, San Diego

PUBLICATIONS

"The specific gravity of mesopelagic fishes from the Northeast Pacific Ocean and its implications for acoustic backscatter", Davison, P., ICES Journal of Marine Science 68(10): 2064-2074, 2011.

"Plastic ingestion by mesopelagic fishes in the North Pacific Subtropical Gyre", Davison, P., Asch, R.G., Marine Ecology Progress Series 432: 173-180, 2011.

Review of J.P. Kritzer and P.F. Sale, Marine Metapopulations (2006), Benham, C., Cawood, A.M., Cook, G.S., Darnell, A., Davison, P.C., Goldstein, M.C., Johnson, A.E., Konotchick, T., Maldonado, E.M., Pasulka, A.L., Prairie, J.S., Moseman, S.M., Tai, V., Tanner, C.A., Vardi, T., Whitty, T.S., Levin, L.A., Marine Ecology 29(2): 319-320, 2008.

"Design and evaluation of a COBIST RISC processor", Davison, P.C., unpublished thesis, University of Wisconsin-Madison, 1990.

ABSTRACT OF THE DISSERTATION

The Export of Carbon Mediated by Mesopelagic Fishes in the Northeast Pacific Ocean

by

Peter Charles Davison

Doctor of Philosophy in Oceanography

University of California, San Diego, 2011

Professor David M. Checkley, Jr., Chair

Mesopelagic fishes are under-studied in relation to their importance in pelagic ecosystems. Traditional sampling methods (trawls and acoustic surveys) are biased, yet synergistic, and it has become clear in recent decades with the increased use of acoustic methods that the biomass of mesopelagic fishes is larger than thought from net sampling. For this research, I investigated the importance of mesopelagic fishes to the biogeochemical flux of carbon in the northeast Pacific Ocean. Calculation of the fluxes mediated by mesopelagic fishes requires an estimate of their abundance, and to this end I developed a new technique using combined trawl and acoustic data. The interpretation of acoustic data requires knowledge regarding the acoustic properties of fishes, and thus I made basic measurements on over 70 species of mesopelagic fishes.

My results indicated that two of the major determinants of the acoustic reflectivity of a fish, body density and swimbladder inflation, vary both between and within species.

Mesopelagic fishes were less dense than epipelagic fishes, and those that did not have inflated swimbladders as adults had decreased body density with increased length.

Acoustic models of captured mesopelagic fishes were used with inverse modeling of multi-frequency acoustic data to estimate the capture efficiency of the Matsuda-Oozeki-Hu trawl (MOHT). Capture efficiency of the MOHT was estimated to be 14% for mesopelagic fishes.

Trawl data, corrected for efficiency of capture, were used to estimate mesopelagic fish biomass at 77 stations in the northeast Pacific Ocean. The export of carbon out of the epipelagic ocean mediated by those fishes ("fish export") was estimated using individual-based metabolic modeling and extrapolated over the study area. Fish export was estimated to be 17% of total carbon export, estimated from satellite data, in the study area. Fish export varied spatially in both magnitude and relative importance. Although overall fish export increased with total export, its fraction of the total export decreased. Fish export exceeded 40% of the total carbon export in the oligotrophic North Pacific Subtropical Gyre. Because subtropical gyres comprise over half of the surface area of the global ocean, mesopelagic fishes are of global biogeochemical importance.

Chapter 1. Introduction

1.1. Background

Mesopelagic fishes are ubiquitous in the open ocean, and they are found in all ocean basins (Gjosaeter and Kawaguchi, 1980). They are dominated numerically by fishes from the families Myctophidae and Gonostomatidae, although other families are of regional importance (Gjosaeter and Kawaguchi, 1980). Myctophids, Bathylagids, Gonostomatids, Phosichthids, and Sternoptychids are chiefly zooplanktivorous, whereas the Stomiids are predominantly piscivorous (Borodulina, 1972; Clarke, 1982). Most of these fishes are <10 cm in length and, with some invertebrates, they belong to a class of moderately-sized and weakly-swimming animals referred to as micronekton.

"Mesopelagic," or "midwater," refers to the depths at which these fishes live. It is the ocean twilight zone located between the well-lit epipelagic euphotic zone, that can support phytoplankton, and the completely dark bathypelagic zone, in which sunlight is totally absent. The mesopelagic is conventionally defined as the depth range of 200-1000 m (Gjosaeter and Kawaguchi, 1980). It is the depth range of the permanent thermocline, in which temperature decreases from ~10°C at 200 m to ~4°C at 1000 m depth (northeast Pacific Ocean). Although sunlight is detectable in the mesopelagic, it is nonetheless very dark there. The animals that inhabit this depth range exhibit a wide variety of adaptations to the low-light environment including enlarged telescopic eyes and the ability to generate their own light (bioluminescence). The release from intense visual predation has lessened the selective pressure for fast swimming (Childress *et al.*, 1980), which has allowed flexibility in body form and composition in comparison to open-ocean epipelagic

fishes. The exotic morphological forms of mesopelagic fishes have inspired colorful common names such as "lanternfishes" (Myctophidae), "hatchetfishes" (Sternoptychidae), "bristlemouths" (Gonostomatidae), and "dragonfishes" (Stomiidae).

The mesopelagic zone is food-poor. Almost all food (carbon) is ultimately derived from autotrophs in the epipelagic zone, and the concentration of both animal biomass and sedimentary carbon decreases exponentially with depth (Angel and Baker, 1982; Martin *et al.*, 1987; Robinson *et al.*, 2010). As a behavioral response to the collocation of food and predation risk, many of these fishes ascend to the surface at night to feed and return to depth before dawn to avoid visual predators (Longhurst, 1976). This daily movement is referred to as diel vertical migration (DVM) and this behavior is common in a wide array of deep-living taxa. As a strategy for avoiding predation, DVM appears to "work." The biomass of mesopelagic fishes is several times that of epipelagic fishes, and the epipelagic and mesopelagic food chains appear to be largely separate (Clarke, 1973; Mann, 1984; Sutton and Hopkins, 1996). Diel horizontal migration has been observed near the Hawaiian coast, presumably in response to a horizontal collocation of food and visual predation risk (Benoit-Bird and Au, 2006; Benoit-Bird *et al.*, 2001). The daily movements of these animals have often been studied acoustically, and they have been described in those terms. Mesopelagic fishes inhabit and, with other midwater taxa, form the acoustic deep scattering layer (DSL). The DSL is a general term for what are usually several acoustic layers of animals present at daytime depths between 75 and 1000m. These layers can be observed to ascend to the surface at dusk and to descend to depth again before dawn, often in complex patterns (Figure 1.1). The animals in the DSL do not appear to form large single-species aggregations in the northeast

Pacific Ocean, and trawls often capture several dozen different species of fishes and large invertebrates.

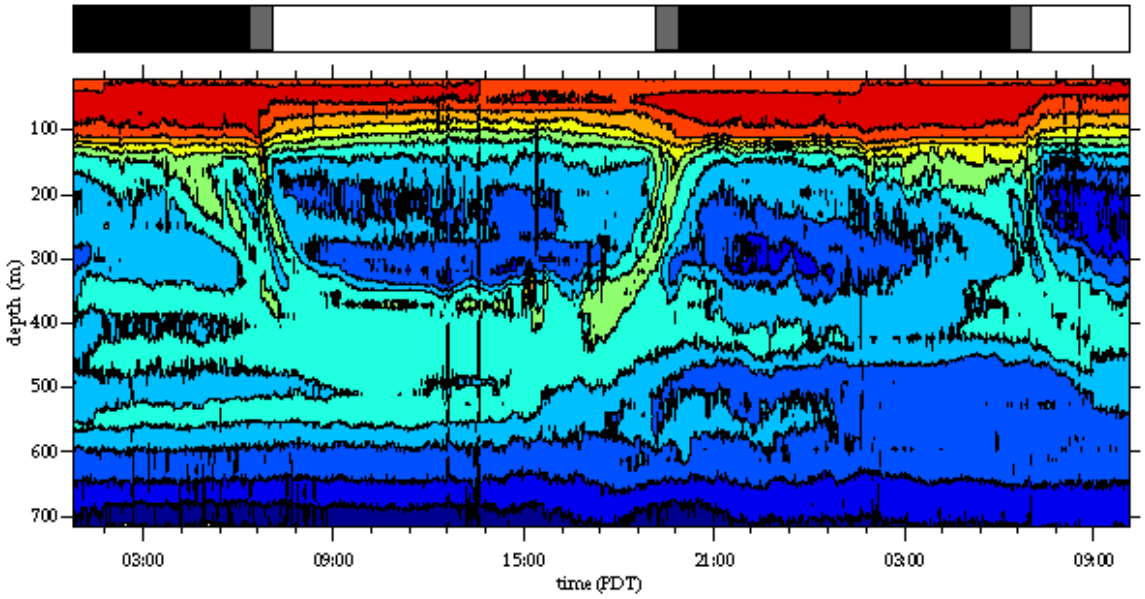

Figure 1.1. Diel vertical migration of the deep scattering layer as observed with an acoustic doppler current profiler (48 kHz, R/V "Roger Revelle", Equatorial Pacific, September 2005). Red is greater and blue lesser intensity. Periods of darkness (black) and daylight (white) are shown in the top bar.

Abundance (ind. m^{-2}) and biomass (g m^{-2}) are fundamental properties of a population required by ecologists for many purposes. The two most common methods used to estimate the abundance of mesopelagic animals are trawling and acoustic surveys. Both of these methods are biased, yet they are complementary. Trawling suffers from net avoidance, poor depth and horizontal resolution, and high effort, but offers taxonomic certainty of the catch and the ability to sample to any depth. Acoustic data have no avoidance bias, fine horizontal and vertical resolution, and can be collected underway with little effort, but suffer from crude taxonomic resolution, blind zones, and limited

sampling depth at high frequencies. Acoustic estimates of abundance are higher than those made from trawls (Kloser *et al.*, 2009; Lawson *et al.*, 2008). Nets are known to undersample abundance, often by approximately an order of magnitude, due to escapement and avoidance by animals (summarized in Chapter 3). Escapement refers to the loss of captured animals through the net mesh, and avoidance results from the ability of animals to swim out of the path of the net. These biases are avoided with acoustic sampling, however the mixing of species in an ensonified water volume makes the interpretation of acoustic data difficult. Multi-frequency acoustic data allow separation of animals with different acoustic properties (such as size or the presence of a gas inclusion) using mathematical inverse methods (Greenlaw, 1979; Holliday and Pieper, 1995), but the categorization is still crude in comparison to taxonomic data from a trawl. The best estimates of mesopelagic fish abundance are made with both nets and trawls, using one method to inform the other.

Enough estimates of biomass have been made, over a wide enough area, to attempt a world-wide synthesis (Gjosaeter and Kawaguchi, 1980), although many regions remain poorly-studied. Gjosaeter and Kawaguchi (1980) estimate the world-wide biomass of mesopelagic fishes to be approximately one billion tons (1 Pg; ~3 g m^{-2}). Since this estimate was largely based upon trawl data, it is likely to be underestimated by a factor of 5-10. For comparison, the world-wide catch by fishermen is less than 0.09 billion tons (including invertebrates; Jennings *et al.*, 2001). This is an astounding quantity of mesopelagic fishes, and anything that they collectively do is likely to be important.

Two such collective activities are the ingestion and release of carbon. In conjunction with the behavior of DVM, mesopelagic fishes have been hypothesized to actively transport material from the epipelagic to the mesopelagic in the forms of excretion, respiration, and mortality (Angel, 1984; Childress and Thuesen, 1992). This active transport of material from the epipelagic to below 150 m depth is thought to completely bypass sediment traps placed at the base of the euphotic zone and other common methods for measuring the flux of material out of the epipelagic (Angel, 1984; Childress and Thuesen, 1992; Fowler and Knauer, 1986). To date, the contribution of mesopelagic fishes to the export of material from the epipelagic has only been studied at a few point locations (Hidaka *et al.*, 2001; Williams *et al.*, 2001).

1.2. Outline of the dissertation

The chapters in this dissertation are arranged in a logical order towards testing my ultimate hypothesis that the export of carbon from the epipelagic mediated by mesopelagic fishes forms a significant portion of the total carbon exported from the epipelagic in the northeast Pacific Ocean. I collected trawl and acoustic data on six research cruises (2008-2010) that spatially covered the entire California Current (U.S.A.). I also sampled the North Pacific Subtropical Gyre (NPSG) on one of those cruises at approximately 33°N 140°W. My study area is bounded at latitudes 30°N, 48°N, longitude 141°W, and by the 200 m isobath of the U.S.A. western coast (~3.3 million km^2).

Mesopelagic fishes are known to differ in acoustic reflectivity both within and between species (Yasuma *et al.*, 2003; Yasuma *et al.*, 2010). Two major properties

governing the acoustic target strength (*TS*) of a fish are the body density and presence of an inflated swimbladder. In Chapter 2, I present data on the ontogenetic changes in body density and swimbladder inflation for over 70 species of mesopelagic fishes from the northeast Pacific Ocean. Those species that have functional swimbladders when large maintain constant body density with increasing body size. Species without functional swimbladders as adults have decreasing body density with increasing body size. I developed acoustic models of mesopelagic fishes, and explored the effect of the observed variation in acoustic properties on *TS*.

Nets are known to undersample mesopelagic micronekton due to the processes of avoidance and escapement (summarized in Chapter 3). We collected concurrent four-frequency acoustic data and midwater trawls at 16 stations off of Point Conception in the California Current Ecosystem (CCE), created acoustic models for each animal captured by the trawl, and then assigned animals to three acoustic groups based upon the shape of the frequency response of their *TS*. The mean group spectra were used with non-negative least squares inverse methods to estimate the acoustic abundance of each group. I estimated the mean capture efficiency of the trawl to be 14% for mesopelagic fishes with inflated swimbladders, and assume that is also representative of the fishes without inflated swimbladders.

In Chapter 4, I estimated the export of carbon out of the epipelagic ocean mediated by mesopelagic fishes ("fish export") with individual-based metabolic modeling of the catch (corrected for capture efficiency) from 77 mesopelagic trawls distributed over the study area. Fish biomass is significantly related to annual net primary productivity estimated from satellite data. I then compared the estimated fish export to

total carbon export estimated from satellite data. I found fish export to vary spatially in both magnitude and relative importance. Although overall fish export increased with total export, its fraction of the total export decreased. Fish export exceeded 40% of the total carbon export in the oligotrophic NPSG, but forms <10% of the total export in the most productive waters of the CCE. Because subtropical gyres comprise over half of the surface area of the global ocean, I conclude that the importance of mesopelagic fishes to global biogeochemistry is greater than previously thought.

1.3. References

Angel, M.V., 1984. Detrital organic fluxes through pelagic ecosystems. In: Fasham, M.J.R. (Ed.), Flows of energy and materials in marine ecosystems, theory and practice. Plenum Press, New York, pp. 475-516.

Angel, M.V., Baker, A.de C., 1982. Vertical distribution of the standing crop of plankton and micronekton at three stations in the Northeast Atlantic. Biological Oceanography 2 (1), 1.

Benoit-Bird, K.J., Au, W.W.L., 2006. Extreme diel horizontal migrations by a tropical nearshore resident micronekton community. Marine Ecology Progress Series 319, 1-14.

Benoit-Bird, K.J., Au, W.W.L., Brainard, R.E., Lammers, M.O., 2001. Diel horizontal migration of the Hawaiian mesopelagic boundary community observed acoustically. Marine Ecology Progress Series 217, 1-14.

Borodulina, O.D., 1972. The feeding of mesopelagic predatory fish in the open ocean. Journal of Ichthyology 12, 692-703.

Childress, J.J., Taylor, S.M., Cailliet, G.M., Price, M.H., 1980. Patterns of growth, energy utilization and reproduction in some meso- and bathypelagic fishes off southern California. Marine Biology 61 (1), 27-40.

Childress, J.J., Thuesen, E.V., 1992. Metabolic potential of deep-sea animals: regional and global scales. In: Rowe, G.T., Pariente, V. (Eds.), Deep-sea food chains and

the global carbon cycle (proceedings of the NATO Advanced Research Workshop, April 1991). Kluwer Academic Press, Boston, pp. 217-236.

Clarke, T.A., 1973. Some aspects of the ecology of lanternfishes (Myctophidae) in the Pacific Ocean near Hawaii. Fishery Bulletin 71 (2), 401-434.

Clarke, T.A., 1982. Feeding habits of stomiatoid fishes from Hawaiian waters. Fishery Bulletin 80 (2), 287-304.

Fowler, S.W., Knauer, G.A., 1986. Role of large particles in the transport of elements and organic compounds through the oceanic water column. Progress in Oceanography 16 (3), 147-194.

Gjosaeter, J., Kawaguchi, K., 1980. A review of the world resources of mesopelagic fish. FAO Fisheries Technical Paper 193, 1-151.

Greenlaw, C.F., 1979. Acoustical estimation of zooplankton populations. Limnology and Oceanography 24 (2), 226-242.

Hidaka, K., Kawaguchi, K., Murakami, M., Takahashi, M., 2001. Downward transport of organic carbon by diel migratory micronekton in the western equatorial Pacific: its quantitative and qualitative importance. Deep-Sea Research 48 (8), 1923-1939.

Holliday, D.V., Pieper, R.E., 1995. Bioacoustical oceanography at high frequencies. ICES Journal of Marine Science 52 (3-4), 279-296.

Jennings, S., Kaiser, M.J., Reynolds, J.D., 2001. Marine fisheries ecology. Blackwell Publishing, Oxford.

Kloser, R.J., Ryan, T.E., Young, J.W., Lewis, M.E., 2009. Acoustic observations of micronekton fish on the scale of an ocean basin: potential and challenges. ICES Journal of Marine Science 66 (6), 998-1006.

Lawson, G.L., Wiebe, P.H., Stanton, T.K., Ashjian, C.J., 2008. Euphausiid distribution along the Western Antarctic Peninsula - Part A: Development of robust multi-frequency acoustic techniques to identify euphausiid aggregations and quantify euphausiid size, abundance, and biomass. Deep-Sea Research II 55 (3-4), 412-431.

Longhurst, A.R., 1976. Vertical migration. In: Cushing, D.H., Walsh, J.J. (Eds.), The ecology of the sea. Blackwell, Oxford, pp. 116-137.

Mann, K.H., 1984. Fish production in open ocean ecosystems. In: Fasham, M.J.R. (Ed.), Flows of energy and materials in marine ecosystems. Plenum Press, New York, pp. 435-458.

Martin, J.H., Knauer, G.A., Karl, D.M., Broenkow, W.W., 1987. VERTEX: carbon cycling in the northeast Pacific. Deep-Sea Research 34 (2), 267-285.

Robinson, C., Steinberg, D.K., Anderson, T.R., Aristegui, J., Carlson, C.A., Frost, J.R., Ghiglione, J.F., Hernandez-Leon, S., Jackson, G.A., Koppelmann, R., Queguiner, B., Ragueneau, O., Rassoulzadegan, F., Robison, B.H., Tamburini, C., Tanaka, T., Wishner, K.F., Zhang, J., 2010. Mesopelagic zone ecology and biogeochemistry - a synthesis. Deep-Sea Research II 57 (16), 1504-1518.

Sutton, T.T., Hopkins, T.L., 1996. Trophic ecology of the stomiid (Pisces: Stomiidae) fish assemblage of the eastern Gulf of Mexico: Strategies, selectivity and impact of a top mesopelagic predator group. Marine Biology 127 (2), 179-192.

Williams, A., Koslow, J.A., Terauds, A., Haskard, K., 2001. Feeding ecology of five fishes from the mid-slope micronekton community off southern Tasmania, Australia. Marine Biology 139 (6), 1177-1192.

Yasuma, H., Sawada, K., Olishima, T., Miyashita, K., Aoki, I., 2003. Target strength of mesopelagic lanternfishes (family Myctophidae) based on swimbladder morphology. ICES Journal of Marine Science 60 (3), 584-591.

Yasuma, H., Sawada, K., Takao, Y., Miyashita, K., Aoki, I., 2010. Swimbladder condition and target strength of myctophid fish in the temperate zone of the Northwest Pacific. ICES Journal of Marine Science 67 (1), 135-144.

Chapter 2. The specific gravity of mesopelagic fish from the northeastern Pacific Ocean and its implications for acoustic backscatter

ICES Journal of Marine Science (2011), 68(10), 2064–2074. doi:10.1093/icesjms/fsr140

The specific gravity of mesopelagic fish from the northeastern Pacific Ocean and its implications for acoustic backscatter

Peter Davison

Scripps Institution of Oceanography, University of California at San Diego, 9500 Gilman Drive, La Jolla, CA 92093-0208, USA; tel: +1 858 5344697; e-mail: pdavison@ucsd.edu

Davison, P. 2011. The specific gravity of mesopelagic fish from the northeastern Pacific Ocean and its implications for acoustic backscatter. – ICES Journal of Marine Science, 68: 2064–2074.

Received 8 February 2011; accepted 7 July 2011; advance access publication 2 September 2011.

Knowledge of the species present, their morphology, and their size distribution is required to infer biomass from acoustic surveys of fish. The gas content and specific gravity of the body (with gas removed), ρ_f, was measured for 71 species of mesopelagic fish in the NE Pacific Ocean. Those species that have functional swimbladders when large maintain constant ρ_f with increasing body size. Species without functional swimbladders as adults show decreased ρ_f with increasing body size. The acoustic-backscattering cross-section, σ_{bs}, was modelled for all individuals collected from three fish species that differed in the presence of a gas-filled swimbladder. The change in σ_{bs} with increasing body size was markedly different between the three. The low body density of those mesopelagic fish without gas-filled swimbladders greatly reduces their σ_{bs}. In species of fish that possess a functional swimbladder as juveniles and in which the swimbladder regresses with growth, the σ_{bs} first decreases, then increases with increased body size. Knowledge of the ontogenetic changes in swimbladder inflation and body density in mesopelagic fish is critical for the construction of the backscattering models used to interpret acoustic surveys.

Keywords: acoustic backscatter, buoyancy, density, mesopelagic fish, swimbladder.

Introduction

Mesopelagic fish are ubiquitous in the world's oceans and are the most abundant vertebrates on earth (Mann, 1984), with an estimated biomass of a billion tonnes (Gjosæter and Kawaguchi, 1980). They are a major component of the acoustic deep-scattering layer (Hersey *et al.*, 1962; Mann, 1984). The sheer numbers of mesopelagic fish make them ecologically important predators and prey, occupying mid-trophic levels (Mann, 1984; Beamish *et al.*, 1999). Mesopelagic fish inhabit depths between 200 and 1000 m by day, and many migrate vertically to the euphotic zone at night to feed (Gjosæter and Kawaguchi, 1980). In mesopelagic fish, diel vertical migration (DVM) is a common behaviour that develops in response to the collocation of food supply and visual predation pressure near the sea surface (Marshall, 1960; Robison, 2003). Their daily vertical movement is often several hundred metres (Pearcy *et al.*, 1977; Karnella, 1987), and it is physiologically difficult for any fish to maintain a gas-filled swimbladder over the pressure changes associated with DVM (Marshall, 1960; D'Aoust, 1971; Alexander, 1972). As the presence and size of a gas inclusion affects the acoustic properties of a fish, the means by which mesopelagic fish maintain buoyancy over their full vertical range are of consequence to fisheries acousticians and acoustic oceanographers.

Acoustic surveys are commonly used to estimate the abundance of fish (Simmonds and MacLennan, 2005). Estimates so derived are critically dependent on the assumed or measured target-strength (*TS*) distribution of the surveyed population or community (Simmonds and MacLennan, 2005). The *TS* (dB re 1 m^2) is the logarithmic form of the acoustic-backscattering cross-section (σ_{bs}, m^2), and the two variables are related by the equation $TS = 10\log_{10}(\sigma_{bs})$ (Simmonds and MacLennan, 2005). Models of the form $TS = m\log_{10}(L_S) + b$ are often used to describe the expected backscatter from a fish, where L_S is the standard length of a fish, and m and b are species-specific constants (Simmonds and MacLennan, 2005). The appropriate *TS* selection is complicated by the diversity of species present, the size distribution of animals, and the orientation of the fish relative to the transducer (Simmonds and MacLennan, 2005). In particular, the presence or the absence of gas in the swimbladder is important, because the gas inclusion is responsible for some 90–95% of the σ_{bs} of a fish (Foote, 1980). Partitioning of measured acoustic backscattering within and between the species that constitute the deep scattering layer requires the use of nets to assess the species present and their size distribution for comparison with acoustic data collected simultaneously (McClatchie *et al.*, 2000; Simmonds and MacLennan, 2005). This remains one of the most common methods of interpreting acoustic data from mixed aggregations such as the deep scattering layer, although the nets used to sample and quantify the targeted assemblage are subject to significant escapement and avoidance biases (Koslow *et al.*, 1997; McClatchie *et al.*, 2000).

Mesopelagic fish may have an extreme departure from length-based *TS* models because of ontogenetic changes in swimbladder morphology and body density. They reduce visual predation risk through occupation of a low-light environment (Mann, 1984). The release from visual predation allows them to optimize buoyancy and metabolic costs through the reduction in dense muscle tissue (Childress *et al.*, 1980). Many fish species accumulate

low-density fluids or lipids as they grow, decreasing their overall body density (Butler and Pearcy, 1972). Other mesopelagic species have negatively buoyant gelatinous tissue (Yancey *et al.*, 1989). The reduction in body density decreases the density contrast with surrounding seawater and hence decreases the acoustic reflectivity of the fish. Some species that have gas in their swimbladder as juveniles do not possess it as adults, and other species vary individually in the presence of a gas-filled swimbladder (Butler and Pearcy, 1972; Neighbors, 1992; Yasuma *et al.*, 2010). Some fish may allow the volume of gas to change over the course of DVM in accordance with Boyle's law, whereas others may maintain a constant gas volume (Hersey *et al.*, 1962; Kalish *et al.*, 1986). Knowledge of variations in body density and gas content within and between species is required before the construction of accurate acoustic models is possible.

As a consequence of the lack of data on the body density of midwater fish, assumptions need to be made to construct acoustic models. The typical body density of an epipelagic fish is 1.076 g ml^{-1} (Taylor, 1921). Several investigations of the buoyancy of mesopelagic fish have found body density to be considerably lower than that of epipelagic fish (Capen, 1967; Butler and Pearcy, 1972; Johnson, 1979; Neighbors and Nafpaktitis, 1982; Yasuma *et al.*, 2006). Unfortunately, just a few species have been subject to such study from the speciose mesopelagic community.

To address some of the issues listed above, this study looked at the specific gravity and swimbladder inflation of some of the species making up the mesopelagic fish communities of two biogeographic provinces in the North Pacific (the California Current and the North Pacific Subtropical Gyre). Three hypotheses were tested: first, that mesopelagic fish have a lower ρ_f than epipelagic fish; second, that fish with functional swimbladders exhibit a constant ρ_f with growth; and third, that the ρ_f of fish species without functional swimbladders decreases with increased size. The implications of these results for the acoustic backscattering from mesopelagic fish were then investigated.

Material and methods

Mesopelagic fish were collected in 2009 and 2010 on three cruises of the RV "New Horizon" and one cruise of the National Oceanic and Atmospheric Administration (NOAA) FSV "Bell Shimada" in the North Pacific (Supplementary Figure S1). All four cruises sampled the California Current off southern California, and one cruise sampled the North Pacific Subtropical Gyre. Fish were captured using midwater trawls, bongo nets, manta nets, and dipnets. Midwater trawls were the main collection method, and 31 were made (Supplementary Table S1, Figure S1). The other nets were used in conjunction with them. Fish were separated from zooplankton within an hour of capture. A subset of the fish catch was then set aside in an ice bath for analysis, which took place within 8 h of capture.

Laboratory measurements

The specific gravity (density relative to freshwater, dimensionless) of fish, ρ_f, was measured by immersion in dense fluids after removal of any gas from the swimbladder. Seawater and glycerine solutions were prepared in 0.0025 increments of specific gravity over the range 1.025–1.090, although most measurements were only made to a precision of 0.005. The specific gravity of each solution was measured periodically with a hydrometer to 0.0005 precision and accuracy, and adjusted when necessary. Variation in specific gravity from dilution or evaporation was never more than ± 0.001. The fish selected for analysis were immersed in room temperature seawater for at least 5 min to equilibrate the temperatures of the fish and glycerine solutions. Room temperature varied between 17 and 24°C over all four cruises. The seawater density change resulting from a 7°C room temperature range is <0.002 g ml^{-1} (Pilson, 1998). The effect of temperature on the density of fish tissue is unknown, but was presumed to be similar to that of seawater. Measurements of ρ_f were neither corrected for temperature variation nor converted to density.

The L_S of each fish was measured to the nearest millimetre. Fish were dissected in seawater under a dissecting microscope to remove any gas from the swimbladder before measurement of ρ_f. The diameter of gas bubbles released from the body cavity during dissection was measured with the ocular micrometer of the microscope. If the swimbladder was not ruptured, the lengths and widths of visible gas bubbles were measured before puncturing the swimbladder. Gas volume was then calculated using the formula for a prolate spheroid: $V = (4/3)\pi ab^2$, where a and b are the major and the minor axis radii, respectively (Capen, 1967). In cases where the gas was released too quickly for measurement, it was simply recorded as present. Volume was then transformed to an equivalent spherical radius (ESR). Transparent fish with no visible gas bubble and opaque fish from taxa with no functional swimbladder at the family level (Stomiidae, Bathylagidae, Alepocephalidae, Platytroctidae, and Notosudidae) were not dissected. Fish with visible damage to the body wall that could have resulted from the escape of gas were recorded as ruptured. Once gas was released from the body cavity, the fish were placed progressively in graduated cylinders containing solutions of different specific gravity to find the highest specific gravity of sinking and the lowest specific gravity of floating. These were recorded as the same if the fish was neutrally buoyant in a cylinder. ρ_f was calculated as the mean of the two measurements. Care was taken to exclude all gas bubbles from the interior and exterior of the fish. After ρ_f measurement, each fish was blotted, then frozen in preweighed plastic bags. Ashore, the bags were weighed and the wet weight of the fish determined by subtracting the weight of the empty bag.

Data analysis

All fish species with a sample size, n, of three or more were included in the data analysis. A decrease in ρ_f with increasing L_S was tested for each species using Kendall's coefficient of rank correlation (τ), with a one-way significance level (p) of 0.05. The parameter τ is not reported for species with three individuals, because the test cannot be significant ($p \leq 0.05$) at that n. Wet weight (W_W) and ρ_f were then standardized within each species to W'_W and ρ'_f using the following equations to allow grouping of data from species of differing size and specific gravity:

$$W'_W = [W_W - W_W(\min)] \times [W_W(\max) - W_W(\min)]^{-1}, \quad (1)$$

$$\rho'_f = \rho_f - \bar{\rho}_f. \quad (2)$$

W'_W is the wet weight standardized to a range 0–1. $W_W(\min)$ and $W_W(\max)$ are, respectively, the wet weights of the smallest and largest fish within a species. The standardized specific gravity ρ'_f is simply the difference from the species mean specific gravity ($\bar{\rho}_f$). Species were assigned to groups based on the presence of gas in the swimbladders of small and large fish. Large fish are defined for this purpose as those with a $W'_W \geq 0.5$, and small fish as those with $W'_W < 0.5$. Group I species had at least

some small and large individuals with inflated swimbladders. The swimbladders of Group II species contained gas in at least some small fish, but not in large ones. Group III species never had inflated swimbladders. Changes in ρ_f with W'_W were tested statistically at the group level using Spearman's rank order correlation (r_s). The maximum L_S for each species (Table 1) was taken from Scripps Institution of Oceanography (SIO) Marine Vertebrate Collection (MVC) records to assess whether or not the sampled fish were representative of the species size range.

Acoustic modelling

The 38-kHz σ_{bs} was estimated for three species of fish (*Ceratoscopelus warmingii*, *Stenobrachius leucopsarus*, and *Idiacanthus antrostomus* from Groups I, II, and III, respectively) for which a large n and broad L_S range were obtained. σ_{bs} as a function of L_S is assumed to vary similarly within each swimbladder inflation group. Fish bodies were modelled acoustically as a fluid-filled cylinder of the same length, volume, and density of the measured fish, following Stanton (1988). The ρ_f of the fish was used in place of density, because the magnitudes differ by just 0.001 g ml^{-1} for seawater at the reference temperature of the hydrometer (15.6°C; Pilson, 1998). The gas from the swimbladder, when present, was modelled as a gas sphere of radius ESR suspended in seawater (Anderson, 1950; Medwin and Clay, 1997). The σ_{bs} of the modelled body and gas were added to form the overall σ_{bs}. Assumed model parameters included: density of seawater, $\rho_w = 1.027$ g ml^{-1}; speed of sound in seawater, $c = 1490$ m s^{-1}; ratio of sound speed in the fish to that in seawater, $h = 1.020$ (Yasuma *et al.*, 2006); angle of scatter 180° (transmitter and receiver collocated); and tilt-angle 0° (dorsal incidence). The gas inside the swimbladder was assumed to be an ideal gas (air) with a temperature of 10.2°C, pressure $P = 1.05$ atm, ratio of specific heats $\gamma = 1.4$, and a speed of sound, c, given by

$$c = (\gamma P \rho_w^{-1})^{0.5}. \quad (3)$$

Body density and the sound-speed ratio, h, were varied across reasonable values to determine their effect on modelled σ_{bs}. The body density range was taken from the measured ρ_f values in this study, and h was varied between 1.01 and 1.05 (Yasuma *et al.*, 2006).

Neutral buoyancy

The gas volume required for neutral buoyancy, V_G, was calculated for each fish from the species *C. warmingii* (Group I) and *S. leucopsarus* (Group II) with the equation

$$V_G = W_W(\rho_w^{-1} - \rho_f^{-1}). \quad (4)$$

ρ_w was assumed to be 1.027 g ml^{-1}, and the weight of gas in the swimbladder was assumed to be negligible.

Results

Measurements and group assignments

In all, 71 species from 16 families were represented by three or more individuals (Supplementary Table S2). Family Myctophidae was by far the most speciose, being represented here by 28 species. Three epipelagic fish were incidentally captured from two species, *Seriola lalandi* and *Cololabis saira*. These fish ($\rho_f = 1.078$, 1.078, and 1.088; Supplementary Table S3) were not included in the analysis, except in comparison with Group I.

Group assignment, n, L_S range, maximum L_S, vertical migration behaviour, ρ_f, and τ for decreasing ρ_f with increasing L_S are summarized in Table 1 for each of the species analysed. Measurements of ρ_f and the gas volume for all fish are listed in Supplementary Table S3. Fish belonging to each of the three groups were collected from both biogeographic provinces (Supplementary Table S2). Biogeographic province may be related to group assignment, although the relationship is not significant (Chi-squared test of contingency table, d.f. = 2, $p = 0.07$). Diel vertical migrators and non-migrators are found in each of the three groups. DVM is not significantly related to group assignment (Chi-squared test of contingency table, d.f. = 2, $p = 0.46$). No full-sized specimens were captured from several species, as determined by comparison with the maximum L_S of fish in the SIO MVC. These species were allocated to group as described herewith. Species from the Stomiidae, Paralepididae, Alepocephalidae, Notosudidae, Platytroctidae, and Bathylagidae were assigned to Group III, because fish from those families do not have functional swimbladders as adults (Marshall, 1960). *Argyropelecus lychnus* was assigned to Group I because of the presence of a gas-filled swimbladder at the family level (Marshall, 1960). *Notoscopelus resplendens*, *Lampadena urophaos*, *Electrona risso*, *Chilara taylori*, and *Microstoma microstoma* were placed in Group I based on literature reports of the presence of gas in the swimbladders of adults (references in Supplementary Table S4). *Diplospinus multistriatus* and *Lampanyctus tenuiformis* were placed in Group I based on the presence of large, thin-walled swimbladders found in dissected specimens from the SIO MVC. No large *Poromitra crassiceps* were captured. This species was assigned to Group II based on published data indicating that gas is not used for buoyancy (references in Supplementary Table S4).

The specific gravities of species (means of large fish, $\bar{\rho}_{f,l}$) from each group were compared. Groups II and III did not have significantly different mean $\bar{\rho}_{f,l}$ (Mann–Whitney rank-sum test, $p = 0.094$), so were combined for comparison of mean $\bar{\rho}_{f,l}$ to Group I (Table 2). Group I has significantly higher mean $\bar{\rho}_{f,l}$ (t-test, 69 d.f., $p < 0.001$) than the combined Groups II and III. Group I has significantly lower mean $\bar{\rho}_{f,l}$ (Mann–Whitney rank-sum test, $p = 0.027$) than the mean $\bar{\rho}_{f,l}$ of epipelagic fish.

Group I fish do not change in ρ_f with increasing W'_W (Figure 1a; $r_s = -0.044$, $n = 459$, $p = 0.347$). Group II fish decrease in ρ_f with increasing W'_W (Figure 1b; $r_s = -0.747$, $n = 305$, $p < 0.001$), as do Group III fish (Figure 1c; $r_s = -0.403$, $n = 213$, $p < 0.001$).

Group I was the most speciose category (40 species; Table 1) followed by Groups III and II (20 and 11 species, respectively; Table 1). Of the 33 species in Group I with $n > 3$, 30 species exhibited no significant relationship between ρ_f and L_S. In Group II, 9 of the 11 species had a significant decline in ρ_f. The results from Group III were less clear, with just five of 18 species (with $n > 3$) exhibiting a significant decline in ρ_f. However, the declining species included all of those with $n > 12$, and those species with no significant decline included eight for which no large individuals were captured.

Acoustic modelling

The fluid cylinder model was used to estimate σ_{bs} for an elongate dragonfish from Group III, *I. antrostomus*. The frequency response of σ_{bs} was modelled for both the body density of a typical epipelagic fish (1.076 g ml^{-1}) and the measured ρ_f (1.034 ≈ 1.034 g ml^{-1}) for this fish. The 38-kHz σ_{bs} of this fish differs by

Table 1. Assignment of species to groups based on the presence or the absence of gas in their swimbladders.

Species	DVM[a]	*n*	L_S range (mm)	Max. L_S (mm)	$\bar{\rho}_{f,s}$	$\bar{\rho}_{f,l}$	τ-value	*p*-value
Group I								
Tarletonbeania crenularis	y	20	22–57	78	1.080	1.085	0.27	0.939
Hygophum reinhardtii	y	4	19–43	64	1.066	1.076	0.66	0.958
Notoscopelus resplendens	y	5	27–42[b]	98	1.073	1.076	0.84	1.000
Diplospinus multistriatus	y	6	18–55[b]	225	1.073	1.074	0.00	0.572
Diogenichthys atlanticus	y	25	16–23	30	1.064	1.073	0.55	1.000
Myctophum nitidulum	y	17	18–78	105	1.074	1.073	−0.16	0.215
Electrona risso	y	3	11–32[b]	81	1.071	1.073	0.82	–
Hygophum proximum	y	5	16–32	61	1.068	1.073	0.44	0.900
Protomyctophum crockeri	n	26	15–37	55	1.070	1.073	0.21	0.920
Nannobrachium fernae	y	5	32–63	81	1.069	1.073	−0.20	0.408
Lampadena urophaos	y	12	19–26[b]	115	1.060	1.073	0.34	0.925[c]
Bolinichthys longipes	y	4	38–42[d]	59	1.071	1.070	−0.40	0.333[c]
Diaphus anderseni	y	13	25–30	55	1.070	1·070	0.20	0.819[c]
Ceratoscopelus warmingii	y	18	19–48	81	1.064	1·070	0.51	0.997
Vinciguerria nimbaria	y	9	17–32	53	1.067	1.069	−0.21	0.269
Vinciguerria poweriae	y	15	18–38	37	1.069	1.069	0.04	0.601
Diaphus fulgens	y	7	36–52[d]	58	1.073	1.068	−0.69	0.029
Lampanyctus tenuiformis	y	13	28–43[b]	153	1.067	1.067	0.13	0.737
Microstoma microstoma	y	6	20–55[b]	210[e]	1.067	1.067	0.17	0.700
Danaphos oculatus	n	23	22–41	46	1.062	1.066	0.49	0.999
Symbolophorus californiensis	y	20	25–88	116	1.072	1.064	−0.26	0.071
Chilara taylori	n	3	35–55[b]	366	1·060	1.064	0.00	–
Taaningichthys bathyphilus	n	3	42–66[d]	85	1·060	1.063	0.82	–
Argyropelecus lychnus	n	3	13–37[b]	78	1·068	1.063	−0.82	–
Argyropelecus sladeni	n	26	12–41	60	1.062	1.062	0.09	0.727
Argyropelecus hemigymnus	n	17	15–30	38	1.064	1.062	−0.25	0.105
Argyropelecus affinis	n	17	14–76	88	1.055	1.059	0.04	0.604
Bathysphyraenops simplex	y	7	17–47	80[e]	1.075	1.058	−0.13	0.429[c]
Cyclothone pseudopallida	n	12	24–43	49	1.055	1.056	−0.08	0.387
Melamphaes simus	y	5	15–29	29	1.069	1.055	−0.89	0.033
Sternoptyx obscura	n	7	12–41	48	1.054	1.053	0.28	0.810
Sternoptyx diaphana	n	6	14–35	60	1.053	1.053	0.00	0.572
Cyclothone signata	n	36	15–35	39	1.058	1.053	−0.21	0.051
Sternoptyx pseudobscura	n	8	17–44	61	1.052	1.049	0.12	0.696
Diaphus theta	y	32	14–73	86	1.059	1.049	−0.38	0.002
Triphoturus nigrescens	y	4	32–41[d]	45	1.064	1.043	−0.91	0.083[c]
Scopeloberyx opisthopterus	n	3	22–33	39	1.053	1.041	−1.00	–
Notolychnus valdiviae	y	8	13–25	29	1.049	1.040	−0.22	0.287[c]
Melamphaes suborbitalis	n	3	24–68	119	1.069	1.040	−0.33	–
Ichthyococcus irregularis	n	3	24–36	63	1.048	1.038	−1.00	–
Group II								
Melamphaes parvus	y	4	21–45	54	1.071	1.055	−0.33	0.375[c]
Cyclothone atraria	n	10	21–47	70	1.051	1.048	−0.33	0.117
Nannobrachium hawaiiensis	y	22	24–92	111	1.052	1.046	−0.35	0.017
Ceratoscopelus townsendi	y	43	21–60	77	1.063	1.045	−0.49	<0.001
Scopelogadus mizolepis	y	19	25–83	97	1.052	1.044	−0.72	<0.001
Poromitra crassiceps	n	14	20–60[b]	204	1.051	1.044	−0.54	0.006
Nannobrachium ritteri	y	56	19–94	124	1.044	1.032	−0.80	<0.001
Triphoturus mexicanus	y	52	17–68	75	1.040	1.031	−0.75	<0.001
Stenobrachius leucopsarus	y	57	20–83	105	1.035	1.029	−0.74	<0.001
Nannobrachium regale	n	19	23–134	171	1.053	1.029	−0.59	<0.001
Melamphaes lugubris	y	9	22–79	98	1.060	1.029	−0.59	0.019
Group III								
Scopelarchus stephensi	y	3	25–55	62	1.076	1.080	0.33	–
Scopelosaurus harryi	y	5	43–52[b]	266	1.063	1.060	−0.24	0.333[c]
Arctozenus risso	n	6	35–124[b]	255	1.068	1.055	−0.97	0.003
Chauliodus macouni	n	6	30–122	236	1.050	1.050	−0.21	0.356
Aristostomias xenostoma	n	5	33–41[b]	108	1.049	1.050	0.17	0.800[c]
Leuroglossus stilbius	y	6	25–29[b]	130	1.043	1.049	0.08	0. 600[c]
Photonectes parvimanus	y	6	30–67[b]	261[f]	1.046	1.048	0.67	0.983[c]
Holtbyrnia latifrons	n	6	20–52[b]	200	1.051	1.048	−0.26	0.350[c]

Continued

Table 1. *Continued*

Species	DVM[a]	*n*	L_S range (mm)	Max. L_S (mm)	$\bar{\rho}_{f,s}$	$\bar{\rho}_{f,l}$	τ-value	*p*-value
Sagamichthys abei	n	5	27–67[b]	239	1.050	1.048	−0.27	0.400[c]
Alepocephalus tenebrosus	n	4	27–50[b]	448	1.045	1.046	0.18	0.750[c]
Bathophilus flemingi	y	6	34–46[b]	140	1.048	1.046	0.57	0.933[c]
Cyclothone acclinidens	n	44	25–61	67	1.051	1.043	−0.62	<0.001
Cyclothone pallida	n	6	30–68	74	1.046	1.043	0.30	0.833[c]
Bathylagoides wesethi	y	55	24–76	104	1.048	1.041	−0.41	<0.001
Tactostoma macropus	y	4	76–254	344	1.042	1.039	−0.55	0.250[c]
Stomias atriventer	n	4	139–187[d]	243	1.041	1.038	−0.55	0.250[c]
Parvilux ingens	n	6	80–160[d]	204	1.044	1.036	−0.69	0.042
Idiacanthus antrostomus	y	21	58–385	372	1.049	1.036	−0.68	<0.001
Lobianchia gemellarii	y	3	55–65[d]	77	1.043	1.035	−1.00	–
Lipolagus ochotensis	y	12	25–110	119	1.047	1.034	−0.29	0.123[c]

Group I species have at least some small and large individuals with inflated swimbladders. Group II species contain gas in at least some small fish, but not in large individuals. Group III fish never contain gas. Maximum standard length, L_S, is taken from the SIO MVC. $\bar{\rho}_{f,s}$ and $\bar{\rho}_{f,l}$ are the mean specific gravities of fish with normalized wet weight, W'_W, <0.5 and $W'_W \geq 0.5$, respectively. Species are ordered within groups by decreasing $\bar{\rho}_{f,l}$. Kendall's coefficient (τ) tests for association between L_S and decreasing ρ_f (one-tailed).

[a]y, yes; n, no.

[b]No full-sized (>50% of maximum L_S) fish were captured.

[c]Small *n* and clusters of fish in a limited size range may have influenced the result.

[d]No small individuals were captured.

[e]Maximum L_S was taken from sources other than the SIO MVC (Cohen, 1986; Kubota *et al.*, 1991).

[f]Maximum L_S from material examined: Australian Museum AMS I.20315023.

Table 2. The specific gravity of species from each group (means of large fish, $\bar{\rho}_{f,l}$).

Fish group	*n*	Mean $\bar{\rho}_{f,l}$	s.d.
I	40	1.062	0.012
II	11	1.039	0.010
III	20	1.046	0.011
II + III	31	1.044	0.011

a factor of six between these two densities (Figure 2). At this frequency, the backscattering is in the Rayleigh region, because the fish is small compared with the acoustic wavelength, and there are no nearby resonant effects that may influence the result. The σ_{bs} (38 kHz) of this fish was modelled for reasonable variation in body density and sound-speed ratio, h (Figure 3). Body density varied between 1.028 and 1.088 g ml^{-1} and is expressed as the ratio, g, to the density of seawater (1.027 g ml^{-1}). Over this range of g and h, σ_{bs} increases by a factor of 84 from the minimum ($TS = -61.5$ dB re 1 m^2 at low g and h) to the maximum ($TS = -42.3$ dB re 1 m^2 at high g and h).

The 38-kHz σ_{bs} was modelled for each individual fish from the representative species *C. warmingii*, *S. leucopsarus*, and *I. antrostomus* (expressed as *TS*; Figure 4). Gas ESR and ρ_f for each of these three species are also shown in Figure 4. The Group I species, *C. warmingii*, exhibits increasing total σ_{bs} with growth. Total σ_{bs} varies by about an order of magnitude between the smallest and largest fish. The contribution of the body to the overall σ_{bs} is ~0.1% for the smallest fish, increasing to 2.7% for the largest fish. When the *x*-axis of Figure 4b is log-transformed, the relationship between *TS* and L_S becomes linear. A regression of *TS* against $\log_{10}(L_S)$ yields a slope of 24.90 and an intercept of −71.07 (L_S in cm, d.f. = 15, $p < 0.01$, $r^2 = 0.61$; Figure 4b). Use of V_G (Figure 5), rather than the observed gas volume for the *C. warmingii TS* regression, results in a slope and intercept of 22.30 and −68.26, respectively, with an r^2 of 0.97 (d.f. = 17, $p < 0.01$; Figure 4b). The Group II species, *S. leucopsarus*, shows dramatic changes in σ_{bs} with growth. σ_{bs} is high for small fish with gas in their swimbladder, drops more than two orders of magnitude for medium-sized fish, no gas present, and reapproaches the juvenile value in the longest fish. The Group III species, *I. antrostomus*, has a steep increase in σ_{bs} from small to moderate lengths, and a lower rate of increase from moderate to large lengths. A regression of *TS* against $\log_{10}(L_S)$ yields a slope of 50.95 and an intercept of −133.80 (L_S in cm, d.f. = 18, $p < 0.01$, $r^2 = 0.97$; Figure 4f). A 250-mm *I. antrostomus* has a σ_{bs} equivalent to that of a 20-mm myctophid with an inflated swimbladder (*S. leucopsarus* and *C. warmingii* in Figure 4).

Gas required for neutral buoyancy

V_G is ~4% of the total body volume for large *C. warmingii* (Figure 5). For *S. leucopsarus*, V_G starts at 2–3% of body volume for the smallest fish, then drops below 0.5% for individuals of $L_S > 40$ mm (Figure 5). The longest *S. leucopsarus* in which gas was present was 37 mm L_S. The similarity in V_G as a percentage of body volume between small *S. leucopsarus* and *C. warmingii* is a result of the similarity of their relative densities. Intermediate values of ρ_f (~1.050–1.060) were found in the smallest individuals of most myctophid species.

Discussion

Group comparison: relative densities and swimbladder inflation

The presence or the absence of a functional swimbladder in the mesopelagic fish examined in this study is significantly associated with whether or not the ρ_f is reduced by other means. In general, fish species in which some large individuals possess gas-filled swimbladders (Group I) have constant or increasing ρ_f with growth. Fish species without functional swimbladders in large individuals (Groups II and III) have a reduced ρ_f with growth.

The ρ_f values of individual species within Group I are high (Table 1), reflecting a reliance on gas for buoyancy or lift from swimming. Even so, most Group I fish species have a lower ρ_f than do epipelagic fish. In *Melamphaes simus* and *Diaphus theta*, ρ_f decreases significantly with an increasing L_S. These species rely less on gas for buoyancy than other Group I species that

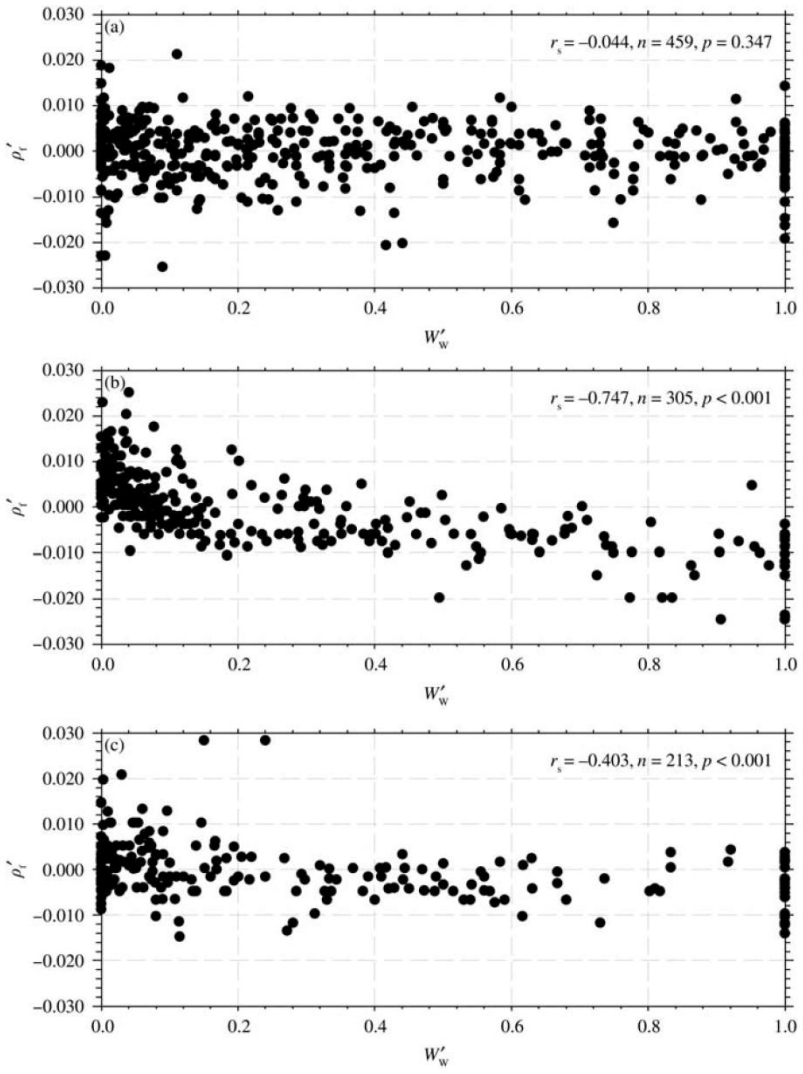

Figure 1. The relationship between standardized specific gravity, ρ', and standardized wet weight, W'_W: (a) Group I, (b) Group II, and (c) Group III fish.

maintain a constant ρ_f with increased size. *Diaphus theta* varies seasonally in lipid content (Neighbors and Nafpaktitis, 1982), so could benefit from the retention of swimbladder function. *Diaphus fulgens* also had significantly decreasing ρ_f with increasing L_S, but because the overall ρ_f range is 0.007 and six of seven fish were within a L_S range of 5 mm, this result may not be representative of this species. *Ichthyococcus irregularis*, *Notolychnus valdiviae*, and *Triphoturus nigrescens* are three other species combining gas with low and apparently decreasing ρ_f with increasing L_S. The low n and narrow L_S distribution of these species limits the power to detect a significant relationship between ρ_f and L_S.

Except *Scopelarchus stephensi*, no Group II or Group III species has a $\bar{\rho}_{f,l} > 1.060$. *Scopelarchus stephensi* would need to be an active swimmer to maintain its place in the water column. Many large individuals of species from Groups II and III have ρ_f values approaching that of seawater. It is possible that $\bar{\rho}_{f,l}$ of some species was overestimated because of a lack of full-sized specimens in the sample. A bias of this nature is conservative and would lead to an overestimation of the slope (less negative) of ρ'_f against W'_W.

Small numbers of large individuals from some species may have resulted in the improper assignment of the species between Groups I and II. Gas was not found in the swimbladders of all fish of similar L_S from many species that use gas for buoyancy. It is possible that gas-filled swimbladders are present in large individuals, but were not detected here. Similarly, the lack of small individuals that may contain gas could have resulted in the incorrect placement of some Group II species into Group III. Only confusion between Groups I and II could have affected the results presented here. The number of individuals from species potentially grouped in error is small compared with the group totals and unlikely to change the results significantly.

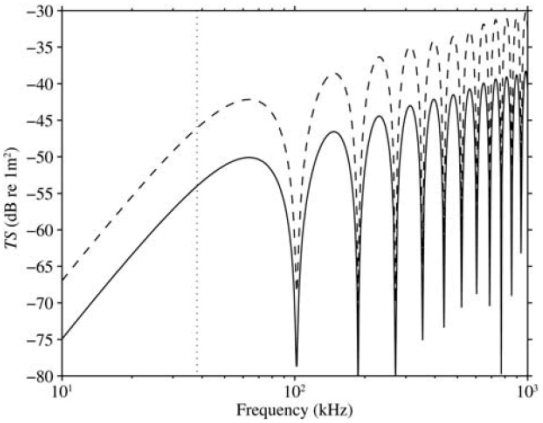

Figure 2. Modelled *TS* as a function of acoustic frequency for a 385 mm, 25.89 g dragonfish (*I. antrostomus*) from Group III. Solid line, measured ρ_f of 1.034 ($\approx$1.034 g ml^{-1}); dashed line, body density 1.076 g ml^{-1}, typical for an epipelagic fish; 38 kHz is marked with a vertical dotted line.

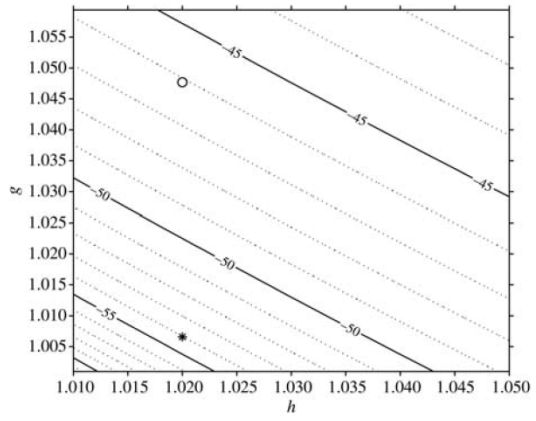

Figure 3. Contour plot of modelled 38 kHz *TS* as a function of the ratio of body density to seawater density, *g*, and the ratio of sound speed in the fish to sound speed in seawater, *h*, for a 385 mm, 25.89 g dragonfish (*I. antrostomus*) from Group III: asterisk, measured ρ_f of 1.034 ($\approx$1.034 g ml^{-1}); open circle, body density 1.076 g ml^{-1}, typical for an epipelagic fish.

A low *n* also affects the power to detect significant relationships. A one-tailed τ-test cannot have a significant *p*-value for $n < 4$. An *n* value of 4 requires perfect rank order for significance. Body density is variable, both from measurement error and individual variation. A group of fish of similar size will show random rank ordering, obscuring the overall pattern if there are few or no points outside of the group. This bias chiefly affects the τ-tests for individual species (Table 1, see footnote c). At the group level, the bias is conservative for Groups II and III. The obfuscation of a true decline in ρ_f in some species with a low *n* is unlikely to affect the overall Group I result, given that it is from 460 fish.

The group assignments of *L. urophaos* (Group I) and *Lobianchia gemellarii* (Group III) are perhaps in error. The *n* for these two species was low, with restricted L_S ranges, limiting the power to detect trends. These two species differ between Atlantic and Pacific populations. Those in the Atlantic Ocean have gas-filled swimbladders of increasing volume with growth consistent with Group I (Bone, 1973; Brooks, 1976; Saenger, 1989). Also consistent with Group I, *L. gemellarii* from the Gulf of Mexico have a low lipid content (Stickney and Torres, 1989). Fish from these species in the Pacific Ocean have high levels of lipid, low body densities, and non-inflated swimbladders when large, consistent with Group II (Neighbors and Nafpaktitis, 1982; Childress *et al.*, 1990). *Lampadena urophaos* has been divided by some authors into Atlantic and Pacific subspecies based on differences in otolith shape and photophores (Wisner, 1976). The apparent developmental differences in buoyancy regulation between Atlantic and Pacific populations of these two species support taxonomic differentiation, so warrant additional investigation.

All three groups contain species that migrate vertically as well as species that are non-migratory. The presence or the absence of gas in large individuals is not significantly related to whether a species migrates vertically, although fish without inflated swimbladders have an energetic advantage and increased potential vertical range over those using gas for buoyancy (Marshall, 1960; Alexander, 1972).

The California Current and North Pacific Subtropical Gyre each contained species from all three groups. Group assignment is not significantly related to biogeographic province, although the significance test is marginal. More Group I and fewer Group II and Group III species are found in the North Pacific Subtropical Gyre than in the California Current. The abundant and lipid-rich Group II myctophid species from the California Current were not common in the North Pacific Subtropical Gyre and were not replaced by other lipid-rich species (Supplementary Tables S2 and S4). Low lipid levels in subtropical fish have been attributed to reduced food levels (Bailey and Robison, 1986) and reduced variability in food supply (Childress *et al.*, 1990).

More than 30 studies have been published on the buoyancy of the fish species discussed here. Supplementary Table S4 summarizes past work for comparison. Only inconsistencies and generalities will be discussed, however, given the large number of species and reports. In general, Group I fish have low lipid content, high body density, and increasing gas volume with increasing L_S. Group II species have low body density, high lipid content, and increasing lipid content with increasing L_S. Group III species have low body density and low lipid content. Three of the Group II species (*Scopelogadus mizolepis*, *P. crassiceps*, and *Cyclothone atraria*) have low lipid content. All these species except *C. atraria*, for which water content is not reported, have water content >85% WW (Childress and Nygaard, 1973) and use dilute body fluids rather than lipids for buoyancy. *Nannobrachium regale* from the western Pacific Ocean are high in lipid (Seo *et al.*, 1996; Saito and Murata, 1998), whereas those from the eastern Pacific have high water content (Butler and Pearcy, 1972; Neighbors and Nafpaktitis, 1982; Bailey and Robison, 1986).

There are four species from Group I (*N. resplendens*, *Myctophum nitidulum*, *L. urophaos*, and *Symbolophorus californiensis*) for which reported body-density measurements are much lower than those measured here (Neighbors and Nafpaktitis, 1982). High lipid levels (Seo *et al.*, 1996; Saito and Murata, 1998) and seasonally high lipid content (Neighbors and Nafpaktitis, 1982) have been reported for *S. californiensis*,

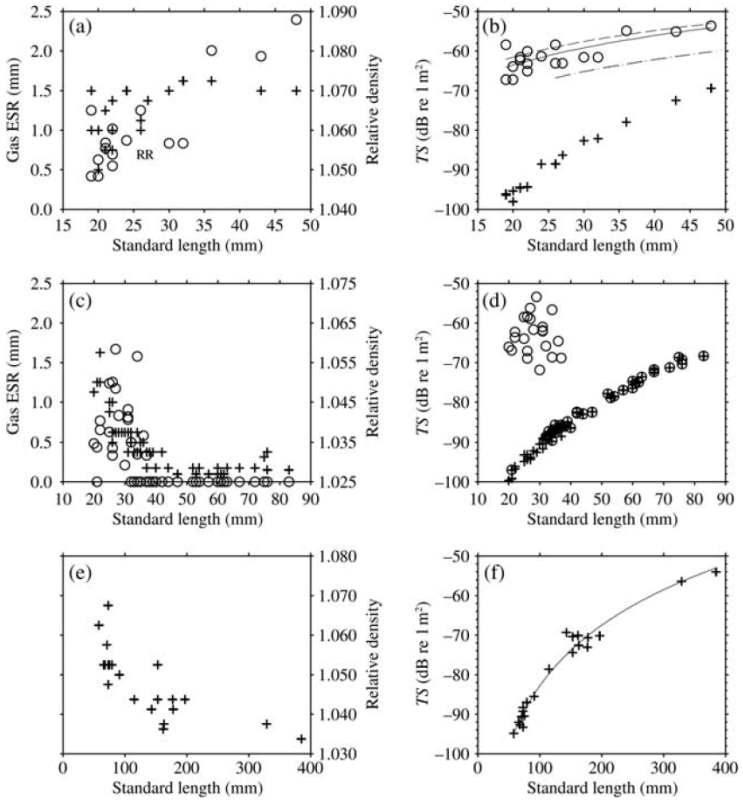

Figure 4. The measured gas ESR (open circle, primary *y*-axis) and body specific gravity, ρ_f, (plus sign, secondary *y*-axis) for individual fish vs. standard length, L_S: (a) *C. warmingii*, Group I; (c) *S. leucopsarus*, Group II; (e) *I. antrostomus*, Group III. The ESR of ruptured bladders is displayed as "R" at an arbitrary value. The modelled 38 kHz *TS* of individual fish for the body only (plus sign) and body summed with the swimbladder (open circle): (b) *C. warmingii*, Group I; (d) *S. leucopsarus*, Group II; (f) *I. antrostomus*, Group III. Transformed $TS = m \log_{10}(L_S) + b$ regressions from the measured data here are shown as solid lines, with the assumption that swimbladder gas volume is that required for neutral buoyancy, V_G, as a dashed line; as a dotted line for modelling by Yasuma *et al.* (2010); and as a dashed-dotted line for the cylinder model using gas-volume measurements from Yasuma *et al.* (2010).

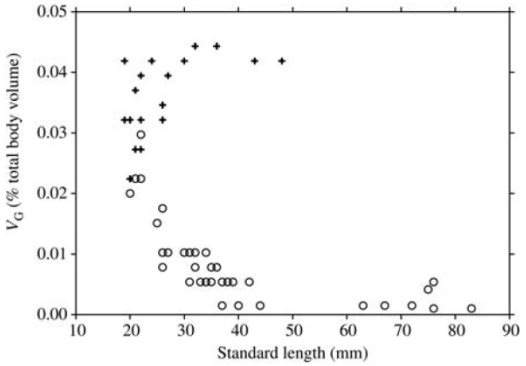

Figure 5. The calculated volume of gas required for neutral buoyancy, V_G, expressed as a percentage of total body volume vs. standard length, L_S: plus sign, *C. warmingii* (Group I); open circle, *S. leucopsarus* (Group II).

but paradoxically, the size class with the highest lipid content also had the highest body density (Neighbors and Nafpaktitis, 1982). Other researchers have found low lipid levels in *N. resplendens*, *M. nitidulum*, and *S. californiensis* (Nevenzel *et al.*, 1969; Brooks, 1976; Neighbors and Nafpaktitis, 1982), and increasing gas volume with length for *M. nitidulum* and *S. californiensis* (Brooks, 1976; Neighbors, 1992). The measurement here of high and constant ρ_f with increasing L_S is consistent with the latter findings.

Presence of gas in the swimbladder

Mesopelagic fish are generally thought to be negatively buoyant (Kanwisher and Ebeling, 1957; Capen, 1967; Bone, 1973; Brooks, 1976; Kalish *et al.*, 1986, Saenger, 1989). A dense-bodied marine fish (i.e. $\rho_f = 1.076$ g ml^{-1}) requires a swimbladder volume of ~5% of the body volume for neutral buoyancy (Taylor, 1921; Marshall, 1960). The gas volume of mesopelagic fish has been measured to be in the range 0–5% of body volume for several species at surface temperature and pressure (Kanwisher and Ebeling, 1957; Capen, 1967; Kleckner and Gibbs, 1972; Kalish *et al.*, 1986; Yasuma *et al.*, 2010). Gas is present or absent on an individual or diel basis rather than uniformly within a species (Capen, 1967; Butler and Pearcy, 1972; Johnson, 1979; Neighbors, 1992; Yasuma *et al.*, 2010). The low ρ_f measurements here demonstrate that many mesopelagic fish require gas

volumes <5% of their body volume to be close to neutral buoyancy (Figure 5). This is especially true for species in Group II. The largest individual *S. leucopsarus* for which gas was present (37 mm) corresponded closely with the L_S at which the V_G drops to 0.5% of body volume.

Volume measurements of swimbladder gas here were variable, with many more than the requirement for neutral buoyancy (Supplementary Table S3). Gas was present or absent in individuals of similar size from the same species. There are several inherent problems with measurements of the volume of gas in the swimbladder of mesopelagic fish at surface temperature and pressure that make accurate quantification difficult. Elasticity of the swimbladder wall adds uncertainty to gas-volume calculations based on swimbladder dimensions. Except for fish collected at the surface, there is uncertainty about the depth of capture. The measured gas volume is subject to a pressure uncertainty of at least 15 atmospheres for midwater trawls and bongo nets as deployed here, plus uncertainty from temperature changes. Gas may be lost during capture, missed during processing, or compressed in life beyond the ambient pressure. Differences between capture methods in the fraction of fish with inflated swimbladders indicate either gas loss during capture or depth-related inflation (Neighbors, 1992). A fish that remains alive in the net for a period may actively remove gas from its swimbladder as the trawl ascends. Removal of swimbladder gas by an ascending fish is rapid compared with the addition of gas, and it can keep pace with the ascent rate of vertical migration (Marshall, 1960; D'Aoust, 1971). The time-frame of a vertical migration, ~1 h, is comparable with the fishing time of a trawl. The absence of measured gas therefore does not mean that gas was not present at the time of capture, even when the fish appears to be undamaged. Given the biases described above with quantitative measurement of gas volume at the surface, it is difficult to know the true degree of swimbladder inflation from these data, except that it is likely to be less than V_G. An assumption of neutral buoyancy is supported by observations of motionless fish from submersibles (Backus *et al.*, 1968; Barham, 1971) and moored echosounders (Kaartvedt *et al.*, 2009). Torpid, non-sinking fish must be close to neutral buoyancy. The buoyancy of fish swimming actively is unclear from visual observations, but there are large energetic advantages to neutral buoyancy. A fish of $\rho_f = 1.077$ swimming one body length per second expends 167% more energy if its swimbladder is not inflated (Alexander, 1966). The question of whether or not individuals of a species vary in their use of gas for buoyancy remains unresolved here. The final solution of the problem will require *in situ* measurements of swimbladder gas volume.

Acoustic model

The simple acoustic models used here are intended to illustrate the relative change in body σ_{bs} through variation in ρ_f. The effects of two of the simplifying assumptions for the swimbladder model are quantified here. The swimbladder of mesopelagic fish is spheroidal rather than spherical (Marshall, 1960; Yasuma *et al.*, 2010). The *TS* of a prolate spheroid and a sphere are similar when the aspect ratio of the spheroid is <3, as is true for mesopelagic fish (Feuillade and Werby, 1994; Barr and Coombs, 2005). The sphere model was compared with a gas-filled prolate spheroid model (Ye, 1997; ESR = 2.4 mm, aspect ratio 3:1, broadside incidence, other parameters as described in "Material and methods" section) and σ_{bs} of the sphere was ~37% less than that of the spheroid in the geometric region. A second simplifying assumption was made to model the swimbladder gas as a free bubble in seawater. Backscattering from the swimbladder occurs at the density interface between the gas and the surrounding medium. Increasing the density of the medium from 1.027 g ml^{-1} to a typical density of fish flesh (1.050 g ml^{-1}) decreases σ_{bs} by <0.01%. Bias derived from the spherical shape and free-bubble assumptions for the swimbladder model is therefore judged to be minimal to exploring the relative change in σ_{bs} brought about by the variation in ρ_f.

A direct comparison can be made between the model used here, measurements, and other models. Yasuma *et al.* (2006) measured the *TS* of a *S. leucopsarus* to be −65.4 dB re 1 m^2. The prolate-spheroid and deformed cylinder models used by Yasuma *et al.* (2006) estimate σ_{bs} to be −64 and −63.6 dB re 1 m^2, respectively. The use of their parameters (64 mm L_S, sound speed in fish c_{fish} = 1518 m s^{-1}, freshwater density, and body density = 1.035 g ml^{-1}) with the fluid-cylinder model results in a *TS* of −62.5 dB re 1 m^2. The simple cylindrical model used here yields results reasonably close to empirical results and more sophisticated models. Yasuma *et al.* (2010) reported a regression of modelled $TS = 26.3 \log_{10}(L_S) - 78.1$ for *C. warmingii* (Figure 4b). The difference between that equation and the one reported here is predominantly a consequence of lower measurements of gas volume by Yasuma *et al.* (2010). When gas volume from Yasuma *et al.* (2010) is used with the spherical model here, the *TS* is almost identical between the two models (Figure 4b).

The tilt-angle of a mesopelagic fish relative to the acoustic beam is important for modelling the σ_{bs} of the body accurately, but less important for the gas inclusion (Yasuma *et al.*, 2010). This important parameter is not addressed here, because dorsal incidence was assumed.

The sound-speed ratio, h, can also have a large impact on backscattering, and it varies with temperature (Yasuma *et al.*, 2006). It seems likely that body density, ambient pressure, and h are not independent, analogous to the behaviour of sound in seawater, but these effects were not measured by Yasuma *et al.* (2006). The value of h used here (1.020 for c = 1490 m s^{-1}; Yasuma *et al.*, 2006) is smaller than the value of 1.050 typically assumed for dense-bodied epipelagic fish (Clay, 1991). Varying h across a reasonable range from 1.010 to 1.050 (Yasuma *et al.*, 2006) in the acoustic-backscattering model for a 385 mm *I. antrostomus* (Figure 3) changes the 38-kHz σ_{bs} by a factor of 10. This parameter needs to be quantified better in future work.

Acoustic implications

Comparison of σ_{bs} from the three fish species in Figure 4 indicates that the σ_{bs} values of 20 mm *C. warmingii* and *S. leucopsarus* are similar to that of a 250 mm *I. antrostomus*. Small *S. leucopsarus* have a σ_{bs} ~10× that of large individuals of the same species. *Stenobrachius leucopsarus* adults do not use gas for buoyancy, and large fish of this species are almost neutrally buoyant (Figures 4 and 5). The σ_{bs} of *C. warmingii* increases with growth because of increased gas volume. For small fish from Groups I and II, the acoustic backscatter from the swimbladder is a much greater proportion of the total than 90%. In myctophids of L_S < 40 mm, the swimbladder contribution to σ_{bs} is 2–4 orders of magnitude greater than that of the body.

The disparity in σ_{bs} between large and small fish of Group II, in combination with larger numbers of small fish, will serve to obscure a direct relationship between acoustic backscattering

and biomass. Four of the Group II myctophid species (*S. leucopsarus*, *T. mexicanus*, *N. ritteri*, and *C. townsendi*) are among the most abundant mesopelagic fish in the California Current. Juvenile fish often greatly outnumber adults, although they may not make up most of the biomass. Trawling is essential to establish the species present and their size distribution for the interpretation of acoustic surveys.

The *TS* for species from Groups I and III can be expressed in the form $TS = m \log_{10}(L_S) + b$ (here, L_S is in cm). The *TS* of Group II fish cannot be represented in equations of this form because of the non-allometric growth of the swimbladder, the major reflector of acoustic energy. The slope and the intercept of the *TS* equation for *I. antrostomus* (Group III) are dramatically different from those of *C. warmingii* (Group I), reflecting the absence of a swimbladder, elongate shape, and decrease in ρ_f with increased L_S of that species.

Estimates for the body density of fish species that do not contain gas are critical for modelling the σ_{bs} of these fish, and hence for acoustic surveys of their abundance and distribution. A change in body density from a typical value for an epipelagic fish to the measured ρ_f of *I. antrostomus* reduced the σ_{bs} sixfold (Figure 2). For those species with functional swimbladders, V_G is affected by body density. Overestimates of body density will result in biased calculations of σ_{bs} for both the body and gas inclusion of these fish.

Conclusions

Body density decreases with size in mesopelagic fish species in which large individuals do not have a functional swimbladder. Species with some large individuals having inflated swimbladders do not decrease in body density with increased weight. Mesopelagic fish in general have lower body density than fish living in shallower water.

The σ_{bs} of a fish is dominated by gas in the swimbladder, if present. The volume of gas in the swimbladder of a mesopelagic fish cannot be measured accurately at the surface as a result of the inherent unknown quantities of capture depth and loss of gas. For accuracy, calculation of the maximum volume of gas in the swimbladder, V_G, requires knowledge of body density.

Information on ontogenetic changes in swimbladder inflation and the body density of fish is critical for the construction of the *TS* models used to interpret acoustic surveys. Knowledge of the fish species present, their relative abundance, their developmental morphology, and their size distribution is required for accurate acoustic surveys of mesopelagic fish. The measurements presented here of ρ_f and swimbladder inflation for 71 species of mesopelagic fish from the Northeast Pacific can be used to improve the accuracy of the backscattering models used to interpret acoustic surveys conducted there. However, those models will also require assumptions or new data regarding tilt-angle and swimbladder volume. Juveniles and adults from Group II species may need to be treated separately because of their disjunct *TS* distributions.

Supplementary material

Supplementary data covering individual trawls, species sampled by cruise, a detailed comparison with previously published work, and measurements for individual fish are available in several tables and a Figure in the ICESJMS online version of this manuscript.

Acknowledgements

I thank the RV "New Horizon" and FSV "Bell Shimada" crew, volunteers, and science parties for their help in deploying nets and processing samples. Equipment and chemicals were provided by the SIO MVC, the SIO Pelagic Invertebrates Collection, J. Koslow, and D. Checkley. Some fish were provided by M. Goldstein, J. Powell, and M. Decima. C. Klepadlo from the SIO MVC provided training, keys, and assistance with the identification of fish. P. Hastings of the SIO MVC allowed the dissection of some fish. D. Checkley, J. Koslow, J. Graham, M. Ohman, F. Powell, and P. Hastings provided valuable suggestions and comments on the manuscript. Wire time for a midwater trawl was provided by L. Levin (SIO 277). The study was supported by a NASA Earth and Space Science Fellowship. Ship time was funded by UC Ship Funds, NOAA, and the Kaisei Foundation/Ocean Voyages Institute.

References

Alexander, R. M. 1966. Physical aspects of swimbladder function. Biological Reviews of the Cambridge Philosophical Society, 41: 141–176.

Alexander, R. M. 1972. The energetics of vertical migration by fishes. Symposia of the Society of Experimental Biology, 26: 273–294.

Anderson, V. C. 1950. Sound scattering from a fluid sphere. Journal of the Acoustical Society of America, 22: 426–431.

Backus, R. H., Craddock, J. E., Haedrich, R. L., Shores, D. L., Teal, J. M., Wing, A. S., Mead, G. W., *et al.* 1968. *Ceratoscopelus maderensis*: peculiar sound-scattering layer identified with this myctophid fish. Science, 160: 991–993.

Bailey, T. G., and Robison, B. H. 1986. Food availability as a selective factor on the chemical compositions of midwater fishes in the eastern North Pacific. Marine Biology, 91: 131–141.

Barham, E. G. 1971. Deep sea fishes: lethargy and vertical orientation. *In* Proceedings of an International Symposium on Biological Sound Scattering in the Ocean, pp. 100–118. Ed. by G. B. Farquhar. US Government Printing Office, Washington DC.

Barr, R., and Coombs, R. F. 2005. The significance of high-order resonances of spherical bubbles to the acoustic response of fish with swimbladders. Journal of the Acoustical Society of America, 117: 3589–3599.

Beamish, R. J., Leask, K. D., Ivanov, O. A., Balanov, A. A., Orlov, A. M., and Sinclair, B. 1999. The ecology, distribution, and abundance of midwater fishes of the Subarctic Pacific Gyres. Progress in Oceanography, 43: 399–442.

Bone, Q. 1973. A note on the buoyancy of some lantern-fishes (Myctophoidei). Journal of the Marine Biological Association of the UK, 53: 619–633.

Brooks, A. L. 1976. Swimbladder allometry of selected midwater fish species. National Technical Information Service, USDOC, Springfield. NUSC Technical Report, 4983: 1–43.

Butler, J. L., and Pearcy, W. G. 1972. Swimbladder morphology and specific gravity of myctophids off Oregon. Journal of the Fisheries Research Board of Canada, 29: 1145–1150.

Capen, R. L. 1967. Swimbladder morphology of some mesopelagic fishes in relation to sound scattering. US Navy Electronics Laboratory San Diego Research Report, 1447: 1–31.

Childress, J. J., and Nygaard, M. H. 1973. Chemical composition of midwater fishes as a function of depth of occurrence off southern California. Deep Sea Research, 20: 1093–1109.

Childress, J. J., Price, M. H., Favuzzi, J., and Cowles, D. 1990. Chemical composition of midwater fishes as a function of depth of occurrence off the Hawaiian Islands: food availability as a selective factor? Marine Biology, 105: 235–246.

Childress, J. J., Taylor, S. M., Cailliet, G. M., and Price, M. H. 1980. Patterns of growth, energy utilization and reproduction in some

meso- and bathypelagic fishes off southern California. Marine Biology, 61: 27–40.

Clay, C. S. 1991. Low-resolution acoustic scattering models: fluid-filled cylinders and fish with swim bladders. Journal of the Acoustical Society of America, 89: 2168–2179.

Cohen, D. M. 1986. Argentinidae. *In* Smith's Sea Fishes, pp. 215–216. Ed. by M. M. Smith, and P. C. Heemstra. Springer, New York.

D'Aoust, B. G. 1971. Physiological constraints on vertical migration by mesopelagic fishes. *In* Proceedings of an International Symposium on Biological Sound Scattering in the Ocean, pp. 86–99. Ed. by G. B. Farquhar. US Government Printing Office, Washington DC.

Feuillade, C., and Werby, M. F. 1994. Resonances of deformed gas bubbles in liquids. Journal of the Acoustical Society of America, 96: 3684–3692.

Foote, K. G. 1980. Importance of the swimbladder in acoustic scattering by fish: a comparison of gadoid and mackerel target strengths. Journal of the Acoustical Society of America, 67: 2084–2089.

Gjosæter, J., and Kawaguchi, K. 1980. A review of the world resources of mesopelagic fish. FAO Fisheries Technical Paper, 193. 151 pp.

Hersey, J. B., Backus, R. H., and Hellwig, J. 1962. Sound-scattering spectra of deep scattering layers in the western North Atlantic Ocean. Deep Sea Research, 8: 196–210.

Johnson, R. K. 1979. Gas bubble sizes for selected myctophids. Oregon State University School of Oceanography Reference, 79: 1–18.

Kaartvedt, S., Rostad, A., Klevjer, T. A., and Staby, A. 2009. Use of bottom-mounted echo sounders in exploring behavior of mesopelagic fishes. Marine Ecology Progress Series, 395: 109–118.

Kalish, J. M., Greenlaw, C. F., Pearcy, W. G., and Van Holliday, D. 1986. The biological and acoustical structure of sound scattering layers off Oregon. Deep Sea Research, 33: 631–653.

Kanwisher, J., and Ebeling, A. 1957. Composition of the swim-bladder gas in bathypelagic fishes. Deep Sea Research, 4: 211–217.

Karnella, C. 1987. Family Myctophidae, lanternfishes. *In* Biology of Midwater Fishes of the Bermuda Ocean Acre, pp. 51–168. Ed. by R. H. J. Gibbs, and W. H. Krueger. Smithsonian Institution Press, Washington DC.

Kleckner, R. C., and Gibbs, R. H. 1972. Swimbladder structure of Mediterranean midwater fishes and a method of comparing swimbladder data with acoustic profiles. *In* Mediterranean Biological Studies Final Report I, pp. 230–281. Smithsonian Institution, Washington DC.

Koslow, J. A., Kloser, R. J., and Williams, A. 1997. Pelagic biomass and community structure over the mid-continental slope off southeastern Australia based upon acoustic and midwater trawl sampling. Marine Ecology Progress Series, 146: 21–35.

Kubota, T., Fujimota, T., and Sato, N. 1991. Some biological aspects of the deepsea fish, *Bathysphyraenops simplex* (family Percichthyidae), from Suruga Bay, Japan. Journal of the Faculty of Marine Science and Technology, Tokai University, 32: 147–155.

Mann, K. H. 1984. Fish production in open ocean ecosystems. *In* Flows of Energy and Materials in Marine Ecosystems, pp. 435–458. Ed. by M. J. R. Fasham. Plenum Press, New York.

Marshall, N. B. 1960. Swimbladder structure of deep-sea fishes in relation to their systematics and biology. Discovery Reports, 31. 122 pp.

McClatchie, S., Thorne, R. E., Grimes, P., and Hanchet, S. 2000. Ground truth and target identification for fisheries acoustics. Fisheries Research, 47: 173–191.

Medwin, H., and Clay, C. S. 1997. Fundamentals of Acoustic Oceanography. Academic Press, Burlington.

Neighbors, M. A. 1992. Occurrence of inflated swimbladders in five species of lanternfishes (family Myctophidae) from waters off southern California. Marine Biology, 114: 355–363.

Neighbors, M. A., and Nafpaktitis, B. G. 1982. Lipid compositions, water contents, swimbladder morphologies and buoyancies of nineteen species of midwater fishes (18 myctophids and 1 neoscopelid). Marine Biology, 66: 207–215.

Nevenzel, J. C., Rodegker, W., Robinson, J. S., and Kayama, M. 1969. Lipids of some lantern fishes (family Myctophidae). Comparative Biochemistry and Physiology, 31: 25–36.

Pearcy, W. G., Krygier, E. E., Mesecar, R., and Ramsey, F. 1977. Vertical distribution and migration of oceanic micronekton off Oregon. Deep Sea Research, 24: 223–245.

Pilson, M. E. Q. 1998. An Introduction to the Chemistry of the Sea. Prentice Hall, Upper Saddle River, NJ.

Robison, B. H. 2003. What drives the diel vertical migrations of Antarctic midwater fish? Journal of the Marine Biological Association of the UK, 83: 639–642.

Saenger, R. A. 1989. Bivariate normal swimbladder size allometry models and allometric exponents for 38 mesopelagic swimbladdered fish species commonly found in the north Sargasso Sea. Canadian Journal of Fisheries and Aquatic Sciences, 46: 1986–2002.

Saito, H., and Murata, M. 1998. Origin of the monoene fats in the lipid of midwater fishes: relationship between the lipids of myctophids and those of their prey. Marine Ecology Progress Series, 168: 21–33.

Seo, H. S., Endo, Y., Fujimoto, K., Watanabe, H., and Kawaguchi, K. 1996. Characterization of lipids in myctophid fish in the Subarctic and tropical Pacific Ocean. Fisheries Science, 62: 447–453.

Simmonds, E. J., and MacLennan, D. N. 2005. Fisheries Acoustics: Theory and Practice. Blackwell Science, Oxford.

Stanton, T. K. 1988. Sound scattering by cylinders of finite length. 1. Fluid cylinders. Journal of the Acoustical Society of America, 83: 55–63.

Stickney, D. G., and Torres, J. J. 1989. Proximate composition and energy content of mesopelagic fishes from the eastern Gulf of Mexico. Marine Biology, 103: 13–24.

Taylor, H. F. 1921. Deductions concerning the air bladder and the specific gravity of fishes. Bulletin of the US Bureau of Fisheries, 38: 121–126.

Wisner, R. L. 1976. The taxonomy and distribution of lanternfishes (family Myctophidae) of the eastern Pacific Ocean. Navy Ocean Research and Development Activity, Bay St Louis.

Yancey, P. H., Lawrence-Berrey, R., and Douglas, M. D. 1989. Adaptations in mesopelagic fishes. 1. Buoyant glycosaminoglycan layers in species without diel vertical migrations. Marine Biology, 103: 453–459.

Yasuma, H., Sawada, K., Takao, Y., Miyashita, K., and Aoki, I. 2010. Swimbladder condition and target strength of myctophid fish in the temperate zone of the Northwest Pacific. ICES Journal of Marine Science, 67: 135–144.

Yasuma, H., Takao, Y., Sawada, K., Miyashita, K., and Aoki, I. 2006. Target strength of the lanternfish, *Stenobrachius leucopsarus* (family Myctophidae), a fish without an airbladder, measured in the Bering Sea. ICES Journal of Marine Science, 63: 683–692.

Ye, Z. 1997. Low-frequency acoustic scattering by gas-filled prolate spheroids in liquids. Journal of the Acoustical Society of America, 101: 1945–1952.

Supplementary material: ICES Journal of Marine Science, 68

The specific gravity of mesopelagic fish from the northeastern Pacific Ocean and its implications for acoustic backscatter

Peter Davison

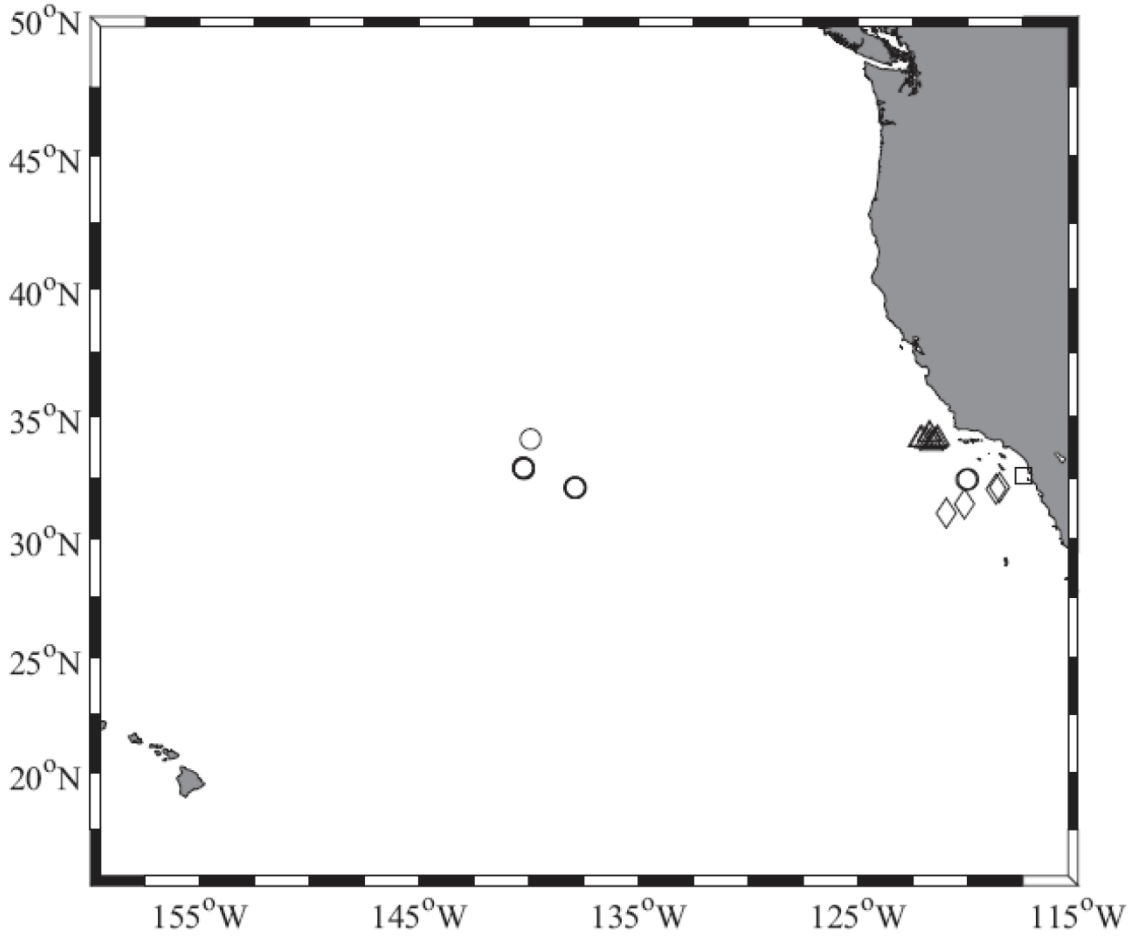

Figure S1. Northeast Pacific Ocean midwater trawl locations for three cruises of the RV "New Horizon" and one of the FSV "Bell Shimada": open triangles, CCE-P0904; open circles, SEAPLEX; open square, DSB; open diamonds, Shimada.

Table S1. Trawl information. The CCE-P0904, SEAPLEX, DSB, and Shimada cruises are abbreviated as "CC," "SP," "DSB"" and "SH," respectively. "Depth" refers to the maximum depth of an oblique trawl profile. "IKMT" refers to an 8 m^2 Isaacs–Kidd midwater trawl (Isaacs and Kidd, 1953), and "MOHT" to a 5 m^2 Matsuda-Oozeki-Hu trawl (Oozeki *et al.*, 2004).

Cruise:tow	Net type	Date (PDT)	Time (PDT)	Latitude (°N)	Longitude (°W)	Light conditions	Depth (m)
CC:1-1	IKMT	25 Apr 2009	07:39	34.276	121.775	day	~800*
CC:1-2	IKMT	25 Apr 2009	17:04	34.229	121.755	day	186
CC:2-1	IKMT	27 Apr 2009	23:40	34.053	122.205	night	165
CC:2-2	IKMT	28 Apr 2009	06:44	34.086	122.114	day	743
CC:2-3	IKMT	28 Apr 2009	16:50	33.976	121.905	day	833
CC:2-4	IKMT	29 Apr 2009	13:44	33.984	121.737	day	805
CC:2-5	IKMT	29 Apr 2009	21:18	33.884	121.673	night	185
CC:F-1	IKMT	1 May 2009	22:43	34.099	121.392	night	162
CC:F-2	IKMT	2 May 2009	02:18	34.037	121.459	night	168
CC:F-3	IKMT	2 May 2009	05:18	33.966	121.541	night	176
SP:1-1	MOHT	3 Aug 2009	07:03	32.426	119.985	day	~900*
SP:1-2	MOHT	3 Aug 2009	14:48	32.414	119.979	day	910
SP:1-3	MOHT	3 Aug 2009	19:59	32.411	119.992	dusk	835
SP:1-4	MOHT	3 Aug 2009	23:46	32.418	120.079	night	231
SP:2-1	MOHT	8 Aug 2009	16:16	32.064	137.899	day	918
SP:2-2	MOHT	8 Aug 2009	20:57	32.076	137.940	dusk	824
SP:2-3	MOHT	9 Aug 2009	01:51	32.106	137.904	night	177
SP:2-4	MOHT	9 Aug 2009	05:49	32.069	137.914	dawn	756
SP:3-1	MOHT	10 Aug 2009	17:04	32.915	140.312	day	878
SP:3-2	MOHT	10 Aug 2009	21:21	32.925	140.303	dusk	797
SP:3-3	MOHT	11 Aug 2009	02:27	32.884	140.265	night	176
SP:3-4	MOHT	11 Aug 2009	06:07	32.883	140.283	dawn	725
SP:4-1	MOHT	14 Aug 2009	00:50	34.063	139.976	night	888
SP:4-2	MOHT	14 Aug 2009	04:57	34.064	139.976	night	197
SP:4-3	MOHT	14 Aug 2009	07:08	34.069	139.979	dawn	797
SP:4-4	MOHT	14 Aug 2009	18:06	34.058	139.998	day	837
DSB:1	IKMT	31 Oct 2009	12:15	32.598	117.463	day	1188
SH:1	MOHT	24 Sep 2010	18:05	32.400	118.457	day	199
SH:2	MOHT	24 Sep 2010	19:27	32.343	118.557	night	214
SH:3	MOHT	25 Sep 2010	11:55	31.678	119.908	day	639
SH:5	MOHT	26 Sep 2010	09:28	31.180	120.919	day	773

* The time-depth recorder malfunctioned on two tows. Depth was estimated from other tows with the same profile.

Table S2. Species included in this study, with sample size from each cruise. The CCE-P0904, SEAPLEX, DSB, and Shimada cruises are abbreviated as "CC," "SP," "DSB", and "SH," respectively. The SEAPLEX samples are further divided into those collected from the California Current, and those from the North Pacific subtropical gyre, respectively.

Family	Species name	Sample size			
		CC	SP	DSB	SH
Microstomatidae	*Microstoma microstoma* (Risso)	3	2+1	0	0
Bathylagidae	*Bathylagoides wesethi* (Bolin)	17	5+1	15	17
	Leuroglossus stilbius Gilbert	0	4+0	2	0
	Lipolagus ochotensis (Schmidt)	2	1+0	4	5
Alepocephalidae	*Alepocephalus tenebrosus* Gilbert	2	0	0	2
Platytroctidae	*Holtbyrnia latifrons* Sazonov	3	3+0	0	0
	Sagamichthys abei Parr	4	0	1	0
Gonostomatidae	*Cyclothone acclinidens* Garman	21	7+4	12	0
	Cyclothone atraria Gilbert	3	1+6	0	0
	Cyclothone pallida Brauer	0	1+5	0	0
	Cyclothone pseudopallida Mukhacheva	1	0+11	0	0
	Cyclothone signata Garman	21	2+12	1	0
Sternoptychidae	*Argyropelecus affinis* Garman	5	1+2	1	8
	Argyropelecus hemigymnus Cocco	7	1+5	0	4
	Argyropelecus lychnus Garman	0	0	2	1
	Argyropelecus sladeni Regan	14	3+0	2	7
	Danaphos oculatus (Garman)	6	2+13	0	2
	Sternoptyx diaphana Hermann	0	0+5	1	0
	Sternoptyx obscura Garman	3	0	0	4
	Sternoptyx pseudobscura Baird	1	0+6	0	1
Phosichthyidae	*Ichthyococcus irregularis* Rechnitzer and Bohlke	1	2+0	0	0
	Vinciguerria nimbaria (Jordan and Williams)	0	0+9	0	0
	Vinciguerria poweriae (Cocco)	0	0+15	0	0
Stomiidae	*Chauliodus macouni* Bean	3	0	0	3
	Stomias atriventer Garman	0	3+0	0	1
	Bathophilus flemingi Aron and McCrery	1	0+5	0	0
	Photonectes parvimanus Regan and Trewavas	0	0+6	0	0
	Aristostomias xenostoma Regan and Trewavas	0	0+5	0	0
	Idiacanthus antrostomus Gilbert	12	2+4	1	2
	Tactostoma macropus Bolin	4	0	0	0
Scopelarchidae	*Scopelarchus stephensi* Johnson	0	0+3	0	0
Notosudidae	*Scopelosaurus harryi* (Mead)	0	0	0	5
Paralepididae	*Arctozenus risso* (Bonaparte)	5	0	0	1
Myctophidae	*Bolinichthys longipes* (Brauer)	0	0+4	0	0
	Ceratoscopelus townsendi (Eigenmann and Eigenmann)	11	1+0	3	28
	Ceratoscopelus warmingii (Lutken)	0	0+18	0	0
	Diaphus anderseni Taning	0	0+13	0	0
	Diaphus fulgens (Brauer)	0	0+7	0	0
	Diaphus theta Eigenmann and Eigenmann	20	4+0	1	7
	Diogenichthys atlanticus (Taning)	5	3+14	0	3
	Electrona risso (Cocco)	0	0+3	0	0
	Hygophum proximum Becker	0	0+5	0	0
	Hygophum reinhardtii (Lutken)	0	0+4	0	0
	Lampadena urophaos Paxton	0	0+12	0	0
	Lampanyctus tenuiformis (Brauer)	0	0+13	0	0
	Lobianchia gemellarii (Cocco)	0	0+3	0	0
	Myctophum nitidulum Garman	0	0+16	0	1

Table S2. (continued)

Family	Species name	Sample size			
		CC	SP	DSB	SH
Myctophidae	*Nannobrachium fernae* (Wisner)	0	0+5	0	0
	Nannobrachium hawaiiensis Zahuranec	0	0+20	0	2
	Nannobrachium regale (Gilbert)	5	5+4	2	3
	Nannobrachium ritteri (Gilbert)	25	13+1	5	12
	Notolychnus valdiviae (Brauer)	0	0+8	0	0
	Notoscopelus resplendens (Richardson)	0	0+5	0	0
	Parvilux ingens Hubbs and Wisner	3	1+0	2	0
	Protomyctophum crockeri (Bolin)	13	8+0	0	5
	Stenobrachius leucopsarus (Eigenmann and Eigenmann)	31	11+0	3	12
	Symbolophorus californiensis (Eigenmann and Eigenmann)	8	6+0	3	3
	Taaningichthys bathyphilus (Taning)	0	0+3	0	0
	Tarletonbeania crenularis (Jordan and Gilbert)	17	3+0	0	0
	Triphoturus mexicanus (Gilbert)	16	5+0	25	6
	Triphoturus nigrescens (Brauer)	0	0+4	0	0
Ophidiidae	*Chilara taylori* (Girard)	0	1+0	1	1
Melamphaeidae	*Melamphaes lugubris* Gilbert	8	0	0	1
	Melamphaes parvus Ebeling	1	1+2	0	0
	Melamphaes simus Ebeling	0	0+5	0	0
	Melamphaes suborbitalis (Gill)	0	0+2	0	1
	Poromitra crassiceps (Gunther)	5	6+0	1	2
	Scopeloberyx opisthopterus (Parr)	0	0+3	0	0
	Scopelogadus mizolepis Gunther	6	1+1	3	8
Howellidae	*Bathysphyraenops simplex* Parr	0	0+6	0	1
Gempylidae	*Diplospinus multistriatus* Maul	0	0+6	0	0

Table S3. Standard length, L_S, wet weight, W_W, body specific gravity after gas removal, ρ_f, measured gas volume, and the gas volume required for neutral buoyancy, V_G, for all individual fish. For gas volume, "P" indicates present but not measured, "R" indicates evidence of rupturing, and "-" indicates not recorded. Species are ordered after Table 1 in the main text, individuals are ordered by increasing L_S.

Group	Family	Species	L_S (mm)	W_W (g)	ρ_f	Gas vol. (mm^3)	Gas vol. (% total)	V_G (% total)
I	Myctophidae	*Tarletonbeania crenularis*	22	0.11	1.0575	R	-	2.884
			23	0.12	1.0575	0	0	2.884
			24	0.13	1.0675	R	-	3.794
			27	0.20	1.0875	0	0	5.563
			32	0.37	1.0850	0	0	5.346
			32	0.28	1.0550	P	-	2.654
			33	0.43	1.0850	P	-	5.346
			35	0.48	1.0875	5.704	1.276	5.563
			36	0.46	1.0825	0	0	5.127
			37	0.61	1.0875	0	0	5.563
			37	0.58	1.0875	4.877	0.906	5.563
			39	0.73	1.0825	4.189	0.617	5.127
			39	0.67	1.0850	4.824	0.775	5.346
			39	0.70	1.0875	1.317	0.204	5.563
			39	0.60	1.0850	8.543	1.521	5.346
			40	0.79	1.0850	5.394	0.735	5.346
			40	0.77	1.0875	0	0	5.563
			43	0.93	1.0850	1.219	0.142	5.346
			45	1.14	1.0850	0	0	5.346
			57	2.01	1.0850	0	0	5.346
I	Myctophidae	*Hygophum reinhardtii*	19	0.10	1.0700	1.012	1.071	4.019
			20	0.09	1.0625	2.090	2.408	3.341
			39	0.85	1.0750	0.085	0.011	4.465
			43	1.13	1.0775	33.112	3.061	4.687
I	Myctophidae	*Notoscopelus resplendens*	27	0.28	1.0700	33.885	11.464	4.019
			28	0.24	1.0750	0	0	4.465
			31	0.38	1.0750	22.984	6.105	4.465
			40	0.84	1.0750	0	0	4.465
			42	0.90	1.0775	0	0	4.687
I	Gempylidae	*Diplospinus multistriatus*	18	0.02	1.0725	0.676	3.496	4.242
			21	0.04	1.0675	1.073	2.784	3.794
			28	0.05	1.0800	-	-	4.907
			38	0.04	1.0725	2.146	5.441	4.242
			49	0.14	1.0775	0.176	0.135	4.687
			55	0.14	1.0700	2.965	2.216	4.019
I	Myctophidae	*Diogenichthys atlanticus*	16	0.06	1.0675	1.053	1.840	3.794
			16	0.08	1.0575	R	-	2.884
			17	0.06	1.0600	3.331	5.558	3.113
			18	0.08	1.0725	0	0	4.242
			18	0.09	1.0575	0.527	0.615	2.884
			18	0.10	1.0575	R	-	2.884
			18	0.09	1.0675	0.066	0.078	3.794
			18	0.08	1.0650	1.553	2.026	3.568
			19	0.13	1.0750	8.230	6.372	4.465
			19	0.12	1.0550	R	-	2.654
			19	0.12	1.0675	3.334	2.880	3.794
			19	0.10	1.0675	0.456	0.484	3.794

Table S3. (continued)

Group	Family	Species	L_S (mm)	W_W (g)	ρ_f	Gas vol. (mm^3)	Gas vol. (% total)	V_G (% total)
I	Myctophidae	*Diogenichthys atlanticus*	20	0.14	1.0750	4.214	3.134	4.465
			20	0.12	1.0675	10.845	8.798	3.794
			20	0.12	1.0700	4.214	3.621	4.019
			21	0.14	1.0750	0.427	0.327	4.465
			21	0.14	1.0725	9.435	6.741	4.242
			21	0.16	1.0650	8.906	5.596	3.568
			22	0.16	1.0775	6.811	4.386	4.687
			22	0.20	1.0700	0.527	0.281	4.019
			22	0.17	1.0700	0.480	0.301	4.019
			22	0.17	1.0750	3.224	1.998	4.465
			22	0.17	1.0700	5.887	3.573	4.019
			23	0.19	1.0800	2.965	1.658	4.907
			23	0.19	1.0750	3.977	2.201	4.465
I	Myctophidae	*Myctophum nitidulum*	18	0.07	1.0600	0.020	0.030	3.113
			21	0.10	1.0775	0.749	0.800	4.687
			22	0.13	1.0725	1.058	0.866	4.242
			30	0.29	1.0750	1.249	0.461	4.465
			31	0.34	1.0775	5.926	1.843	4.687
			31	0.40	1.0775	3.046	0.814	4.687
			32	0.45	1.0700	6.109	1.432	4.019
			32	0.37	1.0750	6.543	1.866	4.465
			36	0.63	1.0775	6.672	1.128	4.687
			37	0.77	1.0750	5.358	0.742	4.465
			46	1.28	1.0725	59.593	4.756	4.242
			65	4.10	1.0725	0	0	4.242
			74	6.76	1.0775	0	0	4.687
			76	6.70	1.0725	P	-	4.242
			76	6.54	1.0725	P	-	4.242
			77	7.02	1.0725	P	-	4.242
			78	7.98	1.0725	P	-	4.242
I	Myctophidae	*Electrona risso*	11	0.03	1.0700	R	-	4.019
			18	0.14	1.0725	0	0	4.242
			32	0.89	1.0725	3.031	0.364	4.242
I	Myctophidae	*Hygophum proximum*	16	0.06	1.0700	0.280	0.498	4.019
			20	0.11	1.0650	0	0	3.568
			29	0.39	1.0725	0	0	4.242
			29	0.35	1.0750	6.653	2.002	4.465
			32	0.52	1.0725	0	0	4.242
I	Myctophidae	*Protomyctophum crockeri*	15	0.06	1.0750	R	-	4.465
			16	0.06	1.0700	R	-	4.019
			17	0.09	1.0675	R	-	3.794
			17	0.09	1.0675	0		3.794
			18	0.14	1.0675	0.156	0.119	3.794
			19	0.10	1.0675	R	-	3.794
			19	0.12	1.0725	R	-	4.242
			19	0.16	1.0700	R	-	4.019
			20	0.16	1.0675	0	0	3.794
			23	0.28	1.0600	2.439	0.915	3.113
			24	0.31	1.0700	4.633	1.574	4.019
			24	0.26	1.0825	13.410	5.288	5.127
			25	0.33	1.0650	1.249	0.401	3.568

Table S3. (continued)

Group	Family	Species	L_S (mm)	W_W (g)	ρ_f	Gas vol. (mm^3)	Gas vol. (% total)	V_G (% total)
I	Myctophidae	*Protomyctophum crockeri*	25	0.30	1.0575	0.305	0.107	2.884
			26	0.37	1.0725	0	0	4.242
			27	0.44	1.0675	0	0	3.794
			28	0.46	1.0725	2.085	0.484	4.242
			28	0.41	1.0775	R	-	4.687
			30	0.47	1.0725	2.190	0.497	4.242
			32	0.66	1.0725	45.012	6.816	4.242
			33	0.74	1.0775	2.439	0.354	4.687
			33	0.74	1.0700	0.836	0.121	4.019
			35	0.83	1.0725	0	0	4.242
			35	0.87	1.0750	14.922	1.810	4.465
			36	0.84	1.0675	0	0	3.794
			37	0.99	1.0725	0	0	4.242
I	Myctophidae	*Nannobrachium fernae*	32	0.25	1.0700	0	0	4.019
			34	0.33	1.0775	18.504	5.698	4.687
			35	0.35	1.0675	4.214	1.269	3.794
			36	0.43	1.0625	0.020	0.005	3.341
			63	2.31	1.0725	69.392	3.121	4.242
I	Myctophidae	*Lampadena urophaos*	19	0.08	1.0625	0.788	1.035	3.341
			19	0.09	1.0600	6.692	7.305	3.113
			20	0.10	1.0600	0	0	3.113
			21	0.12	1.0600	0.836	0.733	3.113
			22	0.13	1.0550	4.233	3.322	2.654
			22	0.13	1.0625	4.214	3.329	3.341
			22	0.13	1.0600	8.386	6.401	3.113
			22	0.11	1.0600	7.662	6.876	3.113
			24	0.16	1.0700	7.131	4.552	4.019
			25	0.18	1.0700	0	0	4.019
			26	0.11	1.0600	3.246	3.033	3.113
			26	0.22	1.0775	5.884	2.801	4.687
I	Myctophidae	*Bolinichthys longipes*	38	0.75	1.0725	19.136	2.664	4.242
			38	0.77	1.0700	30.812	4.106	4.019
			41	0.96	1.0725	3.351	0.373	4.242
			42	1.06	1.0675	44.505	4.290	3.794
I	Myctophidae	*Diaphus anderseni*	25	0.30	1.0700	2.595	0.917	4.019
			26	0.31	1.0700	0	0	4.019
			26	0.35	1.0625	8.230	2.438	3.341
			26	0.37	1.0625	R	-	3.341
			26	0.31	1.0750	0	0	4.465
			27	0.37	1.0625	4.214	1.196	3.341
			27	0.36	1.0725	3.246	0.958	4.242
			27	0.36	1.0750	0.176	0.052	4.465
			27	0.37	1.0725	0	0	4.242
			28	0.45	1.0700	R	-	4.019
			28	0.45	1.0675	7.901	1.840	3.794
			28	0.36	1.0750	0	0	4.465
			30	0.58	1.0725	0.836	0.154	4.242
I	Myctophidae	*Ceratoscopelus warmingii*	19	0.07	1.0700	0.305	0.464	4.019
			19	0.08	1.0600	8.230	9.833	3.113
			20	0.09	1.0600	0.305	0.358	3.113
			20	0.08	1.0500	1.032	1.336	2.190

Table S3. (continued)

Group	Family	Species	L_S (mm)	W_W (g)	ρ_f	Gas vol. (mm^3)	Gas vol. (% total)	V_G (% total)
I	Myctophidae	*Ceratoscopelus warmingii*	21	0.09	1.0650	2.480	2.851	3.568
			21	0.11	1.0550	1.929	1.816	2.654
			22	0.09	1.0675	4.372	4.931	3.794
			22	0.10	1.0600	1.380	1.442	3.113
			22	0.11	1.0550	0.683	0.651	2.654
			24	0.17	1.0700	2.743	1.697	4.019
			26	0.20	1.0600	8.230	4.180	3.113
			26	0.19	1.0625	R	-	3.341
			27	0.23	1.0675	R	-	3.794
			30	0.34	1.0700	2.439	0.762	4.019
			32	0.35	1.0725	2.439	0.742	4.242
			36	0.58	1.0725	33.712	5.868	4.242
			43	1.18	1.0700	30.181	2.664	4.019
			48	1.74	1.0700	57.613	3.422	4.019
I	Phosichthyidae	*Vinciguerria nimbaria*	17	0.03	1.0700	1.778	5.963	4.019
			17	0.04	1.0700	2.439	6.124	4.019
			18	0.04	1.0675	1.553	3.981	3.794
			18	0.04	1.0675	2.080	5.259	3.794
			19	0.04	1.0700	0.066	0.176	4.019
			19	0.05	1.0625	3.551	7.016	3.341
			19	0.06	1.0600	R	-	3.113
			31	0.30	1.0675	30.181	9.698	3.794
			32	0.33	1.0700	14.420	4.467	4.019
I	Phosichthyidae	*Vinciguerria poweriae*	18	0.03	1.0775	4.370	13.566	4.687
			18	0.03	1.0725	2.504	8.218	4.242
			18	0.04	1.0675	0.066	0.175	3.794
			19	0.07	1.0600	R	-	3.113
			20	0.08	1.0650	5.358	6.658	3.568
			22	0.13	1.0650	R	-	3.568
			25	0.18	1.0700	2.802	1.638	4.019
			30	0.31	1.0700	1.249	0.429	4.019
			30	0.33	1.0650	0.856	0.275	3.568
			31	0.37	1.0700	8.296	2.343	4.019
			32	0.38	1.0725	26.798	7.032	4.242
			34	0.58	1.0675	R	-	3.794
			35	0.51	1.0725	53.533	10.119	4.242
			37	0.67	1.0675	R	-	3.794
			38	0.78	1.0675	14.749	1.979	3.794
I	Myctophidae	*Diaphus fulgens*	36	0.69	1.0750	0.305	0.047	4.465
			36	0.77	1.0725	0.371	0.052	4.242
			38	0.87	1.0725	1.249	0.154	4.242
			39	1.07	1.0725	2.524	0.252	4.242
			40	1.04	1.0700	2.305	0.237	4.019
			41	1.19	1.0725	0.156	0.014	4.242
			52	2.46	1.0675	4.590	0.199	3.794
I	Myctophidae	*Lampanyctus tenuiformis*	28	0.17	1.0675	14.222	8.198	3.794
			30	0.21	1.0700	1.778	0.898	4.019
			30	0.27	1.0625	0	0	3.341
			35	0.36	1.0600	27.698	7.541	3.113
			37	0.49	1.0600	0.020	0.004	3.113
			38	0.44	1.0725	30.337	6.885	4.242

Table S3. (continued)

Group	Family	Species	L_S (mm)	W_W (g)	ρ_f	Gas vol. (mm^3)	Gas vol. (% total)	V_G (% total)
I	Myctophidae	*Lampanyctus tenuiformis*	38	0.49	1.0725	6.492	1.401	4.242
			39	0.54	1.0625	-	-	3.341
			40	0.48	1.0700	4.494	0.992	4.019
			42	0.74	1.0700	75.693	9.865	4.019
			43	0.79	1.0675	1.249	0.168	3.794
			43	0.81	1.0675	45.327	5.637	3.794
			43	0.79	1.0700	0	0	4.019
I	Microstomatidae	*Microstoma microstoma*	20	0.05	1.0575	0.305	0.641	2.884
			20	0.04	1.0700	R	-	4.019
			20	0.05	1.0675	R	-	3.794
			28	0.17	1.0700	0.527	0.330	4.019
			31	0.16	1.0700	2.014	1.329	4.019
			55	0.90	1.0675	0	0	3.794
I	Sternoptychidae	*Danaphos oculatus*	22	0.08	1.0575	R	-	2.884
			22	0.06	1.0600	R	-	3.113
			23	0.10	1.0650	R	-	3.568
			23	0.08	1.0600	R	-	3.113
			23	0.05	1.0600	R	-	3.113
			24	0.08	1.0625	R	-	3.341
			25	0.10	1.0600	R	-	3.113
			25	0.09	1.0650	R	-	3.568
			26	0.12	1.0600	R	-	3.113
			28	0.18	1.0625	R	-	3.341
			30	0.21	1.0625	R	-	3.341
			31	0.22	1.0575	R	-	2.884
			33	0.23	1.0675	R	-	3.794
			34	0.33	1.0625	2.370	0.757	3.341
			34	0.33	1.0625	R	-	3.341
			35	0.36	1.0625	1.778	0.522	3.341
			36	0.40	1.0675	1.778	0.472	3.794
			36	0.33	1.0750	21.967	6.678	4.465
			36	0.40	1.0650	R	-	3.568
			36	0.33	1.0650	R	-	3.568
			38	0.50	1.0600	15.188	3.119	3.113
			41	0.53	1.0675	0.305	0.061	3.794
			41	0.52	1.0675	R	-	3.794
I	Myctophidae	*Symbolophorus californiensis*	25	0.14	1.0650	1.731	1.300	3.568
			29	0.22	1.0675	14.420	6.539	3.794
			30	0.26	1.0675	6.692	2.674	3.794
			31	0.32	1.0725	0.593	0.198	4.242
			35	0.40	1.0725	0	0	4.242
			42	0.81	1.0725	0.766	0.101	4.242
			42	0.84	1.0750	0	0	4.465
			43	0.83	1.0750	0	0	4.465
			45	0.99	1.0800	14.817	1.591	4.907
			61	2.29	1.0725	0.085	0.004	4.242
			64	2.78	1.0675	32.263	1.224	3.794
			68	3.71	1.0725	11.220	0.323	4.242
			70	4.05	1.0675	0	0	3.794
			72	4.21	1.0625	P	-	3.341
			73	4.54	1.0575	P	-	2.884

Table S3. (continued)

Group	Family	Species	L_S (mm)	W_W (g)	ρ_f	Gas vol. (mm^3)	Gas vol. (% total)	V_G (% total)
I	Myctophidae	*Symbolophorus californiensis*	74	5.33	1.0650	0	0	3.568
			75	5.46	1.0525	24.867	0.477	2.423
			78	6.37	1.0575	P	-	2.884
			86	6.79	1.0725	8.230	0.130	4.242
			88	7.24	1.0675	P	-	3.794
I	Ophidiidae	*Chilara taylori*	35	0.05	1.0600	0.305	0.642	3.113
			54	0.22	1.0675	0	0	3.794
			55	0.25	1.0600	8.586	3.513	3.113
I	Myctophidae	*Taaningichthys bathyphilus*	42	0.75	1.0575	27.937	3.790	2.884
			43	0.65	1.0625	71.679	10.488	3.341
			66	2.89	1.0625	106.913	3.782	3.341
I	Sternoptychidae	*Argyropelecus lychnus*	13	0.06	1.0675	9.262	14.147	3.794
			36	1.71	1.0625	P	-	3.341
			37	1.84	1.0625	P	-	3.341
I	Sternoptychidae	*Argyropelecus sladeni*	12	0.06	1.0675	10.750	16.055	3.794
			14	0.07	1.0625	16.095	19.634	3.341
			15	0.11	1.0650	R	-	3.568
			15	0.10	1.0525	12.869	11.929	2.423
			15	0.12	1.0575	5.421	4.560	2.884
			16	0.14	1.0675	17.095	11.532	3.794
			17	0.16	1.0675	20.816	12.195	3.794
			18	0.20	1.0725	6.236	3.236	4.242
			18	0.18	1.0725	8.482	4.811	4.242
			20	0.23	1.0525	10.611	4.631	2.423
			21	0.24	1.0525	31.817	12.245	2.423
			23	0.34	1.0500	32.002	8.994	2.190
			24	0.42	1.0675	31.017	7.307	3.794
			25	0.47	1.0525	P	-	2.423
			25	0.44	1.0650	55.440	11.831	3.568
			27	0.62	1.0700	48.366	7.704	4.019
			28	0.71	1.0550	103.145	13.290	2.654
			29	0.74	1.0650	201.376	22.470	3.568
			32	0.94	1.0425	255.488	22.079	1.487
			32	0.97	1.0725	P	-	4.242
			33	1.07	1.0675	150.072	13.022	3.794
			34	1.03	1.0700	P	-	4.019
			35	1.21	1.0625	165.837	12.711	3.341
			35	1.26	1.0725	P	-	4.242
			41	2.06	1.0675	107.300	5.267	3.794
			41	1.99	1.0600	200.273	9.640	3.113
I	Sternoptychidae	*Argyropelecus hemigymnus*	15	0.07	1.0625	R	-	3.341
			15	0.09	1.0675	6.692	7.353	3.794
			16	0.09	1.0725	11.476	12.031	4.242
			17	0.14	1.0650	12.096	8.426	3.568
			18	0.14	1.0625	11.981	8.335	3.341
			18	0.15	1.0600	28.881	16.950	3.113
			19	0.14	1.0575	40.889	23.597	2.884
			20	0.19	1.0600	R	-	3.113
			21	0.25	1.0675	P	-	3.794
			21	0.22	1.0675	9.223	4.284	3.794
			22	0.28	1.0625	81.056	23.523	3.341

Table S3. (continued)

Group	Family	Species	L_S (mm)	W_W (g)	ρ_f	Gas vol. (mm^3)	Gas vol. (% total)	V_G (% total)
I	Sternoptychidae	*Argyropelecus hemigymnus*	25	0.37	1.0625	3.836	1.090	3.341
			27	0.53	1.0625	P	-	3.341
			27	0.46	1.0650	43.461	9.142	3.568
			29	0.61	1.0625	P	-	3.341
			29	0.69	1.0625	P	-	3.341
			30	0.72	1.0575	P	-	2.884
I	Sternoptychidae	*Argyropelecus affinis*	14	0.06	1.0575	1.858	3.171	2.884
			15	0.06	1.0575	14.517	20.374	2.884
			17	0.10	1.0675	P	-	3.794
			17	0.09	1.0600	3.275	3.714	3.113
			20	0.14	1.0400	32.151	19.279	1.250
			21	0.21	1.0550	62.578	23.918	2.654
			28	0.42	1.0575	38.104	8.754	2.884
			33	0.71	1.0475	P	-	1.957
			44	2.17	1.0525	406.136	16.457	2.423
			45	2.02	1.0525	100.289	4.966	2.423
			47	2.38	1.0575	302.070	11.834	2.884
			49	2.53	1.0488	230.732	8.730	2.074
			49	2.79	1.0575	666.969	20.179	2.884
			55	3.22	1.0575	439.482	12.613	2.884
			65	5.82	1.0625	P	-	3.341
			66	6.43	1.0575	780.365	11.374	2.884
			76	10.70	1.0575	780.365	7.160	2.884
I	Howellidae	*Bathysphyraenops simplex*	17	0.06	1.0750	0.156	0.279	4.465
			19	0.09	1.0750	0	0	4.465
			19	0.07	1.0675	1.314	1.965	3.794
			20	0.09	1.0750	0.695	0.823	4.465
			20	0.08	1.0750	1.314	1.736	4.465
			20	0.08	1.0800	0.156	0.210	4.907
			47	1.82	1.0575	0.914	0.053	2.884
I	Gonostomatidae	*Cyclothone pseudopallida*	18	0.01	1.0600	R	-	3.113
			24	0.06	1.0575	1.434	2.465	2.884
			28	0.07	1.0500	R	-	2.190
			29	0.10	1.0525	0.156	0.164	2.423
			33	0.15	1.0575	4.146	2.840	2.884
			38	0.18	1.0575	9.328	5.195	2.884
			39	0.22	1.0575	8.126	3.759	2.884
			41	0.23	1.0550	4.280	1.925	2.654
			42	0.26	1.0550	1.975	0.795	2.654
			42	0.25	1.0525	1.778	0.743	2.423
			42	0.26	1.0550	2.439	0.980	2.654
			43	0.21	1.0600	R	-	3.113
I	Melamphaeidae	*Melamphaes simus*	15	0.07	1.0725	0.856	1.294	4.242
			15	0.06	1.0700	R	-	4.019
			16	0.08	1.0675	-	-	3.794
			16	0.05	1.0650	R	-	3.568
			29	0.56	1.0550	R	-	2.654
I	Sternoptychidae	*Sternoptyx obscura*	12	0.11	1.0525	R	-	2.423
			27	0.93	1.0525	48.419	5.195	2.423
			27	0.83	1.0525	114.311	12.660	2.423
			28	0.86	1.0575	65.243	7.427	2.884

Table S3. (continued)

Group	Family	Species	L_S (mm)	W_W (g)	ρ_f	Gas vol. (mm^3)	Gas vol. (% total)	V_G (% total)
I	Sternoptychidae	*Sternoptyx obscura*	30	1.14	1.0525	153.330	12.401	2.423
			31	1.57	1.0575	181.069	10.870	2.884
			41	3.37	1.0525	R	-	2.423
I	Sternoptychidae	*Sternoptyx diaphana*	14	0.17	1.0525	6.653	3.956	2.423
			19	0.45	1.0550	180.435	29.727	2.654
			23	0.75	1.0500	83.287	10.443	2.190
			25	1.00	1.0525	6.692	0.699	2.423
			32	2.35	1.0488	P	-	2.074
			35	1.90	1.0575	585.496	24.578	2.884
I	Gonostomatidae	*Cyclothone signata*	15	0.02	1.0575	0.702	3.581	2.884
			16	0.02	1.0575	1.075	5.380	2.884
			18	0.02	1.0525	0.966	4.836	2.423
			18	0.04	1.0600	1.314	3.366	3.113
			19	0.03	1.0575	0.836	2.864	2.884
			20	0.03	1.0575	R	-	2.884
			20	0.03	1.0625	R	-	3.341
			20	0.03	1.0650	0	0	3.568
			20	0.02	1.0750	R	-	4.465
			21	0.05	1.0550	R	-	2.654
			22	0.05	1.0625	4.390	8.532	3.341
			22	0.04	1.0775	1.717	4.420	4.687
			24	0.05	1.0500	3.160	6.224	2.190
			24	0.04	1.0475	3.541	8.486	1.957
			24	0.06	1.0575	1.434	2.465	2.884
			25	0.08	1.0525	1.873	2.405	2.423
			25	0.09	1.0550	5.609	6.169	2.654
			26	0.08	1.0525	R	-	2.423
			26	0.09	1.0525	1.873	2.143	2.423
			28	0.11	1.0500	6.321	5.690	2.190
			29	0.12	1.0500	2.963	2.527	2.190
			30	0.09	1.0575	R	-	2.884
			30	0.13	1.0475	1.405	1.119	1.957
			30	0.10	1.0575	1.561	1.624	2.884
			31	0.15	1.0475	10.993	7.130	1.957
			32	0.13	1.0500	3.170	2.497	2.190
			32	0.16	1.0475	15.802	9.376	1.957
			32	0.17	1.0500	0.305	0.188	2.190
			32	0.13	1.0600	9.876	7.453	3.113
			32	0.15	1.0550	1.314	0.916	2.654
			33	0.12	1.0600	R	-	3.113
			33	0.13	1.0575	9.328	7.053	2.884
			34	0.16	1.0500	14.800	8.853	2.190
			35	0.20	1.0575	R	-	2.884
			35	0.19	1.0550	2.439	1.336	2.654
			35	0.13	1.0600	R	-	3.113
I	Sternoptychidae	*Sternoptyx pseudobscura*	17	0.23	1.0475	2.439	1.098	1.957
			19	0.45	1.0500	4.280	0.989	2.190
			20	0.51	1.0475	0	0	1.957
			31	2.05	1.0575	P	-	2.884
			33	2.35	1.0575	554.979	19.983	2.884
			41	3.73	1.0475	R	-	1.957

Table S3. (continued)

Group	Family	Species	L_S (mm)	W_W (g)	ρ_f	Gas vol. (mm^3)	Gas vol. (% total)	V_G (% total)
I	Sternoptychidae	*Sternoptyx pseudobscura*	42	4.72	1.0475	R	-	1.957
			44	4.45	1.0525	1245.536	22.755	2.423
I	Myctophidae	*Diaphus theta*	14	0.04	1.0625	0.305	0.803	3.341
			15	0.05	1.0525	0.344	0.719	2.423
			15	0.05	1.0675	0.851	1.785	3.794
			17	0.07	1.0650	2.241	3.297	3.568
			17	0.08	1.0675	1.695	2.212	3.794
			18	0.08	1.0625	1.141	1.493	3.341
			24	0.25	1.0650	0.066	0.028	3.568
			28	0.46	1.0650	0.524	0.121	3.568
			28	0.37	1.0625	38.104	9.863	3.341
			30	0.50	1.0650	0	0	3.568
			31	0.51	1.0675	0.305	0.064	3.794
			32	0.71	1.0525	0	0	2.423
			33	0.58	1.0675	30.883	5.378	3.794
			34	0.64	1.0625	0	0	3.341
			35	0.86	1.0525	0	0	2.423
			35	0.86	1.0575	7.492	0.913	2.884
			38	1.05	1.0475	0	0	1.957
			38	1.05	1.0525	0	0	2.423
			38	1.01	1.0525	0	0	2.423
			40	1.12	1.0575	0	0	2.884
			41	1.17	1.0525	12.166	1.083	2.423
			45	1.66	1.0600	42.318	2.631	3.113
			45	1.61	1.0650	0	0	3.568
			47	1.75	1.0475	P	-	1.957
			48	1.98	1.0675	R	-	3.794
			54	2.96	1.0625	0	0	3.341
			54	2.58	1.0675	0	0	3.794
			54	2.69	1.0450	P	-	1.722
			55	2.95	1.0375	0	0	1.012
			55	2.99	1.0500	R	-	2.190
			65	5.35	1.0475	P	-	1.957
			73	7.03	1.0500	1.249	0.019	2.190
I	Myctophidae	*Triphoturus nigrescens*	32	0.22	1.0700	1.778	0.857	4.019
			33	0.27	1.0625	R	-	3.341
			33	0.24	1.0600	18.368	7.504	3.113
			41	0.61	1.0425	24.638	4.040	1.487
I	Melamphaeidae	*Scopeloberyx opisthopterus*	22	0.19	1.0525	0.066	0.036	2.423
			30	0.46	1.0450	4.877	1.096	1.722
			33	0.60	1.0375	0.324	0.056	1.012
I	Myctophidae	*Notolychnus valdiviae*	13	0.02	1.0575	0	0	2.884
			19	0.06	1.0400	0.305	0.526	1.250
			22	0.11	1.0375	0	0	1.012
			22	0.09	1.0400	0.461	0.530	1.250
			22	0.11	1.0400	0.222	0.209	1.250
			22	0.10	1.0425	0.324	0.337	1.487
			24	0.13	1.0375	0	0	1.012
			25	0.14	1.0450	R	-	1.722
I	Melamphaeidae	*Melamphaes suborbitalis*	24	0.19	1.0600	8.162	4.355	3.113
			25	0.26	1.0775	14.222	5.566	4.687

Table S3. (continued)

Group	Family	Species	L_S (mm)	W_W (g)	ρ_f	Gas vol. (mm^3)	Gas vol. (% total)	V_G (% total)
I	Melamphaeidae	*Melamphaes suborbitalis*	68	6.10	1.0400	P	-	1.250
I	Phosichthyidae	*Ichthyococcus irregularis*	24	0.37	1.0500	6.692	1.864	2.190
			29	0.63	1.0450	74.274	10.969	1.722
			36	1.09	1.0375	25.967	2.412	1.012
II	Melamphaeidae	*Melamphaes parvus*	21	0.23	1.0700	R	-	4.019
			26	0.43	1.0650	R	-	3.568
			29	0.44	1.0775	19.136	4.476	4.687
			45	2.11	1.0550	0	0	2.654
II	Gonostomatidae	*Cyclothone atraria*	21	0.06	1.0550	0	0	2.654
			24	0.06	1.0525	1.075	1.852	2.423
			26	0.08	1.0575	2.439	3.123	2.884
			28	0.14	1.0425	0	0	1.487
			30	0.15	1.0550	0	0	2.654
			32	0.12	1.0500	0	0	2.190
			32	0.15	1.0450	0	0	1.722
			41	0.30	1.0500	0	0	2.190
			45	0.45	1.0550	0	0	2.654
			47	0.47	1.0400	0	0	1.250
II	Myctophidae	*Nannobrachium hawaiiensis*	24	0.11	1.0600	0.527	0.505	3.113
			26	0.13	1.0525	0.390	0.315	2.423
			46	0.71	1.0525	1.249	0.185	2.423
			47	0.77	1.0575	0.288	0.040	2.884
			47	0.82	1.0475	0	0	1.957
			51	0.97	1.0525	1.778	0.193	2.423
			52	1.59	1.0575	0.856	0.057	2.884
			53	1.03	1.0500	0.836	0.085	2.190
			59	1.85	1.0525	2.751	0.156	2.423
			60	1.72	1.0425	0.749	0.045	1.487
			61	1.80	1.0525	3.026	0.177	2.423
			62	1.93	1.0550	11.476	0.623	2.654
			62	1.83	1.0475	1.778	0.102	1.957
			63	2.04	1.0475	1.358	0.070	1.957
			63	1.85	1.0525	3.843	0.218	2.423
			64	1.76	1.0550	3.773	0.226	2.654
			65	2.33	1.0475	4.302	0.193	1.957
			68	2.69	1.0500	0	0	2.190
			69	2.60	1.0525	1.829	0.074	2.423
			75	2.73	1.0500	0	0	2.190
			78	3.50	1.0450	0	0	1.722
			92	5.63	1.0475	0	0	1.957
II	Myctophidae	*Ceratoscopelus townsendi*	21	0.11	1.0550	0.305	0.292	2.654
			21	0.10	1.0550	0.176	0.185	2.654
			21	0.11	1.0650	2.743	2.587	3.568
			22	0.11	1.0575	0.390	0.374	2.884
			23	0.13	1.0625	0.629	0.512	3.341
			23	0.14	1.0625	5.267	3.844	3.341
			23	0.14	1.0650	0.856	0.647	3.568
			23	0.14	1.0625	1.249	0.939	3.341
			23	0.14	1.0650	0.836	0.632	3.568
			26	0.21	1.0650	9.659	4.670	3.568
			27	0.23	1.0700	5.463	2.478	4.019

Table S3. (continued)

Group	Family	Species	L_S (mm)	W_W (g)	ρ_f	Gas vol. (mm^3)	Gas vol. (% total)	V_G (% total)
II	Myctophidae	*Ceratoscopelus townsendi*	27	0.25	1.0650	10.313	4.208	3.568
			28	0.21	1.0825	15.822	7.541	5.127
			28	0.25	1.0650	10.891	4.434	3.568
			30	0.31	1.0750	13.808	4.569	4.465
			31	0.36	1.0650	19.185	5.371	3.568
			32	0.40	1.0675	0.020	0.005	3.794
			32	0.40	1.0700	32.631	8.028	4.019
			33	0.46	1.0625	17.975	3.986	3.341
			37	0.62	1.0700	29.276	4.809	4.019
			37	0.65	1.0675	0	0	3.794
			39	0.91	1.0575	12.232	1.402	2.884
			39	0.89	1.0575	0	0	2.884
			40	0.82	1.0600	0	0	3.113
			42	1.14	1.0625	0	0	3.341
			42	1.08	1.0575	0	0	2.884
			42	1.10	1.0525	0	0	2.423
			45	1.32	1.0550	0	0	2.654
			46	1.45	1.0375	0	0	1.012
			46	1.46	1.0600	0	0	3.113
			50	2.08	1.0425	0	0	1.487
			50	1.85	1.0475	0	0	1.957
			50	1.90	1.0500	0	0	2.190
			51	2.21	1.0375	0	0	1.012
			52	2.02	1.0575	0	0	2.884
			52	1.73	1.0525	0	0	2.423
			53	2.38	1.0375	0	0	1.012
			53	2.47	1.0425	0	0	1.487
			53	2.22	1.0475	0	0	1.957
			54	2.34	1.0375	0	0	1.012
			54	2.33	1.0475	0	0	1.957
			57	2.57	1.0475	0	0	1.957
			60	2.83	1.0425	0	0	1.487
II	Melamphaeidae	*Scopelogadus mizolepis*	25	0.27	1.0525	0	0	2.423
			29	0.33	1.0575	0.066	0.021	2.884
			39	0.79	1.0575	1.553	0.208	2.884
			40	1.11	1.0525	0	0	2.423
			40	1.10	1.0575	0.836	0.080	2.884
			42	1.26	1.0550	0	0	2.654
			42	1.42	1.0525	0	0	2.423
			48	2.03	1.0525	2.746	0.142	2.423
			55	3.30	1.0525	0	0	2.423
			58	3.55	1.0500	0	0	2.190
			60	3.92	1.0450	0	0	1.722
			61	4.72	1.0475	0	0	1.957
			61	4.32	1.0500	0	0	2.190
			62	4.02	1.0525	0	0	2.423
			63	5.54	1.0475	0	0	1.957
			68	6.66	1.0475	0	0	1.957
			69	6.40	1.0425	0	0	1.487
			74	9.28	1.0475	0	0	1.957
			83	12.96	1.0375	0	0	1.012

Table S3. (continued)

Group	Family	Species	L_S (mm)	W_W (g)	ρ_f	Gas vol. (mm^3)	Gas vol. (% total)	V_G (% total)
II	Melamphaeidae	*Poromitra crassiceps*	20	0.09	1.0550	6.982	7.565	2.654
			25	0.16	1.0625	R	-	3.341
			26	0.19	1.0450	0	0	1.722
			27	0.20	1.0550	17.253	8.342	2.654
			28	0.26	1.0575	0.610	0.247	2.884
			28	0.26	1.0475	0.195	0.079	1.957
			33	0.50	1.0525	2.653	0.555	2.423
			33	0.48	1.0450	0.288	0.063	1.722
			34	0.65	1.0475	22.889	3.557	1.957
			39	0.84	1.0525	0.371	0.046	2.423
			42	1.22	1.0425	2.129	0.182	1.487
			49	2.28	1.0475	P	-	1.957
			51	2.56	1.0425	0.222	0.009	1.487
			60	4.01	1.0425	0.256	0.007	1.487
II	Myctophidae	*Nannobrachium ritteri*	19	0.06	1.0500	0	0	2.190
			25	0.11	1.0525	0	0	2.423
			25	0.12	1.0525	0.527	0.460	2.423
			28	0.14	1.0450	0.836	0.620	1.722
			28	0.17	1.0475	1.249	0.763	1.957
			28	0.14	1.0575	1.717	1.280	2.884
			29	0.17	1.0500	1.195	0.733	2.190
			30	0.21	1.0500	2.439	1.205	2.190
			32	0.26	1.0475	0.020	0.008	1.957
			32	0.26	1.0500	1.434	0.576	2.190
			33	0.29	1.0475	0	0	1.957
			33	0.26	1.0525	0	0	2.423
			34	0.31	1.0425	0.683	0.229	1.487
			34	0.46	1.0425	0	0	1.487
			34	0.31	1.0425	0	0	1.487
			35	0.31	1.0525	0	0	2.423
			35	0.30	1.0500	3.182	1.102	2.190
			36	0.38	1.0450	0	0	1.722
			36	0.33	1.0450	3.312	1.038	1.722
			36	0.36	1.0475	1.668	0.483	1.957
			36	0.35	1.0475	2.695	0.800	1.957
			37	0.40	1.0450	2.765	0.717	1.722
			37	0.37	1.0450	0	0	1.722
			37	0.41	1.0425	0.222	0.056	1.487
			39	0.46	1.0425	0.832	0.188	1.487
			39	0.49	1.0400	3.358	0.708	1.250
			40	0.64	1.0400	0	0	1.250
			40	0.54	1.0425	0	0	1.487
			41	0.57	1.0425	0	0	1.487
			43	0.68	1.0375	0	0	1.012
			44	0.68	1.0425	2.836	0.433	1.487
			45	0.76	1.0425	0	0	1.487
			45	0.79	1.0425	0.156	0.021	1.487
			45	0.69	1.0375	0	0	1.012
			45	0.82	1.0375	0	0	1.012
			48	0.98	1.0375	0	0	1.012
			49	0.92	1.0375	0	0	1.012

Table S3. (continued)

Group	Family	Species	L_S (mm)	W_W (g)	ρ_f	Gas vol. (mm^3)	Gas vol. (% total)	V_G (% total)
II	Myctophidae	*Nannobrachium ritteri*	49	1.11	1.0375	0	0	1.012
			49	1.12	1.0375	0	0	1.012
			49	1.09	1.0375	0	0	1.012
			51	1.38	1.0375	0	0	1.012
			51	1.32	1.0325	0	0	0.533
			55	1.56	1.0350	0	0	0.773
			58	1.79	1.0375	0	0	1.012
			59	1.90	1.0325	0	0	0.533
			77	4.66	1.0285	0	0	0.146
			78	4.82	1.0300	0	0	0.291
			82	4.79	1.0325	0	0	0.533
			85	5.91	1.0363	0	0	0.893
			85	6.50	1.0325	0	0	0.533
			90	8.30	1.0325	0	0	0.533
			91	7.50	1.0285	0	0	0.146
			93	8.36	1.0313	0	0	0.412
			93	8.48	1.0285	0	0	0.146
			94	8.68	1.0325	0	0	0.533
			94	8.10	1.0338	0	0	0.653
II	Myctophidae	*Triphoturus mexicanus*	17	0.04	1.0475	1.141	2.902	1.957
			18	0.03	1.0425	1.778	5.818	1.487
			19	0.05	1.0425	0	0	1.487
			19	0.06	1.0475	0	0	1.957
			20	0.05	1.0525	3.246	6.396	2.423
			20	0.06	1.0475	R	-	1.957
			21	0.05	1.0450	3.246	6.353	1.722
			21	0.05	1.0475	0.156	0.326	1.957
			22	0.07	1.0550	2.439	3.545	2.654
			22	0.04	1.0425	2.497	6.111	1.487
			26	0.12	1.0450	0	0	1.722
			27	0.13	1.0525	1.434	1.148	2.423
			27	0.12	1.0550	0.390	0.342	2.654
			27	0.14	1.0425	0.066	0.049	1.487
			29	0.18	1.0450	0.324	0.188	1.722
			30	0.19	1.0425	1.141	0.622	1.487
			31	0.22	1.0425	0	0	1.487
			32	0.26	1.0375	0	0	1.012
			32	0.26	1.0400	0.312	0.125	1.250
			32	0.25	1.0450	0.324	0.135	1.722
			33	0.28	1.0375	0	0	1.012
			33	0.30	1.0375	1.210	0.417	1.012
			34	0.30	1.0375	0.461	0.159	1.012
			34	0.24	1.0425	0.549	0.238	1.487
			34	0.25	1.0400	0	0	1.250
			34	0.29	1.0375	0	0	1.012
			35	0.35	1.0325	0	0	0.533
			36	0.42	1.0375	0	0	1.012
			36	0.35	1.0325	0	0	0.533
			36	0.38	1.0375	0	0	1.012
			36	0.41	1.0350	0	0	0.773
			38	0.41	1.0350	0	0	0.773

Table S3. (continued)

Group	Family	Species	L_S (mm)	W_W (g)	ρ_f	Gas vol. (mm^3)	Gas vol. (% total)	V_G (% total)
II	Myctophidae	*Triphoturus mexicanus*	39	0.43	1.0325	0	0	0.533
			40	0.56	1.0325	0	0	0.533
			46	0.79	1.0325	0	0	0.533
			48	0.94	1.0325	0	0	0.533
			50	1.10	1.0325	0	0	0.533
			51	1.15	1.0325	0	0	0.533
			51	1.01	1.0325	0	0	0.533
			52	1.23	1.0300	0	0	0.291
			52	1.20	1.0338	0	0	0.653
			52	1.20	1.0285	0	0	0.146
			55	1.58	1.0285	0	0	0.146
			56	1.70	1.0325	0	0	0.533
			58	1.95	1.0338	0	0	0.653
			58	1.92	1.0325	0	0	0.533
			59	1.79	1.0325	0	0	0.533
			59	1.47	1.0325	0	0	0.533
			64	2.09	1.0300	0	0	0.291
			66	2.55	1.0325	0	0	0.533
			66	2.12	1.0285	0	0	0.146
			68	2.82	1.0325	0	0	0.533
II	Myctophidae	*Stenobrachius leucopsarus*	20	0.07	1.0475	0.480	0.714	1.957
			21	0.07	1.0500	0.344	0.513	2.190
			21	0.09	1.0500	0	0	2.190
			22	0.08	1.0575	1.931	2.490	2.884
			22	0.10	1.0500	1.180	1.224	2.190
			25	0.17	1.0425	1.053	0.642	1.487
			25	0.13	1.0450	7.928	5.991	1.722
			26	0.16	1.0450	0.156	0.102	1.722
			26	0.20	1.0350	0.324	0.168	0.773
			26	0.17	1.0375	8.230	4.783	1.012
			27	0.18	1.0375	6.692	3.714	1.012
			27	0.17	1.0375	19.509	10.640	1.012
			28	0.22	1.0375	2.439	1.137	1.012
			29	0.21	1.0375	67.777	25.085	1.012
			30	0.27	1.0375	0.039	0.015	1.012
			31	0.32	1.0375	3.121	1.002	1.012
			31	0.33	1.0325	2.056	0.639	0.533
			31	0.28	1.0325	2.261	0.827	0.533
			32	0.30	1.0350	0.527	0.181	0.773
			32	0.34	1.0350	0	0	0.773
			32	0.34	1.0375	0	0	1.012
			33	0.47	1.0325	0	0	0.533
			33	0.42	1.0325	0	0	0.533
			34	0.35	1.0325	0	0	0.533
			34	0.39	1.0375	0	0	1.012
			34	0.38	1.0375	0.176	0.048	1.012
			34	0.43	1.0375	16.458	3.819	1.012
			35	0.48	1.0325	0	0	0.533
			35	0.45	1.0325	0	0	0.533
			35	0.52	1.0350	0	0	0.773
			36	0.49	1.0350	0.832	0.175	0.773

Table S3. (continued)

Group	Family	Species	L_S (mm)	W_W (g)	ρ_T	Gas vol. (mm^3)	Gas vol. (% total)	V_G (% total)
II	Myctophidae	*Stenobrachius leucopsarus*	37	0.57	1.0325	0	0	0.533
			37	0.48	1.0285	0.156	0.033	0.146
			37	0.53	1.0325	0	0	0.533
			38	0.54	1.0325	0	0	0.533
			39	0.63	1.0325	0	0	0.533
			40	0.62	1.0285	0	0	0.146
			42	0.83	1.0325	0	0	0.533
			42	0.82	1.0325	0	0	0.533
			44	0.94	1.0285	0	0	0.146
			47	1.07	1.0270	0	0	0.000
			52	1.78	1.0285	0	0	0.146
			53	1.66	1.0270	0	0	0.000
			54	1.62	1.0285	0	0	0.146
			57	2.15	1.0270	0	0	0.000
			60	2.28	1.0270	0	0	0.000
			60	2.67	1.0285	0	0	0.146
			61	2.65	1.0270	0	0	0.000
			62	2.77	1.0270	0	0	0.000
			63	3.10	1.0285	0	0	0.146
			67	4.02	1.0285	0	0	0.146
			67	3.63	1.0285	0	0	0.146
			72	4.23	1.0285	0	0	0.146
			75	5.36	1.0313	0	0	0.412
			76	4.56	1.0325	0	0	0.533
			76	4.91	1.0280	0	0	0.097
			83	6.65	1.0280	0	0	0.097
II	Myctophidae	*Nannobrachium regale*	23	0.10	1.0525	14.222	13.020	2.423
			26	0.14	1.0575	3.246	2.393	2.884
			29	0.16	1.0550	8.733	5.445	2.654
			33	0.20	1.0650	1.429	0.755	3.568
			39	0.51	1.0625	0	0	3.341
			43	0.55	1.0550	1.775	0.339	2.654
			46	0.71	1.0525	0.198	0.029	2.423
			48	0.97	1.0525	1.075	0.117	2.423
			48	1.09	1.0525	46.334	4.282	2.423
			51	1.24	1.0425	2.651	0.222	1.487
			51	1.13	1.0525	7.023	0.650	2.423
			51	1.08	1.0725	42.862	4.083	4.242
			53	1.41	1.0525	2.029	0.151	2.423
			53	1.52	1.0475	10.398	0.711	1.957
			61	2.11	1.0525	0.156	0.008	2.423
			61	2.07	1.0475	1.229	0.062	1.957
			79	4.81	1.0438	0	0	1.605
			99	8.92	1.0438	0	0	1.605
			134	27.31	1.0285	0	0	0.146
II	Melamphaeidae	*Melamphaes lugubris*	22	0.18	1.0625	2.439	1.419	3.341
			26	0.35	1.0675	0	0	3.794
			26	0.35	1.0525	11.476	3.336	2.423
			32	0.72	1.0675	8.230	1.206	3.794
			39	1.13	1.0650	P	-	3.568
			43	1.86	1.0625	62.705	3.458	3.341

Table S3. (continued)

Group	Family	Species	L_S (mm)	W_W (g)	ρ_f	Gas vol. (mm^3)	Gas vol. (% total)	V_G (% total)
II	Melamphaeidae	*Melamphaes lugubris*	50	2.84	1.0425	30.815	1.118	1.487
			75	13.30	1.0285	0	0	0.146
			79	14.65	1.0285	0	0	0.146
III	Scopelarchidae	*Scopelarchus stephensi*	25	0.17	1.0700	0	0	4.019
			38	0.50	1.0825	0	0	5.127
			55	1.87	1.0800	0	0	4.907
III	Notosudidae	*Scopelosaurus harryi*	43	0.16	1.0625	0	0	3.341
			48	0.26	1.0600	0	0	3.113
			48	0.28	1.0600	0	0	3.113
			50	0.28	1.0575	0	0	2.884
			52	0.34	1.0625	0	0	3.341
III	Paralepididae	*Arctozenus risso*	35	0.05	1.0800	0	0	4.907
			40	0.11	1.0675	0	0	3.794
			53	0.22	1.0650	0	0	3.568
			55	0.23	1.0625	0	0	3.341
			56	0.27	1.0625	0	0	3.341
			124	2.32	1.0550	0	0	2.654
III	Stomiidae	*Chauliodus macouni*	30	0.10	1.0550	0	0	2.654
			34	0.10	1.0475	0	0	1.957
			38	0.13	1.0450	0	0	1.722
			83	1.79	1.0525	0	0	2.423
			113	4.07	1.0525	0	0	2.423
			122	6.41	1.0475	0	0	1.957
III	Stomiidae	*Aristostomias xenostoma*	33	0.18	1.0500	0	0	2.190
			38	0.23	1.0500	0	0	2.190
			38	0.22	1.0475	0	0	1.957
			39	0.28	1.0500	0	0	2.190
			41	0.30	1.0500	0	0	2.190
III	Bathylagidae	*Leuroglossus stilbius*	25	0.14	1.0525	0	0	2.423
			26	0.16	1.0475	0	0	1.957
			26	0.13	1.0400	0	0	1.250
			26	0.13	1.0375	0	0	1.012
			29	0.18	1.0500	0	0	2.190
			29	0.19	1.0500	0	0	2.190
III	Stomiidae	*Photonectes parvimanus*	30	0.15	1.0450	0	0	1.722
			32	0.16	1.0450	0	0	1.722
			32	0.17	1.0425	0	0	1.487
			33	0.20	1.0475	0	0	1.957
			33	0.19	1.0475	0	0	1.957
			67	1.37	1.0475	0	0	1.957
III	Platytroctidae	*Holtbyrnia latifrons*	20	0.06	1.0475	0	0	1.957
			21	0.05	1.0525	0	0	2.423
			22	0.05	1.0525	0	0	2.423
			24	0.07	1.0525	0	0	2.423
			32	0.25	1.0475	0	0	1.957
			52	1.08	1.0475	0	0	1.957
III	Platytroctidae	*Sagamichthys abei*	27	0.14	1.0525	0	0	2.423
			28	0.13	1.0475	0	0	1.957
			28	0.14	1.0475	0	0	1.957
			36	0.36	1.0525	0	0	2.423
			67	3.00	1.0475	0	0	1.957

Table S3. (continued)

Group	Family	Species	L_S (mm)	W_W (g)	ρ_f	Gas vol. (mm^3)	Gas vol. (% total)	V_G (% total)
III	Alepocephalidae	*Alepocephalus tenebrosus*	27	0.10	1.0425	0	0	1.487
			35	0.27	1.0475	0	0	1.957
			47	1.03	1.0500	0	0	2.190
			50	1.11	1.0425	0	0	1.487
III	Stomiidae	*Bathophilus flemingi*	34	0.31	1.0425	0	0	1.487
			35	0.19	1.0475	0	0	1.957
			42	0.32	1.0425	0	0	1.487
			43	0.33	1.0475	0	0	1.957
			43	0.41	1.0475	0	0	1.957
			46	0.43	1.0475	0	0	1.957
III	Gonostomatidae	*Cyclothone acclinidens*	25	0.07	1.0525	0	0	2.423
			25	0.07	1.0525	0	0	2.423
			26	0.09	1.0500	0	0	2.190
			28	0.10	1.0700	0	0	4.019
			29	0.22	1.0775	0	0	4.687
			29	0.31	1.0775	0	0	4.687
			29	0.14	1.0475	0	0	1.957
			29	0.11	1.0500	0	0	2.190
			30	0.14	1.0575	0	0	2.884
			31	0.17	1.0475	0	0	1.957
			31	0.13	1.0625	0	0	3.341
			32	0.15	1.0525	0	0	2.423
			33	0.14	1.0550	0	0	2.654
			33	0.16	1.0575	0	0	2.884
			33	0.16	1.0525	0	0	2.423
			33	0.18	1.0475	0	0	1.957
			35	0.15	1.0425	0	0	1.487
			35	0.23	1.0475	0	0	1.957
			37	0.27	1.0475	0	0	1.957
			40	0.31	1.0475	0	0	1.957
			41	0.19	1.0475	0	0	1.957
			42	0.46	1.0475	0	0	1.957
			43	0.16	1.0475	0	0	1.957
			44	0.40	1.0425	0	0	1.487
			45	0.47	1.0425	0	0	1.487
			46	0.56	1.0475	0	0	1.957
			46	0.48	1.0475	0	0	1.957
			46	0.47	1.0425	0	0	1.487
			47	0.39	1.0500	0	0	2.190
			47	0.49	1.0450	0	0	1.722
			48	0.48	1.0475	0	0	1.957
			49	0.51	1.0525	0	0	2.423
			50	0.70	1.0450	0	0	1.722
			50	0.52	1.0450	0	0	1.722
			51	0.60	1.0425	0	0	1.487
			51	0.66	1.0425	0	0	1.487
			51	0.66	1.0425	0	0	1.487
			51	0.80	1.0375	0	0	1.012
			51	0.63	1.0475	0	0	1.957
			52	0.75	1.0425	0	0	1.487
			52	0.61	1.0425	0	0	1.487

Table S3. (continued)

Group	Family	Species	L_S (mm)	W_W (g)	ρ_f	Gas vol. (mm^3)	Gas vol. (% total)	V_G (% total)
III	Gonostomatidae	*Cyclothone acclinidens*	55	0.88	1.0450	0	0	1.722
			58	0.35	1.0375	0	0	1.012
			61	1.07	1.0375	0	0	1.012
III	Gonostomatidae	*Cyclothone pallida*	30	0.12	1.0400	0	0	1.250
			40	0.24	1.0575	0	0	2.884
			54	0.71	1.0400	0	0	1.250
			56	0.82	1.0400	0	0	1.250
			62	1.04	1.0425	0	0	1.487
			68	1.37	1.0475	0	0	1.957
III	Bathylagidae	*Bathylagoides wesethi*	24	0.13	1.0425	0	0	1.487
			25	0.10	1.0525	0	0	2.423
			25	0.13	1.0500	0	0	2.190
			27	0.15	1.0575	0	0	2.884
			28	0.16	1.0575	0	0	2.884
			28	0.19	1.0475	0	0	1.957
			28	0.18	1.0475	0	0	1.957
			30	0.28	1.0500	0	0	2.190
			30	0.23	1.0525	0	0	2.423
			30	0.14	1.0525	0	0	2.423
			30	0.18	1.0450	0	0	1.722
			30	0.21	1.0425	0	0	1.487
			30	0.14	1.0600	0	0	3.113
			31	0.27	1.0525	0	0	2.423
			31	0.19	1.0525	0	0	2.423
			32	0.31	1.0475	0	0	1.957
			33	0.32	1.0575	0	0	2.884
			33	0.30	1.0575	0	0	2.884
			35	0.29	1.0575	0	0	2.884
			36	0.40	1.0450	0	0	1.722
			37	0.40	1.0525	0	0	2.423
			37	0.36	1.0550	0	0	2.654
			39	0.57	1.0325	0	0	0.533
			41	0.66	1.0425	0	0	1.487
			41	0.67	1.0425	0	0	1.487
			41	0.65	1.0425	0	0	1.487
			42	0.67	1.0525	0	0	2.423
			42	0.64	1.0450	0	0	1.722
			43	0.70	1.0575	0	0	2.884
			44	0.84	1.0425	0	0	1.487
			44	0.72	1.0475	0	0	1.957
			45	0.78	1.0525	0	0	2.423
			45	0.85	1.0425	0	0	1.487
			47	0.94	1.0500	0	0	2.190
			49	0.99	1.0450	0	0	1.722
			49	1.00	1.0500	0	0	2.190
			50	1.32	1.0450	0	0	1.722
			51	1.27	1.0425	0	0	1.487
			52	1.38	1.0375	0	0	1.012
			53	1.44	1.0425	0	0	1.487
			53	1.44	1.0425	0	0	1.487
			55	1.61	1.0475	0	0	1.957

Table S3. (continued)

Group	Family	Species	L_S (mm)	W_W (g)	ρ_T	Gas vol. (mm^3)	Gas vol. (% total)	V_G (% total)
III	Bathylagidae	*Bathylagoides wesethi*	56	1.48	1.0425	0	0	1.487
			57	1.67	1.0425	0	0	1.487
			58	1.51	1.0450	0	0	1.722
			60	1.77	1.0475	0	0	1.957
			61	1.91	1.0450	0	0	1.722
			62	1.92	1.0475	0	0	1.957
			63	2.10	1.0425	0	0	1.487
			63	2.21	1.0425	0	0	1.487
			64	2.43	1.0425	0	0	1.487
			66	2.46	1.0400	0	0	1.250
			69	3.39	1.0425	0	0	1.487
			70	3.45	1.0425	0	0	1.487
			76	4.20	1.0375	0	0	1.012
III	Stomiidae	*Tactostoma macropus*	76	0.40	1.0475	0	0	1.957
			215	13.14	1.0363	0	0	0.893
			226	18.74	1.0413	0	0	1.369
			254	30.13	1.0363	0	0	0.893
III	Stomiidae	*Stomias atriventer*	139	6.90	1.0400	0	0	1.250
			153	9.40	1.0425	0	0	1.487
			156	13.30	1.0400	0	0	1.250
			187	20.54	1.0375	0	0	1.012
III	Myctophidae	*Parvilux ingens*	80	3.87	1.0475	0	0	1.957
			91	5.78	1.0425	0	0	1.487
			99	7.89	1.0438	0	0	1.605
			120	15.66	1.0413	0	0	1.369
			128	17.29	1.0425	0	0	1.487
			160	44.14	1.0363	0	0	0.893
III	Stomiidae	*Idiacanthus antrostomus*	58	0.09	1.0625	0	0	3.341
			66	0.15	1.0525	0	0	2.423
			68	0.14	1.0525	0	0	2.423
			71	0.16	1.0575	0	0	2.884
			73	0.13	1.0525	0	0	2.423
			73	0.16	1.0675	0	0	3.794
			73	0.26	1.0475	0	0	1.957
			75	0.18	1.0525	0	0	2.423
			79	0.27	1.0525	0	0	2.423
			91	0.34	1.0500	0	0	2.190
			115	0.88	1.0438	0	0	1.605
			143	2.87	1.0413	0	0	1.369
			153	1.43	1.0438	0	0	1.605
			153	1.89	1.0525	0	0	2.423
			162	3.03	1.0363	0	0	0.893
			163	2.14	1.0375	0	0	1.012
			177	1.67	1.0438	0	0	1.605
			178	2.40	1.0413	0	0	1.369
			197	2.35	1.0438	0	0	1.605
			329	15.99	1.0375	0	0	1.012
			385	25.89	1.0338	0	0	0.653
III	Bathylagidae	*Lipolagus ochotensis*	25	0.10	1.0475	0	0	1.957
			29	0.14	1.0525	0	0	2.423
			31	0.26	1.0425	0	0	1.487

Table S3. (continued)

Group	Family	Species	L_S (mm)	W_W (g)	ρ_f	Gas vol. (mm^3)	Gas vol. (% total)	V_G (% total)
III	Bathylagidae	*Lipolagus ochotensis*	32	0.28	1.0500	0	0	2.190
			36	0.42	1.0475	0	0	1.957
			42	0.63	1.0475	0	0	1.957
			45	0.82	1.0500	0	0	2.190
			45	0.80	1.0475	0	0	1.957
			45	0.78	1.0525	0	0	2.423
			48	1.01	1.0475	0	0	1.957
			74	3.40	1.0325	0	0	0.533
			110	12.25	1.0338	0	0	0.653
III	Myctophidae	*Lobianchia gemellarii*	55	2.93	1.0450	0	0	1.722
			57	3.25	1.0400	0	0	1.250
			65	4.83	1.0350	0	0	0.773
(epip.)	Carangidae	*Seriola lalandi*	83	12.39	1.0775	P	0	4.687
(epip.)	Scomberesocidae	*Cololabis saira*	33	0.13	1.0875	0	0	5.563
			157	15.35	1.0775	P	-	4.687
-	Nemichthyidae	*Nemichthys scolopaceus*	544	3.64	1.0675	0	0	3.794
-	Platytroctidae	*Mirorictus taningi*	47	0.83	1.0475	0	0	1.957
-	Gonostomatidae	*Diplophos taenia*	33	0.05	1.0750	2.614	0	4.465
			40	0.08	1.0725	0.020	0	4.242
-	Sternoptychidae	*Valenciennellus tripunctulatis*	24	0.17	1.0775	0.156	0	4.687
			28	0.19	1.0700	R	0	4.019
-	Phosichthyidae	*Vinciguerria lucetia*	18	0.06	1.0650	2.439	4.150	3.568
			24	0.15	1.0700	0.156	0.111	4.019
-	Stomiidae	*Aristostomias scintillans*	43	0.36	1.0500	0	0	2.190
-	Stomiidae	*Opostomias mitsuii*	65	1.07	1.0475	0	0	1.957
-	Stomiidae	*Eustomias* sp.	64	0.37	1.0475	0	0	1.957
-	Stomiidae	*Photonectes* sp.	31	0.13	1.0475	0	0	1.957
			40	0.24	1.0450	0	0	1.722
-	Stomiidae	*Bathophilus kingi*	76	1.93	1.0425	0	0	1.487
-	Stomiidae	*Bathophilus pawneei*	22	0.08	1.0525	0	0	2.423
-	Stomiidae	*Astronesthes nigroides*	28	0.23	1.0475	0	0	1.957
-	Scopelarchidae	*Scopelarchus analis*	36	0.30	1.0750	0	0	4.465
-	Scopelarchidae	*Scopelarchus guentheri*	34	0.14	1.0650	0	0	3.568
			38	0.23	1.0700	0	0	4.019
-	Paralepididae	*Lestidiops ringens*	85	0.69	1.0700	0	0	4.019
			90	0.96	1.0675	0	0	3.794
-	Paralepididae	*Lestidiops pacificum*	68	0.68	1.0500	0	0	2.190
-	Myctophidae	*Diaphus phillipsi*	43	1.42	1.0775	30.059	0	4.687
-	Myctophidae	*Nannobrachium bristori*	106	11.60	1.043	0	0	1.487
-			121	14.48	1.043	0	0	1.487
-	Myctophidae	*Nannobrachium lineatum*	57	1.12	1.0525	P	0	2.423
-	Melamphaeidae	*Melamphaes polylepis*	90	16.24	1.0250	0	0	-0.195
-	Melamphaeidae	*Melamphaes laeviceps*	16	0.08	1.0625	0	0	3.341

Table S4. Swimbladder inflation, lipid content, and body specific gravity for species in this and previous studies. In the "Gas" column, ratios represent the fraction of animals containing gas in their swimbladder. High lipid levels are defined as >9% of wet weight or 40% of dry weight. Dense density refers to species which were identified as dense-bodied, but for which no measurements were reported. Brackets indicate data from this study. Numbered references are listed in the table footnote. Species are ordered as in Table S3, and omitted where no data are available.

Fish group	Species	Gas	Lipid content	Density (g ml^{-1}) or specific gravity
I	*T. crenularis*	9/14 < 34 mm, 4/19 > 30 mm[5]; some[22]; 3/90 trawl, 66/128 surface[24]; 13/25[13]; 7/9[15]; no gas[7]; increases with L_S[13,24]; [12/20]	Low[5,7,22,25]; does not increase with L_S[5,22]	1.086-1.089[5]; 1.074-1.080[22]; 1.055-1.080[13]; [1.055-1.080]
I	*H. reinhardtii*	Gas[3]; [4/4]	Low[7,34]	[1.063-1.078]
I	*N. resplendens*	Gas[4,22,29]; increases with L_S[29]; [2/5]	Low[19,22,34]; high[31]	1.050[22]; [1.070-1.078]
I	*D. atlanticus*	Gas[4,20,29]; increases with L_S[29]; [24/25]	-	[1.055-1.080]
I	*M. nitidulum*	Gas[4,10,22,33]; increases with L_S[4,10,33]; [15/17]	Low[17,22,19,34]	1.050[22]; [1.060-1.078]
I	*E. risso*	Gas[18,20]; increases with L_S[18]; [2/3]	-	[1.070-1.073]
I	*H. proximum*	-	Low[32]	[1.065-1.075]
I	*P. crockeri*	Gas[5,7,15,22,28];44/51[13]; [19/28]	Low[5,22]	Dense[22]; 1.065-1.080[13]; [1.058-1.083]
I	*L. urophaos*	Gas[4,29]; smaller fish only[22]; increases with L_S[4,29]; decr. with L_S[22]; [10/12]	High, increases with L_S[22]	1.030-1.044[22]; [1.050-1.078]
I	*B. longipes*	Gas[22]; [4/4]	Low[8,22]	Dense[22]; [1.068-1.073]
I	*C. warmingii*	Gas, increases with L_S[4,29,38]; [18/18]	Low[8,9,32]; high[1,30,31]	1.036[38]; [1.050-1.073]
I	*V. nimbaria*	Gas[20]; [9/9]	Low[8]	[1.060-1.070]
I	*V. poweriae*	Gas, increases with L_S[4,18,29]	-	[1.060-1.078]
I	*D. fulgens*	[7/7]	Low[17]	[1.068-1.075]
I	*L. tenuiformis*	[10/13]	Low[8]	[1.060-1.073]
I	*M. microstoma*	Gas[20]; [5/6]	-	[1.058-1.070]
I	*D. oculatus*	Gas[23]; [23/23]	Low[8,23,26]	[1.058-1.075]
I	*S. californiensis*	Gas[3,7,15]; dipnet only[22]; no gas[36]; 7/90 trawl, 267/289 surface, increases with L_S[24]; [15/20]	Low[25]; high[30,31,32]; seasonally high, increases with L_S[22]	1.044-1.060[22]; [1.053-1.080]
I	*C. taylori*	Gas[27]	-	[1.060-1.068]
I	*T. bathyphilus*	Gas[4,22,29]; increases with L_S[4,29]; [3/3]	Low[8,22,34]	Dense[22]; [1.058-1.063]
I	*A. lychnus*	Gas[6,7,16]	Low[7]	[1.063-1.068]
I	*A. sladeni*	Gas[6,7,20,23,28]; increases with L_S[28]; [26/26]	Low[1,7,19,23]	[1.043-1.073]
I	*A. hemigymnus*	Gas[4,18,20,29]; increases with L_S[4,18,29]; [17/17]	Low[34]	1.050[29]; [1.058-1.073]
I	*A. affinis*	Gas[6,7,16,23]; [17/17]	Low[1,7,23]	[1.040-1.068]
I	*C. pseudopallida*	Gas[21]; [12/12]	Low[8,17,26]	[1.050-1.060]
I	*M. simus*	Gas[11]; [4/5]	'-	[1.055-1.073]
I	*S. obscura*	Gas[7,16]; [7/7]	Low[7]	[1.053-1.058]
I	*S. diaphana*	Gas[4,20,29,33]; incr. with L_S[4,29,33]; [6/6]	Low[1,8,17,19,34]	[1.049-1.058]
I	*C. signata*	Gas[21,23]; [35/36]	Low[1,23,26]	[1.048-1.078]

Table S4. (continued)

Fish group	Species	Gas	Lipid content	Density (g ml^{-1}) or specific gravity
I	*S. pseudobscura*	-	Low[34]	[1.048-1.058]
I	*D. theta*	0/6[6]; 61/109[13]; 33/33[15]; 12/114[22]; 11/13 17-24 mm, 9/39 29-70 mm[5]; 176/176[36]; some[2]; no gas[7]; increases with L_S[13,22]; decreases with L_S[36]; [20/32]	High[5,7,25,32]; increases with L_S[5]; seasonally high[22]; low[30,31]	1.025-1.045[13]; 1.025-1.062[5]; [1.038-1.068]
I	*T. nigrescens*	[4/4]	Low[8]	[1.043-1.070]
I	*S. opisthopterus*	Gas[4,16,29]; increases with L_S[4,29]; [3/3]	-	[1.038-1.053]
I	*N. valdiviae*	Gas[4,34]; [5/8]	Low[8]; High[34]	[1.038-1.058]
I	*M. suborbitalis*	Gas[11]; [3/3]	-	[1.040-1.078]
I	*I. irregularis*	Gas[23]; [3/3]	High[23]	[1.038-1.050]
II	*M. parvus*	No gas[11]; [3/4]	-	[1.055-1.078]
II	*C. atraria*	-	Low[17]	[1.040-1.058]
II	*C. townsendi*	1/23[22]; [17/43, no gas > 39 mm]	High[1,22]; increases with L_S[22]	1.041-1.057[22]; [1.038-1.083]
II	*S. mizolepis*	Regressed swimbladder[12,20]; no gas[7,8,23]; [4/19 , no gas > 48 mm]	Low[7,8,23,34]	[1.038-1.058]
II	*P. crassiceps*	No gas[7,8]; [13/14]	Low[1,7,23]	[1.043-1.068]
II	*N. ritteri*	No gas[7,22,25]; no gas > 23 mm[24]; no gas > 50 mm[5]; [19/56, no gas > 45 mm]	High[1,5,7,22,25]; increases with L_S[22]	1.034-1.051[22]; 1.023-1.048[5]; [1.029-1.058]
II	*T. mexicanus*	No gas[7,22]; no gas > 49mm[6];gas > 33 mm[28]; [18/52, no gas > 34 mm]	High[7,22,25]; increases with L_S[22]	1.029-1.062[6]; 1.025-1.033[22]; [1.029-1.055]
II	*S. leucopsarus*	No gas[7,37]; no gas > 57 mm[6]; no gas > 35 mm[15]; no gas > 39 mm[5]; some[2]; decreasing fraction up to 85 mm[13]; [22/57, no gas > 42 mm]	High[5,7,25,30,31,32]; increases with L_S[5]	1.015-1.025[13]; 1.025-1.048[5]; 1.027-1.044[37]; [1.027-1.058]
II	*N. regale*	No gas[7,22]; no gas > 61 mm[24]; no gas > 49 mm[5]; [14/18, no gas > 61 mm]	Low[1,5,7,22]; high[30,31,32]	1.021[22]; 1.040-1.041[5]; [1.029-1.073]
II	*M. lugubris*	Gas[7]; no gas[11]; [6/9, no gas > 50 mm]	-	[1.029-1.068]

Table S4. (continued)

Fish group	Species	Gas	Lipid content	Density (g ml^{-1}) or specific gravity
III	*S. stephensi*	No gas[14]	-	[1.070-1.083]
III	*S. harryi*	No gas[14]	Low[23]	[1.058-1.063]
III	*A. risso*	No gas[14]	-	[1.055-1.080]
III	*C. macouni*	No gas[7,23,35]	Low[23]; high[1]	[1.045-1.055]
III	*L. stilbius*	No gas[7,23]	Low[7,23]	[1.038-1.053]
III	*S. abei*	No gas[7,23]	Low[7,23]	[1.048-1.053]
III	*C. acclinidens*	No gas[7,20]	Low[1,7,26]	[1.038-1.078]
III	*C. pallida*	-	Low[8,17,26,34]	[1.040-1.058]
III	*B. wesethi*	No gas[7,23]	Low[7,23]	[1.033-1.060]
III	*T. macropus*	No gas[35]	-	[1.036-1.048]
III	*S. atriventer*	No gas[7,23]	Low[23]; high[7]	[1.038-1.043]
III	*P. ingens*	No gas[7,22]; [0/6]	Low[22]	1.021[22]; [1.036-1.048]
III	*I. antrostomus*	No gas[7,23]	Low[1,7,23]	[1.034-1.068]
III	*L. ochotensis*	No gas[23]	High[23]	[1.033-1.053]
III	*L. gemellarii*	Gas[3,4,29]; [no gas 55-65 mm]	Low[3,34]; high[8]	[1.035-1.045]

1. (Bailey and Robison, 1986); 2. (Barham, 1957); 3. (Bone, 1973); 4. (Brooks, 1976); 5. (Butler and Pearcy, 1972); 6. (Capen, 1967); 7. (Childress and Nygaard, 1973); 8. (Childress *et al.*, 1990); 9. (Culkin and Morris, 1970); 10. (Dunlap, 1971); 11. (Ebeling, 1962); 12.(Ebeling and Weed, 1963); 13. (Johnson, 1979); 14. (Johnson, 1982); 15. (Kalish *et al.*, 1986); 16. (Kanwisher and Ebeling, 1957); 17. (Kayama and Ikeda, 1975); 18. (Kleckner and Gibbs, 1972); 19. (Lee and Hirota, 1973); 20. (Marshall, 1960); 21. (Marshall, 1980); 22. (Neighbors and Nafpaktitis, 1982); 23. (Neighbors, 1988); 24. (Neighbors, 1992); 25. (Nevenzel *et al.*, 1969); 26. (Nevenzel and Menon, 1980); 27. (Nielsen *et al.*, 1999); 28. (Pieper and Bargo, 1980); 29. (Saenger, 1989); 30. (Saito and Murata, 1996); 31. (Saito and Murata, 1998); 32. (Seo *et al.*, 1996); 33. (Shearer, 1971); 34. (Stickney and Torres, 1989); 35. (Yancey *et al.*, 1989); 36. (Yasuma *et al.*, 2003); 37. (Yasuma *et al.*, 2006); 38. (Yasuma *et al.*, 2010)

References

Bailey, T. G., and Robison, B. H. 1986. Food availability as a selective factor on the chemical compositions of midwater fishes in the eastern North Pacific. Marine Biology, 91: 131–141.

Barham, E. G. 1957. The ecology of sonic scattering layers in the Monterey Bay area. Hopkins Marine Station of Stanford University, Pacific Grove. Technical Report 1: 1–182.

Bone, Q. 1973. A note on the buoyancy of some lantern-fishes (Myctophoidei). Journal of the Marine Biological Association of the United Kingdom, 53: 619–633.

Brooks, A. L. 1976. Swimbladder allometry of selected midwater fish species. National Technical Information Service, Springfield. USDOC, NUSC Technical Report 4983: 1–43.

Butler, J. L., and Pearcy, W. G. 1972. Swimbladder morphology and specific gravity of myctophids off Oregon. Journal of the Fisheries Research Board of Canada, 29: 1145–1150.

Capen, R. L. 1967. Swimbladder morphology of some mesopelagic fishes in relation to sound scattering. US Navy Electronics Laboratory San Diego Research Report 1447: 1–31.

Childress, J. J., and Nygaard, M. H. 1973. Chemical composition of midwater fishes as a function of depth of occurrence off southern California. Deep-Sea Research, 20: 1093–1109.

Childress, J. J., Price, M. H., Favuzzi, J., and Cowles, D. 1990. Chemical composition of midwater fishes as a function of depth of occurrence off the Hawaiian Islands: food availability as a selective factor? Marine Biology, 105: 235–246.

Culkin, F., and Morris, R. J. 1970. Fatty acids of some marine teleosts. Journal of Fish Biology, 2: 107–112.

Dunlap, C. R. 1971. A reconnaissance of the deep scattering layers in the eastern tropical Pacific and the Gulf of California. *In* Proceedings of an International Symposium on Biological Sound Scattering in the Ocean, pp. 395–408. Ed. by G. B. Farquhar. US Government Printing Office, Washington DC.

Ebeling, A. W. 1962. Melamphaidae I. Systematics and zoogeography of the species in the bathypelagic fish genus *Melamphaes* Gunther. Dana Report, 58: 1–164.

Ebeling, A. W., and Weed, W. H. 1963. Melamphaidae III. Systematics and distribution of the species in the bathypelagic fish genus *Scopelogadus* Vaillant. Dana Report, 60: 1–58.

Isaacs, J. D., and Kidd, L. W. 1953. Isaacs–Kidd midwater trawl final report. Scripps Institution of Oceanography Oceanographic Equipment Report, 1: 1–21.

Johnson, R. K. 1979. Gas bubble sizes for selected myctophids. Oregon State University School of Oceanography Reference 79-6: 1–18..

Johnson, R. K. 1982. Fishes of the families Evermannellidae and Scopelarchidae: systematics, morphology, interrelationships, and zoogeography. Fieldiana Zoology, N.S. 12: 1–252.

Kalish, J. M., Greenlaw, C. F., Pearcy, W. G., and Holliday, D. V. 1986. The biological and acoustical structure of sound scattering layers off Oregon. Deep-Sea Research, 33: 631–653.

Kanwisher, J., and Ebeling, A. 1957. Composition of the swim-bladder gas in bathypelagic fishes. Deep-Sea Research, 4: 211–217.

Kayama, M., and Ikeda, Y. 1975. Studies on the lipids of micronektonic fishes caught in Sagami and Suruga Bays, with special reference to their wax esters. Journal of Japan Oil Chemists' Society, 24: 435–440.

Kleckner, R. C., and Gibbs, R. H. 1972. Swimbladder structure of Mediterranean midwater fishes and a method of comparing swimbladder data with acoustic profiles. *In* Mediterranean Biological Studies Final Report I, pp. 230–281. Smithsonian Institution, Washington DC.

Lee, R. F., and Hirota, J. 1973. Wax esters in tropical zooplankton and nekton and geographical distribution of wax esters in marine copepods. Limnology and Oceanography, 18: 227–239.

Marshall, N. B. 1960. Swimbladder structure of deep-sea fishes in relation to their systematics and biology. Discovery Reports, 31: 122.

Marshall, N. B. 1980. Deep-Sea Biology: Developments and Perspectives, Garland STPM Press, New York.

Neighbors, M. A. 1988. Triacylglycerols and wax esters in the lipids of deep midwater teleost fishes of the Southern California Bight. Marine Biology, 98: 15–22.

Neighbors, M. A. 1992. Occurrence of inflated swimbladders in five species of lanternfishes (family Myctophidae) from waters off southern California. Marine Biology, 114: 355–363.

Neighbors, M. A., and Nafpaktitis, B. G. 1982. Lipid compositions, water contents, swimbladder morphologies and buoyancies of nineteen species of midwater fishes (18 Myctophids and 1 Neoscopelid). Marine Biology, 66: 207–215.

Nevenzel, J. C., and Menon, N. K. 1980. Lipids of midwater marine fish: family Gonostomatidae. Comparative Biochemistry and Physiology, 65B: 351–355.

Nevenzel, J. C., Rodegker, W., Robinson, J. S., and Kayama, M. 1969. Lipids of some lantern fishes (family Myctophidae). Comparative Biochemistry and Physiology, 31: 25–36.

Nielsen, J. G., Cohen, D. M., Markle, D. F., and Robins, C. R. 1999. Ophidiiform fishes of the world (Order Ophidiiformes). An annotated and illustrated catalogue of pearlfishes, cusk-eels, brotulas and other ophidiiform fishes known to date, FAO, Rome.

Oozeki, Y., Hu, F. X., Kubota, H., Sugisaki, H., and Kimura, R. 2004. Newly designed quantitative frame trawl for sampling larval and juvenile pelagic fish. Fisheries Science, 70: 223–232.

Pieper, R. E., and Bargo, B. G. 1980. Acoustic measurements of a migrating layer of the Mexican Lampfish, *Triphoturus mexicanus*, at 102 kilohertz. Fishery Bulletin US, 77: 935–942.

Saenger, R. A. 1989. Bivariate normal swimbladder size allometry models and allometric exponents for 38 mesopelagic swimbladdered fish species commonly found in the north Sargasso Sea. Canadian Journal of Fisheries and Aquatic Sciences, 46: 1986–2002.

Saito, H., and Murata, M. 1996. The high content of monoene fatty acids in the lipids of some midwater fishes: family Myctophidae. Lipids, 31: 757–763.

Saito, H., and Murata, M. 1998. Origin of the monoene fats in the lipid of midwater fishes: relationship between the lipids of myctophids and those of their prey. Marine Ecology Progress Series, 168: 21–33.

Seo, H. S., Endo, Y., Fujimoto, K., Watanabe, H., and Kawaguchi, K. 1996. Characterization of lipids in myctophid fish in the subarctic and tropical Pacific Ocean. Fisheries Science, 62: 447–453.

Shearer, L. W. 1971. Comparisons between surface-measured swimbladder volumes, depth of resonance, and 12-kHz echograms at the time of capture of sound-scattering fishes. *In* Proceedings of an

International Symposium on Biological Sound Scattering in the Ocean, pp. 453-473. Ed. by G. B. Farquhar. US Government Printing Office, Washington DC.

Stickney, D. G., and Torres, J. J. 1989. Proximate composition and energy content of mesopelagic fishes from the eastern Gulf of Mexico. Marine Biology, 103: 13–24.

Yancey, P. H., Lawrence-Berrey, R., and Douglas, M. D. 1989. Adaptations in mesopelagic fishes. I. buoyant glycosaminoglycan layers in species without diel vertical migrations. Marine Biology, 103: 453–459.

Yasuma, H., Sawada, K., Olishima, T., Miyashita, K., and Aoki, I. 2003. Target strength of mesopelagic lanternfishes (family Myctophidae) based on swimbladder morphology. ICES Journal of Marine Science, 60: 584–591.

Yasuma, H., Sawada, K., Takao, Y., Miyashita, K., and Aoki, I. 2010. Swimbladder condition and target strength of myctophid fish in the temperate zone of the Northwest Pacific. ICES Journal of Marine Science, 67: 135–144.

Yasuma, H., Takao, Y., Sawada, K., Miyashita, K., and Aoki, I. 2006. Target strength of the lanternfish, *Stenobrachius leucopsarus* (family Myctophidae), a fish without an airbladder, measured in the Bering Sea. ICES Journal of Marine Science, 63: 683–692.

Chapter 2, in full, is a reprint of the material as it appears in ICES Journal of Marine Science 68 (10), 2064-2074, Davison, P., 2011. The dissertation author was the primary investigator and author of this paper.

Chapter 3. The efficacy of acoustic and trawl-based estimates of the biomass of a complex aquatic community

3.1. Abstract

Concurrent acoustic and trawl data were collected offshore of southern California to estimate the abundance of vertically migratory mesopelagic micronekton. Acoustic data were obtained with a multi-frequency scientific sonar, while animals were collected with a midwater trawl. Target strength (*TS*) models were created of the captured animals, which were then assigned to three acoustic groups based upon the frequency spectrum shape of their modeled *TS*: I) animals with a gas inclusion, II) "large" animals with no gas inclusion, and III) "small" animals with no gas inclusion. The mean spectra of the acoustic groups were used with non-negative least squares inverse methods to estimate abundances from the multi-frequency volume backscattering (S_v). The resulting acoustic abundances were compared to the trawl catches, and capture efficiency of the net is estimated to be 14%, 38%, and 81% for Groups I-III respectively. The ability of the inverse method to correctly decompose S_v was tested with Monte Carlo analyses of artificial echograms. The inverse method is accurate when averaged, but variance is high for individual ensonified volumes. The high variance in acoustic estimates of abundance is caused by individual variation in *TS* frequency spectra, which is greatest for the geometric scatterers in Group II.

3.2. Introduction

The deep scattering layer (DSL) is a sound-reflecting layer of small fishes and zooplankton found worldwide in the open ocean at mesopelagic depths (Longhurst, 1976). The global biomass of the animals forming this layer is immense (Gjosaeter and Kawaguchi, 1980). A portion of the DSL migrates vertically to the surface at night to feed (Longhurst, 1976; Gjosaeter and Kawaguchi, 1980), and this constitutes the largest mass migration on earth (Robison, 1983). The great abundance and world-wide distribution of the animals forming the DSL makes them trophically and even biogeochemically important (Mann, 1984; Robinson *et al.*, 2010). Despite the importance of the DSL and decades of attention by oceanographers, many fundamental aspects of its ecology remain poorly-known due to the difficulty of making direct observations.

The principal sampling techniques for the study of the DSL are acoustic surveys and nets. Acoustic estimates of abundance are generally higher than those made from trawls (Lawson *et al.*, 2008; Kloser *et al.*, 2009). Nets are known to undersample abundance, often by an unknown amount, due to escapement and avoidance by animals (Gartner *et al.*, 1989). Escapement refers to the loss of captured animals through the net mesh, and avoidance results from the ability of animals to swim out of the path of the net. Capture efficiency therefore varies with the size, shape, and swimming ability of animals, and also between net designs, meshes, and trawling speeds (Gartner *et al.*, 1989; Itaya *et al.*, 2007). These biases are avoided with acoustic sampling, however the mixing of acoustically different individuals in an ensonified water volume makes the interpretation of volume backscattering (S_v) difficult. The animals that comprise the DSL form a mixed assemblage, although vertical and horizontal structure has been observed (Pearcy, 1964; Backus *et al.*, 1968; Greenblatt, 1982; Robison, 1983).

The recent commercial availability of scientific multi-frequency acoustic instruments (and software to process the data) offers a means to make improved abundance estimates. Inverse analysis of multi-frequency S_v data is effective for separation by size of fluid-filled shapes, if the frequency range encompasses the transition between Rayleigh scattering and geometric scattering (Greenlaw, 1979; Holliday and Pieper, 1995). For fluid-filled shapes, the Rayleigh-geometric transition occurs at approximately $ka = 1$, where k is the wavenumber and a is the spherical or cylindrical radius (Anderson, 1950; Stanton, 1988). The frequency range of 38-200 kHz spans the Rayleigh-geometric transition for radii of 1-6 mm, and is appropriate for the large zooplankters and small fishes that form the DSL. Researchers have successfully used this technique to estimate the abundance of differently-sized zooplankton and mesopelagic fishes (Greenlaw, 1979; Kalish *et al.*, 1986; Holliday and Pieper, 1995). Inverse analysis requires a model target strength (*TS*) frequency spectrum for each acoustic group (Greenlaw and Johnson, 1983). These spectra can be derived from the trawl catch by modeling *TS* for each animal present, sorting the spectra into similarly-shaped groups, and then calculating the mean spectrum for each group. Abundance surveys that combine net deployments with acoustic data collection can thus quantify both abundance and taxonomic composition of the DSL.

A study is made here of the efficacy of acoustic estimates of biomass made from inverse modeling and of the capture efficiency of the Matsuda-Oozeki-Hu trawl (MOHT; Oozeki *et al.*, 2004). This net design, in conjunction with a Simrad EK60 multi-frequency sonar, has recently been incorporated into the sampling program of the California Cooperative Oceanic Fisheries Investigations (CalCOFI) time series to measure the

abundance and distribution of mesopelagic micronekton and small pelagic fishes. The ability of inverse methods to correctly decompose multi-frequency acoustic data from mixed aggregations was tested with a series of Monte Carlo simulations. In addition, the Monte Carlo method was used to explore the cost to accuracy resulting from the addition of more categorical resolution.

3.3. Materials and Methods

3.3.1. EK60 data collection

Acoustic backscattering data were collected using a Simrad EK60 split-beam echosounder equipped with four frequencies (38, 70, 120, and 200 kHz). The EK60 transducers were calibrated using the standard sphere technique (Foote *et al.*, 1987). Pulse length was set to 0.512 ms with a ping rate of 0.5 s^{-1}. Beam angles were 6° for the 70, 120, and 200 kHz transducers, and 12° for the 38 kHz. Acoustic data were processed and cleaned using Echoview software (Myriax Software Pty Ltd) without ping-averaging. S_v was calculated at the minimum Echoview depth resolution of 1 m to the maximum depth of the trawl for the time periods corresponding to the trawling. The surface blind zone (transducer depth plus near-field) encompassed the top 10 m of the water column. For night abundance estimates, the blind zone was assumed to contain animals equivalent to the difference between day and night 38 kHz S_a (S_v integrated to 700 m). For daylight abundance estimates, the blind zone was assumed to contain animals equivalent to the 10-20 m depth stratum. Schooling epipelagic fishes were present in two of the trawl echograms and, because these fishes were not captured by the trawl, the time periods in which epipelagic fish schools were present were excluded from the analysis.

3.3.2. Collection and processing of animals

Mesopelagic micronekton were collected in October 2008 on a cruise of the RV "Melville" to the California Current System off Point Conception (cruise P0810 of the California Current Ecosystem Long Term Ecology Research program). Sampling was performed at six Lagrangian stations (around a subsurface drifter) in a region with complex mesoscale features (Figure 3.1). Animals were captured using a 5-m^2 MOHT with a uniform 1.7 mm square mesh towed at 1.25-1.50 m s^{-1}. A total of 16 oblique trawls were made to a depth of approximately 200 m. Trawl depth and water temperature were recorded using a Wildlife Computers Mk9 archival tag fixed to the frame of the MOHT. Water flow through the net was measured with a TSK flowmeter. The catch was preserved in 5% Formalin within one hour after recovery of the net. Ashore, fishes were identified to species, weighed, and standard length (L_S) measured to the nearest millimeter. The invertebrate catch was sub-sampled with a Folsom splitter and Stempel pipette. Invertebrates were not sorted to species, but to higher taxonomic categories. Length and width of invertebrates were measured with the ocular micrometer of a dissecting microscope.

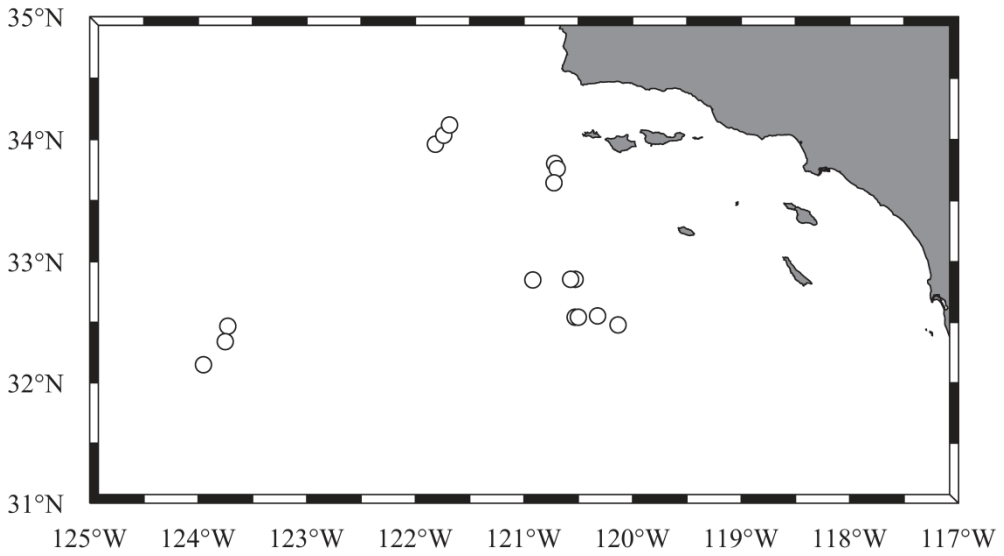

Figure 3.1. Sampling locations off of southern California for the October 2008 cruise of the R/V "Melville".

3.3.3. Forward modeling

3.3.3.1. Fishes

Fish bodies were acoustically modeled as fluid-filled cylinders of the same length, volume, and density as the measured fishes, following Stanton (1988). The gas from the swimbladder (when deemed present) was modeled as a gas sphere following Anderson (1950). Gas was arbitrarily assumed to have 80% of the volume required for neutral buoyancy. The acoustic backscattering cross sections (σ_{bs}) of the modeled body and gas were summed to form the total σ_{bs}. *TS* (dB re 1 m^2) is the decibel form of the σ_{bs} (m^2), and the two variables are related by the equation $TS = 10\log10(\sigma_{bs})$. The density of water was calculated per the High Pressure International Equation of State of Seawater, 1980 (Millero *et al.*, 1980). The speed of sound in seawater, c, was calculated based upon the pressure, temperature, and salinity at 50 m depth following Mackenzie (1981). The ratio of sound speed in the fish body to that in seawater, *h*, was assumed to be 1.020 (Yasuma

et al., 2006). Because this value of h was determined for c = 1490 m s^{-1} at ~1 atm pressure, and the change in h with decreased temperature and increased pressure is unknown, σ_{bs} of the fish body was calculated at a depth of 0.5 m and c = 1490 m s^{-1}, i.e., sound speed in fish flesh is assumed to change proportionally to that of seawater with identical temperature and pressure. Tilt angle of the fishes was assumed to be 0° (dorsal incidence). The gas inside the swimbladder was assumed to be an ideal gas (air) at the temperature and pressure, P, of the ambient water, with a ratio of specific heats γ = 1.4, and a speed of sound, c_g, given by $c_g = (\gamma P \rho_w^{-1})^{0.5}$, where ρ_w is the density of the ambient water. Temperature and pressure of the gas were assumed to be that found at 50 m depth.

Several of the most common mesopelagic fishes in the California Current have functional swimbladders as larvae and juveniles, but non-functional swimbladders as adults (Davison, 2011). Information on body density as a function of L_S and the L_S at which gas ceases to be present were taken from Davison (2011), and are summarized in Table 3.1. For those fish species in which the swimbladder regresses with growth, individuals with L_S greater than the maximum L_S in which inflated swimbladders are found were assumed to have no gas in their swimbladder. Individuals less than or equal to the maximum L_S in which inflated swimbladders were found were all assumed to have gas in their swimbladder. Non-vertically migratory fish species that were captured by the MOHT were excluded from the forward modeling, as they were most likely caught at a depth below that corresponding to the signal-to-noise threshold of the higher frequencies.

Table 3.1. Fish density and swimbladder inflation assumptions. Body density (ρ) parameters a and b correspond to the expression $\rho = aL_S + b$ (g ml^{-1}, L_S in m). Two sets of parameters are given for those species with a pronounced knee in their body density relationship against L_S ($L_S \leq$ knee, $L_S >$ knee respectively).

Species	Inflated swimbladder	Knee in ρ (mm)	a	b
Nemichthyidae				
Nemichthys scolopaceus	no	-	0	1.050*
Microstomatidae				
Microstoma microstoma	yes	-	0	1.067
Bathylagidae				
Bathylagoides wesethi	no	-	-0.242	1.058
Leuroglossus stilbius	no	-	0	1.046
Lipolagus ochotensis	no	-	-0.218	1.056
Photichthyidae				
Vinciguerria lucetia	yes	-	0	1.067
Stomiidae				
Aristostomias scintillans	no	-	0	1.050*
Bathophilus flemingi	no	-	0	1.046
Idiacanthus antrostomus	no	-	-0.076	1.058
Stomias atriventer	no	-	0	1.040
Scopelarchidae				
Scopelarchus analis	no	-	0	1.075
Notosudidae				
Scopelosaurus harryi	no	-	0	1.061
Myctophidae				
Ceratoscopelus townsendi	<40 mm	-	-0.643	1.082
Diaphus theta	yes	-	-0.278	1.068
Diogenichthys atlanticus	yes	-	2.190	1.025
Diogenichthys laternatus	yes	-	2.190**	1.025**
Hygophum reinhardtii	yes	-	0	1.071
Nannobrachium hawaiiensis	<70 mm	-	0	1.051
Nannobrachium regale	<62 mm	-	-0.259	1.066
Nannobrachium ritteri	<46 mm	58	-0.563	1.065
			0	1.032
Notolychnus valdiviae	yes	-	-1.340	1.071
Notoscopelus resplendens	yes	-	0	1.075
Stenobrachius leucopsarus	<38 mm	39	-1.030	1.069
			0	1.029
Symbolophorus californiensis	yes	-	0	1.068
Tarletonbeania crenularis	yes	28	6.430	0.913
			0	1.084
Triphoturus mexicanus	<35 mm	39	-0.679	1.062
			0	1.032
Ophidiidae				
Chilara taylori	yes	-	0	1.063
Melamphaeidae				
Melamphaes lugubris	<51 mm	-	-0.677	1.082
Melamphaes parvus	<30 mm	-	0	1.067

Table 3.1. (continued)

Species	Inflated swimbladder	Knee in ρ (mm)	*a*	*b*
Poromitra crassiceps	yes	-	-0.353	1.062
Scopelogadus mizolepis	<49 mm	-	-0.280	1.065
Howellidae				
Bathysphyraenops simplex	yes	-	-0.599	1.086

* body density is set to 1.050 g ml^{-1} for those species (and larvae) for which no data are available

** no data are available, density data from congener *D. atlanticus* are used

3.3.3.1. Invertebrates

Invertebrates from the midwater trawl catch were modeled with a variety of shapes, model types, and acoustic parameters. Fluid shapes were modeled using the distorted wave Born approximation (DWBA; Stanton *et al.*, 1998; Stanton and Chu 2000), whereas pteropods and physonect siphonophores were modeled as spherical elastic shells and gas bubbles respectively. The taxonomic groups, fluid shapes, model parameters, and references for invertebrates are summarized in Table 3.2. Invertebrate models were averaged over tilt angle per Table 3.2.

3.3.3.1. Acoustic grouping

The forward-modeled frequency spectra of the animals were sorted into three acoustic groups by shape. Group I corresponded to animals with gas inclusions, Group II to "large" ($ka > 1$) animals without gas inclusions that scatter geometrically in the EK60 frequency range, and Group III to "small" ($ka < 1$) animals that scatter entirely in the Rayleigh region for the EK60 frequency range. σ_{bs} was averaged by frequency to generate a mean frequency spectrum for each acoustic group. Because the sample size of

some acoustic groups was small, the modeled catches from all trawls were lumped together to calculate mean frequency spectra. Modeled invertebrates were multiplied out corresponding to the subsample fraction of each trawl catch before their spectra were averaged together with those from modeled fish. Because the beam angle for the 38 kHz transducer was wider than that of the other frequencies, an artificial acoustic group ("Group IV") was created for strong scatterers that were detected at 38 kHz but not at the higher frequencies.

Table 3.2. Invertebrate acoustic models. *g* and *h* refer to the density and sound-speed contrasts respectively.

Taxa	Shape	*g*	*h*	Tilt angle	Tilt angle SD
euphausiids	bent cylinder	1.037[a]	1.011[a]	15[b]	24.2[b]
copepods	prolate spheroid	1.000[c]	1.012[c]	0[d]	30[d]
pteropods	spherical elastic shell	1.732[e]	1.732[e]	-	-
decapods (≤ 25 mm)	bent cylinder	1.043[f]	1.065[f]	20[g]	20[g]
decapods (>25 mm)	bent cylinder	1.041[h]	1.078[h]	20[g]	20[g]
siphonophore pneumatophores	hybrid gas sphere	0.001[i]	0.225[i]	-	-
amphipods	bent cylinder	1.058[d,e]	1.058[d,e]	0[d]	30[d]
chaetognaths	bent cylinder	1.014[j]	1.030[d]	0[d]	30[d]
ostracods	bent cylinder	1.030[d]	1.030[d]	0[d]	30[d]
polychaetes	bent cylinder	1.030[d]	1.030[d]	0[d]	30[d]
salps	bent cylinder	1.002[k]	1.010[k]	0[d]	30[d]
zoea	bent cylinder	1.058[d,e]	1.058[d,e]	0[d]	30[d]

[a](Mikami *et al.*, 2000; *Euphausia pacifica*, September)
[b](Miyashita *et al.* 1996; swimming *E. pacifica*)
[c](Matsukura *et al.*, 2009; *Neocalanus cristatus*, mean at 10° C)
[d](Lawson *et al.*, 2004; assumptions when little or no information available)
[e](Stanton *et al.*, 1994)
[f](Chu *et al.*, 2000)
[g](Chu *et al.*, 1993)
[h](Chu and Wiebe, 2005)
[i](Lavery *et al.*, 2007; carbon monoxide)
[j](Smith *et al.*, 2010)
[k](Wiebe *et al.*, 2010; *Salpa thompsoni*)

3.3.4. Inverse modeling

A non-negative least squares (NNLS) inverse method was used to estimate the abundance of animals of each acoustic group from the multi-frequency S_v data for each ensonified water parcel (Greenlaw and Johnson, 1983; Holliday and Pieper, 1995). Abundance is reported in units of "mean scatterers" per volume ensonified, i.e. the number of average animals that scatter sound according to one of the four mean *TS* frequency spectra contained in the water parcel. Abundances for each water parcel were vertically integrated to the trawl depth and then averaged over the time period of the trawl (mean scatterers m^{-2}). For each trawl period, the Group IV inverse-modeled abundance was converted to 38 kHz area scattering and assigned to Groups I and II in proportion to the forward-modeled backscattering from those groups as represented in the trawl catch. Finally, abundance was converted to biomass (g m^{-2}) through multiplication by the mean wet weight of animals from each acoustic group captured by the MOHT. Capture efficiency is defined as the ratio of the MOHT biomass estimate to the acoustic biomass estimate.

A series of Monte Carlo simulations was performed to test the ability of the NNLS inverse method to correctly decompose S_v. In the simplest case, an artificial echogram of 50,000 water parcels was constructed from random integers of mean backscattering spectra from each acoustic group (0-9, 0-9, 1-10, 0-9 for Groups I-IV respectively). At least one animal was required to be present in each water parcel (Group III in this case) because the NNLS function did not handle a true zero well. The presence of zero backscattering is an artificial situation, because measured S_v will always include noise, even when no targets are ensonified. The inverse model was then applied to the

artificial echogram. The abundances resulting from the inverse model were then compared to the known abundance of animals from each acoustic group. Subsequent Monte Carlo tests explored the effect of the use of randomly selected individuals rather than mean spectra, and also the effect of underdetermination (i.e., the condition when acoustic categories outnumber acoustic frequencies) on NNLS results. Individual variability in the shape of *TS* frequency spectra is a source of error, and increased categorical resolution is desirable in acoustic surveys. For the underdetermination series of Monte Carlo simulations, the group with the most variable frequency spectra (Group II) was progressively subdivided into seven groups of more homogenously-shaped frequency spectra, each with 0-9 randomly selected individuals per ensonified water parcel. Only model fishes (no zooplankton models) were used for the individual and acoustic group spectra in the Monte Carlo simulations. These model fishes were the same ones that were used to generate the mean frequency spectra (in combination with the zooplankton models) for the biomass survey. They varied individually in their proximity to the Rayleigh-geometric transition and in the presence or absence of high-frequency resonant spikes and nulls.

3.4. Results

3.4.1. Trawl catch and forward model

Overall trawl biomass was dominated by invertebrates, with almost no fishes captured in the daylight tows (Figure 3.2). The mean night catch was 6.6-times larger than the mean day catch, indicating substantial diel vertical migration into epipelagic

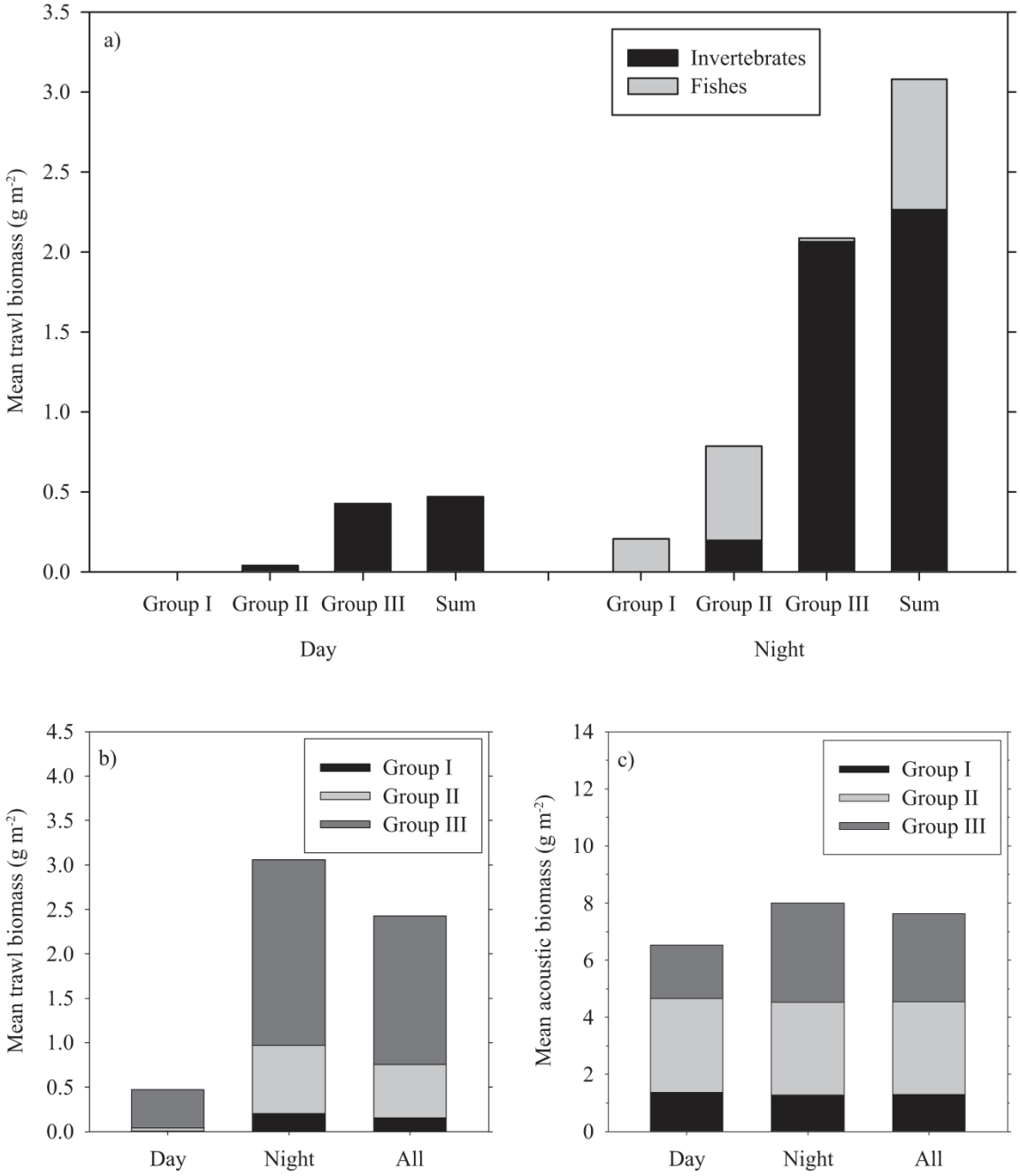

Figure 3.2. (a) Catch composition of MOHT within each acoustic group (day and night). (b) MOHT catch composition of the MOHT by acoustic group and daylight. (c) Acoustic biomass estimate by acoustic group and daylight. Note that the scale differs in all three panels. Group I corresponds to animals with gas inclusions, Group II to "large" (ka > 1) animals without gas inclusions that scatter geometrically in the EK60 frequency range, and Group III to "small" (ka < 1) animals that scatter entirely in the Rayleigh region for the EK60 frequency range.

depths at night and/or increased avoidance of the net by day. By acoustic group, the resident (non-migratory) fraction of biomass in the epipelagic zone (as defined by the ratio of the mean day catch to the mean night catch) was 2.5%, 4.8%, and 20.4% for Groups I-III respectively. At night, fishes comprised over 99% of Group I, 74% of Group II, and less than 1% of Group III by weight. The fraction of the total epipelagic biomass contributed by each acoustic group increased from Groups I-II-III both day and night (Figure 3.2).

Frequency spectra from the modeled trawl catch were found to separate into three basic shapes (Figure 3.3). Group I (fishes with gas-filled swimbladders and physonect siphonophores) have a relatively flat frequency spectrum, with slightly decreasing σ_{bs} with increasing frequency. Group II (large fish without inflated swimbladders, pteropods, and large invertebrates) show a sharp increase in σ_{bs} between 38 and 70 kHz, with complex behavior (but positive average slope) at higher frequencies. The σ_{bs} of Group III (small zooplankters and small fishes without inflated swimbladders) has a steep slope with increasing frequency over the entire frequency range, a characteristic of Rayleigh scattering. Variability was observed in the modeled σ_{bs} of Groups I and II at 120 and 200 kHz due to resonant effects (Figure 3.3). Small changes in animal length can align resonant nulls with the sampling frequency (Figure 3.4). The variability was more pronounced in Group II than in Group I.

3.4.2. Inverse model

The capture efficiency (mean of all 16 trawls) was lowest for Group I and highest for Group III (Table 3.3). A day-night difference in capture efficiency is significant only

for Group I (Table 3.3), with a greater fraction of Group I biomass captured at night by the MOHT. Acoustic estimates of the overall epipelagic biomass were ~3-fold higher than those from nets when biomass is averaged over all trawl periods (Figure 3.2). For individual trawls, the acoustic to trawl biomass ratio ranged widely from 0.7 to 182.9 (Figure 3.5). Similarly to the trawl catch, the fraction of total epipelagic biomass contributed by each acoustic group increased from Groups I-II-III both day and night (Figure 3.2).

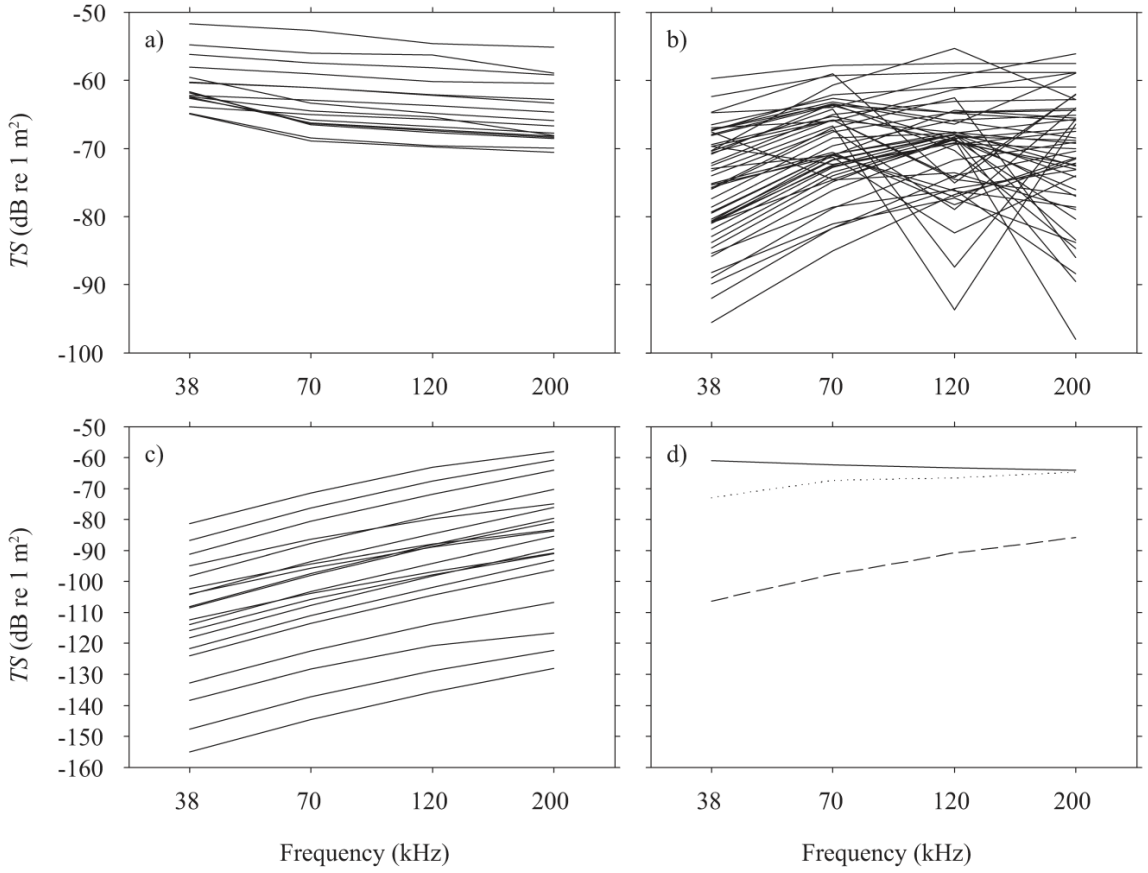

Figure 3.3. (a-c) Example frequency spectra of animals belonging to the three acoustic groups determined from forward models of the trawl catch, showing the full range of *TS*. (d) Mean frequency spectra for the three acoustic groups. Group I (solid line) corresponds to animals with a gas inclusion, Group II (dotted line) is large invertebrates and fishes with no gas inclusion, and Group III (dashed line) is composed of small invertebrates and fishes.

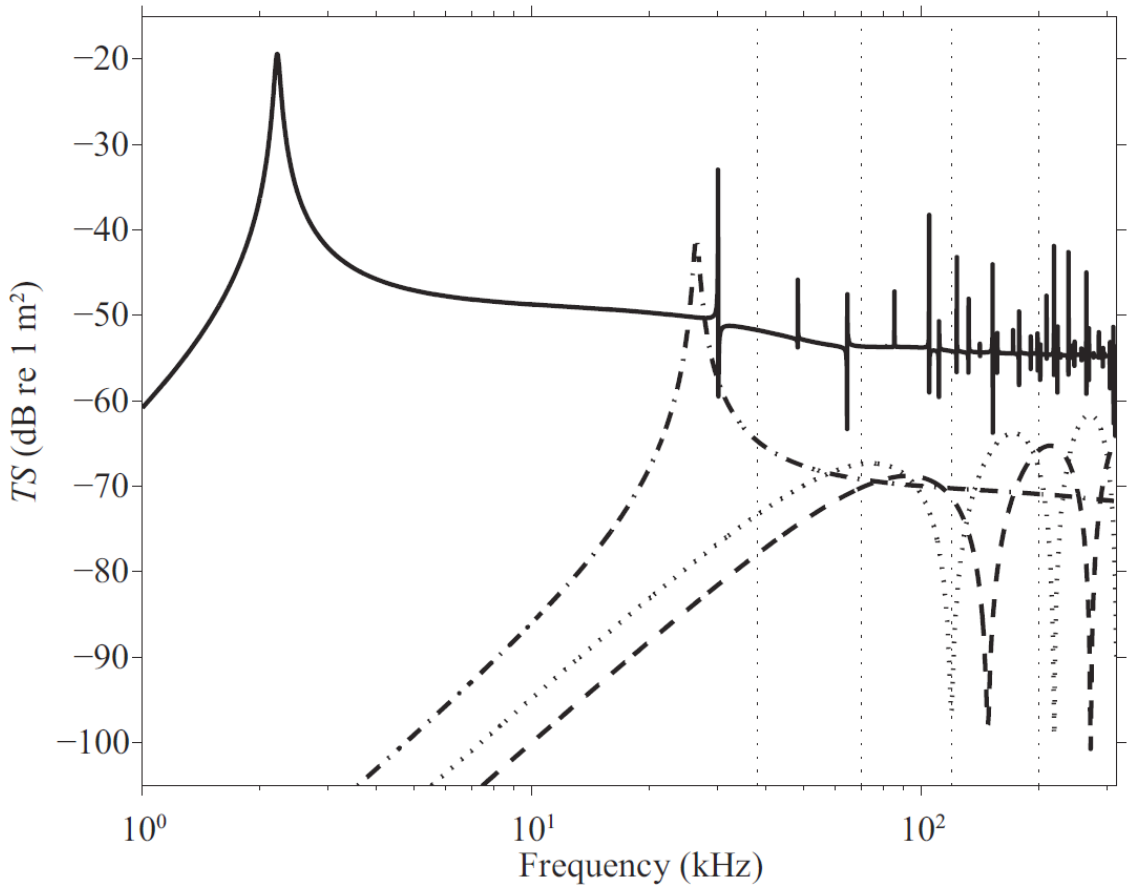

Figure 3.4. Frequency spectra of the largest (radius 3.7 mm, solid line) and smallest (radius 0.3 mm, dash-dot line) gas inclusions of Group I animals captured by the MOHT. No gas inclusions resonate at the sampling frequencies of the EK60 (38-200 kHz). The frequency spectra of 54 and 64 mm fluid-filled cylinders (*S. leucopsarus*, Group II, dashed and dotted lines respectively) are also shown for comparison. The 64 mm modeled fish has a resonant null aligned with the 120 kHz EK60 sampling frequency. Small changes in the length of geometric scatterers result in large differences in spectral shape measured at the discrete frequencies of the EK60. EK60 frequencies are marked with vertical dotted lines.

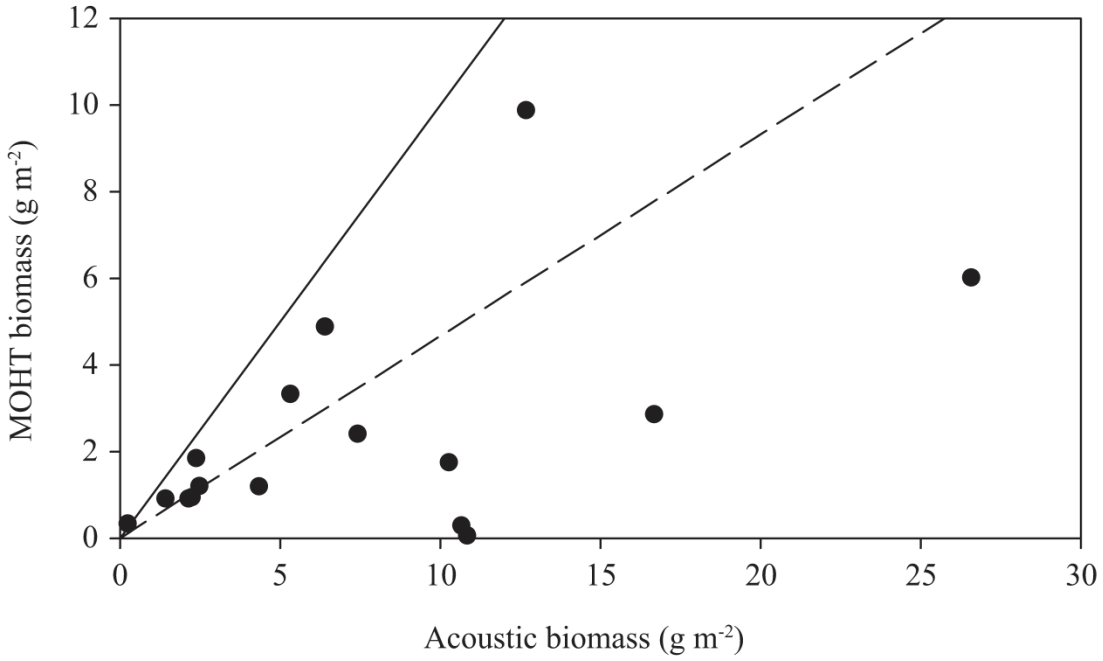

Figure 3.5. Overall capture efficiency of mesopelagic micronekton by the MOHT for each deployment. The lines indicate the mean capture efficiency (dashed) and a capture efficiency of 1.00 (solid).

Table 3.3. Mean capture efficiency by acoustic group for 16 epipelagic trawls. Numbers in parentheses are the standard deviation. *U* is the Mann-Whitney Rank Sum statistic for a difference between day and night capture efficiency.

	Day trawls (n = 4) (%)	Night trawls (n = 12) (%)	All trawls (n = 16) (%)	*U*	*P*
Group I	1.1 (1.3)	18.7 (12.9)	14.3 (13.6)	0	0.004
Group II	23.3 (44.4)	42.3 (25.9)	37.5 (30.9)	21	0.130
Group III	92.2 (134.0)	76.8 (46.4)	80.7 (72.2)	19	0.585
Total	41.2 (63.2)	48.4 (23.1)	46.6 (34.7)	15	0.303

The relative contribution of Groups I-III to the overall S_a is frequency dependent. The fraction of S_a was lowest for Group II and highest for Group I at all frequencies. Group I contributed 94% of the backscattering at 38 kHz, and this decreased to 49% at 200 kHz.

The ability of the inverse model to correctly decompose artificial echograms constructed from mean backscattering spectra was essentially errorless (Table 3.4, "All mean spectra" test). When mean spectra were replaced with random modeled individuals for each acoustic group in isolation, both mean and standard deviation of the error increased. A fifth Monte Carlo simulation (Table 3.4, "All ind. spectra" test) addressed the case where echograms are composed of backscattering spectra from randomly selected modeled fishes from all four acoustic groups, most closely matching our biomass

Table 3.4. Monte Carlo simulations. Groups I-IV are consistent with the acoustic groups used for the biomass survey methods (Group IV consists of strong scatterers present in the wider 38 kHz beam that were subsequently allocated to Groups I and II). Mean spectra for all acoustic groups were used to construct artificial echograms except as noted in the first column, where "ind." refers to the use of randomly selected (modeled) fishes rather than an acoustic group mean. The same random number range of animals (0-9, 0-9, 1-10, 0-9 for Groups I-IV respectively) was used for each water parcel (n = 50,000) for all Monte Carlo simulations. Results are reported in units of individuals as the mean error with the standard deviation of the error in parentheses. NNLS inverse modeling performs perfectly when mean spectra are used, but becomes noisy when variable individual spectra are used.

test	Group I error (SD)	Group II error (SD)	Group III error (SD)	Group IV error (SD)
All mean spectra	0.00 (0.00)	0.00 (0.00)	0.00 (0.00)	0.00 (0.00)
Group I ind.	0.06 (1.53)	-0.26 (3.80)	0.19 (3.13)	0.64 (20.29)
Group II ind.	-0.47 (1.53)	1.37 (5.23)	-1.00 (6.29)	6.01 (20.22)
Group III ind.	0.00 (0.20)	-0.01 (0.68)	-0.01 (3.83)	-0.03 (2.45)
All ind. spectra	0.06 (2.05)	-0.609 (5.79)	2.535 (14.25)	-0.314 (19.12)

survey conditions. In this configuration of the model, the mean error of the NNLS inverse model was lowest for the strong scatterers (0.06 individuals from a range of 0-9 for Group I) and highest for the weak scatterers (2.54 individuals from a range of 1-10 for Group III). The error of all acoustic groups combined was 1.7 individuals from a range of 1-37 individuals per water parcel. The results of this test systematically overcounted Group III and undercounted (negative error) Groups II and IV. Groups III and IV had very high maximum errors of over 200 individuals in a few water parcels. The SD of the error exceeded the mean error for all four acoustic groups in all simulations.

A second series of Monte Carlo simulations explored the effect of underdetermination on NNLS inversion (i.e., changes in performance when the number of acoustic groups exceeds the number of measured frequencies, four here). For these tests, the most variable acoustic group (Group II, Figure 3.3) was successively divided into seven groups of homogenously-shaped frequency spectra, representing various combinations of Rayleigh-geometric transition frequencies and resonant nulls. The underdetermination factor (ratio of acoustic groups to frequencies) increased from 1 to 2.5 with the addition of acoustic groups (Figure 3.6). The mean across all acoustic groups of the absolute value of the error roughly doubled over this range, while the mean SD of the error decreased ~60% (Figure 3.6).

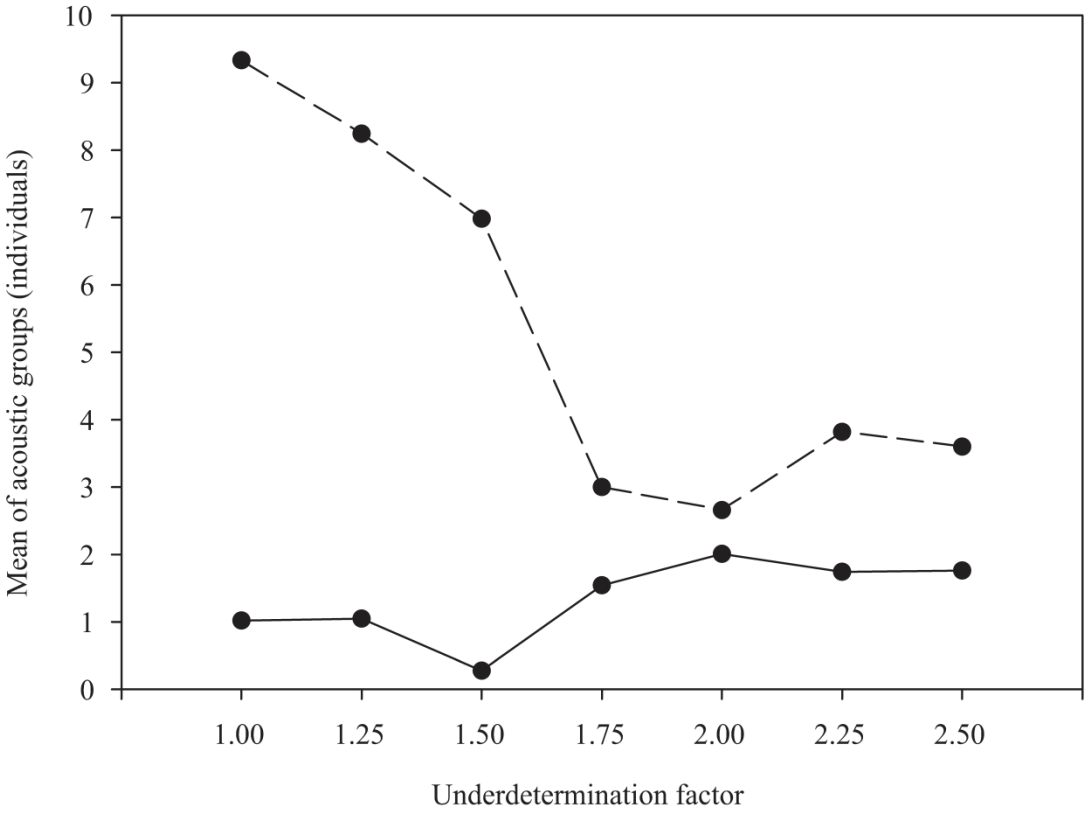

Figure 3.6 Effect of underdetermination on NNLS accuracy. The lines indicate the mean absolute error of acoustic groups (solid) and the mean standard deviation of the error (dashed).

3.5. Discussion

3.5.1. Forward modeling

The true shape of the inflated swimbladders of mesopelagic fishes is spheroidal (Marshall, 1960; Yasuma *et al.*, 2010), but we assumed a spherical shape. The difference in σ_{bs} between the two shapes is small as long as the aspect ratio is less than three, as is the case for mesopelagic fishes (Feuillade and Werby, 1994; Barr and Coombs, 2005). Measurements of the σ_{bs} of tethered myctophids with inflated swimbladders show that σ_{bs} is insensitive to tilt angle, consistent with a spherical shape (Yasuma *et al.*, 2003;

Yasuma *et al.*, 2010). The swimbladder gas volumes required for neutral buoyancy of the fishes captured here (equivalent spherical radius varied from 0.3-3.6 mm) are too large to be resonant at the EK60 frequencies (Figure 3.4). However, addition of an 18 kHz transducer would allow separation of fishes with gas inclusions of radii less than 0.3 mm because 18 kHz is close enough to the resonant frequency of these bubbles to show a resonant increase in σ_{bs}.

Our assumption of an L_S threshold for the presence or absence of gas in the swimbladder for myctophids (and perhaps other mesopelagic fishes) is simplistic. There is evidence that myctophids vary individually or on a diel basis in the presence of gas, even within a species and age group (reviewed in Davison, 2011). However, the measurement of gas volume, or even presence, in the swimbladder of a mesopelagic fish at the surface after capture is problematic and subject to several forms of bias (Davison, 2011). Different researchers have arrived at different conclusions regarding swimbladder inflation for the same species of mesopelagic fish (reviewed in Davison, 2011). Mesopelagic fishes are thought to be slightly negatively buoyant (reviewed in Davison, 2011). Our assumption that gas is present in 80% of the volume required for neutral buoyancy is arbitrary, but consistent with "slight" negative buoyancy. Given the lack of consensus and unbiased (*in situ*) data on swimbladder inflation, the simple assumptions made here were deemed better than more complex alternatives. Variation in swimbladder inflation by mesopelagic fishes remains an area in need of research.

Many mesopelagic animals do not contain a gas inclusion that dominates acoustic backscatter. The use of fluid-filled cylinders, or any other simple shape, to model the backscattering from the body of an animal is not likely to exactly match the true σ_{bs}. The

fact that the cylindrical radius of mesopelagic animals is smaller than the wavelength of the EK60 frequencies makes fine structural details of these animals less important to σ_{bs}. However, tilt angle is important. Tilt angle only strongly affects Group II animals, because the backscattering from Group I is dominated by gas and Group III animals scatter in the Rayleigh region. Resonant nulls in σ_{bs} have been observed and modeled in mesopelagic micronekton at moderate tilt angles (Stanton and Chu, 2000; Yasuma *et al.*, 2003; Yasuma *et al.*, 2006; Yasuma *et al.*, 2010). The effect of tilt angle on a cylindrical geometric scatterer (Figure 3.7) shows that a null is present at one or more tilt angles (less than 20°) at every frequency over 25 kHz, including all of the EK60 frequencies used in this study. No data are available for the statistical tilt angle distribution of mesopelagic fishes, although the night trawls here captured vertically migratory fishes that were presumably actively feeding and roughly horizontal in tilt. Mesopelagic fishes have been observed to hang motionless in the water at odd angles (Barham, 1971), but these observations have been made at depth on inactive fishes. The dorsal incidence assumption for fishes represents an σ_{bs} maximum. Error due to tilt angle distribution would underestimate the acoustic abundance of fishes here, and thus overestimate capture efficiency (i.e., the dorsal incidence assumption is a conservative one in regards to acoustic biomass estimation). The zooplankton models suffer similarly from simplified shapes and uncertain tilt angle, although they were averaged over a tilt angle distribution (Table 3.2). Simple shapes have been shown to adequately represent backscattering from animals when the tilt angle distribution includes 0° (Stanton and Chu, 2000). The large changes in σ_{bs} over small areas in frequency-tilt space make tilt angle assumptions crucial

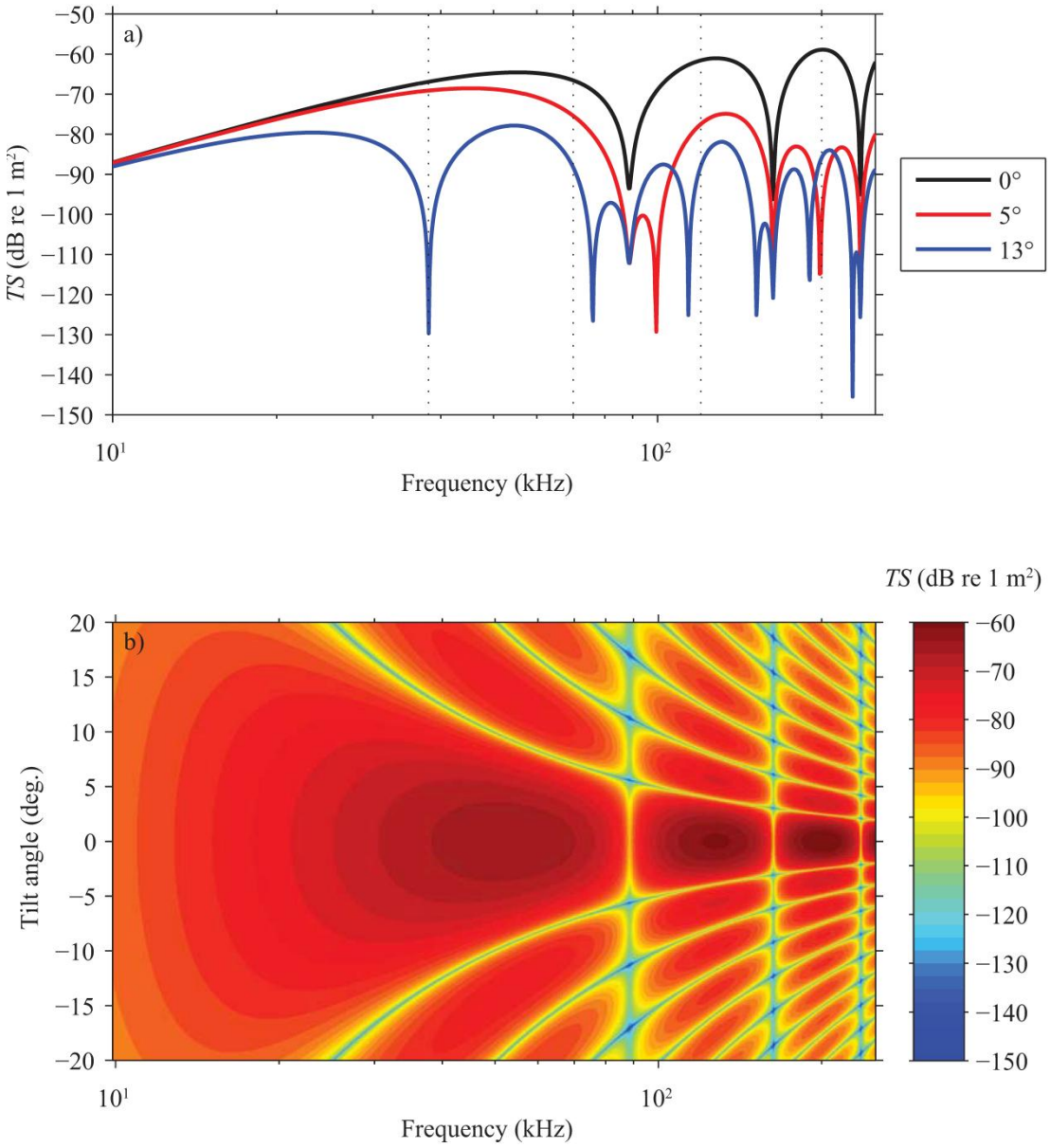

Figure 3.7. (a) Frequency spectrum of a fluid cylinder (86 mm *S. leucopsarus*, radius of 5.2 mm) at 0° tilt (black line), 5° tilt (red line), and 13.2° tilt (blue line). EK60 frequencies are marked with vertical dotted lines. (b) *TS* of the same fish mapped over tilt angle and frequency.

to acoustic biomass estimates. Because null location varies from model to model (Figure 3.8), with size of the animal (Figure 3.4), and perhaps between model and animal, averaging over a tilt angle distribution is perhaps the best approach. Unfortunately, this

parameter is poorly known, and conceivably changes with species, population, time of day, feeding history of the individual, depth, season, animal size, oxygen content of the water, and other environmental properties. More research is necessary to establish the tilt angle assumptions that produce the most accurate results.

Comparison of the cylindrical model to a DWBA prolate spheroid model (Chu and Ye, 1999) and the two-mode solution of the cylindrical model (Stanton, 1988) shows that modeled *TS* is similar through the first null (Figure 3.8). A fourth model, the DWBA deformed cylinder, performs similarly to the prolate spheroid model (Yasuma *et al.*, 2003). The models diverge at higher frequencies, where they all become less likely to match the *TS* of a real animal as heterogeneities within the animal become larger in relation to the acoustic wavelength.

3.5.2. Efficacy of the inverse method

The Monte Carlo analyses of artificial echograms showed that the inverse method is successful at decomposing multi-frequency S_v into accurate counts of model animals when average frequency spectra are used (Table 3.4). The differences between Groups I-III are sufficient to distinguish them and to make accurate abundance surveys. The results of subsequent Monte Carlo analyses (echograms constructed from individual animal models rather than from average spectra) qualify the results of the first analysis. The abundance measurements are still accurate (low mean error), but they are extremely variable (Table 3.4). In the Monte Carlo configuration matching the survey conditions, the combined NNLS inverse model error from all acoustic groups was 1.7 individuals from a range of 1-37 individuals ensonified. This is quite good by trawling standards.

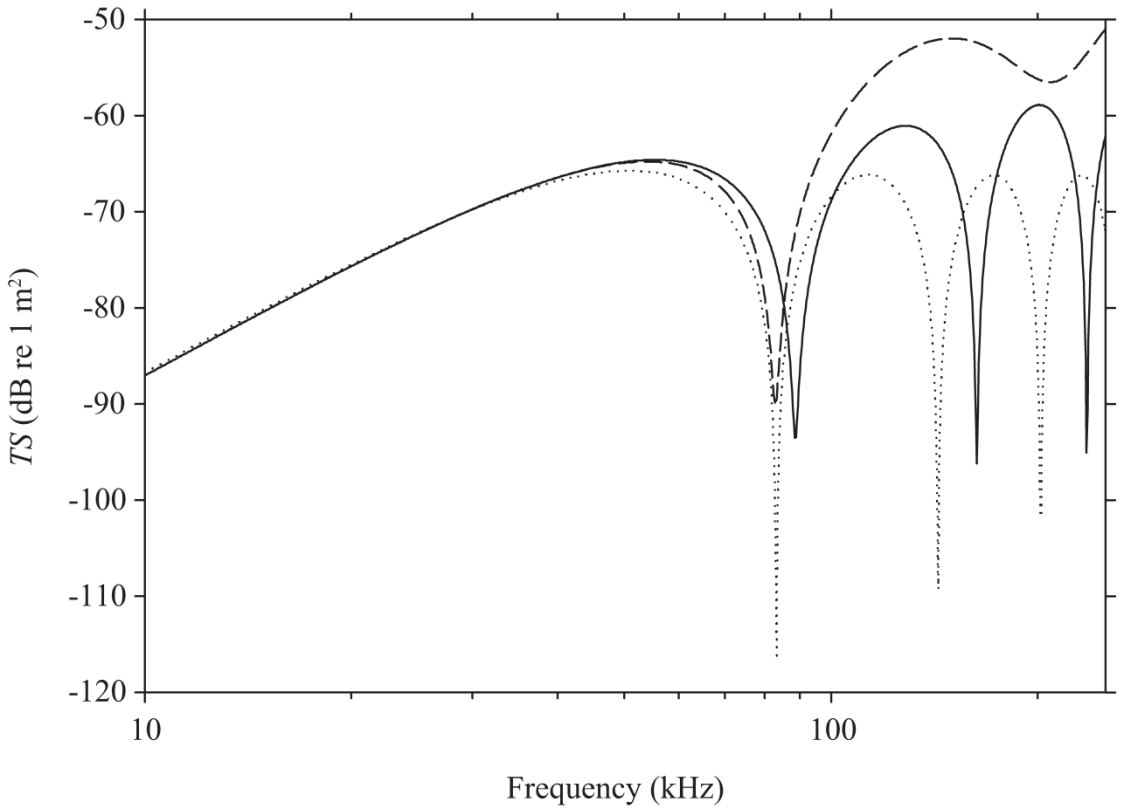

Figure 3.8. Frequency spectra of a fish (86 mm *S. leucopsarus*, radius of 5.2 mm) as represented by the full fluid cylinder model (solid line), the 2-mode solution of the fluid cylinder model (dashed line), and the DWBA prolate spheroid model (dotted line).

However, large numbers of samples must be taken in order to make a good abundance estimate. The source of most error in the results of the Monte Carlo analyses is individual variation in the modeled spectra. If enough animals are ensonified, the use of average spectra is appropriate. In the case of sparsely present strong scatterers (Groups I and II), accurate abundance estimates for individual water parcels are probably not possible using this method due to differences between the model frequency spectra used for inverse analysis (means derived from simple fluid shapes and assumed tilt angle distributions) and those of individual animals with complex internal and external structure, unknown size, and unknown tilt angle. The error measured by the Monte Carlo simulation is not

identical to the error in our acoustic survey, although care was taken to match the simulation to the survey. This is due to differences between the *TS* frequency spectra of *in situ* animals and our forward models, as well as the sampling bias of the MOHT, both of which contribute to uncertainty by an unknown amount.

Group II is composed of geometric scatterers, and contains spectra of heterogenous shape (Figure 3.3). The heterogeneity of the spectra within this group is a source of error when inverse methods are used to decompose measured S_v (Table 3.4). The question of whether or not the performance of inverse methods can be improved with the addition of more acoustic groups was explored with Monte Carlo simulations. In other words, does the benefit from more homogenous acoustic groups outweigh the cost of underdetermination? NNLS inversion has been reported to provide solutions for cases that are underdetermined by factors of 1.5-2 (Holliday and Pieper, 1995). We found that NNLS inversion remained accurate for up to ten acoustic groups with four measured frequencies (underdetermination by a factor of 2.5; Figure 3.6). Our results indicate that the subdivision of Group II into more acoustic groups with the current set of frequencies (underdetermination) can reduce variability in the error of the inverse methods, although the mean error approximately doubles. However, because a single Group II scatterer can have a resonant null at any measured frequency and some moderate tilt angle (Figure 3.7), it may belong to any of several different acoustic groups composed of homogenously-shaped acoustic spectra depending on its tilt angle. Care must be taken to ensure that fine division of geometrically-scattering acoustic groups remains biologically meaningful. For this reason, the addition of measured frequencies or acoustic groups in the geometric scattering region may not improve survey accuracy. The use of an

appropriate averaging scheme for geometric scatterers is required, and resolution will be limited in the case where few animals are ensonified.

The smallest gas inclusions of Group I animals resonate at frequencies just below the lowest EK60 frequency (~20-30 kHz here for a swimbladder ESR of 0.03 mm; Figure 3.4). The addition of new frequencies below 38 kHz would allow subdivision of Group I into resonant and non-resonant animals. It may be possible to separate fish larvae from juvenile and adult fishes in this manner, although the problem will be complicated by the presence of fish species that regress in swimbladder gas volume with growth (Davison, 2011) and the possibility that some fishes may allow swimbladder gas volume to compress with a decrease in depth.

3.5.3. Capture efficiency

The biomass estimate of mesopelagic fishes from the MOHT (night mean of 0.8 g m^{-2}) is lower than the published trawling estimates for the California Current (3.6 g m^{-2}, 6' IKMT; Gjosaeter and Kawaguchi, 1980). This discrepancy results from the shallow depth of the trawls used in this study, where only the vertically migrant portion of the population was sampled. Mean fish biomass from 21 tows of the MOHT to ~750 m depth (Chapter 4, Table 4.6) was 3.9 g m^{-2}.

The depth of MOHT tows (~200 m) exceeded the usable depth range of the highest frequency of the EK60 (~150 m). The depth discrepancy between the two biomass estimation methods used here may result in an overestimate of biomass by the MOHT in comparison to the acoustic results, and thus an overestimate of capture efficiency. Exclusion of non-vertically migratory fishes from the forward modeling was

intended to correct for the expected bias, but this method is imperfect, and it did not include a similar correction for invertebrates. Inspection of the echograms of the lower frequencies indicated that the depth range of 150-200 m was largely empty, and the bias is likely to be small.

The inverse modeling results here indicate that the MOHT captures an average of 47% of the micronekton biomass (Table 3.3). It is not possible to fully partition the capture efficiency of fishes from invertebrates within the acoustic groups, although the capture efficiency of a group is most influenced by the numerically dominant members. The capture efficiency of Group I (14%) is thus representative of small fishes with inflated swimbladders, while the capture efficiency of Group III (81%) is representative of "small" zooplankton. Group II is composed of a more even mixture of fishes and large invertebrates, so their relative contribution to the overall capture efficiency of the group (38%) is unknown, although it seems reasonable that small fishes without inflated swimbladders have similar avoidance capabilities to those with swimbladders (Group I).

Capture efficiency of Group I animals by the MOHT is significantly less in daylight than at night (Table 3.3). This result is possibly due to a combination of increased visibility of the trawl (Wiebe *et al.*, 1982; Pearcy, 1983) and a difference in the taxonomic composition of Group I between day and night. Vertically migratory mesopelagic fishes were not present at trawl depths during daylight, so acoustic detections were likely to be epipelagic fishes, which are known to easily avoid framed trawls similar to the MOHT (Barkley, 1972; Itaya *et al.*, 2007).

The lower capture efficiencies for Groups I and II reflect the increased swimming ability of these larger animals. The net mesh used here (1.7 mm) can be expected to retain

these large animals, although more delicate forms (such as jellies) may be torn up and extruded through the mesh. Zooplankters are less able to avoid the net, but more likely to be extruded through the mesh. These include small zooplankters which were not forward modeled (as they were not retained), but undoubtedly contribute to measured S_v. These small zooplankters scatter in the Rayleigh region, similarly to our Group III. Extruded small zooplankters would therefore be interpreted by the inverse model as fewer, but larger, Group III animals. Thus, extrusion error in Group III abundance is not likely to contribute much to error in abundance estimates of Groups I and II.

The Group I capture efficiency estimate for the MOHT is consistent with previous estimates for fishes using other trawl designs of similar size, and perhaps coincidentally, consistent with that reported for very large trawls (Table 3.5). Group II capture efficiency for the MOHT is higher than that reported for similarly-sized invertebrates, likely due to the larger net area and faster towing speed of the MOHT in comparison to the MOCNESS, BIONESS, and MIK (Table 3.5). Similar differences in capture efficiency are observed between the MOHT and smaller nets for Group III animals (small euphausiids; Table 3.5).

3.6. Conclusions

The inverse methods presented here successfully separated a diverse assemblage of mesopelagic micronekton into three groups for abundance estimation. The Monte Carlo results indicate that errors from NNLS inversion are low, but variable (Figure 3.6, Table 3.4). It is desirable to improve the resolution of the methods, which can be accomplished via the addition of frequencies and/or acoustic categories. Small resonant

gas inclusions from acoustic Group I will be separable with the addition of frequencies below 38 kHz. Subdivision of Group II is possible at a relatively low cost to accuracy with either underdetermination or the addition of frequencies between 38 and 200 kHz.

Table 3.5. Measurements of the capture efficiency (CE) of pelagic trawls for mesopelagic micronekton. Studies are sorted by increasing mouth area of the net.

Reference	Net	Mouth area	Mesh	Towing speed	Animals	Baseline	CE
Lawson *et al.* (2008)	MOCNESS	1 m^2	335 μm	1 m s^{-1}	Antarctic krill	acoustics	~1-10%
Mitson *et al.* (1996)	BIONESS	1 m^2	330 μm	not given	euphausiids	acoustics	46-78%
Warren *et al*. (2003)	MOCNESS	1 m^2	335 μm	not given	15 mm euphausiids	acoustics	>9%
Zhou *et al*. (1994)	MOCNESS	1 m^2	333 μm	1 m s^{-1}	Antarctic euphausiids	acoustics	1-100%
Mitson *et al.* (1996)	MIK	2 m^2	2 mm	not given	large shrimp	acoustics	0.1-0.5%
Barkley (1972)	6' IKMT	2.9 m^2	12 mm	1.2 m s^{-1}	mesopelagic fishes	avoidance theory	7%
Barkley (1972)	6' IKMT	2.9 m^2	12 mm	2.0 m s^{-1}	mesopelagic fishes	avoidance theory	31%
Baird *et al.* (1974)	6' Tucker trawl	3.2 m^2	11 mm	1.16 m s^{-1}	mesopelagic fishes	acoustics	2-8%
this study	MOHT	5 m^2	1.7 mm	1.25-1.5 m s^{-1}	mesopelagic fishes with swimbladder	multi-frequency acoustics	14%
this study	MOHT	5 m^2	1.7 mm	1.25-1.5 m s^{-1}	mesopelagic micronekton with no gas inclusion	multi-frequency acoustics	38%
this study	MOHT	5 m^2	1.7 mm	1.25-1.5 m s^{-1}	large zooplankton	multi-frequency acoustics	81%
Koslow *et al.* (1997)	IYGPT	105 m^2	100-10 mm	1.5 m s^{-1}	mesopelagic fishes	acoustics	4-14%
May and Blaber (1989)	Engel 152 pelagic trawl	266 m^2	1,800-9 mm	1.5 m s^{-1}	mesopelagic fishes	catchability coefficient model	6-20%
Gjosaeter (1984)	Commercial pelagic trawl	250, 500, and 800 m^2	200-9 mm	1-1.5 m s^{-1}	mesopelagic fishes	acoustics	35%

Addition of frequencies higher than 200 kHz will shift the classification of some Group III animals to Group II. Improvements in the categorical resolution of Group II may not correspond to natural taxonomic groups, because the frequency spectra of the geometrically backscattering animals in this group are confounded by resonant nulls that are strongly influenced by orientation (Figure 3.4, Figure 3.7). Thus, the same animal will belong to different acoustic groups depending upon its tilt angle. Acoustic surveys of the complex DSL micronekton community using inverse methods are likely to be limited to a handful of categories due to this fundamental limitation of the technique. Furthermore, results will be accurate only when averaged over a great many samples.

The relation between acoustic and trawl estimates of the biomass of the DSL is variable (Figure 3.5). The sources of this variability are many, including patchiness in the distribution of animals, differential capture efficiency within acoustic groups, error in blind zone assumptions, differences between simplified models and real animals, imperfect understanding of acoustic parameters (g, h, tilt angle, gas volume), and high frequency nulls in the frequency spectra of relatively large scatterers. Some of these problems can be overcome with large sample sizes, as illustrated by the performance of Monte Carlo simulations, while others (acoustic parameters, blind zone, and oversimplified models) cannot. Capture efficiency of the MOHT for mesopelagic micronekton is estimated to be 14% for small fishes, 81% for small zooplankton, and 38% for larger animals with no gas inclusion. Mesopelagic trawls such as the MOHT with mm-range mesh are not used for zooplankton biomass estimates, because an unknown fraction of zooplankters is lost through the mesh. The capture efficiencies

reported here will be most useful for improving trawl-based biomass estimates of mesopelagic micronekton in the 2-10 cm size range.

3.7. Acknowledgements

Advice and support for EK60 calibration was provided by D. Demer (NOAA SWFSC) and his laboratory. J. Liu installed and operated the EK60 and calibration electrical equipment. MATLAB code for zooplankton models was provided by L. McGarry and written by D. Chu (NOAA NWFSC) and A. Lavery (WHOI). MATLAB code for the NNLS inverse models was provided by P. Wiebe (WHOI). A. Townsend (SIO PIC) provided advice and assistance for processing the invertebrate samples. Funding for the EK60 and MOHT was provided by the Moore Foundation. P. Davison was supported by a NASA Earth and Space Science Fellowship. A. Lara-Lopez was supported by JIMO. Wire time for midwater trawling was provided by the California Current Ecosystem LTER site, supported by NSF. The authors thank the captain, crew, and science party of the R/V "Melville" for assistance deploying the MOHT and processing the samples.

3.8. References

Anderson, V.C., 1950. Sound scattering from a fluid sphere. Journal of the Acoustical Society of America 22 (4), 426-431.

Backus, R.H., Craddock, J.E., Haedrich, R.L., Shores, D.L., Teal, J.M., Wing, A.S., Mead, G.W., Clarke, W.D., 1968. *Ceratoscopelus maderensis*: peculiar sound-scattering layer identified with this myctophid fish. Science 160 (3831), 991-993.

Barham, E.G., 1971. Deep-sea fishes: lethargy and vertical orientation. In: Farquhar, G.B. (Ed.), Proceedings of an international symposium on biological sound scattering in the ocean. U.S. Government Printing Office, Washington D.C., pp. 100-118.

Barkley, R.A., 1972. Selectivity of towed-net samplers. Fishery Bulletin 70 (3), 799-820.

Barr, R., Coombs, R.F., 2005. The significance of high-order resonances of spherical bubbles to the acoustic response of fish with swimbladders. Journal of the Acoustical Society of America 117 (6), 3589-3599.

Chu, D., Wiebe, P.H., 2005. Measurements of sound-speed and density contrasts of zooplankton in Antarctic waters. ICES Journal of Marine Science 62 (4), 818-831.

Chu, D.Z., Foote, K.G., Stanton, T.K., 1993. Further analysis of target strength measurements of Antarctic krill at 38 and 120 kHz: comparison with deformed cylinder model and inference of orientation distribution. Journal of the Acoustical Society of America 93 (5), 2985-2988.

Chu, D.Z., Wiebe, P., Copley, N., 2000. Inference of material properties of zooplankton from acoustic and resistivity measurements. ICES Journal of Marine Science 57 (4), 1128-1142.

Chu, D.Z., Ye, Z., 1999. A phase-compensated distorted wave Born approximation representation of the bistatic scattering by weakly scattering objects: Application to zooplankton. Journal of the Acoustical Society of America 106 (4), 1732-1743.

Davison, P., 2011. The buoyancy of mesopelagic fishes from the northeast Pacific Ocean and its implications for acoustic backscatter. ICES Journal of Marine Science 68 (10), 2064-2074.

Feuillade, C., Werby, M.F., 1994. Resonances of deformed gas bubbles in liquids. Journal of the Acoustical Society of America 96 (6), 3684-3692.

Foote, K.G., Knudsen, H.P., Vestnes, G., MacLennan, D.N., Simmonds, E.J., 1987. Calibration of acoustic instruments for fish density estimation: a practical guide. ICES Cooperative Research Report No. 144.

Gartner, J.V., Conley, W.J., Hopkins, T.L., 1989. Escapement by fishes from midwater trawls - a case study using lanternfishes (Pisces: Myctophidae). Fishery Bulletin 87 (1), 213-222.

Gjosaeter, J., Kawaguchi, K., 1980. A review of the world resources of mesopelagic fish. FAO Fisheries Technical Paper 193, 1-151.

Greenblatt, P.R., 1982. Small-scale horizontal distributions of zooplankton taxa. Marine Biology 67 (1), 97-111.

Greenlaw, C.F., 1979. Acoustical estimation of zooplankton populations. Limnology and Oceanography 24 (2), 226-242.

Greenlaw, C.F., Johnson, R.K., 1983. Multiple frequency acoustical estimation. Biological Oceanography 2, 227-252.

Holliday, D.V., Pieper, R.E., 1995. Bioacoustical oceanography at high frequencies. ICES Journal of Marine Science 52 (3-4), 279-296.

Itaya, K., Fujimori, Y., Shimizu, S., Komatsu, T., Miura, T., 2007. Effect of towing speed and net mouth size on catch efficiency in framed midwater trawls. Fisheries Science 73 (5), 1007-1016.

Kalish, J.M., Greenlaw, C.F., Pearcy, W.G., Van Holliday, D., 1986. The biological and acoustical structure of sound scattering layers off Oregon. Deep-Sea Research 33 (5), 631-653.

Kloser, R.J., Ryan, T.E., Young, J.W., Lewis, M.E., 2009. Acoustic observations of micronekton fish on the scale of an ocean basin: potential and challenges. ICES Journal of Marine Science 66 (6), 998-1006.

Lavery, A.C., Wiebe, P.H., Stanton, T.K., Lawson, G.L., Benfield, M.C., Copley, N., 2007. Determining dominant scatterers of sound in mixed zooplankton populations. Journal of the Acoustical Society of America 122 (6), 3304-3326.

Lawson, G.L., Wiebe, P.H., Ashjian, C.J., Gallager, S.M., Davis, C.S., Warren, J.D., 2004. Acoustically-inferred zooplankton distribution in relation to hydrography west of the Antarctic Peninsula. Deep-Sea Research II 51 (17-19), 2041-2072.

Lawson, G.L., Wiebe, P.H., Stanton, T.K., Ashjian, C.J., 2008. Euphausiid distribution along the Western Antarctic Peninsula - Part A: Development of robust multi-frequency acoustic techniques to identify euphausiid aggregations and quantify euphausiid size, abundance, and biomass. Deep-Sea Research II 55 (3-4), 412-431.

Longhurst, A.R., 1976. Vertical migration. In: Cushing, D.H., Walsh, J.J. (Eds.), The ecology of the sea. Blackwell, Oxford, pp. 116-137.

Mackenzie, K.V., 1981. Nine-term equation for sound speed in the oceans. Journal of the Acoustical Society of America 70 (3), 807-812.

Mann, K.H., 1984. Fish production in open ocean ecosystems. In: Fasham, M.J.R. (Ed.), Flows of energy and materials in marine ecosystems. Plenum Press, New York, pp. 435-458.

Marshall, N.B., 1960. Swimbladder structure of deep-sea fishes in relation to their systematics and biology. Discovery Reports 31, 122.

Matsukura, R., Yasuma, H., Murase, H., Yonezaki, S., Funamoto, T., Honda, S., Miyashita, K., 2009. Measurements of density contrast and sound-speed contrast for target strength estimation of Neocalanus copepods (*Neocalanus cristatus* and *Neocalanus plumchrus*) in the North Pacific Ocean. Fisheries Science 75 (6), 1377-1387.

Mikami, H., Mukai, T., Iida, K., 2000. Measurements of density and sound speed contrasts for estimating krill target strength using theoretical scattering models. Nippon Suisan Gakkaishi 66 (4), 682-689.

Millero, F.J., Chen, C.T., Schleicher, K., Bradshaw, A., 1980. A new high pressure equation of state for seawater. Deep-Sea Research 27 (3-4), 255-264.

Mitson, R.B., Simard, Y., Goss, C., 1996. Use of a two-frequency algorithm to determine size and abundance of plankton in three widely spaced locations. ICES Journal of Marine Science 53 (2), 209-215.

Miyashita, K., Aoki, I., Inagaki, T., 1996. Swimming behaviour and target strength of isada krill (*Euphausia pacifica*). ICES Journal of Marine Science 53 (2), 303-308.

Oozeki, Y., Hu, F.X., Kubota, H., Sugisaki, H., Kimura, R., 2004. Newly designed quantitative frame trawl for sampling larval and juvenile pelagic fish. Fisheries Science 70 (2), 223-232.

Pearcy, W.G., 1964. Some distributional features of mesopelagic fishes off Oregon. Journal of Marine Research 22 (1), 83-102.

Pearcy, W.G., 1983. Quantitative assessment of the vertical distributions of micronektonic fishes with opening/closing midwater trawls. Biological Oceanography 2, 289-310.

Robinson, C., Steinberg, D.K., Anderson, T.R., Aristegui, J., Carlson, C.A., Frost, J.R., Ghiglione, J.F., Hernandez-Leon, S., Jackson, G.A., Koppelmann, R., Queguiner, B., Ragueneau, O., Rassoulzadegan, F., Robison, B.H., Tamburini, C., Tanaka, T., Wishner, K.F., Zhang, J., 2010. Mesopelagic zone ecology and biogeochemistry - a synthesis. Deep-Sea Research II 57 (16), 1504-1518.

Robison, B.H., 1983. Midwater biological research with the WASP ADS. Marine Technology Society Journal 17 (3), 21-27.

Smith, J.N., Ressler, P.H., Warren, J.D., 2010. Material properties of euphausiids and other zooplankton from the Bering Sea. Journal of the Acoustical Society of America 128 (5), 2664-2680.

Stanton, T.K., 1988. Sound scattering by cylinders of finite length. I. Fluid cylinders. Journal of the Acoustical Society of America 83 (1), 55-63.

Stanton, T.K., Chu, D.Z., 2000. Review and recommendations for the modelling of acoustic scattering by fluid-like elongated zooplankton: euphausiids and copepods. ICES Journal of Marine Science 57 (4), 793-807.

Stanton, T.K., Chu, D.Z., Wiebe, P.H., 1998. Sound scattering by several zooplankton groups. II. Scattering models. Journal of the Acoustical Society of America 103 (1), 236-253.

Stanton, T.K., Wiebe, P.H., Chu, D.Z., Benfield, M.C., Scanlon, L., Martin, L., Eastwood, R.L., 1994. On acoustic estimates of zooplankton biomass. ICES Journal of Marine Science 51 (4), 505-512.

Wiebe, P.H., Boyd, S.H., Davis, B.M., Cox, J.L., 1982. Avoidance of towed nets by the euphausiid *Nematoscelis megalops*. Fishery Bulletin 80 (1), 75-91.

Wiebe, P.H., Chu, D.Z., Kaartvedt, S., Hundt, A., Melle, W., Ona, E., Batta-Lona, P., 2010. The acoustic properties of *Salpa thompsoni*. ICES Journal of Marine Science 67 (3), 583-593.

Yasuma, H., Sawada, K., Olishima, T., Miyashita, K., Aoki, I., 2003. Target strength of mesopelagic lanternfishes (family Myctophidae) based on swimbladder morphology. ICES Journal of Marine Science 60 (3), 584-591.

Yasuma, H., Sawada, K., Takao, Y., Miyashita, K., Aoki, I., 2010. Swimbladder condition and target strength of myctophid fish in the temperate zone of the Northwest Pacific. ICES Journal of Marine Science 67 (1), 135-144.

Yasuma, H., Takao, Y., Sawada, K., Miyashita, K., Aoki, I., 2006. Target strength of the lanternfish, *Stenobrachius leucopsarus* (family Myctophidae), a fish without an airbladder, measured in the Bering Sea. ICES Journal of Marine Science 63 (4), 683-692.

Zhou, M., Nordhausen, W., Huntley, M., 1994. ADCP measurements of the distribution and abundance of euphausiids near the Antarctic Peninsula in winter. Deep-Sea Research 41 (9), 1425-1445.

Chapter 3, in full, has been submitted for publication of the material as it may appear in the Journal of the Acoustical Society of America, Davison, P., Lara-Lopez, A., and Koslow, J.A., 2011. The dissertation author was the primary investigator and author of this paper.

Chapter 4. Carbon export mediated by mesopelagic fishes in the northeast Pacific Ocean

4.1. Abstract

The role of mesopelagic fishes in the global carbon cycle is poorly known and often neglected. We estimate the export of carbon out of the epipelagic ocean mediated by mesopelagic fishes ("fish export") with individual-based metabolic modeling of the catch from 77 mesopelagic trawls distributed over a wide area of the northeast Pacific Ocean. The biomass of mesopelagic fishes increases with increasing annual net primary productivity, and is estimated to be approximately 55 million metric tons (17 g m^{-2}) off the continental U.S.A. west to longitude 141°W. We found that 25% of this biomass ascends to the epipelagic zone at night. Fish export forms 17% (24.8 mg C m^{-2} d^{-1}) of the total carbon exported in the study area (144.4 mg C m^{-2} d^{-1}), as estimated from satellite data. Fish export varies spatially in both magnitude and relative importance. Although overall fish export increases with total export, its fraction of the total export decreases. Fish export exceeds 40% of the total carbon export in the oligotrophic North Pacific Subtropical Gyre, but forms <10% of the total export in the most productive waters of the California Current. Because the daytime residence depth of these fishes is below the depths where most remineralization of sinking particles occurs, fish export is approximately equal to the passive transport at a depth of 400 m.

4.2. Introduction

The global carbon cycle is of interest due to the large and increasing amount of anthropogenic CO_2 that has been released into the atmosphere since the beginning of the industrial age, and its impact on world climate (IPCC, 2007). Approximately 31% of anthropogenic CO_2 (~2.2 Pg C y^{-1}) is currently taken up by the ocean, a carbon reservoir ~50 times the size of the atmosphere (Denman *et al.*, 2007). A portion of the oceanic carbon is exported from the surface mixed layer, where it is in contact with the atmosphere, to the deep ocean, where it is sequestered for decades to centuries. Deep ocean water has a higher CO_2 partial pressure than the atmosphere when brought to the surface and warmed, and will therefore outgas as a result of oceanic circulation (Watson and Orr, 2003). The larger size of the deep ocean carbon reservoir and higher CO_2 partial pressure in comparison to the atmosphere means that upper ocean processes critically affect atmospheric CO_2 concentration (Falkowski *et al.*, 2003; Watson and Orr, 2003).

The air-sea flux of CO_2 results from concentration and solubility gradients between the atmosphere, the ocean surface, and deeper water (Watson and Orr, 2003). About 70% of the CO_2 concentration gradient in the top 1000 m of the ocean is maintained by biological processes in the form of exported production, the "biological pump" (Volk and Hoffert, 1985). The biological pump is not a single mechanism, but rather several different processes mediated by a wide array of organisms (Angel, 1984, 1989a). It is broadly divided into passive and active transport terms. Passive transport refers to the sinking of organic material through the water column. Active transport is the flux of material physically transported by animals as they move daily or seasonally across a depth range. This flux depends on the relative locations in the water column of ingestion, respiration, excretion, defecation, and mortality of these animals. Most

passively sinking particles are remineralized high in the water column, so large rapidly sinking particles such as fecal pellets and aggregates dominate passive export to the deep ocean (Angel, 1984; Buesseler *et al.*, 2007b; Fowler and Knauer, 1986). Passive transport is often measured with sediment traps set at various depths in the water column. However, the carbon export measured by sediment traps is expected to be biased low in comparison to total carbon export, because sediment traps undercount large and sparsely-distributed particles, as well as flux events on short time scales, and because they may completely miss active transport (Angel, 1984, 1985; Fowler and Knauer, 1986; Robison *et al.*, 2005; Silver *et al.*, 1998). Carbon export measured via the Thorium disequilibrium technique also does not include active transport (Falkowski *et al.*, 2003). Estimates of carbon export made using sediment traps are indeed lower than those estimated by other methods (Buesseler *et al.*, 2007a; Knauer *et al.*, 1990; Martz *et al.*, 2008; Usbeck *et al.*, 2003). Carbon actively transported by fishes may be proportionally greater in the mesopelagic in comparison to total carbon export because these relatively large and strongly-swimming animals can carry carbon below the depths where most mesopelagic remineralization occurs (150-400 m; Buesseler and Boyd, 2009).

The animals that conduct active transport form the deep scattering layer (DSL), a strong and ubiquitous sound-reflecting layer of organisms that rises at night and descends during the day (Diel Vertical Migration, DVM). A portion of the DSL remains at depth during the night. At 38 kHz in our study area, the DSL is chiefly composed of midwater fishes with swim bladders and, to a lesser extent, other micronekton and zooplankton (Chapter 3). Although not moving vertically themselves, some midwater fishes contribute to active transport through the consumption of vertically-migratory

zooplankton (Figure 4.1). The global biomass of midwater (mesopelagic) fishes that populate the DSL has been estimated as at least one billion metric tons, or 1 Pg wet weight (Gjosaeter and Kawaguchi, 1980). During the time spent at depth, these fishes "lose" carbon in the form of respired CO_2, feces, excreta, and mortality (Figure 4.1). A simple calculation indicates that 1 Pg of fishes will consume 1.5 Pg C y^{-1} assuming a daily ration of 5% of wet weight, a dry weight to wet weight ratio of 0.2 for zooplankton (Childress and Nygaard, 1974), and a carbon to dry weight ratio of 0.4 for zooplankton

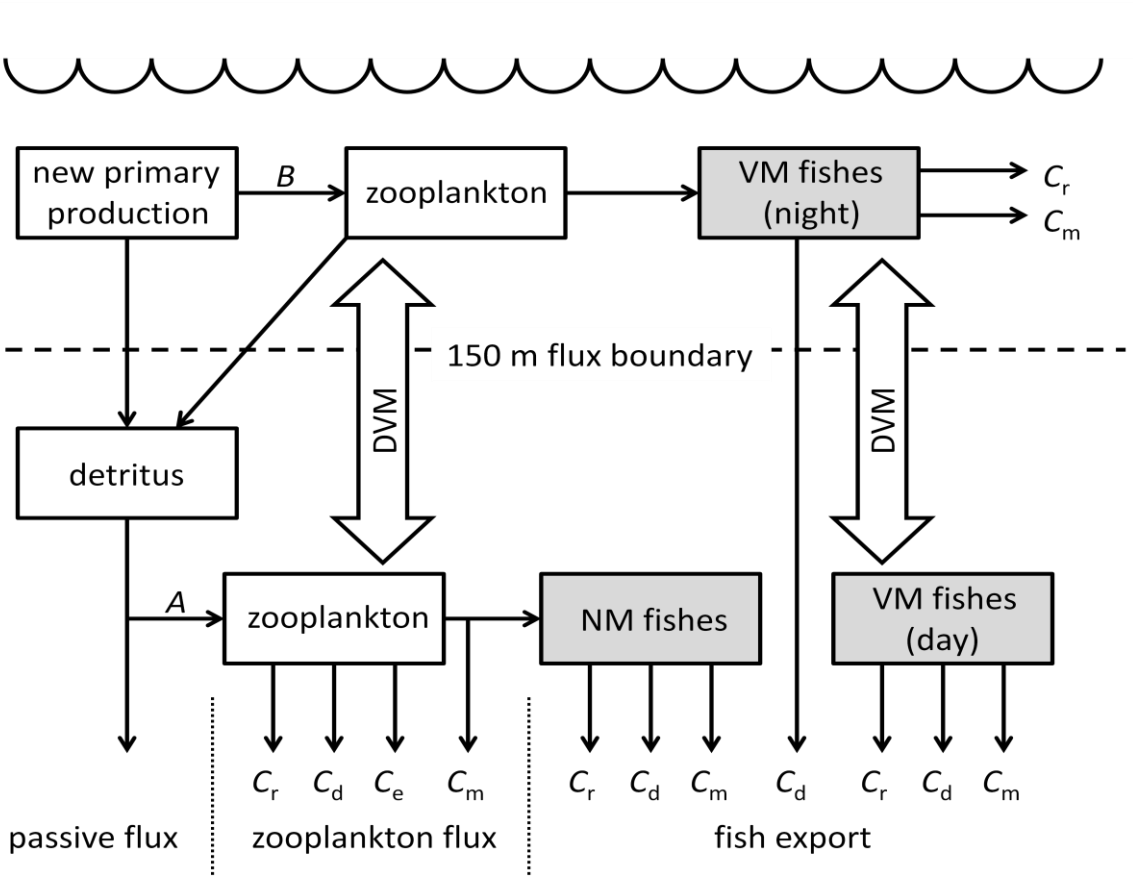

Figure 4.1. Carbon flux diagram of the biological pump. Fish export is defined as the sum of respiratory (C_r), defecation (C_d), and mortality (C_m) carbon fluxes of all fishes below the 150 m flux boundary and C_d of VM fishes above the 150 m flux boundary. The fraction of zooplankton carbon of detrital origin, $C_{do} = A(A+B)^{-1}$, is defined in terms of the fluxes marked *A* and *B*. Only mesopelagic fishes (shaded boxes) are studied here. An additional carbon export flux term for excretion (C_e) is shown for zooplankton.

(Putzeys and Hernandez-Leon, 2005). This is a large and significant quantity in relation to net air-sea exchange (1.6 Pg y^{-1}; Denman *et al.*, 2007) and global estimates of new production (11 Pg y^{-1}; Falkowski *et al.*, 2003), and it invites closer examination.

The export of carbon by fishes is expected to vary regionally with changes in temperature and fish abundance (ind. m^{-2}). Local mesopelagic fish biomass (g m^{-2} wet weight) can exceed 500 g m^{-2}, much greater than the global mean value of ~3 g m^{-2} (Gjosaeter and Kawaguchi, 1980). Current estimates of the distribution of mesopelagic fishes are based upon widely dispersed measurements, largely from trawls, extrapolated across zoogeographical regions and thus have low spatial and temporal resolution (Gjosaeter and Kawaguchi, 1980). Trawl-based measurements of fish biomass have been shown to be biased low due to avoidance and escapement of the net, and capture efficiency may be less than 10% for some commonly-used net designs (summarized in Chapter 3). This large bias in net-based sampling has encouraged the development of alternative and complementary methods for estimating biomass, such as acoustic techniques.

Previous studies of the biological pump have generally either neglected the role of mesopelagic fishes (Buesseler *et al.*, 2007a; Buesseler and Boyd, 2009; Buesseler *et al.*, 2007b; Emerson *et al.*, 1997; Falkowski *et al.*, 2003; Karl *et al.*, 1996) or considered them to play a minor role (Angel, 1989a, b; Longhurst *et al.*, 1990; Longhurst and Harrison, 1989). This was the result of previous low estimates of fish abundance and neglect of some flux terms. More recent work that corrects fish abundance for the low capture efficiency of nets (Hidaka *et al.*, 2001; Williams and Koslow, 1997) indicates that carbon export by fishes is considerably larger relative to the total flux. We hypothesize

that the export of carbon from the epipelagic mediated by mesopelagic fishes ("fish export"; Figure 4.1) forms a significant portion of the total carbon exported from the epipelagic ("total export"). For this purpose, we define the epipelagic as the top 150 m of the water column and mesopelagic fishes as those species found shallower than 1000 m but not present in the epipelagic during daylight. Observations of water temperature, fish biomass, size distribution, and migratory behavior are used with published physiological and ecological rates to inform a flux model in order to estimate the fish export across a region of the northeast Pacific Ocean. Fish export is compared to measurements of the passive flux in the study area (Martin *et al.*, 1987) and to total export, as estimated with the Laws (2004) model from satellite-derived measurements of net primary productivity (NPP), sea surface temperature (SST), and depth of the euphotic zone. Sensitivity of the flux model to variation in measured, assumed, and calculated parameters is explored, and model predictions for fish respiration rate and daily ration are compared to independent measurements from the literature.

4.3. Materials and Methods

Mesopelagic fishes were collected in 2008 and 2009 from 77 stations on cruises of the R/V "Melville" (cruise P0810 of the California Current Ecosystem Long Term Ecological Research program), R/V "New Horizon" ("SEAPLEX"), and the National Oceanic and Atmospheric Administration (NOAA) FSV "McArthur II" ("ORCAWALE") in the North Pacific (Figure 4.2). All three cruises sampled the California Current ecosystem (CCE), and one cruise (SEAPLEX) also sampled the eastern North Pacific subtropical gyre (NPSG). At each sampling station, oblique midwater trawls were

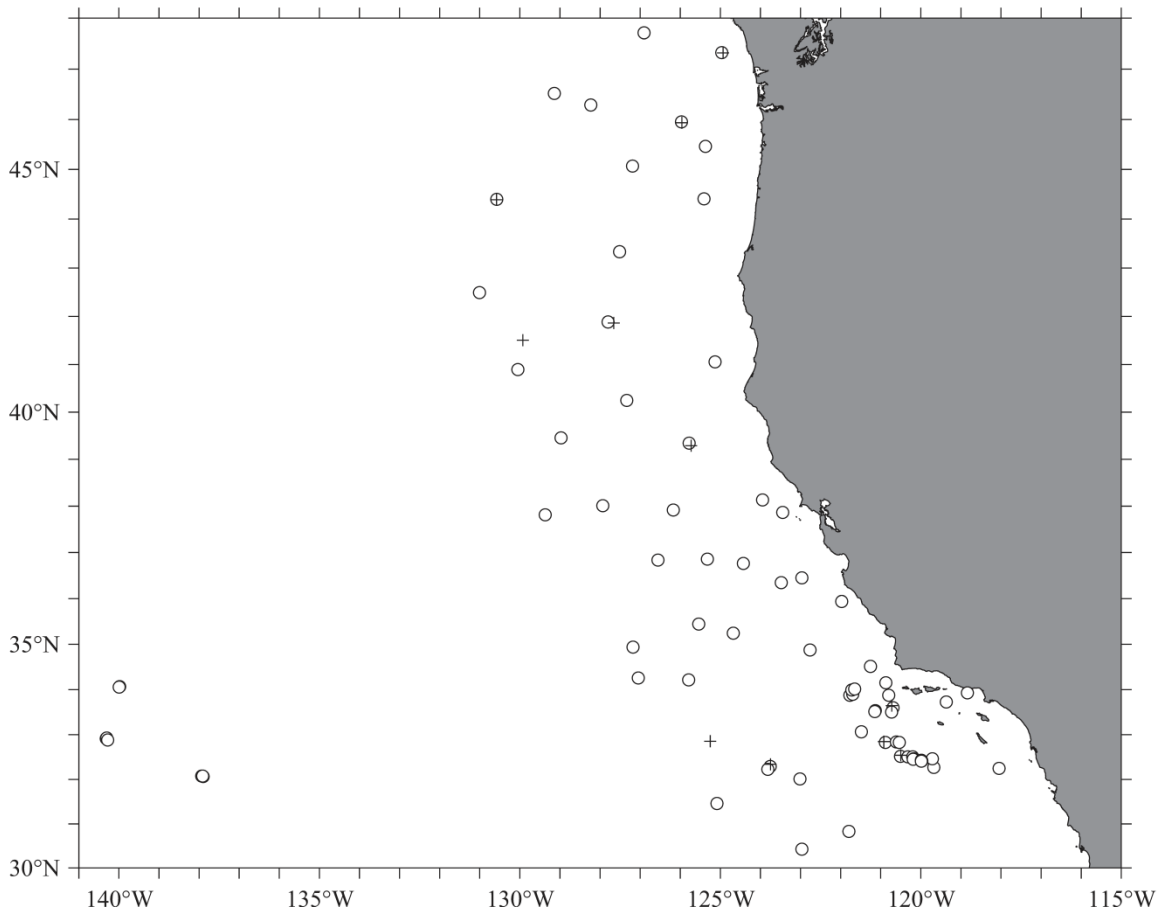

Figure 4.2. Sampling locations of midwater trawls. The field of view is the study area for which the carbon flux mediated by mesopelagic fishes was calculated. Sampling locations are marked as open circles and shallow day trawls are marked as crosses.

conducted to a depth of at least 500 m at a towing speed of ~1.5 m s^{-1} (Table 4.6). Epipelagic tows were made at each station in darkness after the ascent of the DSL to directly estimate the vertically-migratory fish abundance and biomass. In addition, daylight epipelagic tows to ~200 m depth were made on eleven occasions. On the P0810 cruise, six deployments of a sub-surface Lagrangian drifter were made, and sampling occurred over multiple days following each drifter deployment. SEAPLEX sampling occurred over 24 h period at each of four Eulerian stations. For these cruises, deep tows

were treated as separate stations, but night epipelagic trawls were averaged together (by Lagrangian or Eulerian station) for estimates of vertically-migratory abundance and biomass. All three vessels were equipped with Simrad EK60 multi-frequency echosounders, although the acoustic data were not used quantitatively here. Fishes were captured using an Isaacs-Kidd midwater trawl (IKMT; Isaacs and Kidd 1953; 3 m^2 mouth area; FSV "McArthur II") and a 5-m^2 Matsuda-Oozeki-Hu trawl (MOHT; Oozeki *et al.* 2004; R/V "Melville" and R/V "New Horizon") that each had a uniform square mesh of 1.7 mm. Trawl depth and ambient water temperature were measured with a Wildlife Computers MK9 archival tag mounted to the net frame. The archival tag temperature and depth measurements were calibrated on each cruise from casts of a Sea-Bird SBE 911plus CTD. Water flow through the trawl mouth was measured with a TSK flowmeter for the MOHT, and calculated from ship speed for the IKMT because the flowmeter (and spare) malfunctioned on the FSV "McArthur II". Fishes were separated from zooplankton at sea, and preserved with a solution of 5% Formalin in seawater, 90% ethanol, or by freezing until they could be processed ashore.

In the laboratory, fishes were identified to species, the standard length (L_S) was measured to the nearest mm, and the wet weight was measured to a precision of 0.01 g or calculated from a length-weight curve constructed from a subset of the material. Fishes of the genus *Cyclothone* were weighed in aggregate by species to save time because they often numbered several hundred per trawl, and mean weights of *Cyclothone* spp. were used for metabolic modeling. Each fish species was classified as either "vertically migratory" (VM) or "non-migratory" (NM). VM fishes included *Vinciguerria* spp., *Scopelarchus* spp., *Diplophos taenia*, *Bregmaceros japonicus*, all Bathylagidae (except

Bathylagus pacificus and *Pseudobathylagus milleri*), and all Myctophidae (except *Protomyctophum* spp., *Taaningichthys bathyphilus*, *Stenobrachius nannochir*, *Parvilux ingens*, *Nannobrachium regale*, *Nannobrachium bristori*, *Nannobrachium fernae*, and *Nannobrachium lineatum*). Larval, epipelagic, and piscivorous fishes (*Benthalbella dentata* and most fishes of the family Stomiidae) were not included in modeling or analysis, and are not considered further. The stomiids *Tactostoma macropus*, *Bathophilus flemingi*, *Malacosteus niger*, and *Photostomias* sp. were considered to be planktivores (Borodulina, 1972; Clarke, 1982) and included in all analyses.

4.3.1. Carbon exported by fishes

The overall carbon flux model for an individual mesopelagic fish was constructed from sub-models, including a respiratory rate sub-model, a diel activity cycle sub-model, and an energy budget sub-model. The energy usage of a fish was calculated from its size, temperature, daily activity pattern, and routine metabolic rate. The energy budget equation was then solved for ingestion rate, and converted to units of carbon, as described in detail below. Note that symbols are defined in Table 4.1. The model estimates carbon flux across a 150 m depth plane (the assumed epipelagic boundary) partitioned into respiration, fecal, and mortality categories. Non-fecal excretory carbon flux was found to be very small in comparison to the other terms, and was therefore neglected. Each fish from each deep trawl was modeled, and then carbon flux was summed by trawl. Piscivorous fishes were excluded from the analysis because their ingestion of carbon is included in the mortality term of other mesopelagic fishes. The carbon fluxes at the trawl-level were then adjusted for capture efficiency of the IKMT (relative to the MOHT)

Table 4.1. Notation. No value is given if a term varies, no units are given for ratios, and no reference is given when the term is calculated from others. Symbol subscripts containing "nm" and "vm" refer to differing values for non-migratory and vertically-migratory fishes.

Symbol	Meaning	Value	Units	Reference
a	Regressed intercept for RMR of fishes	14.47		Gillooly *et al.*, 2001
AMR	Active metabolic rate (feeding fish)		J min^{-1}	
b_{nm}	Constant resulting from simplification of Eq. 2-3	0.29		
B_s	Biomass of VM fishes from shallow trawls		g m^{-2}	
b_{vm}	Constant resulting from simplification of Eq. 2-3	0.43		
B_{vm}	Biomass of VM fishes determined taxonomically		g m^{-2}	
c	Regressed slope for RMR of fishes	-5.02		Gillooly *et al.*, 2001
C_c	Ratio of carbon:carbohydrate of zooplankton	0.44		Harris *et al.* 2000
C_d	Carbon defecated by a fish per day		g d^{-1}	
C_{do}	Fraction of zooplankton carbon of detrital origin	0.33		
$C_{f,nm}$	Ratio of carbon:wet weight of NM fish	0.40[3]		Childress and Nygaard 1973
$C_{f,vm}$	Ratio of carbon:wet weight of VM fish	0.49[3]		Childress and Nygaard 1973
C_l	Ratio of carbon:lipid of zooplankton	0.78		Harris *et al.* 2000
C_m	Carbon lost by fish to growth (mortality) per day		g d^{-1}	
$C_{nm,adj}$	$C_{nm,tot}$ adjusted for C_{do}, V_f, and D_s		g m^{-2} d^{-1}	
$C_{nm,tot}$	Carbon exported by a fish per day		g d^{-1}	
C_p	Ratio of carbon:protein of zooplankton	0.53		Harris *et al.* 2000
C_r	Carbon respired by a fish per day		g d^{-1}	
$C_{vm,adj}$	$C_{vm,tot}$ adjusted for B_s:B_{vm}, V_f, and D_s		g m^{-2} d^{-1}	
$C_{vm,tot}$	Carbon exported by a fish per day		g d^{-1}	
C_z	Ratio of carbohydrate:dry weight of zooplankton	0.06[1,2]		Childress and Nygaard 1974
D_c	Fish digestive efficiency of carbohydrate	0.40		Brett and Groves 1979
D_l	Fish digestive efficiency of lipid	0.85		Brett and Groves 1979
D_p	Fish digestive efficiency of protein	0.90		Brett and Groves 1979
D_s	Sampling depth of the trawl		m	
E	Loss of ingested energy to non-fecal excretion	0.07I	J d^{-1}	Brett and Groves, 1979
ef ratio	Ratio of total exported production to NPP			Laws, 2004
F	Loss of ingested energy to feces	0.20I	J d^{-1}	Brett and Groves, 1979
G_{nm}	Daily growth of a fish (from lifetime G:M)	0.28M	J d^{-1}	Childress *et al.*, 1980
G_{vm}	Daily growth of a fish (from lifetime G:M)	0.71M	J d^{-1}	Childress *et al.*, 1980
H_c	Carbohydrate energy content	16.74	kJ g^{-1}	Brett and Groves 1979
H_l	Lipid energy content	39.55	kJ g^{-1}	Brett and Groves 1979
H_p	Protein energy content	18.25	kJ g^{-1}	Brett and Groves 1979
I	Daily energy requirement of a fish		J d^{-1}	
L_s	Standard length of a fish		mm	

Table 4.1. (continued)

Symbol	Meaning	Value	Units	Reference
L_z	Ratio of lipid:dry weight of zooplankton	0.24[1]		Childress and Nygaard 1974
M_{nm}	Daily metabolism of a fish	0.43I	J d^{-1}	
M_{vm}	Daily metabolism of a fish	0.57I	J d^{-1}	
NPP	Difference between autotrophic fixed and respired C		g m^2 d^{-1}	Behrenfeld and Falkowski, 1997
P_z	Ratio of protein:dry weight of zooplankton	0.37[1]		Childress and Nygaard 1974
$Q_{f,nm}$	$W_{w,f}$ -specific energy content of NM fish	3.06[3]	kJ g^{-1}	Childress and Nygaard 1973
$Q_{f,vm}$	$W_{w,f}$ -specific energy content of VM fish	5.84[3]	kJ g^{-1}	Childress and Nygaard 1973
Q_{ox}	Oxycalorific equivalent (energy obtained from respired oxygen)	13.6	J mg^{-1}	Brett and Groves, 1979
Q_z	Caloric value of zooplankton per gram wet weight	3.63	kJ g^{-1}	
R_d	Daily ration of a fish, expressed in terms of $W_{w,z}$		g d^{-1}	
R_e	Ratio of fish export between non-migratory and vertically-migratory behavior of a VM fish	1.03		
RMR	Routine metabolic rate (normal spontaneous activity)		J min^{-1}	Gillooly *et al.*, 2001
r_{nm}	Residence depth of fish	400	m	
RQ	Respiratory quotient (molar ratio CO_2:O_2)	0.90		Brett and Groves, 1979
r_{vm}	Residence depth of fish	50	m	
R_z	Ratio of zooplankton active transport to carbon demand at depth	2.0		Steinberg *et al.*, 2008
SDA	Energetic cost of food absorption and assimilation	0.14I	J d^{-1}	Brett and Groves, 1979
SMR	Standard metabolic rate (torpid fish)		J min^{-1}	
T	Temperature of fish		°C	
t	Time		d	
V_f	Volume filtered by the trawl		m^3	
$W_{d,f,nm}$	Ratio of dry weight:wet weight of NM fish	0.18[3]		Childress and Nygaard 1973
$W_{d,f,vm}$	Ratio of dry weight:wet weight of VM fish	0.26[3]		Childress and Nygaard 1973
$W_{d,z}$	Ratio of dry weight:wet weight of zooplankton	0.21[1]		Childress and Nygaard 1974
$W_{w,f}$	Wet weight of fish		g	
$W_{w,z}$	Wet weight of zooplankton consumed by a fish		g	

[1]mean of species with minimum depth of occurrence ≤400 m

[2]chitin included

[3]mean of species captured in this study

and the MOHT (relative to concurrent acoustic biomass estimates, 14%; Chapter 3).

The routine metabolic rate (RMR, J min^{-1}) of fishes was assumed to be a function of fish wet weight ($W_{w,f}$) and temperature (T) following Gillooly *et al.* (2001),

$$\mathrm{RMR} = e^{a} W_{w,f} e^{\left(\frac{1000c}{273.15+T}\right)}, \quad (1)$$

where a = 14.47 and c = -5.020. The standard metabolic rate (SMR, J min^{-1}) of resting, inactive fishes is assumed to be 50% of the RMR (Winberg, 1956). The active, feeding metabolic rate (AMR, J min^{-1}) is assumed to be four times the SMR (Brett and Groves, 1979; Smith and Laver, 1981). Because the metabolic rate of fishes decreases with the depth inhabited (in addition to temperature effects), the metabolic rates of NM fishes were reduced by an additional factor of 0.49 corresponding to the ratio of RMR between 400 and 50 m residence depths (Torres *et al.*, 1979).

VM fishes were assumed to ascend and descend at 5 cm s^{-1} from 400 m to 50 m in depth at a swimming speed of 2 body-lengths (BL) s^{-1}, resulting in a transit time of ~2 h. The energetically optimal swimming speed for fishes of 0.1-10.0 g $W_{w,f}$ ranges from 4.0-2.1 BL s^{-1} (Videler, 1993). NM fishes were assumed to remain at 400 m depth for the entire diel period. The measured temperature at 400 m was used for fishes at depth, whereas the mean epipelagic (1-150 m) temperature was used for VM fishes at night (Table 4.6). Temperature is assumed to vary linearly between 50 m and 400 m depths. All fishes (including NM fishes; Smith and Laver 1981) were assumed to spend half of a

24 h period actively feeding with a metabolic rate equivalent to the AMR and half of the day inactive with a metabolic rate equal to the SMR.

The general balanced energy equation for a fish can be expressed as follows (Brett and Groves, 1979; Jobling, 1993):

$$I = M(I, T, W_{w,f}) + G(I) + F(I) + E(I), \quad (2)$$

with

$$M = \text{activity}(t)\text{SMR}(T, W_{w,f}, r) + \text{SDA}(I), \quad (3)$$

where I is the ingestion rate (J d^{-1}), M the metabolic rate (J d^{-1}), T the temperature (°C), r the residence depth (m), G the growth rate (J d^{-1}), F the fecal loss (J d^{-1}), E non-fecal excretion (J d^{-1}), t the time (d), and SDA the specific dynamic action or heat increment (J d^{-1}). Activity refers to the time-partitioned use of SMR and AMR. Growth was assumed to be equal to mortality on an annual basis (no population growth). The partitioning of ingested energy to F, E, and SDA was assumed to follow the general model for a carnivorous fish (Brett and Groves, 1979), whereas the ratio of lifetime growth to metabolism was taken from Childress *et al.* (1980; mean of VM fishes and mesopelagic zooplanktivorous NM fishes). Equations 2-3 thus reduce to

$$I = \frac{1}{b}\text{activity}(t)\text{SMR}(T, W_{w,f}, r), \quad (4)$$

where $b = 0.43$ for VM fishes and $b = 0.29$ for NM fishes. Energy was converted to units of zooplankton wet weight ($W_{w,z}$) using a caloric value (Q_z) of 3.629 kJ g^{-1} $W_{w,z}$ calculated from the lipid, protein, and carbohydrate content of zooplankton (L_z, P_z, C_z), dry weight fraction of zooplankton ($W_{d,z}$), heats of combustion (H_l, H_p, H_c), and fish digestive efficiencies (D_l, D_p, D_c; Table 4.1) with the equation

$$Q_z = W_{d,z}(D_l L_z H_l + D_p P_z H_p + D_c C_z H_c), \tag{5}$$

and it follows that the daily ration of a fish (R_d, g d^{-1} $W_{w,z}$) is then

$$R_d = \frac{I}{Q_z}. \tag{6}$$

Respired energy rate was converted to respired carbon rate (C_r, g d^{-1}) using a respiratory quotient (RQ) of 0.90, the molar weights of carbon and O_2, and an oxycalorific equivalent (Q_{ox}) of 13.6 J mg O_2 (Brett and Groves, 1979) according to the equation

$$C_r = \frac{12\text{RQ}}{32Q_{ox}}\,\text{activity}(t)\text{SMR}(T, W_{w,f}, r). \tag{7}$$

Only respiration below 150 m was counted as "exported". Defecated carbon (C_d, g d^{-1}) was estimated from proximate analysis of zooplankton, absorption efficiency of fishes, and carbon content of lipids, protein, and carbohydrates (C_l, C_p, C_c; Table 4.1) as follows;

$$C_d = R_d W_{d,z}\left[L_z C_l(1 - D_l) + P_z C_p(1 - D_p) + C_z C_c(1 - D_c)\right]. \quad (8)$$

All fecal production was assumed to be exported, because the feces of mesopelagic fishes are large and fast-sinking (Robison and Bailey, 1981). The fraction of carbon devoted to growth, or mortality (C_m, g d^{-1}), was calculated from the fraction of ingested energy devoted to growth, the energy content of fishes (Q_f, kJ g^{-1} $W_{w,f}$), the carbon content of fishes (C_f; Table 4.1), and the percentage of mortality occurring at depth (89%; Sutton and Hopkins, 1996) with the equation

$$C_m = 0.89G\frac{C_f}{Q_f}. \quad (9)$$

As it is known that not all individuals of nominally VM species are present in the epipelagic layer on a given night (Clarke, 1973; Clarke, 1971; Pearcy *et al.*, 1977), the carbon exported by VM fishes ($C_{vm,tot} = C_r + C_d + C_m$) was discounted by the ratio of measured biomass (B_s, from shallow trawls) to the expected VM biomass (B_{vm}, determined taxonomically from the catch of deep trawls), and then normalized by volume filtered (V_f) and sampling depth (D_s) using the equation

$$C_{\mathrm{vm,adj}} = \frac{D_{\mathrm{s}}}{V_{\mathrm{f}}} C_{\mathrm{vm,tot}} \left[R_{\mathrm{e}} \left(1 - \frac{B_{\mathrm{s}}}{B_{\mathrm{vm}}} \right) + \frac{B_{\mathrm{s}}}{B_{\mathrm{vm}}} \right], \tag{10}$$

where R_{e} is the modeled ratio of the carbon exported by a non-migratory VM fish to that of a migratory VM fish and $C_{\mathrm{vm,adj}}$ (g C m^{-2} d^{-1}) is the adjusted carbon export mediated by VM fishes. The carbon export mediated by NM fishes was similarly adjusted for V_{f}, D_{s}, and the fraction of carbon of detrital origin (C_{do}) as follows,

$$C_{\mathrm{nm,adj}} = \frac{D_{\mathrm{s}}}{V_{\mathrm{f}}} C_{\mathrm{nm,tot}} (1 - C_{\mathrm{do}}) . \tag{11}$$

Equating bacterial and NM zooplankton carbon demand with particulate organic carbon remineralization and VM zooplankton carbon flux from Steinberg *et al.* (2008), and solving for the ratio (R_{z}) of VM zooplankton carbon flux to NM zooplankton carbon demand results in $R_{\mathrm{z}} = 2.0$ (the smallest and most conservative value from reported data ranges). C_{do} is then $(1 + R_{\mathrm{z}})^{-1}$, and has a (highest) value of 0.33. Approximately 33% of the carbon content of a zooplankter at depth is thus assumed to originate from material that had already left the epipelagic via passive sinking, and 67% is assumed to have been consumed in the epipelagic and actively transported to the mesopelagic.

A sensitivity analysis was performed on the carbon export model, in which the parameters were varied within reasonable ranges and the effects noted to the results.

4.3.2. Total carbon export

In order to establish a baseline for comparison, as well as to provide a basis for areal extrapolation of the fish export, MODIS satellite measurements of chlorophyll and SST were used to estimate annual NPP (g C m^{-2} y^{-1}; Behrenfeld and Falkowski 1997) and exported production as a fraction of NPP (*ef* ratio; Laws, 2004; Laws *et al.*, 2000). Depth of the euphotic zone was calculated following Morel and Berthon (1989) for conversion between area- and volume-specific NPP. The above satellite data (monthly averages) were processed to estimate total export for bottom depths greater than 200 m over a latitude/longitude grid encompassing the study area (Figure 4.2) at 4 km resolution, and then averaged to produce an annual rate. The annual rate of total export was calculated for each year between 2003 and 2010, and then averaged over the eight-year period. The regression of fish export on total export from our sampling locations was used to estimate fish export over the entire study area from the total export.

4.4. Results

4.4.1. Fish catch

In all, 25,013 zooplanktivorous mesopelagic fishes from 26 families were collected from 77 deep trawls in the study area. Forty-four deep trawls suitable for biomass measurements of mesopelagic fishes were made with the IKMT, and 33 with the MOHT. Fishes from the family Gonostomatidae (almost entirely *Cyclothone* spp.) were most abundant (58% of the total), while fishes from the family Myctophidae dominated the overall biomass (52% of the total, Table 4.2). The dominance of myctophids amongst VM fishes was pronounced, with myctophids comprising 94% of the abundance and 95%

Table 4.2. Fraction of total mesopelagic fish abundance and biomass by family (deep trawls). Piscivores, epipelagic fishes, and larval fishes are excluded.

Family	VM abundance	NM abundance	Total abundance	VM biomass	NM biomass	Total biomass
Bathylagidae	0.04	0.00	0.01	0.04	0.07	0.06
Gonostomatidae	0.00	0.85	0.58	0.01	0.26	0.14
Melamphaeidae	0.00	0.01	0.01	0.00	0.15	0.08
Myctophidae	0.94	0.04	0.33	0.95	0.12	0.52
Phosichthyidae	0.02	0.00	0.01	0.00	0.00	0.00
Platytroctidae	0.00	0.01	0.01	0.00	0.06	0.03
Sternoptychidae	0.00	0.07	0.05	0.00	0.11	0.06
Stomiidae	0.00	0.01	0.00	0.00	0.20	0.10
other	0.00	0.00	0.00	0.00	0.03	0.01

of the biomass in this category (Table 4.2). Within NM fishes, *Cyclothone* spp. formed 85% of the abundance but only 26% of the biomass. Biomass prior to correction for capture efficiency of the trawls ranged from 0.56-5.55 g m^{-2}, with a mean of 2.34 g m^{-2}. The mean wet weight of individual captured fishes was 0.43 g, and the mean abundance prior to capture efficiency adjustment was 5.47 fishes m^{-2}. The IKMT has a smaller mouth opening than the MOHT, and it was found that it collected fewer fishes than the MOHT when normalized by V_f and D_s (*t*-test, $t = 7.4$, df = 66, $p < 0.001$). Because the MOHT trawls in the CCE were concentrated off of southern California, whereas the IKMT tows were made along the entire western coast of the U.S.A., the IKMT biomass measurements were tested for meridional dependence prior to calculation of the relative capture efficiency of the IKMT. No meridional trend in biomass was found (Spearman rank correlation, $r_s = -0.02$, $p = 0.89$, n = 44), so all IKMT trawls were compared to the MOHT trawls (24 CCE trawls only) for the relative capture efficiency estimate. The mean biomass of the IKMT trawls was 1.73 g m^{-2} versus 3.69 g m^{-2} for the MOHT

trawls. Therefore, each IKMT catch was multiplied by a factor of 2.1. Capture efficiency of the MOHT is 0.14 (of biomass, SD = 0.14) for mesopelagic fishes with inflated swim bladders, and all trawl catches were adjusted by this factor (Chapter 3). Corrected biomass ranged from 7.50-70.47 g m^{-2}, with a mean of 24.70 g m^{-2}. The corrected abundance ranged from 5.07-136.33 fishes m^{-2}, with a mean of 54.40 fishes m^{-2}. In general, a higher biomass of mesopelagic fishes was found close to the continental shelf break and lower biomass was measured offshore (Figure 4.3). The relationship between estimated mesopelagic fish biomass and estimated annual NPP was tested and biomass was found to increase significantly (df = 76, $p < 0.001$, $R^2 = 0.410$) with increasing annual NPP (Figure 4.4).

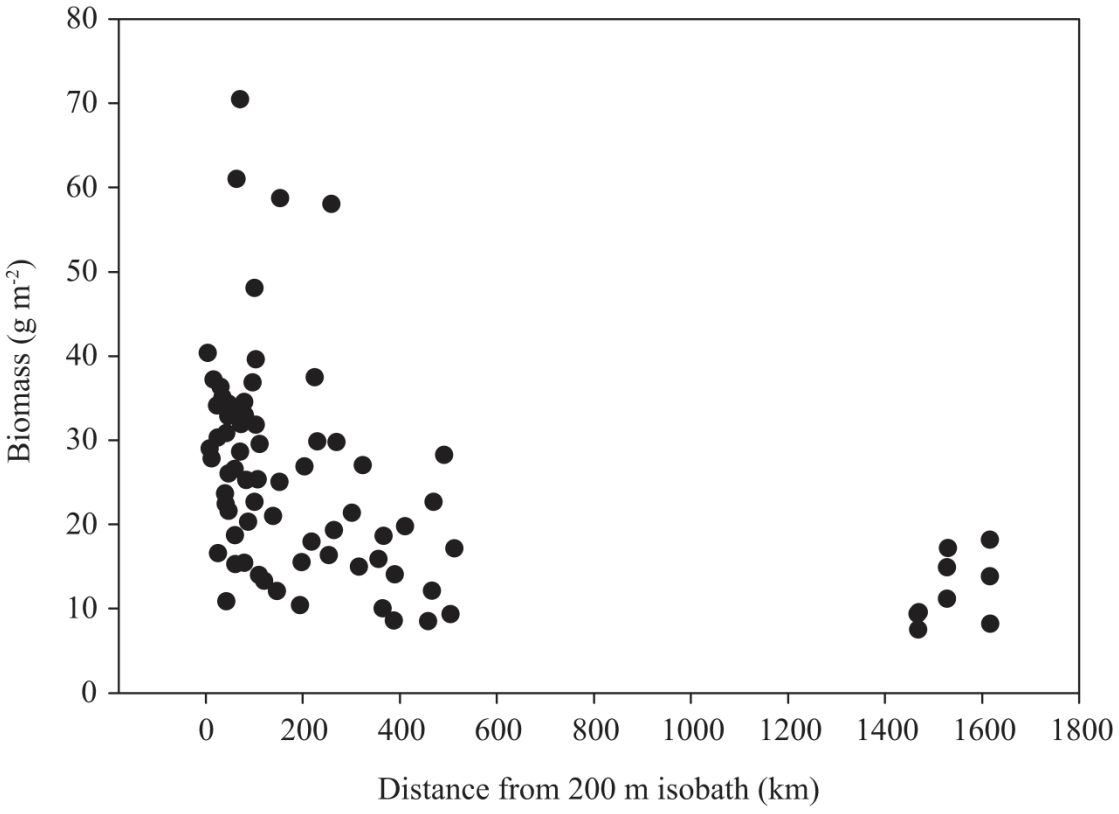

Figure 4.3. Biomass of mesopelagic fishes in relation to the distance from the continental shelf, as defined by the 200 m isobath.

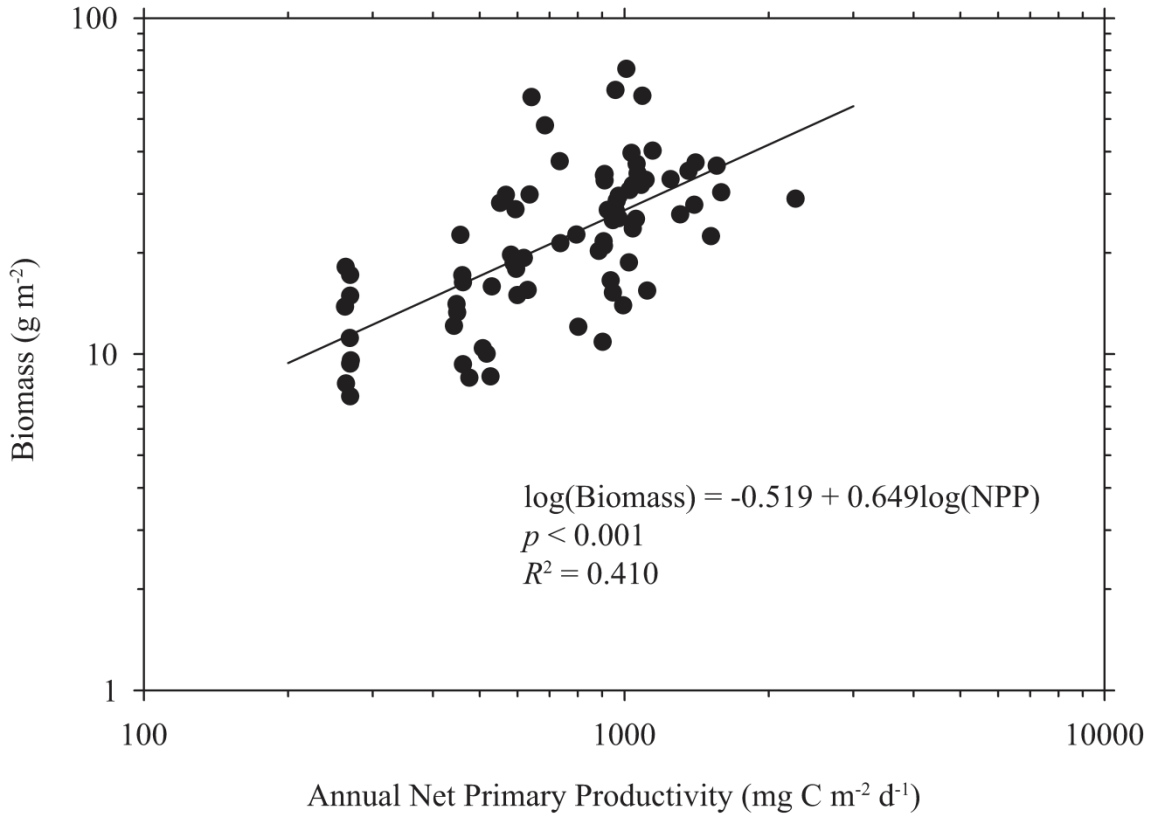

Figure 4.4. Biomass of mesopelagic fishes in relation to annual Net Primary Productivity as estimated by the VGPM model from satellite data (Behrenfeld and Falkowski, 1997). A linear regression of the log-transformed variables was found to be significant (df = 76, $p < 0.001$, $R^2 = 0.410$).

Taxonomic categorization of migratory behavior results in 34% of the overall mesopelagic fish abundance and 46% of the biomass classified as vertically-migratory (average of deep trawls). However, direct measurements of VM biomass with shallow trawls average 54.1% (B_s:B_{vm}, Equation 10) of the taxonomically-determined VM fish biomass. The biomass of VM fish taxa varied from 12-97% of the total catch for deep trawls. The mean weight of individual VM and NM fishes was 0.71 and 0.31 g, respectively. The preponderance of small fishes was marked, 68.6% of the VM and

82.7% of the NM fishes weighed less than 0.2 g. However, for both VM and NM categories most of the biomass was contributed by fishes of mass >1 g (Figure 4.5).

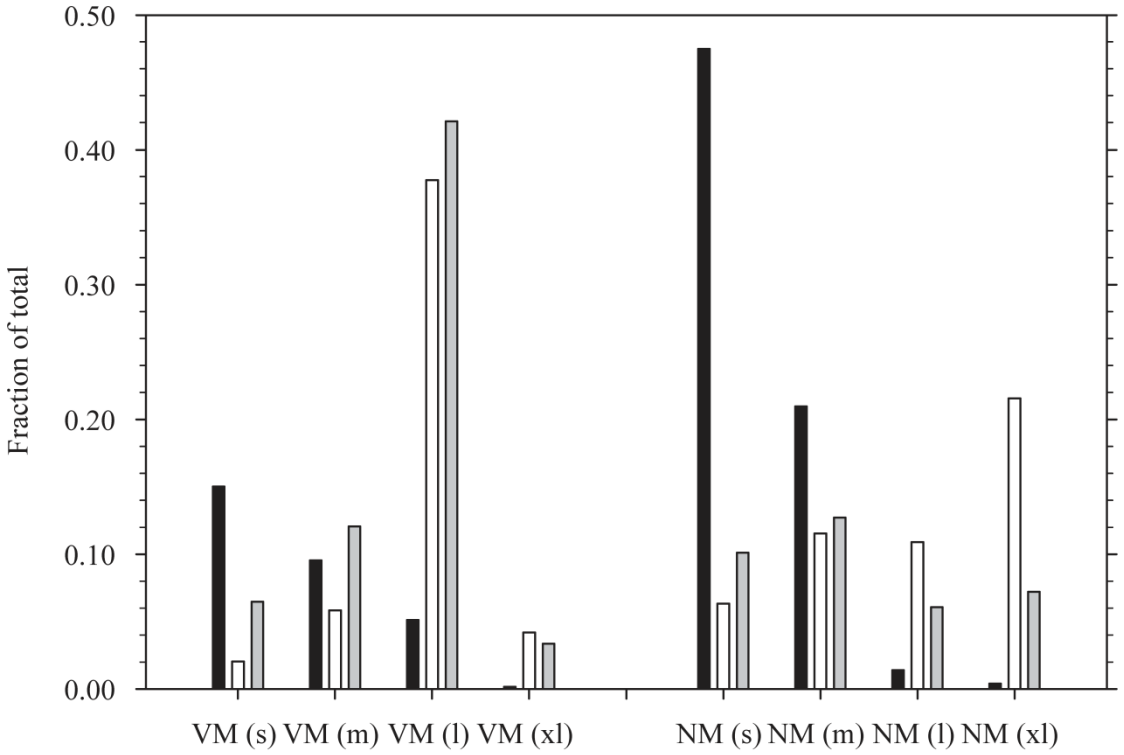

Figure 4.5. Abundance (black), biomass (white), and carbon export (grey) for all captured vertically migratory (VM) and non-migratory (NM) mesopelagic fishes by size classes 0.01-0.1 g (s), 0.1-1 g (m), 1-10 g (l), and 10-100 g (xl).

4.4.2. Fish export

The VM and NM fish export models were compared using a 1-g virtual fish (Table 4.3). Under a common set of assumptions ("baseline scenario"), the two models produce similar estimates of daily energy usage, daily ration, and carbon flux (Table 4.3). The baseline scenario for each model was then progressively modified to the configuration used for analysis.

The baseline scenario of the VM model was first altered to reflect the decreased energy available for growth by VM fishes (Equation 4, Table 4.1; Childress *et al.*, 1980). This change directly reduces the estimated mortality flux, and also results in decreased ingested energy, rations, and defecation rate because the fish is respiring at the same rate but is not feeding enough to maintain the same ratio of growth to metabolism assumed by the baseline Brett and Groves (1979) budget. The second modification of the VM fish model was to decrease the night depth to 50 m. With this change, 72% of the respired

Table 4.3. Carbon flux model scenarios for a 1-g fish. The baseline scenarios for the vertically-migratory (VM, shaded) and non-migratory (NM) fish models use a common set of assumptions; night depth (D_n) = day depth (D_d), night temperature (T_n) = day temperature (T_d), no elevated metabolic rate for swimming between day and night depths ("swim"), no modification of metabolic rate for residence depth (DE), prey detritivory fraction (C_{do}) = 0, and the general growth:metabolism ratio (G:M; 0.66; Brett and Groves, 1979). The models produce results for daily energy requirement (I), daily ration (R_d), and carbon exported via respiration, defecation, and mortality (C_r, C_d, C_m respectively). The baseline scenarios are cumulatively modified to the configurations used to estimate fish export (indicated with asterisks).

Scenario	D_n:D_d (m)	T_n:T_d (°C)	G:M	Swim	DE	C_{do}	C_r mg C d^{-1}	C_d mg C d^{-1}	C_m mg C d^{-1}	C_{total} mg C d^{-1}	R_d %$W_{w,f}$	I J d^{-1}
Baseline (VM)	400:400	7:7	0.66	no	1	0	1.42	0.71	1.11	3.24	5.26	190.7
VM G:M	400:400	7:7	0.28	no	1	0	1.42	0.49	0.42	2.34	3.67	133.0
Add ascent	50:400	7:7	0.28	no	1	0	0.40	0.50	0.42	1.32	3.67	133.1
Add swimming	50:400	7:7	0.28	yes	1	0	0.67	0.63	0.54	1.84	4.66	169.0
Add warm surface*	50:400	7:13	0.28	yes	1	0	0.74	0.83	0.70	2.27	6.12	222.2
Baseline (NM)	400:400	7:7	0.66	no	1	0	1.42	0.71	1.27	3.40	5.25	190.7
NM G:M	400:400	7:7	0.71	no	1	0	1.42	0.73	1.36	3.51	5.44	197.2
Add DE	400:400	7:7	0.71	no	0.49	0	0.70	0.36	0.67	1.73	2.68	97.3
Add C_{do}*	400:400	7:7	0.71	no	0.49	0.33	0.47	0.24	0.45	1.16	2.68	97.3

carbon is no longer exported, as it occurs shallower than 150 m. The number is larger than 50% because the AMR (night) is higher than the SMR (day). Because thus far the temperature is constant and vertical swimming has no metabolic cost, the daily energy requirement and daily ration remain unchanged. If the metabolic cost of swimming is assumed to equal the swimming speed (BL s^{-1}) to an exponent of 2.5, and fishes swim at 2 BL s^{-1} with a vertical velocity 5 cm s^{-1}, then the VM fish now spends ~4 h d^{-1} travelling vertically with an elevated metabolic rate equivalent to 6.7 times the SMR. This has the effect of increasing by 27% the ingestion, daily ration, fecal export, and mortality export. Respired carbon flux increases by 68% because most of the elevated respiration for swimming occurs below the 150 m export threshold depth. The final adjustment to the model was to set the 50 m temperature to 13°C. This change increased daily ingestion, daily ration, fecal export, and mortality export by 31%. Respiratory flux increased by 10% with this change because part of the thermocline is deeper than the 150 m export threshold depth. In this configuration of the model, nominally matching trawl conditions for a 1-g fish, the daily ration is 6.1% $W_{w,f}$, daily energy expenditure is 222 J, and 2.27 mg C d^{-1} is exported, 33% as respired carbon, 36% as fecal flux, and 31% as mortality. The ratio of carbon exported by a VM fish that does not migrate ("VM *G*:*M*" scenario, Table 4.3) to that by one that ascends "normally" at night (R_e, Equation 10) is 1.03.

The NM model modifications from the baseline scenario were simpler, and consisted first of an adjustment to the *G*:*M* ratio based upon measurements of NM mesopelagic fishes (Equation 4, Table 4.1; Childress *et al.*, 1980), and then scaling the metabolic rate by 49% to reflect the lower SMR of fishes residing at 400 m in

comparison to vertical migrators (Torres *et al.*, 1979). This lowered all export terms, daily ration, and daily energy budget by ~50%. The third modification was to apply C_{do}, the fraction of consumed prey that is detrital in origin (Equation 11), resulting in a 33% reduction to all carbon export terms, but no change to daily energy or daily ration. In this nominal configuration of the model for a 1-g fish, the daily ration is 2.7% $W_{w,f}$, daily energy expenditure is 97 J, and 1.16 mg C d^{-1} is exported, 40% as respired carbon, 21% as fecal flux, and 39% in the form of mortality.

The overall carbon flux mediated by a 1-g NM fish is thus 31% of that from a similarly-sized VM fish. The higher flux from VM fishes results from a higher SMR, consumption of a higher fraction of prey that is non-detrital in origin, and the greater rations required to support elevated energy expenditures in warmer temperatures and for vertical movement.

Carbon export model parameters were varied independently for these example fishes to determine the sensitivity of the model to uncertainty (Table 4.4). The modeled fish export is most sensitive to parameters of the respiration model (a = 14.47 and c = -5.02, Equation 1; Gillooly *et al.*, 2001). Changes of ±1 SE in these parameters resulted in changes to the estimated fish export of 0.17-5.87 times the nominal value. Reasonable variation of other parameters results in flux reductions of 23% or less and flux increases of 43% or less.

4.4.3. Total carbon export

Mean annual NPP, *ef* ratio, and total export were calculated from satellite data for the northeast Pacific Ocean area bounded by 30/48°N latitudes and from the USA coastal

200 m isobath west to 141°W longitude (Figure 4.6). The surface area of the study area is 3.273×10^6 km^2. Estimated annual NPP ranged from 259.7-4607.7 mg C m^{-2} d^{-1} in the study area. The annual *ef* ratio for this region ranged from 0.16 to 0.57. Total export was 144.4 mg C m^{-2} d^{-1} (0.173 Pg C y^{-1}) in the study area, varying from 42.1 mg C m^{-2} d^{-1} in the oligotrophic central water mass to 2460.4 mg C m^{-2} d^{-1} in the productive coastal upwelling area of the CCE.

Table 4.4. Sensitivity analysis of the VM and NM metabolic models, measured as the summed carbon exported (C_{total}) by a 1-g NM fish and a 1-g VM fish and expressed as a ratio to the C_{total} for nominal values of parameters (C_{nom}, 3.4 mg C m^{-2} d^{-1}). Where parameters differ for VM and NM fishes, both values are expressed separated by a colon in the order VM:NM.

Parameter	Units	Low	Nominal	High	$C_{total,low}$:C_{nom}	$C_{total,high}$:C_{nom}
Temperature (50 m)	°C	8	13	23	0.89	1.31
Temperature (400 m)	°C	5	7	8	0.93	1.04
Depth (shallow)	m	1	50	149	1.01	0.95
Depth (deep)	m	200	400	800	0.84	1.32
Night length	h	8	12	16	0.88	1.12
Swim MR exponent		2.2	2.5	2.8	0.95	1.06
Swim speed	BL s^{-1}	1	2	3	0.80	1.43
AMR:RMR		1.5	2.0	2.5	0.87	1.13
SMR:RMR		0.25	0.50	0.75	0.77	1.24
RMR *a*		12.97	14.47	15.97	0.22	4.48
RMR *c*		-5.52	-5.02	-4.52	0.17	5.87
C_{do}		0:0	0:0.33	0:0.67	1.17	0.83
Depth effect on RMR		1:0.20	1:0.49	1:0.70	0.80	1.14
RQ		0.80	0.90	0.95	0.96	1.02
Q_{ox}	J mg^{-1} O_2	13.39	13.60	15.07	1.01	0.97
G:*M*		0.17:0.38	0.28:0.71	0.34:1.12	0.81	1.20
Q_z	kJ g^{-1}	3.51	3.63	4.04	1.01	0.97
Q_f	kJ g^{-1}	2.85:1.67	5.57:3.22	8.57:4.86	1.10	0.94
Mortality export fraction		0.50:0.90	0.89:1.00	0.95:1.00	0.90	1.01
$W_{w,f}$	g	0.95	1.00	1.05	0.96	1.04

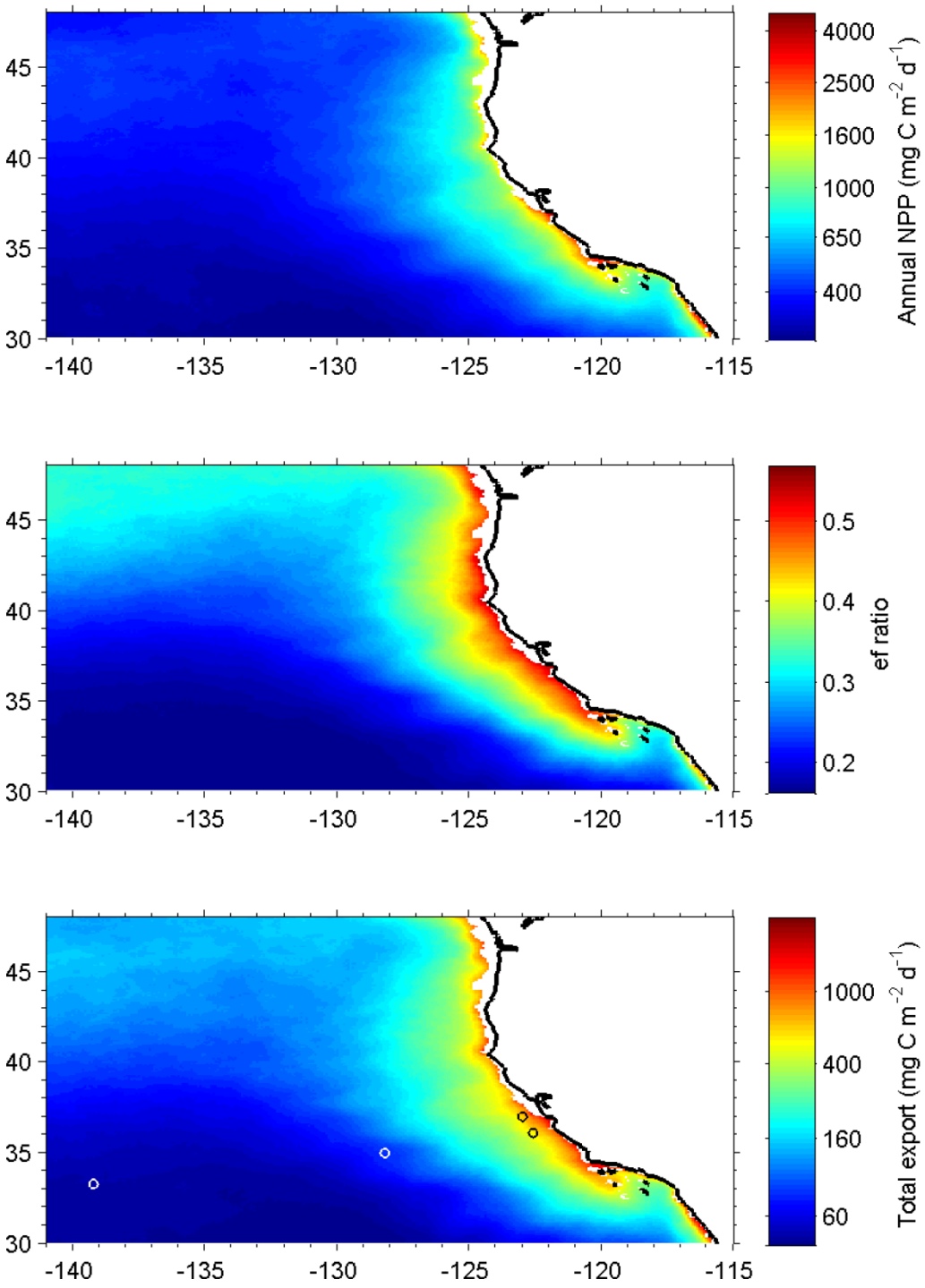

Figure 4.6. a) Annual Net Primary Productivity as estimated by the VGPM model from satellite data (Behrenfeld and Falkowski, 1997) averaged over 2003-2010, b) annual *ef* ratio (Laws, 2004) averaged over 2003-2010, and c) annual carbon export averaged over 2003-2010. Sediment trap stations for VERTEX (Martin *et al.*, 1987) are marked as black or white open circles.

The carbon exported from each captured fish was estimated, summed by trawl, and then adjusted for capture efficiency, volume of water sampled, and "non-migratory" VM biomass (Equations 10-11). From the trawl data, fish export ranged from 13.7-75.8 mg C m^{-2} d^{-1}, with a mean of 34.3 mg C m^{-2} d^{-1}. Fish export does not form a constant fraction of the total export. A linear regression of log fish export against log total export yields a slope of 0.315 and an intercept of 0.742 (d.f. = 76, $p < 0.001$, $R^2 = 0.34$; Figure 4.7). Fish export is largest in productive waters and smallest in oligotrophic waters (Figure 4.7). However the ratio of fish export to total export is approximately seven-fold higher at the oligotrophic stations in comparison to the eutrophic stations (Figures 4.7,

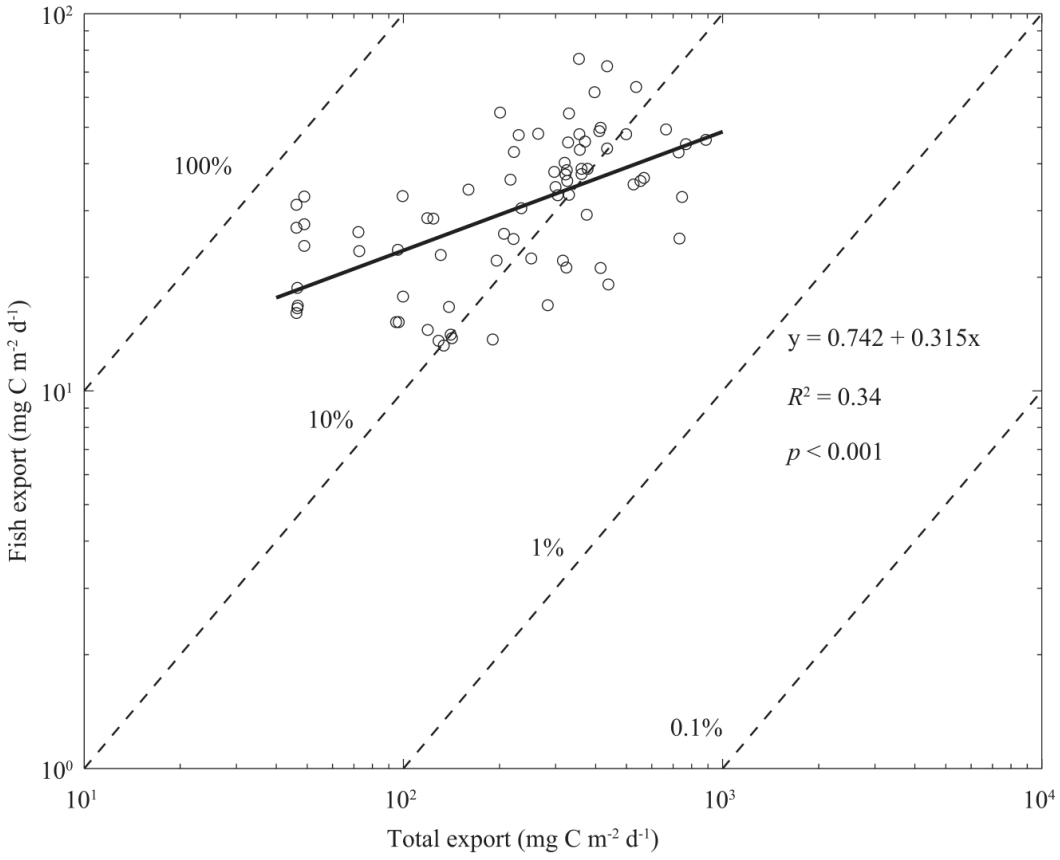

Figure 4.7. Carbon export mediated by mesopelagic fishes in relation to satellite-derived total carbon export.

4.8). The relationship between fish export and total export was used to estimate fish export for the entire study area (24.8 mg C m^{-2} d^{-1}, 0.030 Pg C y^{-1}).

The fraction of annual NPP consumed by mesopelagic fishes was estimated at each sampling station from modeled R_d following Barlow *et al.* (2008) using a trophic transfer efficiency for carbon of 10% (Pauly and Christensen, 1995) and a zooplankton trophic level of 2.2 (Pauly *et al.*, 1998). The fraction of NPP consumed by mesopelagic fishes increases significantly with oligotrophy, rising from ~20% in the most productive areas of the CCE to over 80% in the oligotrophic NPSG (Figure 4.9).

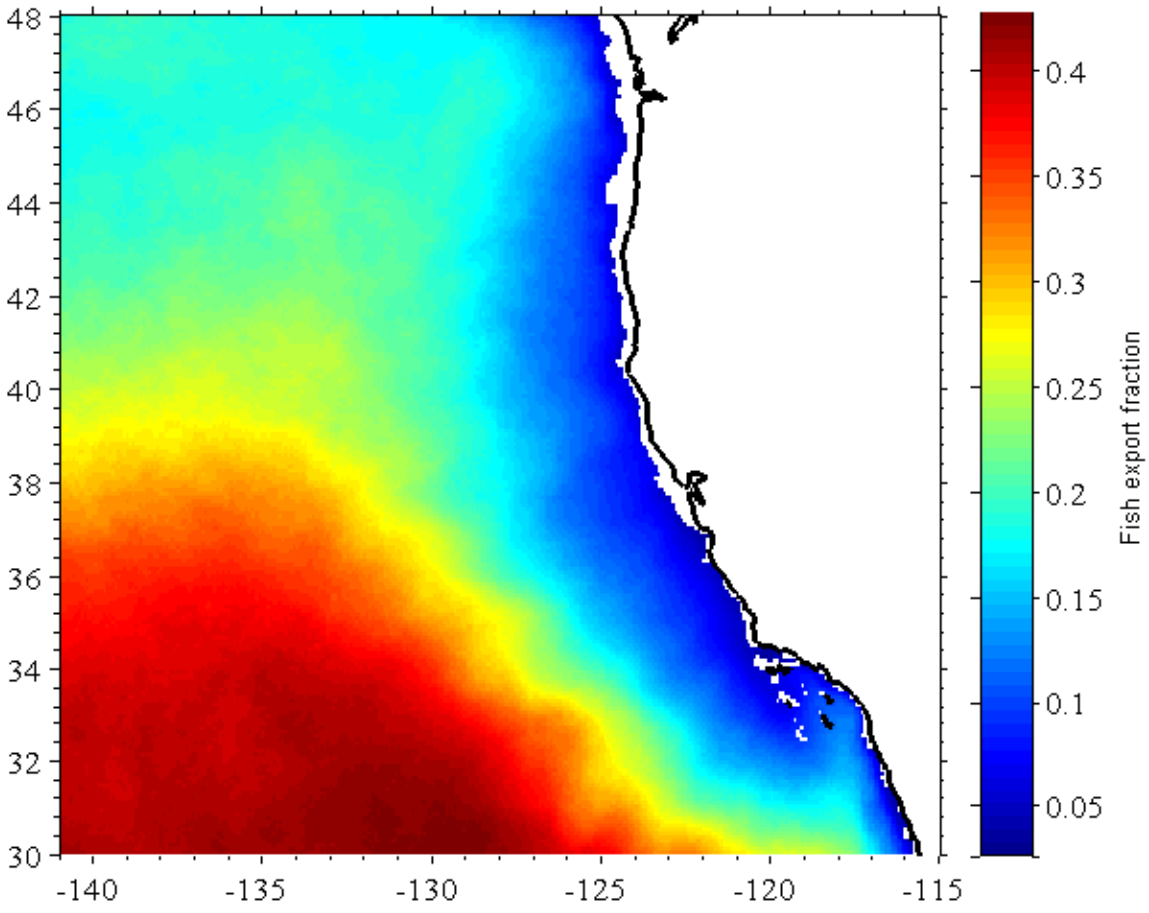

Figure 4.8. Carbon export mediated by mesopelagic fishes in relation to satellite-derived total carbon export within the study area.

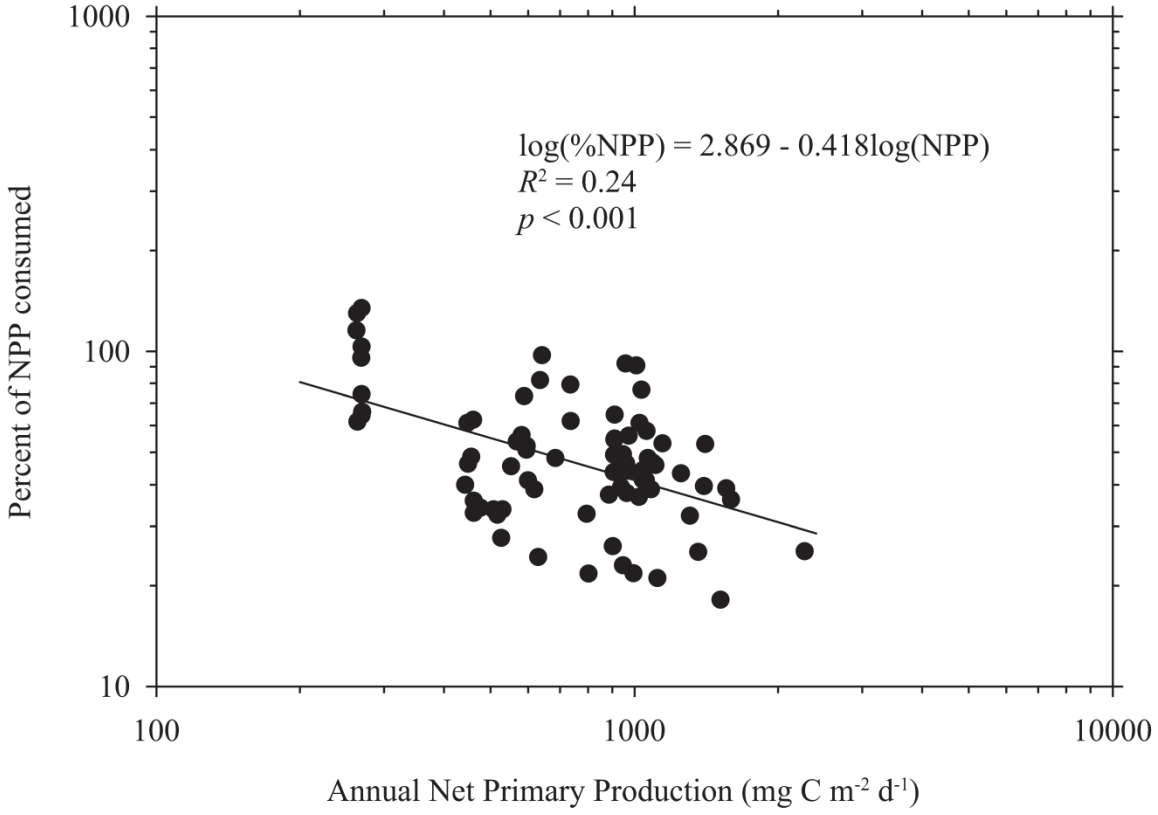

Figure 4.9. Fraction of annual NPP consumed by mesopelagic fishes.

Because fish export for the entire study area was estimated from the relationship to total export, it is difficult to exactly partition it by size class and migratory behavior as the trawling effort was not distributed in proportion to the ocean surface area of differing productivity levels. With that caveat, Figure 4.5 presents size-partitioned abundance, biomass, and fish export for all captured VM and NM fishes. VM fishes >1 g in wet weight mediate 45% of the overall fish export, and they form 5% of the overall abundance and 42% of the biomass. Biomass increases with size class for NM fishes, but peaks sharply in the 1-10 g size class for VM fishes. Abundance decreases with weight for both VM and NM fishes. Fish export peaks in the 0.1-1.0 g size class for NM fishes,

and in the 1-10 g size class for VM fishes. The fractions of respiratory, fecal, and mortality carbon export (Table 4.3) are size and temperature independent, depending wholly on the assumed energy budget, behavior, proximate compositions, and activity patterns of the VM and NM fishes.

4.5. Discussion

4.5.1. Fish catch

The biomass of fishes here, 0.6-5.5 g m^{-2} (mean of 2.4 and 1.7 g m^{-2} for the CCE and NPSG trawls respectively) as measured by nets and prior to correction for capture efficiency, is consistent with prior estimates for the sampling area (3.6 and 2.0 g m^{-2} for the CCE and NPSG respectively; Gjosaeter and Kawaguchi, 1980; Pearcy and Laurs, 1966), which also were not corrected for capture efficiency. Nets are known to underestimate mesopelagic fish biomass by approximately an order of magnitude due to the processes of avoidance and escapement (summarized in Chapter 3). Capture efficiency of the MOHT has been measured from concurrent acoustic data to be, on average, 14% for small mesopelagic fishes (Chapter 3). The capture efficiency of the IKMT is 46.8% of that of the MOHT, equivalent to an absolute capture efficiency of 6.6%. This is an overall value, as capture efficiency is expected to vary with size and swimming ability of the fish. Thus, capture efficiency is lower for large, fast-swimming fishes and higher for small, slow-swimming fishes. The size distribution of captured fishes matches this expectation, with numbers dominated by smaller fishes. It is unknown how much capture efficiency size-bias contributes to the observed numerical dominance of very small (<0.2 g) fishes in comparison to the similar expectation from

mortality. In contrast to abundance, biomass is dominated by larger individuals for both VM and NM fishes (Figure 4.5). Thus, the portion of the size spectrum least well-sampled contributes most of the biomass. Because almost half of the modeled fish export is mediated by large (>1 g) VM fishes that are undersampled in relation to the whole, the fish export estimate here is expected to be conservative.

The biomass of mesopelagic fishes is not evenly distributed. Although no meridional trend in biomass was found, biomass generally decreases with distance from the continental shelf (Figure 4.3). Near the continental shelf break, the biomass of fishes is variable, with both extremely high values and low values that approximate the biomass well offshore. The decrease in variability with increasing distance from the continental shelf may coincide with changes in habitat patchiness at the scale of the trawl. There is some evidence of a biomass peak over the continental slope, which has been reported both in the CCE and in other places (Brodeur *et al.*, 2003; Gjosaeter and Kawaguchi, 1980; Pearcy, 1976; Radchenko, 2007). This biomass peak is theorized to result from the collocation of forage (high productivity) and predation risk from demersal and coastal predators (Pearcy, 1976).

The importance of food availability to mesopelagic fish biomass is illustrated by the significantly increasing relationship between satellite-derived annual NPP (Behrenfeld and Falkowski, 1997) and mesopelagic fish biomass (Figure 4.4). Application of the regressed relationship between mesopelagic fish biomass and annual NPP (2008) for the study area produces a mesopelagic fish biomass estimate of 55.1 million metric tons (MMT; 16.8 g m^{-2}; 18.5 MMT for the CCE area <300 km from the 200 m isobath). The combined stock of sardines (2008; Hill *et al.*, 2010) and anchovies

(1991, not annually assessed; Jacobson *et al.*, 1994) in the same region is <2 MMT. We estimate the large stock of mesopelagic fishes to consume a correspondingly large fraction of annual NPP. A significant relationship was found between annual NPP and fraction of NPP consumed by mesopelagic fishes (Figure 4.9). This fraction is lower in productive CCE waters and higher in the oligotrophic NPSG. This pattern is consistent with increased competition for NPP, top-down control of mesopelagic fish biomass, and increased passive flux efficiency in eutrophic waters. The fraction of NPP consumed by mesopelagic fishes seems rather high in the NPSG (0.6-1.2) in light of the expected consumption of 10-50% of NPP by the microbial loop alone (Azam *et al.*, 1983). Possible confounding factors include an increase in capture efficiency offshore (fishes tend to be smaller offshore, and perhaps less able to avoid the net), a reduction in trophic level of mesopelagic fishes in the NPSG, and underestimation of annual NPP by the VGPM model. A reduction of trophic level below 3.0 (our assumed value was 3.2) requires some herbivory. This has only been observed once in mesopelagic fishes (Robison, 1984), but it was for *Ceratoscopelus warmingii*, one of the dominant myctophid species of the NPSG. Previous attempts to reconcile the productivity of subtropical mesopelagic fishes with NPP have concluded that there is not enough NPP to support them if trophic level is >3 and trophic transfer efficiency is 10% (Clarke, 1973; Mann, 1984). Some recent evidence suggests that global gross primary production has been underestimated (Welp *et al.*, 2011; but the authors attribute it to terrestrial sources), and that nitrogen fixation plays a larger role in the oligotrophic eastern North Pacific than previously believed at depths below those observed by satellites (Montoya *et al.*, 2004), supporting the possibility that NPP is underestimated here. It has also been found that

there is not enough NPP in the western subarctic Pacific to support *Neocalanus* spp. copepods, important prey of mesopelagic fishes, if trophic efficiency is less than 13% (Kobari et al., 2003). Reconciliation of these diverse fields of ecological study will require more research.

4.5.2. Flux model

The model used to estimate fish export is individual-based, with many assumptions made at the individual, species, and higher taxonomic levels. Several of the more critical assumptions are discussed below.

All fishes were assumed to inhabit a depth of 400 m during the day and to experience the measured temperature there, with the VM fishes assumed to ascend to 50 m at night where they experience the mean epipelagic temperature (1-150 m). The densest portion of the (daytime) 38 kHz DSL is at approximately 400 m in the study area, as observed from concurrently collected acoustic data. Less-dense layers were often observed both above and below the 400 m layer. Temperature changes slowly (by ~0.01°C m^{-1}) at 400 m, and lower metabolic rates of fishes below 400 m will be offset by higher metabolic rates of fishes above 400 m. We view the choice of 400 m as the daytime depth of mesopelagic fishes to be both appropriate and conservative because the densest portion of the DSL was observed acoustically at approximately 400 m, biomass generally decreases with depth, temperature increases more quickly from 400-150 m depth than it decreases blow 400 m, and because the effort of vertical migration to below 400 m will offset the effect on metabolic rate from slowly decreasing temperatures. Because VM fishes are distributed throughout the epipelagic, the choice of 50 m as their

night depth represents a compromise between the observed dense acoustic layer from ~10-50 m and the bottom of the epipelagic zone. The model is not sensitive to this depth choice, as the mean epipelagic temperature is used and the night depth is only used to estimate swimming effort (Table 4.4).

Vertical migration was treated at the species level in the modeling for this study. There is evidence that not all individuals of VM species ascend to epipelagic depths on a given night (Clarke, 1973; Clarke, 1971; Pearcy *et al.*, 1977), and that the fraction may vary seasonally or with the lunar cycle (Clarke, 1973; Kaartvedt *et al.*, 2009; Linkowski, 1996). In contrast, it is thought that all individuals of VM species that do ascend to the epipelagic at night return to depth at dawn (Clarke, 1973; Pearcy, 1964). Eleven epipelagic tows made in daylight captured few mesopelagic fishes (mean biomass of 0.013 g m^{-2}), indicating either that capture efficiency is dramatically less in daylight, or that almost no mesopelagic fishes occupy epipelagic depths during daylight. The deep oblique trawls used to estimate biomass and carbon export were not vertically resolved, and thus it is impossible to know the depth of capture of individual fishes. VM species constituted 33.7% of the overall mesopelagic fish abundance and 46.4% of the biomass when averaged by trawl. An alternate estimate of the migratory fraction of mesopelagic fishes was made from the shallow tows associated with the deeper tows used to estimate biomass. A mean of 25.1% of the abundance and 24.4% of the biomass of mesopelagic fishes in the deep tows were found in the epipelagic tows. The difference between estimates of the migratory fraction of biomass from these two methods is consistent with approximately half of the nominally VM biomass remaining at depth during the night. It is possible that there is a capture efficiency difference between active fishes near the

surface at night and lethargic fishes at depth in daylight. We found no clear evidence of a night-day capture efficiency difference, as the VM fraction of total biomass was not significantly different between day and night tows (*t*-test, $t = 1.44$, df = 75, $p = 0.15$). Some species of nominally NM fishes have been reported to be present in the epipelagic zone at night (Baird, 1971; Benoit-Bird and Au, 2006), or may be VM as juveniles but not as adults (Bailey and Robison, 1986; Clarke, 1973). Our trawl data support the finding of nocturnal vertical range expansion, because some individuals of several NM species were captured in shallow trawls. NM fishes found in the epipelagic at night formed 6.9% of the abundance and 12.7% of the biomass of the shallow tows. These fishes were not present in shallow trawls to the same depth conducted in daylight. For carbon export purposes, the presence of these fishes in the epipelagic zone at night partially offsets the fishes from VM species that do not migrate. The modeled fish export by VM fishes was adjusted for the difference between taxonomic and trawl-based estimates of the vertically-migratory biomass (Equation 10). This adjustment is approximate, as it includes the small fraction of NM fishes found in the epipelagic which have (on average) lower metabolic rates, and it does not resolve size- and species-specific differences in DVM behavior. The adjustment is also small, as R_e (the ratio of carbon export by a non-migrating VM fish to that of a migrating VM fish) is 1.03.

The energy budget for an idealized carnivorous fish (Brett and Groves, 1979), as modified for the lifetime *G*:*M* ratios of VM and NM mesopelagic fish species (Childress *et al.*, 1980), was used to calculate daily ration for the purposes of estimating the carbon exported by an individual fish. It is likely that this energy budget varies with ontogeny, temperature, season, and species. Some mesopelagic species are theorized to be

semelparous, reproducing in their last year of life, while others are known to be iteroparous (Childress *et al.*, 1980). No attempt was made here to separate reproductive and somatic growth, and we assumed that fishes do not change the fraction of ingested energy allocated to overall growth with the onset of reproductive activity. In addition, the assumption that growth is equivalent to mortality is only valid for a population that is not changing in size and on a generational time scale. Few data are available concerning the physiological energetics of mesopelagic fishes, as they are notoriously difficult to keep alive in captivity (Robison, 1973). Given the lack of detailed knowledge, the annual time scales assumed, the large number of mesopelagic fish species, and the wide variety of size classes considered, the use of generalized energy budgets was deemed appropriate.

Additional assumptions were made as to what constitutes "fish export" (Figure 4.1). The first of these assumptions is the 150 m flux boundary, chosen as a conventional depth of both sediment trap sampling and of the epipelagic layer. The most appropriate depth to use for a flux boundary is likely variable (Buesseler and Boyd, 2009), but the model here is not sensitive to the precise location of this boundary because all fishes are assumed inhabit a depth of 400 m during the day, with the VM fishes assumed to ascend to 50 m at night.

The second "fish export" assumption is the inclusion of fecal flux. This flux could be reasonably included in the passive transport category, as all mesopelagic fish feces are assumed to be exported regardless of the depth of defecation. Feces are included here due to their high speed of sinking (Robison and Bailey, 1981) and their rarity relative to zooplankton fecal pellets, properties that make fish fecal export difficult to measure using the sediment trap and ^{234}Th depletion methods usually used to estimate

the passive flux (Angel, 1985). It is possible that epipelagic fish feces are also largely exported, but our sampling methods were not suited to assess the biomass and size distribution of epipelagic fishes. The contribution of NM fishes to carbon export is via consumption of VM zooplankton (Figure 4.1), and may thus be considered a portion of the zooplankton mortality export flux. A "detrital fraction" of 33% was assumed for the diet of NM fishes, representing the fraction of zooplankton carbon that was acquired by the zooplankter below the 150 m threshold (Figure 4.1). It assumes that NM fishes are not selecting VM zooplankton in preference to NM zooplankton as prey, or vice versa. This was the largest (and most conservative for estimation of fish export) fraction resulting from the range of measurements of bacterial and zooplankton carbon demand by Steinberg *et al.* (2000) at two stations in the North Pacific. Although not counted as export here, a portion of this material is repackaged as rapidly-sinking feces by NM fishes. NM fishes may thus play a role in the transformation of slowly-sinking detritus at mesopelagic depths to fast-sinking detritus that may reach the sea floor.

The last general assumption regarding "fish export" is that 89% of VM fish mortality occurs below the 150 m flux depth boundary. This value is taken from an estimate of the food requirements of piscivorous stomiids in the Gulf of Mexico (Sutton and Hopkins, 1996), and is supported by less-specific estimates of stomiid predation from the NPSG (Clarke, 1982; Mann, 1984) that suggest that most mesopelagic fish production is isolated from epipelagic food chains, i.e. that the most important predators of open-ocean mesopelagic fishes are deep-living.

The RMR sub-model used here (Gillooly *et al.*, 2001) results from a regression of many studies from many species of fishes, most of which were not mesopelagic. This

model is similar to other published general estimates for fishes in the temperature range present in our study area (5-23°C; Figure 4.10; Clarke and Johnston, 1999; Winberg, 1956). This RMR model was then modified to represent a diel cycle of 50% inactivity (SMR) and 50% feeding (AMR). The RMR:SMR and AMR:RMR ratios were both set to 2 based upon general estimates from the literature (Brett and Groves, 1979; Winberg, 1956) and one published in situ measurement of the diel respiratory cycle of *Cyclothone acclinidens* (Smith and Laver, 1981), an abundant NM fish species from our study area. The fish export model is very sensitive to variation of the respiration rate parameters (Table 4.4). Therefore, we compared the respiration model and published respiratory rates in order to assess whether or not the modeled respiratory rates are representative of mesopelagic fishes. Once scaled to a common $W_{w,f}$ (1 g) and residence depth, the measured respiratory rates of mesopelagic fishes correspond well to the model (Figure 4.10).

The metabolic rate of fishes, and thus the ingested energy required to support it, is strongly and exponentially dependent upon both weight and temperature (Equation 1, Figure 4.11; Winberg 1956, Jobling 1993, Brett and Groves 1979). Variation of $W_{w,f}$ from 0.01-20 g and temperature from 2-30°C results in a 36-fold change in the expected weight-specific daily ration of a fish (Figure 4.11). However, published ingestion rates are often based upon weight and temperature averaged across wide ranges, making them sensitive to the sample distribution, which is often not reported. Uncertainties in temperature and weight aside, our calculations of daily ration based upon first principles, estimates of DVM behavior, and general energy budgets give reasonable results in the context of reported ingestion rates (Figure 4.12). The modeled R_d for a 1-g fish is lower

(above 7°C) than the relationship reported by Winberg (1956; 1-g fish), and higher than most measured values, although these measurements are often averaged over a wide range of temperature and span a range of $W_{w,f}$ between 0.05 and 116 g. The modeled R_d is also consistent with R_d calculated from measured respiration rates (Figure 4.10) assuming Q_{ox} = 13.6 J mg^{-1} O_2 and Q_z = 3.6 kJ g^{-1} $W_{w,z}$.

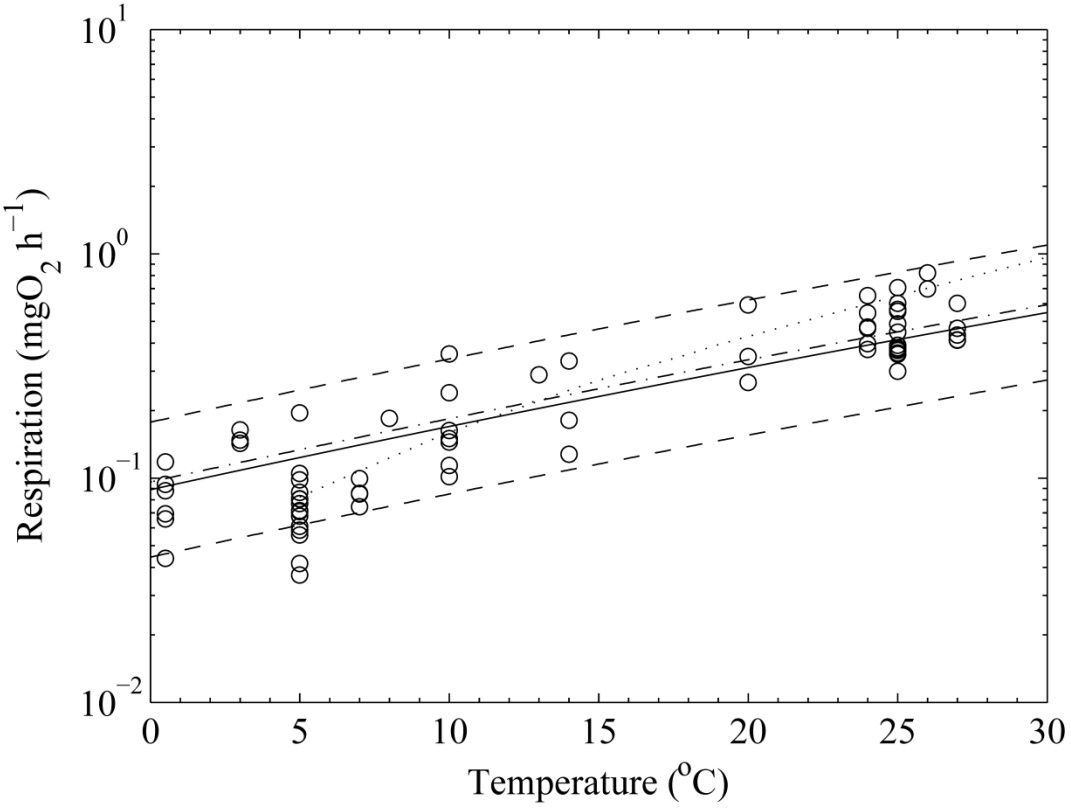

Figure 4.10. Metabolic model for RMR as a function of temperature for a 1-g fish (solid line; Gillooly *et al.*, 2001), and as modified for SMR (lower dashed line) and AMR (upper dashed line). The Clarke and Johnston (1999) and Winberg (1956) models are also shown for comparison (dash-dot line and dotted line respectively). Published measurements of the respiratory rate for mesopelagic fishes are shown (Childress and Somero, 1979; Donnelly and Torres, 1988; Ikeda, 1989; Smith and Laver, 1981; Torres *et al.*, 1979; Torres and Somero, 1988). Respiration rates of non-migratory fish species were divided by 0.49 to correct for the effect of residence depth on metabolism (Torres *et al.*, 1979).

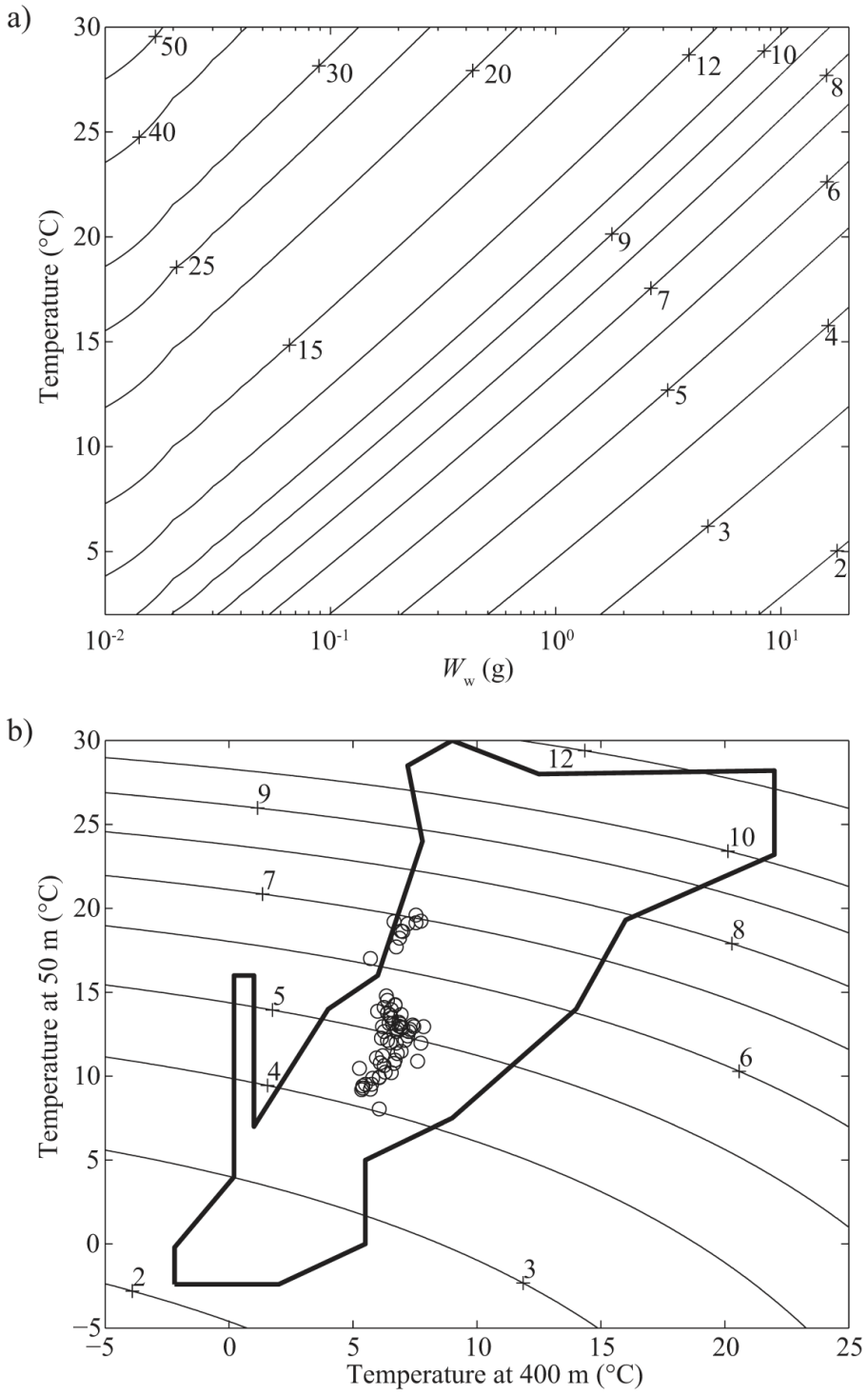

Figure 4.11. Modeled daily ration of fishes; a) effect of wet weight and temperature, b) daily ration of a 2-g vertically-migratory fish (~6 cm L_S) as a function of temperature at 50 and 400 m depths. The polygon contains the approximate range of these temperatures found in nature (annual average, World Ocean Atlas 2009; Locarnini *et al.* 2010).

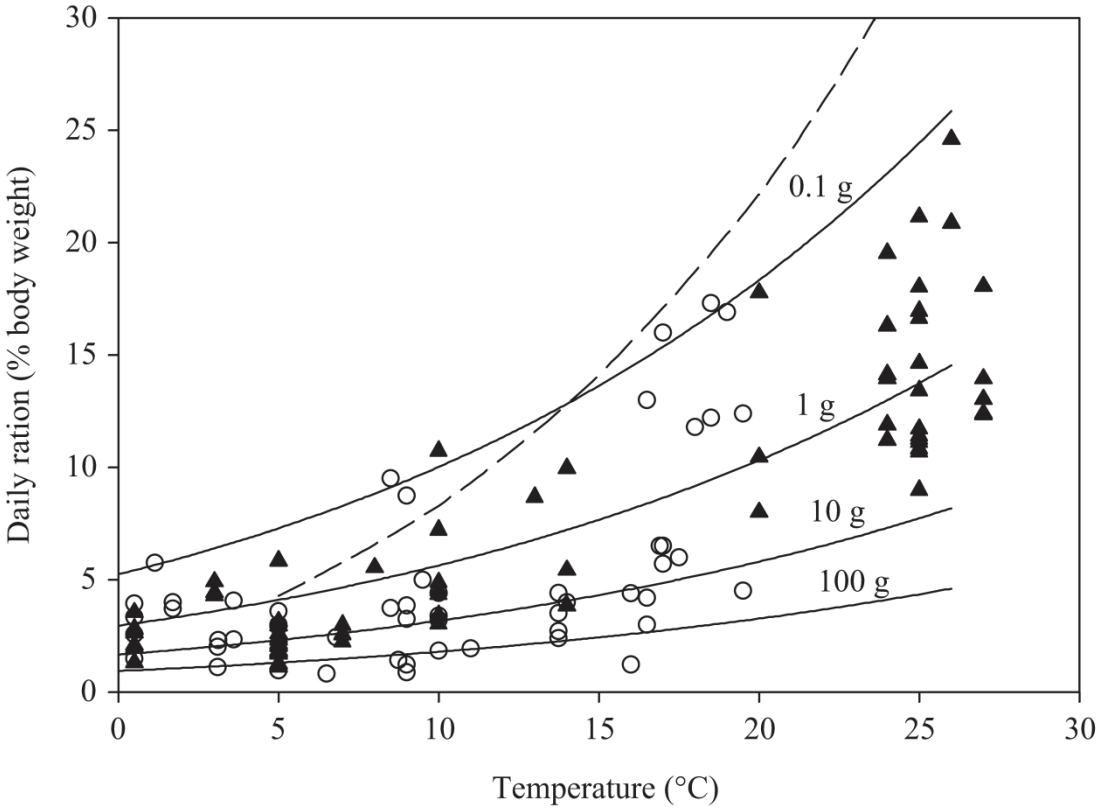

Figure 4.12. Modeled daily ration of a 0.1, 1, 10, and 100 g vertically-migratory fish as a function of temperature (solid lines). The daily ration estimate of Winberg (1956) for fishes is shown as a dashed line for wet weight of 1 g and 29% growth fraction of ingested energy. Measured values of mesopelagic fish daily ration (daily ration of NM fishes were divided by 0.49 to correct for the effect of residence depth on metabolism; Torres *et al.*, 1979) are marked as open circles (Childress *et al.*, 1980; Clarke, 1978; Dalpadado and Gjosaeter, 1988; Gerasimova, 1990; Gorbatenko and Il'inskii, 1991; Gorelova, 1984; Gorelova and Tseitlin, 1979; Holton, 1969; Hopkins and Baird, 1985; Legand and Rivaton, 1969; Pakhomov *et al.*, 1996; Rowedder, 1979; Sameoto, 1989; Sameoto, 1988; Tseytlin and Gorelova, 1978; Watanabe and Kawaguchi, 2003; Williams *et al.*, 2001), and daily ration calculated from measured respiration rates (Figure 9; 1-g $W_{w,f}$; assuming Q_{ox} = 13.6 J mg^{-1} O_2 and Q_z = 3.6 kJ g^{-1} $W_{w,z}$) are shown as closed triangles. Where temperature was not reported, World Ocean Atlas 2009 values (mean of 50 and 400 m temperatures; Locarnini *et al.* 2010) were used from the study location.

The daily energy expenditure of a NM fish is smaller than that of a VM fish, and thus it requires lower R_d and will process a smaller amount of carbon (Table 4.3),

resulting in lower weight-specific carbon export. The carbon exported by a 1-g NM fish is 31% of that of a similarly-sized VM fish. The respiratory fraction of overall fish export will be to shallow depths (150-400 m) with moderate ventilation times. The fecal fraction will be exported quickly to greater depths (mesopelagic fish feces sink at ~1000 m d^{-1}; Robison and Bailey 1981), and may be sequestered from the atmosphere on a time scale of centuries. The fate of the mortality export term is predator-specific. Given the assumption that 89% of mesopelagic zooplanktivore production is consumed by dragonfishes (Sutton and Hopkins, 1996) , it is likely that carbon lost to mortality will be transformed at a similar depth and in similar ratios as that of NM fishes (40% respired, 21% defecated, and 39% passed on to the next predator). The energy expenditure for vertical swimming is 27% of the daily ingested energy of a VM fish. Increased energy expenditure resulting from higher temperatures encountered near the surface can also be considered part of the cost of vertical migration. Vertical migration thus increases daily energy expenditure by about 67% under the conditions in Table 4.3. Looked at another way, if a VM fish can meet 60% of its normal daily energy requirement at depth, or if it consumed 160% of R_d the previous night in the epipelagic, it does not need to ascend to the surface to feed. Non-migration may be advantageous to fish if vertical migration elevates predation risk, either in transit or at the surface. There is evidence of partial population migration and feeding at depth by VM fishes that supports conditional vertical migration (Gorbatenko and Il'inskii, 1991; Pearcy et al., 1977; Pearcy et al., 1979), but if so, it is unclear whether or not fishes of nominally VM species make a daily decision to migrate based upon hunger.

4.5.3. Carbon export

Recent estimates of worldwide carbon export are ~10-11 Pg y^{-1} (83-91 mg C m^{-2} d^{-1} assuming an open ocean area of $332x10^6$ km^2; Falkowski *et al.*, 2003; Schlitzer, 2002; Usbeck *et al.*, 2003). Global estimates made from sediment trap data are 30-50% lower (Karl *et al.*, 1996; Martin *et al.*, 1987; Usbeck *et al.*, 2003). Active transport of carbon by zooplankton and mesopelagic fishes is at least partially responsible for the discrepancy between ecosystem modeling and empirical measurements of passive transport. Several researchers have estimated portions of the active transport at specific locations (Table 4.5). Direct comparisons of magnitude between the studies are difficult, because the studies varied in the form of the active transport estimated as well as by ecosystem. With two exceptions (Angel, 1985; Angel and Pugh, 2000; no correction for capture efficiency), the fish export studies are consistent given the partial populations and partial export terms studied. Estimates of zooplankton active transport have a wide range, and are generally lower than those for mesopelagic fishes, although many of the zooplankton studies are partial taxonomically or in terms of the flux terms (Table 4.5). Larger invertebrates likely avoid nets similarly to mesopelagic fishes, resulting in underestimates of biomass and carbon fluxes. If the midpoint is taken where a range is given, the mean zooplankton active transport across all studies is 12.7 mg C m^{-2} d^{-1} and the mean fish export rate is 12.6 mg C m^{-2} d^{-1}. Together, mean fish and zooplankton export is ~30% of the mean global carbon export (83-91 mg C m^{-2} d^{-1}). It must be emphasized that these studies may not be distributed across the range of NPP in the same ratio as NPP is over the ocean surface, and that there is some overlap between "zooplankton export" and "fish export." Even so, it is apparent that active transport by zooplankton and fishes may

explain a 30-50% gap between empirical data from sediment traps and ecological modeling, especially when the missing flux terms from the studies in Table 4.5 are considered.

Table 4.5. Active transport of carbon by vertically-migratory taxa. "DVM" and "OVM" refer to dielly vertically migratory and ontogenetically vertically migratory zooplankton respectively. In the "Terms" column, "R" refers to respiratory loss, "E" to excretion, "F" to fecal, and "M" to mortality. The first row of the table is a global carbon export estimate made with the Laws (2000) model (converted to mg C m^{-2} d^{-1} using an open ocean area of $332x10^6$ km^2).

Author	Location	Taxa	Carbon export (mg C m^{-2} d^{-1})	Terms
Falkowski *et al.* (2003)	global	n/a, global export	91.6	-
Al-Mutairi and Landry (2001)	Hawaii	DVM zooplankton[1]	7.1	R, E, F, M
Dam *et al.* (1995)	Bermuda	DVM zooplankton	14.5	R
Hidaka *et al.* (2001)	W. Eq. Pac.	DVM zooplankton[2]	10.2-24.8	R, F
Kobari *et al.* (2003)	N.W. Pac.	OVM copepods	11.8	R, M
Kobari *et al.* (2008)	N.W. Pac.	OVM, DVM copepods	9.4-22.4	R, F, M
Le Borgne and Rodier (1997)	E. Eq. Pac.	DVM zooplankton	6.3-7.9	R
Le Borgne and Rodier (1997)	W. Eq. Pac.	DVM zooplankton	3.1	R
Longhurst *et al.* (1990)	Sargasso Sea, E. Trop. Pac.	DVM zooplankton[1]	2.8-8.8	R
Longhurst and Williams (1992)	Bermuda	OVM copepods	0.3	M
Morales (1999)	Bermuda	OVM, DVM copepods	7.3-133.0	R, F, M
Putzeys and Hernandez-Leon (2005	Canary Is.	DVM zooplankton	4.0-7.0	R
Schnetzer and Steinberg (2002)	Bermuda	DVM zooplankton	0.9	F
Steinberg *et al.* (2000)	Bermuda	DVM zooplankton	2.0	R, E
Steinberg *et al.* (2008)	Hawaii	DVM zooplankton	1.8-7.7	R, E
Steinberg *et al.* (2008)	N.W. Pac.	DVM zooplankton	15.6-46.0	R, E
Takahashi *et al.* (2009)	N.W. Pac.	DVM copepods	8.0	R, M
Zhang and Dam (1997)	Eq. Pac.	DVM zooplankton	7.1-12.7	R, M
Angel (1985)	Azores Is.	DVM fishes	2.5	F
Angel and Pugh (2000)	N.E. Atl.	DVM fishes	0.1-0.6	E, F, M
Hidaka *et al.* (2001)	W. Eq. Pac.	DVM fishes	8.4-24.0	R, F
Radchenko (2007)	Bering Sea	DVM fishes	12.5[3]	F
Williams and Koslow (1997)	Tasmania	DVM fishes	5.8-20.3	M
This study	N.E. Pac.	Mesopelagic fishes	24.8	R, F, M

[1] Some fishes were included.

[2] Shrimp and euphausiid data were added to zooplankton.

[3] Assumes Bering Sea basin area is 1.2 million km^2

Fish export is 29.6 MMT y^{-1} (24.8 mg C m^{-2} d^{-1}) in the study area, forming 17.2% of the total export (144.4 mg C m^{-2} d^{-1}) as estimated by the model of Laws (2004). Most of the fish export is to depths of 400 m or more, as respiration during transit between 150 and 400 m is small in comparison to respiration at depth, defecation, and mortality (Table 4.3). This depth of export increases the importance of the fish export in relation to the passive flux, because as much as 80% of the passive flux is remineralized between 150 and 500 m (Buesseler *et al.*, 2007b). A comparison between sediment trap estimates of passive flux and fish export is possible in our study area (Figure 4.6c; Martin *et al.* 1987). Fish export varies from 6.4-39.5% of the overall carbon export at these four stations, and from 24.4-53.2% of the passive flux at 150 m (Figure 4.13). At a depth of 400 m, fish export averages 95% of the passive flux.

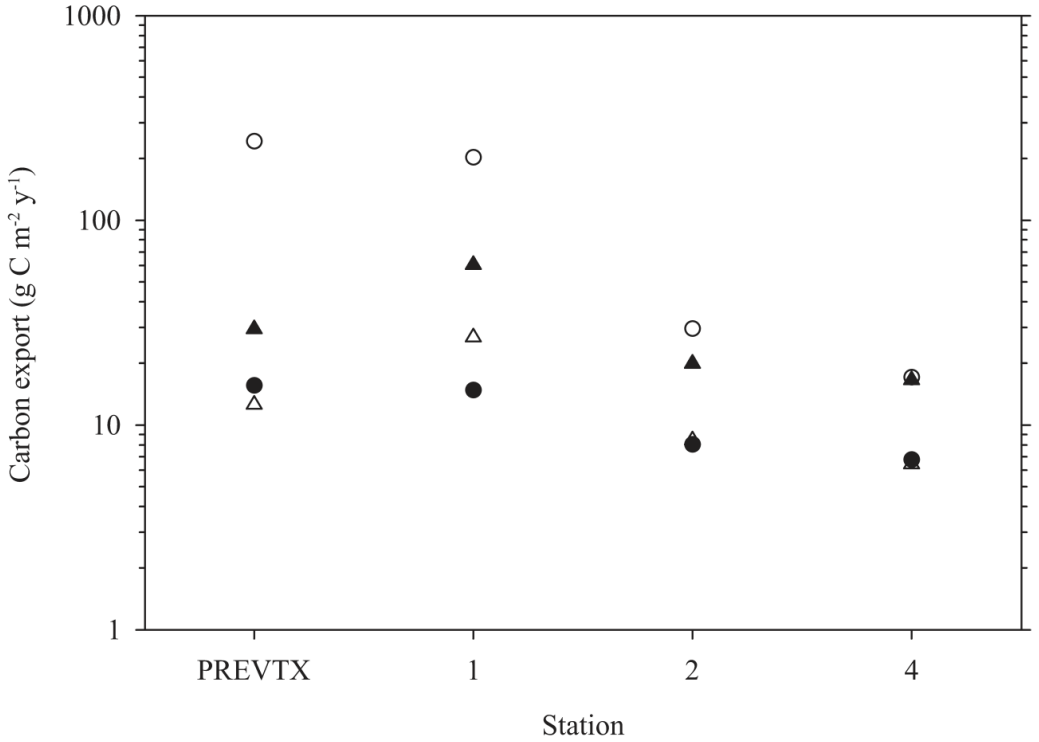

Figure 4.13. Comparison of total carbon export (open circles; Laws, 2004), passive flux (150 m, closed triangles; 400 m, open triangles; Martin et al., 1987), and fish export (closed circles) at the four VERTEX sediment trap stations in the study area.

The distributions of annual NPP, *ef* ratio, total carbon export, and fish export all have similar areal patterns, i.e., high in the coastal upwelling zone, low in the offshore central water mass, and moderate offshore to the north in the North Pacific Drift (Figure 4.6). However, the ratio of fish export to total export has an inverted pattern in relation to those ecological properties (Figure 4.8). This pattern inversion occurs because the biomass of mesopelagic fishes (and thus fish export) decreases in proportion to the amount of food available (proportional to annual NPP, Figure 4.4), whereas the total export decreases in proportion to the square of annual NPP because the multiplicative *ef* ratio is itself a function of annual NPP. The occurrence of relatively high fish export in subtropical waters is important because these oligotrophic waters form ~60% of overall ocean area (Eppley and Peterson, 1979) and are the site of approximately half of oceanic carbon export (Emerson *et al.*, 1997; Laws *et al.*, 2000). Although the linear regression between estimated fish export and total export was significant, visual inspection of Figure 4.7 suggests that the relationship may have different slopes to either side of an inflection point at 200 mg C m^{-2} d^{-1} of total export. If so, fish export may form a roughly constant 10% of total export above the inflection point and a rapidly increasing fraction of total export below the inflection point.

4.6. Conclusion

Quantifying the efficiency of the biological pump is a prerequisite for forming accurate global carbon models (Usbeck *et al.*, 2003). Few studies of the biological pump to date have quantified the role of mesopelagic fishes in the export of carbon from the

epipelagic. Our results indicate that not only is the fish export large in comparison to zooplankton flux estimates (Table 4.5), but that it is approximately equal to the passive flux at 400 m depth (Figure 4.13), and that it varies spatially in both magnitude and relative importance (Figures 4.7, 4.8). The size, swimming ability, and abundance of mesopelagic fishes serve to elevate their importance to the biological pump. Their feces sink rapidly, and they are isolated from epipelagic predators. Their daily vertical movements, or those of their prey, take them through the upper thermocline, and they release carbon in the form of defecation, respiration, and mortality below the depth zone in which most remineralization occurs (Figure 4.1). Mesopelagic fishes mediate a mean of 17.2% (24.8 mg C m^{-2} d^{-1}) of the total carbon export in the study area. Approximately half of this export passes through vertical-migrants of $W_{w,f}$ >1 g, over 90% of which are myctophids (Table 4.2, Figure 4.5). The magnitude of fish export exceeds 40% of the total export in the oligotrophic NPSG, where remineralization of passive carbon flux is most efficient (Figure 4.7). Fish export is larger in productive coastal upwelling areas, but forms a smaller fraction of the total export (Figure 4.8). Fish export is likely to be high in ocean regions that have warm water at mesopelagic depths due to elevated metabolic rates, but no such conditions were present in our study area. As fish export largely bypasses direct measurements of passive carbon export, it is additive to estimates of the biological pump made with them. This often-neglected component of the biological pump is large enough to affect global biogeochemical models that are currently fit to sediment trap data.

Quantification of fish export can be improved with more research on size-, temperature-, depth-, and taxonomically-specific energy budgets, respiration, and daily

rations of mesopelagic fishes. Depth-stratified sampling will serve to better describe the vertical distribution patterns of mesopelagic fishes, and thus depths of carbon ingestion and release. The major predators of mesopelagic fishes in the northeast Pacific Ocean are still unknown (Mann, 1984), and therefore the fate of mesopelagic fish production is also unknown, although it has been estimated that 34.6 mg C m^{-2} y^{-1} of mesopelagic fishes (~0.4 g m^{-2} y^{-1} wet weight cf. the mean biomass of 29.8 g m^{-2}) are consumed by cetaceans in the CCE (Barlow *et al.*, 2008). More in situ respiration experiments similar to that of Smith and Laver (1981) will improve understanding of daily variation in the metabolic rates of fishes. Finally, the export of nitrogen from the epipelagic by mesopelagic fishes and the fecal export of carbon by epipelagic fishes, although not studied here, are likely to prove ecologically important.

4.7. Acknowledgements

The authors thank the captains, crews, and science parties of the R/V "Melville," R/V "New Horizon," and FSV "McArthur II" for assistance deploying the trawls and processing the samples. A. Suntsov performed many of the trawls. C. Klepadlo from the Scripps Institution of Oceanography Marine Vertebrate Collection helped with the identification of mesopelagic fishes. R. Raymond provided assistance processing some of the samples. Funding for the MOHT was provided by the Moore Foundation. P. Davison was supported by a NASA Earth and Space Science Fellowship. Funding for the SEAPLEX cruise was provided by University of California Ship Funds, Project Kaisei, and NSF IGERT Grant #0333444. Wire time for midwater trawling was provided by the California Current Ecosystem LTER site, supported by NSF. Chemicals, equipment, and

laboratory space were provided by the SIO Marine Vertebrate and Pelagic Invertebrate Collections, D. Checkley, and J. Koslow.

4.8. Supplementary Material

Table 4.6. Trawl information. The P0810, ORCAWALE, and SEAPLEX cruises are abbreviated as "LTER," "O," and "SP," respectively. "IKMT" refers to a 3-m^2 Isaacs–Kidd midwater trawl (Isaacs and Kidd, 1953), and "MOHT" to a 5-m^2 Matsuda-Oozeki-Hu trawl (Oozeki *et al.*, 2004). "Light" refers to light conditions at the time of the trawl, "Depth" to the maximum depth of an oblique trawl profile, "Vol. filt." to the volume of water filtered by the net, "T_{top}" to the mean temperature of the top 150 m, "T_{bottom}" to the temperature at 400 m depth, and "$W_{w,f}$" to the wet weight of fishes collected per m^2. T_{top} and T_{bottom} are only reported for the 66 deep trawls used to estimate fish export.

Cruise:tow	Net	Date (PDT/PST)	Time (PDT/PST)	Lat. (°N)	Long. (°W)	Light	Depth (m)	Vol. filt. (m^3)	T_{top} (°C)	T_{bottom} (°C)	$W_{w,f}$ (g m^{-2})
LTER:1-1	MOHT	6 Oct. 2008	07:40	34.150	120.871	day	605	67046	12.4	7.2	4.243
LTER:1-2	MOHT	6 Oct. 2008	17:55	33.873	120.803	day	769	42411	12.7	7.3	5.085
LTER:1-3	MOHT	6 Oct. 2008	21:41	33.802	120.720	night	194	17308			0.533
LTER:1-4	MOHT	7 Oct. 2008	00:56	33.760	120.696	night	210	17203			1.322
LTER:1-5	MOHT	7 Oct. 2008	14:49	33.645	120.725	day	182	16383			0.000
LTER:1-6	MOHT	7 Oct. 2008	16:30	33.599	120.688	day	758	48567	12.1	7.1	3.644
LTER:1-7	MOHT	8 Oct. 2008	04:23	33.502	120.725	night	745	41897	12.8	7.3	4.644
LTER:2-1	MOHT	12 Oct. 2008	01:15	32.470	123.724	night	199	16882			0.326
LTER:2-2	MOHT	12 Oct. 2008	14:36	32.339	123.749	day	232	18143			0.000
LTER:2-3	MOHT	12 Oct. 2008	16:09	32.291	123.752	day	903	45518	14.8	6.4	2.226
LTER:2-4	MOHT	12 Oct. 2008	23:46	32.233	123.813	night	760	45757	14.5	6.4	1.405
LTER:2-5	MOHT	14 Oct. 2008	03:35	32.148	123.953	night	169	29957			0.104
LTER:3-1	MOHT	15 Oct. 2008	05:09	33.961	121.815	night	218	19717			1.122
LTER:3-2	MOHT	15 Oct. 2008	07:07	33.871	121.767	day	727	45469	13.1	6.6	4.138
LTER:3-3	MOHT	16 Oct. 2008	05:55	34.033	121.739	night	189	20107			0.792
LTER:3-4	MOHT	16 Oct. 2008	08:15	33.896	121.695	day	746	46129	13.0	6.2	4.457
LTER:3-5	MOHT	16 Oct. 2008	15:09	33.990	121.718	day	694	47888	13.0	6.9	5.546
LTER:3-6	MOHT	16 Oct. 2008	21:33	34.016	121.651	night	693	45084	13.2	6.9	5.160
LTER:3-7	MOHT	17 Oct. 2008	00:45	34.119	121.685	night	143	18596			0.964
LTER:4-1	MOHT	20 Oct. 2008	15:30	33.534	121.138	day	687	48325	13.1	7.4	2.162
LTER:4-2	MOHT	20 Oct. 2008	20:56	33.518	121.147	night	889	38623	13.0	7.5	4.615
LTER:4-3	MOHT	21 Oct. 2008	01:28	33.545	121.165	night	200	20888			0.810
LTER:4-4	MOHT	21 Oct. 2008	05:07	33.549	121.179	night	179	21926			1.926
LTER:5-1	MOHT	22 Oct. 2008	06:52	32.824	120.884	day	741	39062	12.0	6.8	3.551
LTER:5-2	MOHT	22 Oct. 2008	09:28	32.846	120.921	day	211	15619			0.006
LTER:5-3	MOHT	23 Oct. 2008	14:35	32.842	120.605	day	986	31451	12.1	6.4	3.541
LTER:5-4	MOHT	23 Oct. 2008	20:24	32.831	120.532	night	841	34676	12.7	6.3	4.835
LTER:5-5	MOHT	24 Oct. 2008	00:51	32.854	120.531	night	213	16192			1.780
LTER:5-6	MOHT	24 Oct. 2008	04:30	32.852	120.568	night	191	15331			1.165
LTER:6-1	MOHT	26 Oct. 2008	05:12	32.539	120.527	night	171	18156			0.429
LTER:6-2	MOHT	26 Oct. 2008	06:50	32.512	120.505	day	719	39831	13.2	6.5	2.844
LTER:6-3	MOHT	26 Oct. 2008	09:19	32.541	120.500	day	209	16524			0.011
LTER:6-4	MOHT	26 Oct. 2008	20:42	32.510	120.323	night	784	37694	14.0	6.6	4.009
LTER:6-5	MOHT	27 Oct. 2008	00:02	32.553	120.319	night	207	16642			0.919
LTER:6-6	MOHT	27 Oct. 2008	08:44	32.505	120.203	day	754	38049	13.6	6.5	2.622
LTER:6-7	MOHT	27 Oct. 2008	14:29	32.461	120.177	day	691	43245	13.8	6.4	3.719
LTER:6-8	MOHT	27 Oct. 2008	17:31	32.447	120.188	day	672	44445	12.0	6.5	2.135
LTER:6-9	MOHT	27 Oct. 2008	22:55	32.481	120.136	night	192	17626			0.543
LTER:7-1	MOHT	28 Oct. 2008	13:13	32.273	119.681	day	449	26582	13.7	7.0	1.523

Table 4.6. (continued)

Cruise:tow	Net	Date (PDT/PST)	Time (PDT/PST)	Lat. (°N)	Long. (°W)	Light	Depth (m)	Vol. filt. (m^3)	T_{top} (°C)	T_{bottom} (°C)	$W_{w.f.}$ (g m^{-2})
O:1-1	IKMT	30 Jul. 2008	20:40	45.939	125.957	day	176	10530[2]			0.000
O:1-2	IKMT	31 Jul. 2008	00:14	45.956	125.973	night	449	29160[2]	9.5	5.8	3.151
O:1-3	IKMT	31 Jul. 2008	02:27	45.958	125.998	night	165	10530[2]			0.207
O:1-4	IKMT	31 Jul. 2008	20:23	47.320	124.932	day	161	15660[2]			0.000
O:1-5	IKMT	31 Jul. 2008	23:49	47.332	124.858	night	167	14310[2]			0.791
O:1-6	IKMT	1 Aug. 2008	01:31	47.329	124.970	night	425	32400[2]	8.0	6.1	1.825
O:1-7	IKMT	1 Aug. 2008	23:56	47.730	126.853	night	126	11880[2]			0.229
O:1-8	IKMT	2 Aug. 2008	00:51	47.710	126.897	night	535	34830[2]	9.3	5.4	1.487
O:1-11	IKMT	3 Aug 2008	01:02	46.514	129.138	night	165	13500[2]			0.357
O:1-12	IKMT	3 Aug 2008	02:13	46.515	129.143	night	486	31860[2]	9.0	5.1	0.873
O:1-15	IKMT	5 Aug. 2008	23:52	46.283	128.197	night	186	12960[2]			0.505
O:1-16	IKMT	6 Aug. 2008	01:11	46.295	128.233	night	462	31050[2]	9.2	5.4	0.683
O:1-17	IKMT	6 Aug. 2008	23:54	45.031	127.035	night	146	13770[2]			0.322
O:1-18	IKMT	7 Aug. 2008	01:08	45.066	127.191	night	436	31590[2]	9.5	5.5	1.017
O:1-24	IKMT	9 Aug. 2008	19:50	44.393	130.583	day	173	14580[2]			0.000
O:1-26	IKMT	10 Aug 2008	00:19	44.394	130.577	night	147	12960[2]			0.065
O:1-27	IKMT	10 Aug 2008	01:33	44.403	130.580	night	469	32400[2]	9.3	5.0	1.073
O:1-28	IKMT	10 Aug. 2008	23:53	42.494	131.010	night	121	12960[2]			0.320
O:1-29	IKMT	11 Aug. 2008	01:08	42.496	131.007	night	430	32940[2]	10.5	5.3	0.795
O:1-34	IKMT	13 Aug 2008	23:25	40.901	130.051	night	162	13500[2]			0.115
O:1-35	IKMT	14 Aug 2008	00:38	40.899	130.052	night	502	33480[2]	12.0	6.0	0.559
O:1-36	IKMT	14 Aug. 2008	18:52	41.508	129.927	day	140	14670[2]			0.000
O:1-48	IKMT	19 Aug. 2008	00:31	44.411	125.417	night	134	13500[2]			1.652
O:1-49	IKMT	19 Aug. 2008	01:43	44.409	125.409	night	508	34290[2]	9.9	5.8	2.021
O:2-52	IKMT	26 Aug. 2008	00:48	45.247	125.366	night	134	14040[2]			1.618
O:2-53	IKMT	26 Aug. 2008	02:11	45.460	125.374	night	468	32940[2]	9.2	5.7	4.621
O:2-56	IKMT	27 Aug. 2008	23:15	43.330	127.515	night	164	14040[2]			0.225
O:2-57	IKMT	28 Aug. 2008	00:35	43.330	127.515	night	469	34020[2]	11.6	5.7	1.177
O:2-58	IKMT	28 Aug. 2008	19:15	41.864	127.656	day	150	9180[2]			0.000
O:2-60	IKMT	28 Aug. 2008	23:16	41.889	127.804	night	166	14040[2]			0.433
O:2-61	IKMT	29 Aug. 2008	00:36	41.884	127.804	night	471	33750[2]	10.4	5.4	3.805
O:2-65	IKMT	4 Sep. 2008	22:46	36.761	124.418	night	156	13770[2]			0.426
O:2-67	IKMT	5 Sep. 2008	01:56	36.759	124.419	night	457	33210[2]	10.8	6.1	1.643
O:2-73	IKMT	11 Sep. 2008	22:57	38.129	123.963	night	156	13770[2]			0.499
O:2-75	IKMT	12 Sep. 2008	01:08	38.129	123.952	night	458	34290[2]	10.0	6.1	1.554
O:2-77	IKMT	12 Sep. 2008	23:00	37.918	126.170	night	142	13500[2]			0.425
O:2-80	IKMT	13 Sep. 2008	02:36	37.916	126.173	night	449	32670[2]	10.6	6.3	2.456
O:3-81	IKMT	18 Sep. 2008	17:58	39.290	125.731	day	159	14040[2]			0.001
O:3-82	IKMT	18 Sep. 2008	23:41	39.335	125.780	night	144	12690[2]			1.151
O:3-83	IKMT	19 Sep. 2008	00:54	39.338	125.781	night	541	31590[2]	9.4	5.4	0.791
O:3-84	IKMT	19 Sep. 2008	23:01	41.081	125.114	night	153	12960[2]			1.320
O:3-85	IKMT	20 Sep. 2005	00:18	41.057	125.127	night	613	33210[2]	9.9	6.1	4.001
O:3-88	IKMT	21 Sep. 2005	22:36	40.249	127.327	night	168	13.230[2]			0.641
O:3-89	IKMT	21 Sep. 2005	23:55	40.248	127.329	night	625	33750[2]	10.4	5.6	1.956
O:3-90	IKMT	22 Sep. 2005	22:34	39.448	128.962	night	155	13.230[2]			0.017
O:3-91	IKMT	22 Sep. 2005	23:56	39.450	128.969	night	540	34830[2]	13.4	6.1	0.563
O:3-94	IKMT	24 Sep. 2008	22:29	37.795	129.336	night	148	13500[2]			0.047
O:3-95	IKMT	24 Sep. 2008	23:44	37.813	129.374	night	499	33480[2]	13.9	6.0	1.851
O:3-102	IKMT	27 Sep. 2008	23:37	35.435	125.472	night	132	13500[2]			0.240
O:3-103	IKMT	28 Sep. 2008	00:38	35.446	125.538	night	479	32940[2]	14.2	6.7	0.984
O:3-105	IKMT	28 Sep. 2008	23:11	36.904	125.327	night	142	13500[2]			0.378
O:3-106	IKMT	29 Sep. 2008	00:12	36.859	125.323	night	601	33210[2]	11.2	6.2	1.762
O:3-107	IKMT	29 Sep. 2008	22:25	36.835	126.559	night	136	13500[2]			0.534
O:3-108	IKMT	29 Sep. 2008	23:42	36.833	126.557	night	517	34290[2]	17.0	5.7	1.400

Table 4.6. (continued)

Cruise:tow	Net	Date (PDT/PST)	Time (PDT/PST)	Lat. (°N)	Long. (°W)	Light	Depth (m)	Vol. filt. (m^3)	T_{top} (°C)	T_{bottom} (°C)	$W_{w.f.}$ ($g\ m^{-2}$)
O:3-109	IKMT	30 Sep. 2008	22:26	34.931	127.178	night	139	13500[2]			0.166
O:3-110	IKMT	30 Sep. 2008	23:45	34.932	127.174	night	507	36450[2]	14.3	6.7	1.486
O:3-111	IKMT	1 Oct. 2008	22:11	34.209	125.789	night	146	13230[2]			0.120
O:3-112	IKMT	1 Oct. 2008	23:35	34.212	125.786	night	431	34560[2]	12.3	6.2	1.296
O:3-113	IKMT	2 Oct. 2008	22:12	35.246	124.678	night	144	13500[2]			0.036
O:3-114	IKMT	2 Oct. 2008	23:30	35.243	124.677	night	910	41175[2]	14.1	6.3	1.268
O:3-116	IKMT	3 Oct. 2008	22:02	34.872	122.769	night	129	13230[2]			0.353
O:3-117	IKMT	3 Oct. 2008	23:20	34.873	122.767	night	489	35100[2]	10.9	7.6	3.851
O:3-118	IKMT	4 Oct. 2008	21:53	34.517	121.254	night	132	13230[2]			0.284
O:3-119	IKMT	4 Oct. 2008	23:09	34.516	121.251	night	503	32940[2]	11.5	7.0	1.470
O:3-120	IKMT	5 Oct. 2008	21:31	33.937	118.850	night	149	13230[2]			0.721
O:3-121	IKMT	5 Oct. 2008	22:49	33.933	118.842	night	457	35640[2]	13.0	7.9	1.903
O:3-122	IKMT	6 Oct. 2008	21:34	33.726	119.356	night	123	13230[2]			0.466
O:3-123	IKMT	6 Oct. 2008	22:50	33.726	119.359	night	481	36450[2]	12.0	7.8	2.440
O:3-124	IKMT	7 Oct. 2008	21:41	32.466	119.715	night	131	13230[2]			0.213
O:3-125	IKMT	7 Oct. 2008	22:56	32.464	119.714	night	455	37260[2]	13.1	6.9	1.088
O:3-126	IKMT	8 Oct. 2008	21:28	32.233	118.103	night	161	13500[2]			0.119
O:3-127	IKMT	8 Oct. 2008	23:18	32.242	118.046	night	482	34560[2]	13.4	7.9	2.236
O:4-130	IKMT	16 Oct. 2008	22:46	33.068	121.489	night	169	13500[2]			0.552
O:4-131	IKMT	17 Oct. 2008	00:28	33.064	121.479	night	796	32670[2]	12.9	7.0	1.378
O:4-136	IKMT	20 Oct. 2008	21:44	38.007	127.924	night	145	13230[2]			0.642
O:4-137	IKMT	20 Oct. 2008	22:57	38.011	127.970	night	448	33750[2]	11.1	6.0	1.224
O:4-140	IKMT	23 Oct. 2008	21:02	37.863	123.452	night	153	13500[2]			0.716
O:4-141	IKMT	23 Oct. 2008	22:19	37.861	123.450	night	500	33210[2]	10.2	6.6	2.644
O:4-142	IKMT	24 Oct. 2008	21:42	36.445	122.967	night	134	13500[2]			1.119
O:4-143	IKMT	24 Oct. 2008	22:53	36.447	122.969	night	423	32940[2]	10.8	6.7	2.094
O:4-144	IKMT	25 Oct. 2008	21:21	36.358	123.496	night	157	13230[2]			0.289
O:4-145	IKMT	25 Oct. 2008	22:40	36.350	123.487	night	482	33480[2]	10.9	6.7	0.917
O:4-151	IKMT	29 Oct. 2008	22:16	35.955	122.043	night	127	13770[2]			0.466
O:4-152	IKMT	29 Oct. 2008	23:52	35.935	121.976	night	453	33210[2]	10.3	6.3	2.303
O:5-158	IKMT	8 Nov. 2008	20:28	34.266	127.036	night	144	13500[2]			0.078
O:5-159	IKMT	8 Nov. 2008	21:39	34.265	127.047	night	493	32670[2]	13.5	6.6	0.612
O:5-160	IKMT	9 Nov. 2008	15:47	32.856	125.253	day	139	13230[2]			0.000
O:5-163	IKMT	10 Nov. 2008	20:36	31.460	125.090	night	153	13230[2]	15.6	6.5	0.036
O:5-164	IKMT	10 Nov. 2008	21:52	31.459	125.090	night	483	32670[2]			1.125
O:5-178	IKMT	17 Nov. 2008	20:01	30.825	121.798	night	131	13230[2]	12.2	6.6	0.120
O:5-179	IKMT	17 Nov. 2008	21:15	30.825	121.795	night	490	32670[2]			1.953
O:5-181	IKMT	18 Nov. 2008	20:08	30.350	122.967	night	136	12960[2]			0.219
O:5-182	IKMT	18 Nov. 2008	21:19	30.430	122.966	night	474	32940[2]	13.9	6.6	0.923
O:5-185	IKMT	27 Nov. 2008	19:59	31.982	122.972	night	145	13500[2]			0.204
O:5-186	IKMT	27 Nov. 2008	21:00	32.009	123.018	night	479	32940[2]	12.7	6.8	1.773
SP:1-1	MOHT	3 Aug. 2009	07:03	32.426	119.985	day	~900[1]	39244	12.8	6.8	4.809
SP:1-2	MOHT	3 Aug. 2009	14:48	32.414	119.979	day	910	37931	12.9	7.0	4.600
SP:1-3	MOHT	3 Aug. 2009	19:59	32.411	119.992	dusk	835	44001	11.4	6.8	3.029
SP:1-4	MOHT	3 Aug. 2009	23:46	32.418	120.079	night	231	21974			0.676
SP:2-1	MOHT	8 Aug. 2009	16:16	32.064	137.899	day	918	37827	19.1	7.6	1.312
SP:2-2	MOHT	8 Aug. 2009	20:57	32.076	137.940	dusk	824	45585	19.6	7.6	1.342
SP:2-3	MOHT	9 Aug. 2009	01:51	32.106	137.904	night	177	20212			0.172
SP:2-4	MOHT	9 Aug. 2009	05:49	32.069	137.914	dawn	756	50398	19.2	7.8	1.050
SP:3-1	MOHT	10 Aug. 2009	17:04	32.915	140.312	day	878	41107	19.2	6.7	1.146
SP:3-2	MOHT	10 Aug. 2009	21:21	32.925	140.303	dusk	797	52453	18.2	6.9	2.541
SP:3-3	MOHT	11 Aug. 2009	02:27	32.884	140.265	night	176	18317			0.261
SP:3-4	MOHT	11 Aug. 2009	06:07	32.883	140.283	dawn	725	49817	17.7	6.8	1.939
SP:4-1	MOHT	14 Aug. 2009	00:50	34.063	139.976	night	888	42191	18.6	7.0	1.563
SP:4-2	MOHT	14 Aug. 2009	04:57	34.064	139.976	night	197	16800[2]			0.289

Table 4.6. (continued)

Cruise:tow	Net	Date (PDT/PST)	Time (PDT/PST)	Lat. (°N)	Long. (°W)	Light	Depth (m)	Vol. filt. (m^3)	T_{top} (°C)	T_{bottom} (°C)	$W_{w.f.}$ ($g\ m^{-2}$)
SP:4-3	MOHT	14 Aug. 2009	07:08	34.069	139.979	dawn	797	47959	18.6	7.0	2.092
SP:4-4	MOHT	14 Aug. 2009	18:06	34.058	139.998	day	837	40701	19.1	7.2	2.408

4.9. References

Al-Mutairi, H., Landry, M.R., 2001. Active export of carbon and nitrogen at Station ALOHA by diel migrant zooplankton. Deep-Sea Research Part II 48 (8-9), 2083-2103.

Angel, M.V., 1984. Detrital organic fluxes through pelagic ecosystems. In: Fasham, M.J.R. (Ed.), Flows of energy and materials in marine ecosystems, theory and practice. Plenum Press, New York, pp. 475-516.

Angel, M.V., 1985. Vertical migrations in the oceanic realm: possible causes and probable effects. In: Rankin, M.A. (Ed.), Migration. Mechanisms and adaptive significance, pp. 45-70.

Angel, M.V., 1989a. Does mesopelagic biology affect the vertical flux? In: Berger, W.H., Smetacek, V.S., Wefer, G. (Eds.), Productivity of the ocean: present and past. John Wiley & Sons Limited, New York, pp. 155-173.

Angel, M.V., 1989b. Vertical profiles of pelagic communities in the vicinity of the Azores Front and their implications to deep ocean ecology. Progress in Oceanography 22 (1), 1-46.

Angel, M.V., Pugh, P.R., 2000. Quantification of diel vertical migration by micronektonic taxa in the northeast Atlantic. Hydrobiologia 440 (1-3), 161-179.

Azam, F., Fenchel, T., Field, J.G., Gray, J.S., Meyerreil, L.A., Thingstad, F., 1983. The ecological role of water-column microbes in the sea. Marine Ecology Progress Series 10 (3), 257-263.

Bailey, T.G., Robison, B.H., 1986. Food availability as a selective factor on the chemical compositions of midwater fishes in the eastern North Pacific. Marine Biology 91 (1), 131-141.

Baird, R.C., 1971. The systematics, distribution, and zoogeography of the marine hatchetfishes (family Sternoptychidae). Bulletin of the Museum of Comparative Zoology 142 (1), 1-128.

Barlow, J., Kahru, M., Mitchell, B.G., 2008. Cetacean biomass, prey consumption, and primary production requirements in the California Current ecosystem. Marine Ecology Progress Series 371, 285-295.

Behrenfeld, M.J., Falkowski, P.G., 1997. Photosynthetic rates derived from satellite-based chlorophyll concentration. Limnology and Oceanography 42 (1), 1-20.

Benoit-Bird, K.J., Au, W.W.L., 2006. Extreme diel horizontal migrations by a tropical nearshore resident micronekton community. Marine Ecology Progress Series 319, 1-14.

Borodulina, O.D., 1972. The feeding of mesopelagic predatory fish in the open ocean. Journal of Ichthyology 12, 692-703.

Brett, J.R., Groves, T.D.D., 1979. Physiological energetics. In: Hoar, W.S., Randall, D.J. (Eds.), Bioenergetics and growth. Academic Press, New York, pp. 279-351.

Brodeur, R.D., Pearcy, W.G., Ralston, S., 2003. Abundance and distribution patterns of nekton and micronekton in the Northern California Current Transition Zone. Journal of Oceanography 59 (4), 515-535.

Buesseler, K.O., Antia, A.N., Chen, M., Fowler, S.W., Gardner, W.D., Gustafsson, O., Harada, K., Michaels, A.F., van der Loeff, M.R., Sarin, M., Steinberg, D.K., Trull, T., 2007a. An assessment of the use of sediment traps for estimating upper ocean particle fluxes. Journal of Marine Research 65 (3), 345-416.

Buesseler, K.O., Boyd, P.W., 2009. Shedding light on processes that control particle export and flux attenuation in the twilight zone of the open ocean. Limnology and Oceanography 54 (4), 1210-1232.

Buesseler, K.O., Lamborg, C.H., Boyd, P.W., Lam, P.J., Trull, T.W., Bidigare, R.R., Bishop, J.K.B., Casciotti, K.L., Dehairs, F., Elskens, M., Honda, M., Karl, D.M., Siegel, D.A., Silver, M.W., Steinberg, D.K., Valdes, J., Van Mooy, B., Wilson, S., 2007b. Revisiting carbon flux through the ocean's twilight zone. Science 316 (5824), 567-570.

Childress, J.J., Nygaard, M., 1974. Chemical composition and buoyancy of midwater crustaceans as function of depth of occurrence off southern California. Marine Biology 27 (3), 225-238.

Childress, J.J., Somero, G.N., 1979. Depth-related enzymic activities in muscle, brain and heart of deep-living pelagic marine teleosts. Marine Biology 52 (3), 273-283.

Childress, J.J., Taylor, S.M., Cailliet, G.M., Price, M.H., 1980. Patterns of growth, energy utilization and reproduction in some meso- and bathypelagic fishes off southern California. Marine Biology 61 (1), 27-40.

Clarke, A., Johnston, N.M., 1999. Scaling of metabolic rate with body mass and temperature in teleost fish. Journal of Animal Ecology 68 (5), 893-905.

Clarke, T.A., 1973. Some aspects of the ecology of lanternfishes (Myctophidae) in the Pacific Ocean near Hawaii. Fishery Bulletin 71 (2), 401-434.

Clarke, T.A., 1978. Diel feeding patterns of 16 Species of mesopelagic fishes from Hawaiian waters. Fishery Bulletin 76 (3), 495-513.

Clarke, T.A., 1982. Feeding habits of stomiatoid fishes from Hawaiian waters. Fishery Bulletin 80 (2), 287-304.

Clarke, W.D., 1971. Comparison of different investigative techniques for studying the deep scattering layers. In: Farquhar, G.B. (Ed.), Proceedings of an international symposium on biological sound scattering in the ocean. U.S. Government Printing Office, Washington D.C., pp. 550-562.

Dalpadado, P., Gjosaeter, J., 1988. Feeding ecology of the lanternfish *Benthosema pterotum* from the Indian Ocean. Marine Biology 99 (4), 555-567.

Dam, H.G., Roman, M.R., Youngbluth, M.J., 1995. Downward export of respiratory carbon and dissolved inorganic nitrogen by diel-migrant mesozooplankton at the JGOFS Bermuda time-series station. Deep-Sea Research 42 (7), 1187-1197.

Denman, K.L., Brasseur, G., Chidthaisong, A., Ciais, P., Cox, P.M., Dickinson, R.E., Hauglustaine, D., Heinze, C., Holland, E., Jacob, D., Lohmann, U., Ramachandran, S., da Silva Dias, P.L., Wofsy, S.C., Zhang, X., 2007. Couplings between changes in the climate system and biogeochemistry. In: Solomon, S., Qin, D., Manning, M., Chen, Z., Marquis, M., Averyt, K.B., Tignor, M., Miller, H.L. (Eds.), Climate change 2007: the physical science basis. Contribution of Working Group I to the fourth assessment report of the Intergovernmental Panel on Climate Change, New York, pp. 499-587.

Donnelly, J., Torres, J.J., 1988. Oxygen consumption of midwater fishes and crustaceans from the eastern Gulf of Mexico. Marine Biology 97 (4), 483-494.

Emerson, S., Quay, P., Karl, D., Winn, C., Tupas, L., Landry, M., 1997. Experimental determination of the organic carbon flux from open-ocean surface waters. Nature 389 (6654), 951-954.

Eppley, R.W., Peterson, B.J., 1979. Particulate organic matter flux and planktonic new production in the deep ocean. Nature 282 (5740), 677-680.

Falkowski, P.G., Laws, E.A., Barber, R.T., Murray, J.W., 2003. Phytoplankton and their role in primary, new, and export production. In: Fasham, M.J.R. (Ed.), Ocean biogeochemistry. Springer-Verlag, Berlin, pp. 99-121.

Fowler, S.W., Knauer, G.A., 1986. Role of large particles in the transport of elements and organic compounds through the oceanic water column. Progress in Oceanography 16 (3), 147-194.

Gerasimova, O., 1990. Feeding and food intake of *Electrona carlsbergi* (Taning, 1932) Myctophidae. Selected Science Paper CCAMLR 7, 411-416.

Gillooly, J.F., Brown, J.H., West, G.B., Savage, V.M., Charnov, E.L., 2001. Effects of size and temperature on metabolic rate. Science 293 (5538), 2248-2251.

Gjosaeter, J., Kawaguchi, K., 1980. A review of the world resources of mesopelagic fish. FAO Fisheries Technical Paper 193, 1-151.

Gorbatenko, K.M., Il'inskii, E.N., 1991. Feeding behavior of the most common mesopelagic fishes in the Bering Sea. Journal of Ichthyology 31 (5), 816-821.

Gorelova, T.A., 1984. A quantitative assessment of consumption of zooplankton by epipelagic lanternfishes (family Myctophidae) in the equatorial Pacific Ocean. Journal of Ichthyology 23, 106-113.

Gorelova, T.A., Tseitlin, V.B., 1979. Feeding of mesopelagic fish of the genus *Cyclothone*. Okeanologiya 19 (6), 1110-1115.

Hidaka, K., Kawaguchi, K., Murakami, M., Takahashi, M., 2001. Downward transport of organic carbon by diel migratory micronekton in the western equatorial Pacific: its quantitative and qualitative importance. Deep-Sea Research 48 (8), 1923-1939.

Hill, K.T., Lo, N.C.H., Macewiz, B.J., Crone, P.R., Felix-Uraga, R., 2010. Assessment of the Pacific sardine resource in 2010 for U.S. Management in 2011. NOAA Technical Memorandum NMFS SWFSC-469, pp. 1-142.

Holton, A.A., 1969. Feeding behavior of a vertically migrating lanternfish. Pacific Science 23 (3), 325-331.

Hopkins, T.L., Baird, R.C., 1985. Feeding ecology of four hatchetfishes (Sternoptychidae) in the eastern Gulf of Mexico. Bulletin of Marine Science 36 (2), 260-277.

Ikeda, T., 1989. Estimated respiration rate of myctophid fish from the enzyme activity of the electron-transport-system. Journal of the Oceanographical Society of Japan 45, 167-173.

IPCC, 2007. Summary for policymakers. In: Solomon, S., Qin, D., Manning, M., Chen, Z., Marquis, M., Averyt, K.B., Tignor, M., Miller, H.L. (Eds.), Climate change 2007: the physical science basis. Contribution of Working Group I to the fourth assessment report of the Intergovernmental Panel on Climate Change, New York.

Isaacs, J.D., Kidd, L.W., 1953. Isaacs-Kidd midwater trawl final report. Scripps Institution of Oceanography Oceanographic equipment report 1 (53-3), 1-21.

Jacobson, L.D., Lo, N.C.H., Barnes, J.T., 1994. A biomass-based assessment model for northern anchovy, *Engraulis mordax*. Fishery Bulletin 92, 711-724.

Jobling, M., 1993. Bioenergetics: feed intake and energy partitioning. In: Rankin, J.C., Jensen, F.B. (Eds.), Fish ecophysiology. Chapman and Hall, London, pp. 1-44.

Kaartvedt, S., Rostad, A., Klevjer, T.A., Staby, A., 2009. Use of bottom-mounted echo sounders in exploring behavior of mesopelagic fishes. Marine Ecology Progress Series 395, 109-118.

Karl, D.M., Christian, J.R., Dore, J.E., Hebel, D.V., Letelier, R.M., Tupas, L.M., Winn, C.D., 1996. Seasonal and interannual variability in primary production and particle flux at Station ALOHA. Deep-Sea Research Part II 43 (2-3), 539-568.

Knauer, G.A., Redalje, D.G., Harrison, W.G., Karl, D.M., 1990. New production at the VERTEX time-series site. Deep-Sea Research 37 (7), 1121-1134.

Kobari, T., Shinada, A., Tsuda, A., 2003. Functional roles of interzonal migrating mesozooplankton in the western subarctic Pacific. Progress in Oceanography 57 (3-4), 279-298.

Kobari, T., Steinberg, D.K., Ueda, A., Tsuda, A., Silver, M.W., Kitamura, M., 2008. Impacts of ontogenetically migrating copepods on downward carbon flux in the western subarctic Pacific Ocean. Deep-Sea Research Part II 55 (14-15), 1648-1660.

Laws, E., 2004. Export flux and stability as regulators of community composition in pelagic marine biological communities: implications for regime shifts. Progress in Oceanography 60 (2-4), 343-354.

Laws, E.A., Falkowski, P.G., Smith, W.O., Ducklow, H., McCarthy, J.J., 2000. Temperature effects on export production in the open ocean. Global Biogeochemical Cycles 14 (4), 1231-1246.

Le Borgne, R., Rodier, M., 1997. Net zooplankton and the biological pump: a comparison between the oligotrophic and mesotrophic equatorial Pacific. Deep-Sea Research Part II 44 (9-10), 2003-2023.

Legand, M., Rivaton, J., 1969. Biological cycles of mesopelagic fishes of eastern Indian Ocean 3: predatory activity of micronektonic fishes. Cahiers Orstom Oceanographie 7 (3), 29-45.

Linkowski, T.B., 1996. Lunar rhythms of vertical migrations coded in otolith microstructure of North Atlantic lanternfishes, genus *Hygophum* (Myctophidae). Marine Biology 124 (4), 495-508.

Locarnini, R.A., Mishonov, A.V., Antonov, J.I., Boyer, T.P., Garcia, H.E., Baranova, H.A., Zweng, M.M., Johnson, D.R., 2010. World Ocean Atlas 2009, Volume 1: Temperature. U.S. Government Printing Office, Washington, D.C.

Longhurst, A., Williams, R., 1992. Carbon flux by seasonal vertical migrant copepods is a small number. Journal of Plankton Research 14 (11), 1495-1509.

Longhurst, A.R., Bedo, A.W., Harrison, W.G., Head, E.J.H., Sameoto, D.D., 1990. Vertical flux of respiratory carbon by oceanic diel migrant biota. Deep-Sea Research 37 (4), 685-694.

Longhurst, A.R., Harrison, W.G., 1989. The biological pump: profiles of plankton production and consumption in the upper ocean. Progress in Oceanography 22 (1), 47-123.

Mann, K.H., 1984. Fish production in open ocean ecosystems. In: Fasham, M.J.R. (Ed.), Flows of energy and materials in marine ecosystems. Plenum Press, New York, pp. 435-458.

Martin, J.H., Knauer, G.A., Karl, D.M., Broenkow, W.W., 1987. VERTEX: carbon cycling in the northeast Pacific. Deep-Sea Research 34 (2), 267-285.

Martz, T.R., Johnson, K.S., Riser, S.C., 2008. Ocean metabolism observed with oxygen sensors on profiling floats in the South Pacific. Limnology and Oceanography 53 (5, part 2), 2094-2111.

Montoya, J.P., Holl, C.M., Zehr, J.P., Hansen, A., Villareal, T.A., Capone, D.G., 2004. High rates of N_2 fixation by unicellular diazotrophs in the oligotrophic Pacific Ocean. Nature 430 (7003), 1027-1031.

Morales, C.E., 1999. Carbon and nitrogen fluxes in the oceans: the contribution by zooplankton migrants to active transport in the North Atlantic during the Joint Global Ocean Flux Study. Journal of Plankton Research 21 (9), 1799-1808.

Morel, A., Berthon, J.F., 1989. Surface pigments, algal biomass profiles, and potential production of the euphotic layer: relationships reinvestigated in view of remote-sensing applications. Limnology and Oceanography 34 (8), 1545-1562.

Oozeki, Y., Hu, F.X., Kubota, H., Sugisaki, H., Kimura, R., 2004. Newly designed quantitative frame trawl for sampling larval and juvenile pelagic fish. Fisheries Science 70 (2), 223-232.

Pakhomov, E.A., Perissinotto, R., McQuaid, C.D., 1996. Prey composition and daily rations of myctophid fishes in the Southern Ocean. Marine Ecology Progress Series 134 (1-3), 1-14.

Pauly, D., Christensen, V., 1995. Primary production required to sustain global fisheries. Nature 374, 255-257.

Pauly, D., Trites, A.W., Capuli, E., Christensen, V., 1998. Diet composition and trophic levels of marine mammals. ICES Journal of Marine Science 55 (3), 467-481.

Pearcy, W.G., 1964. Some distributional features of mesopelagic fishes off Oregon. Journal of Marine Research 22 (1), 83-102.

Pearcy, W.G., 1976. Seasonal and inshore-offshore variations in standing stocks of micronekton and macrozooplankton off Oregon. Fishery Bulletin 74 (1), 70-80.

Pearcy, W.G., Krygier, E.E., Mesecar, R., Ramsey, F., 1977. Vertical distribution and migration of oceanic micronekton off Oregon. Deep-Sea Research 24 (3), 223-245.

Pearcy, W.G., Laurs, R.M., 1966. Vertical migration and distribution of mesopelagic fishes off Oregon. Deep-Sea Research 13, 153-165.

Pearcy, W.G., Lorz, H.V., Peterson, W., 1979. Comparison of the feeding habits of migratory and non-migratory *Stenobrachius leucopsarus* (Myctophidae). Marine Biology 51 (1), 1-8.

Putzeys, S., Hernandez-Leon, S., 2005. A model of zooplankton diel vertical migration off the Canary Islands: implication for active carbon flux. Journal of Sea Research 53 (4), 213-222.

Radchenko, V.I., 2007. Mesopelagic fish community supplies "biological pump". Raffles Bulletin of Zoology, 265-271.

Robison, B.H., 1973. System for maintaining midwater fishes in captivity. Journal of the Fisheries Research Board of Canada 30 (1), 126-128.

Robison, B.H., 1984. Herbivory by the myctophid fish *Ceratoscopelus warmingii*. Marine Biology 84 (2), 119-123.

Robison, B.H., Bailey, T.G., 1981. Sinking rates and dissolution of midwater fish fecal matter. Marine Biology 65 (2), 135-142.

Robison, B.H., Reisenbichler, K.R., Sherlock, R.E., 2005. Giant larvacean houses: rapid carbon transport to the deep sea floor. Science 308 (5728), 1609-1611.

Rowedder, U., 1979. Feeding ecology of the Myctophid *Electrona antarctica* (Gunther, 1878) (Teleostei). Meeresforschung-Reports on Marine Research 27 (4), 252-263.

Sameoto, D., 1989. Feeding ecology of the lantern fish *Benthosema glaciale* in a subarctic region. Polar Biology 9 (3), 169-178.

Sameoto, D.D., 1988. Feeding of lantern fish *Benthosema glaciale* off the Nova Scotia shelf. Marine Ecology Progress Series 44 (2), 113-129.

Schlitzer, R., 2002. Carbon export fluxes in the Southern Ocean: results from inverse modeling and comparison with satellite-based estimates. Deep-Sea Research Part II 49 (9-10), 1623-1644.

Schnetzer, A., Steinberg, D.K., 2002. Active transport of particulate organic carbon and nitrogen by vertically migrating zooplankton in the Sargasso Sea. Marine Ecology Progress Series 234, 71-84.

Silver, M.W., Coale, S.L., Pilskaln, C.H., Steinberg, D.R., 1998. Giant aggregates: importance as microbial centers and agents of material flux in the mesopelagic zone. Limnology and Oceanography 43 (3), 498-507.

Smith, K.L., Laver, M.B., 1981. Respiration of the bathypelagic fish *Cyclothone acclinidens*. Marine Biology 61 (4), 261-266.

Steinberg, D.K., Carlson, C.A., Bates, N.R., Goldthwait, S.A., Madin, L.P., Michaels, A.F., 2000. Zooplankton vertical migration and the active transport of dissolved organic and inorganic carbon in the Sargasso Sea. Deep-Sea Research 47 (1), 137-158.

Steinberg, D.K., Van Mooy, B.A.S., Buesseler, K.O., Boyd, P.W., Kobari, T., Karl, D.M., 2008. Bacterial vs. zooplankton control of sinking particle flux in the ocean's twilight zone. Limnology and Oceanography 53 (4), 1327-1338.

Sutton, T.T., Hopkins, T.L., 1996. Trophic ecology of the stomiid (Pisces: Stomiidae) fish assemblage of the eastern Gulf of Mexico: Strategies, selectivity and impact of a top mesopelagic predator group. Marine Biology 127 (2), 179-192.

Takahashi, K., Kuwata, A., Sugisaki, H., Uchikawa, K., Saito, H., 2009. Downward carbon transport by diel vertical migration of the copepods *Metridia pacifica* and *Metridia okhotensis* in the Oyashio region of the western subarctic Pacific Ocean. Deep-Sea Research 56 (10), 1777-1791.

Torres, J.J., Belman, B.W., Childress, J.J., 1979. Oxygen consumption rates of midwater fishes as a function of depth of occurrence. Deep-Sea Research 26 (2), 185-197.

Torres, J.J., Somero, G.N., 1988. Metabolism, enzymic activities and cold adaptation in Antarctic mesopelagic fishes. Marine Biology 98 (2), 169-180.

Tseytlin, V.B., Gorelova, T.A., 1978. Studies of the feeding of the lanternfish *Myctophum nitidulum* (Myctophidae, Pisces). Okeanologiya 18 (4), 742-749.

Usbeck, R., Schlitzer, R., Fischer, G., Wefer, G., 2003. Particle fluxes in the ocean: comparison of sediment trap data with results from inverse modeling. Journal of Marine Systems 39 (3-4), 167-183.

Videler, J.J., 1993. Fish swimming. Chapman and Hall, New York.

Volk, T., Hoffert, M.I., 1985. Ocean carbon pumps: analysis of relative strengths and efficiencies in ocean-driven atmospheric CO_2 changes. In: Sundquist, E., Broecker, W.S. (Eds.), The carbon cycle and atmospheric CO_2: natural variations archean to present.

Watanabe, H., Kawaguchi, K., 2003. Decadal change in the diets of the surface migratory myctophid fish *Myctophum nitidulum* in the Kuroshio region of the western North

Pacific: predation on sardine larvae by myctophids. Fisheries Science 69 (4), 716-721.

Watson, A.J., Orr, J.C., 2003. Carbon dioxide fluxes in the global ocean. In: Fasham, M.J.R. (Ed.), Ocean biogeochemistry. Springer-Verlag, Berlin, pp. 123-143.

Welp, L.R., Keeling, R.F., Meijer, H.A.J., Bollenbacher, A.F., Piper, S.C., Yoshimura, K., Francey, R.J., Allison, C.E., Wahlen, M., 2011. Interannual variability in the oxygen isotopes of atmospheric CO_2 driven by El Nino. Nature 477 (7366), 579-582.

Williams, A., Koslow, J.A., 1997. Species composition, biomass and vertical distribution of micronekton over the mid-slope region off southern Tasmania, Australia. Marine Biology 130 (2), 259-276.

Williams, A., Koslow, J.A., Terauds, A., Haskard, K., 2001. Feeding ecology of five fishes from the mid-slope micronekton community off southern Tasmania, Australia. Marine Biology 139 (6), 1177-1192.

Winberg, G.G., 1956. Rate of metabolism and food requirements of fishes. Belorussian State University, Minsk.

Zhang, X.S., Dam, H.G., 1997. Downward export of carbon by diel migrant mesozooplankton in the central equatorial Pacific. Deep-Sea Research Part II 44 (9-10), 2191-2202.

Chapter 4, in full, is currently being prepared for submission for publication of the material. Davison, P.C., Checkley, D.M., Koslow, J.A., and Barlow, J. The dissertation author was the primary investigator and author of this paper.